

**A Comparative Analysis of Passive and Active Daylight
Redirecting Blinds in Support of the Schematic Design Process**

Samson Yip

A Thesis in the Department of
Building, Civil, and Environmental Engineering

Presented in Partial Fulfillment of the Requirements for the Degree of

Master of Applied Science (Building Engineering) at

Concordia University

Montréal, Québec, Canada

April 2015

©Samson Yip, 2015

CONCORDIA UNIVERSITY
School of Graduate Studies

This is to certify that the thesis prepared

By: Samson Yip

Entitled: A Comparative Analysis of Passive and Active Daylight Redirecting Blinds in Support of the Schematic Design Process

and submitted in partial fulfillment of the requirements for the degree of

Master of applied Science (Building Engineering)

complies with the regulations of the University and meets the accepted standards with respect to originality and quality.

Signed by the final examining committee:

Dr. B. Lee Chair

Dr. S. Mudur Examiner

Dr. H. Ge Examiner

Dr. A. Athienitis Supervisor

Approved by _____
Chair of Department or Graduate Program Director

Dean of Faculty

Date _____

Abstract

A Comparative Analysis of Passive and Active Daylight Redirecting Blinds in Support of the Schematic Design Process

Samson Yip

Daylight redirecting blinds are a class of sun control device that are designed specifically to increase daylighting levels in buildings in addition to preventing unwanted solar gain and glare. Because they rely on many parameters such as complex geometry and may require automated controls to achieve their high illuminance performance, their angle-dependent optical characteristics cannot be represented or simulated accurately using the simple tools that are normally used at the beginning of the design process when rapid assessments are needed. Instead they require time- and resource-intensive simulation methods that are difficult to integrate into existing building design workflows at such an early stage of design. Therefore design guidance for these daylight redirecting blinds is needed in support of design decisions at the beginning of the schematic design phase – to assist in answering questions such as: *How deep can a floor plate be for the entire floor area in an open-plan office to be considered sufficiently daylit?*

The daylighting illuminance performance of two classes of blinds, passive and active, are investigated to generalize this design guidance. A representative model of each class of blind is used. Through the use of a high-performance multi-storey open-plan double-perimeter zone office building in Golden, USA (40°N, 105°W) as a case study, a simplified simulation model using the radiosity method is validated.

The simulation model is used to examine the effect of different parameters such as blind type, location, glazing properties, building depth, façade orientation, window to wall ratio, and window head height on daylighting illuminance in the office space. Simple correlations between building geometry and interior daylight illuminance sufficiency are sought that can be used as design guidance in early schematic design in lieu of simulations.

Based on the results, the conclusion is that for most combinations tested active blinds will perform as well as or better than passive blinds. While a passive blind may be acceptable for mild, temperate climates, it may cause excessive overheating in climates with high cooling loads. In this respect, the greatest flexibility is offered by the class of active blinds which can control when daylight or solar heat is desired in the interior. Using the $sDA_{300/50}$ metric from the IES LM-83-12 standard, the study found that the maximum building depth for a South-oriented open-plan space that provides ‘nominally acceptable’ daylight illuminance is 14.5 m for Golden (actual building depth is 18 m). This calculated maximum building depth is between 11.5 m (Vancouver) and 15 m (Montreal) for different locations. This variation is due to the different total annual sunshine hours and visible transmittance of the glazing and blind at different solar incidence angles at each location. A correlation is made between window head height and maximum building depth for an open-plan office space.

Acknowledgements

I wish to express my deepest gratitude to my supervisor, Professor Andreas K. Athienitis, for providing me the opportunity to pursue this work and in the process open up a world to me. I have learned immensely under his guidance and I am inspired by his passion and dedication to research and teaching. It has been a privilege to be a participant in his research group.

I wish to thank my friend and colleague, Dr. Yuxiang Chen, for his guidance and constructive criticism throughout the process of realizing this thesis. His insight is rare and has been invaluable to me.

I am indebted to my friends and colleagues at the Solar Lab and in the CZEBS group. I thank them for all their support and the numerous serious and not so serious ideas and moments that we shared over the last few years.

My time at Concordia University was enriched with lively discussions with the late Professor Paul Fazio. I always looked forward to our exchanges on architecture and engineering.

Special thanks go to my family, and my dearest friends, Naomi, Edward, and Jennifer. They provided intellectual and emotional support throughout this entire adventure. I am especially grateful for their patience during difficult times.

This work is dedicated to my mother, So King, for her love and support and to the memory of my father, Wah Fong, who worked selflessly and tirelessly to support us and help us realize our many dreams. He is dearly missed but not forgotten.

Finally, I wish to acknowledge funding from the Natural Sciences and Engineering Research Council of Canada (NSERC) Smart Net-zero Energy Buildings strategic Research Network (SNEBRN), and the Graduate Student Support Program of the Faculty of Engineering and Computer Science of Concordia University, Montreal, Canada. Additional in-kind support was provided by the National Renewable Energy Laboratory (NREL) of the USA.

Table of Contents

LIST OF FIGURES.....	XII
LIST OF TABLES.....	XVI
NOMENCLATURE.....	XIX
CHAPTER 1 INTRODUCTION	1
Section 1.1 Daylighting renaissance	1
Section 1.2 Importance of daylighting.....	3
Section 1.3 The role of design process.....	5
Section 1.4 Motivation and goals.....	8
Section 1.5 Thesis objectives	11
Section 1.6 Thesis overview.....	11
CHAPTER 2 LITERATURE REVIEW	13
Section 2.1 Introduction	13
Section 2.2 Building fenestration elements	13
1. Window properties	13
2. Sun control devices: blinds, louvers, and daylight redirection	14
3. Advanced sun control devices	16
4. Sun control devices selected for investigation	19
5. Three-section façade	20
6. Occupant behaviour and blinds	22
7. Open-plan office spaces.....	23
Section 2.3 Daylighting design and analysis tools	24

1. Charts and graphical methods.....	24
2. Rules of thumb: useful daylight building depth calculator.....	26
3. Scale models.....	27
4. Optical characterization of blinds.....	27
5. Daylighting simulation software.....	30
6. Radiosity model.....	32
7. Sky models for daylighting.....	34
8. Contingency at schematic design and model resolution.....	35
9. Recommended illuminance levels.....	37
10. Metrics for daylighting design.....	37
Section 2.4 Summary	42
CHAPTER 3 METHODOLOGY PART 1: SIMULATION MODEL.....	43
Section 3.1 Introduction.....	43
Section 3.2 Case study building	44
Section 3.3 Radiosity model	49
1. Room geometry.....	49
2. Effective visible reflectances of surfaces.....	52
3. Simulation time step and length of simulation	52
4. Modeling assumptions	52
5. Weather data.....	53
6. Solar geometry calculations	54
7. Window data	54
8. LightLouver visible light transmittance	55
9. Vision Control visible light transmittance and control strategy	56
Section 3.4 Daylighting metrics	57
Section 3.5 Model calibration.....	57
Section 3.6 Model verification for LEED v2.2.....	63
Section 3.7 Illuminance analysis grid resolution.....	65

CHAPTER 4 METHODOLOGY PART 2: BUILDING DESIGN PARAMETERS 69

Section 4.1 Base case: comparative analysis of the LightLouver and the Vision Control blind (existing location) 69

Section 4.2 Base building: extended daylighting study (effect of climate, building orientations, window properties) 71

Section 4.3 Effect of building depth on $sDA_{300/50}$ 79

Section 4.4 Window to wall ratio and window head height..... 82

Section 4.5 Design inquiry: maximum building depth for daylit open-plan building 91

CHAPTER 5 DISCUSSION AND CONCLUSIONS..... 95

Section 5.1 Further research needs 99

REFERENCES..... 101

APPENDICES 109

A1. Mathematical daylighting model..... 109

 A1.1. Daylighting model flowchart..... 109

 A1.2. Active blind control strategy flowchart 110

 A1.3. General building inputs..... 111

 A1.4. Solar geometry calculations..... 112

 A1.5. Room geometry 113

 A1.6. Sample view factor calculations 115

 A1.7. Sample configuration factor calculations 121

A2. Model calibration support data..... 124

 A2.1. RSF weather station irradiance data (sample)..... 124

 A2.2. Simulation analysis grid data for LEED v2.2 verification..... 125

 A2.3. Analysis grid resolution..... 128

A3. Supporting data for methodology part 2..... 130

 A3.1. Comparative analysis of the LightLouver and Vision Control blinds (existing location)
 130

A3.2. Base building: location, window properties, daylight redirecting blind, orientation	132
A3.3. Base building: from Golden to Montreal	132
A3.4. Base building: from Golden to Phoenix	134
A3.5. Base building: all locations, low VLT, daylight redirecting blind, $\psi = -45^\circ$ to 45°	136
A3.6. Changing window visible light transmittance (VLT) properties	138
A3.7. Configuration A: a taller daylighting window	140
A3.8. Configuration B: increase daylighting window head height to ceiling height	142
A3.9. Configuration C: increase daylighting window height and window width	144
A3.10. Configuration D: increase daylighting window WWR and WHH	146
A3.11. Configuration E: increasing WHH without changing WWR	148
A3.12. Configuration F: lower WHH on North façade	149
A3.13. All window to wall ratio and window head height configurations	151
A3.14. Design inquiry: maximum building depth for daylit open-plan area	155
A4. Tables of simulation results	159
A4.1. Base building, building depth 11 m	159
A4.2. Base building, building depth 12 m	159
A4.3. Base building, building depth 13 m	160
A4.4. Base building, building depth 14 m	160
A4.5. Base building, building depth 14.5 m	161
A4.6. Base building, building depth 15 m	161
A4.7. Base building, building depth 16 m	162
A4.8. Base building, building depth 17 m	162
A4.9. Base building, building depth 18 m	163
A4.10. Configuration A, building depth 18 m	163
A4.11. Configuration B, building depth 18 m	164
A4.12. Configuration C, building depth 18 m	164
A4.13. Configuration D, building depth 18 m	165
A4.14. Configuration D, building depth 18.5 m	165
A4.15. Configuration E, building depth 10 m	166
A4.16. Configuration E, building depth 11 m	166
A4.17. Configuration E, building depth 12 m	167
A4.18. Configuration E, building depth 13 m	167
A4.19. Configuration E, building depth 14 m	168
A4.20. Configuration E, building depth 15 m	168

A4.21. Configuration E, building depth 16 m	169
A4.22. Configuration E, building depth 17 m	169
A4.23. Configuration E, building depth 18 m	170
A4.24. Configuration F, building depth 18 m	170

List of Figures

FIGURE 1.1: MEAN DAILY GLOBAL INSOLATION (ANNUAL) ON A SOUTH-FACING VERTICAL SURFACE
(NATURAL RESOURCES CANADA, 2014).2

FIGURE 1.2: SCHEMATIC OF AN ARCHETYPAL SOLAR NET-ZERO ENERGY BUILDING.5

FIGURE 2.1: SELECTED DAYLIGHT REDIRECTING BLINDS, LEFT TO RIGHT, TOP TO BOTTOM: CLEARSHADE,
SERRAGLAZE DAYLIGHT REDIRECTING FILM, OKASOLAR W, 3M DAYLIGHT REDIRECTING FILM,
CONTROLITE, DLS ECKLITE EVOLUTION, RETROLUXTHERM.18

FIGURE 2.2: LIGHTLOUVER (PHOTO: DENNIS SCHROEDER, NREL).19

FIGURE 2.3: VISION CONTROL WINDOW (PHOTO: QIAN PENG).20

FIGURE 2.4: MULTIFUNCTIONAL SOLAR FAÇADE.22

FIGURE 2.5: WINTER SUN SHADING STUDY FROM YIP AND CORY (2013).25

FIGURE 2.6: VIEW FACTOR BETWEEN TWO ARBITRARY SURFACES.33

FIGURE 3.1: MAIN ENTRANCE OF THE RSF (PHOTO: DENNIS SCHROEDER, NREL).44

FIGURE 3.2: GENERAL FLOOR PLANS OF PHASE I OF THE RSF (DRAWINGS COURTESY OF RNL DESIGN).45

FIGURE 3.3: ENERGY USE BREAKDOWN OF THE RSF.46

FIGURE 3.4: SCHEMATIC CROSS-SECTION SHOWING WINDOW DESIGN FOR DAYLIGHTING SYSTEM.48

FIGURE 3.5: SIMPLIFIED FLOWCHART OF A) DAYLIGHTING MODEL, B) ACTIVE BLIND CONTROL STRATEGY.49

FIGURE 3.6: KEY PLAN OF RSF SHOWING LOCATION OF REPRESENTATIVE CROSS-SECTION.50

FIGURE 3.7: REPRESENTATIVE CROSS-SECTION UNFOLDED, ITS SURFACES LABELED, AND DIMENSIONED. ..51

FIGURE 3.8: VISIBLE LIGHT TRANSMITTANCE OF LIGHTLOUVER AND VISION CONTROL BLINDS.56

FIGURE 3.9: SIMULATED (S) AND MEASURED (M) ILLUMINANCE VALUES FOR MODEL CALIBRATION.59

FIGURE 3.10: MAKESHIFT SUNSHADE INSTALLED AT A WORKSTATION.62

FIGURE 3.11: ECOTECT SUN SHADING ANALYSIS OF THE RSF FOR 14:00 ON 16 JANUARY.62

FIGURE 3.12: ECOTECT SUN SHADING ANALYSIS OF THE RSF FOR 14:00 ON 16 JANUARY; CLOSER VIEW
SHOWING SELF-SHADING.63

FIGURE 3.13: ANALYSIS GRID ILLUMINANCE; 12:00, 22 SEPTEMBER; $\Psi=0$; LIGHTLOUVER (TOP) AND VISION
CONTROL (MIDDLE); ILLUMINANCE X-Y PLOT (BOTTOM) [LX].65

FIGURE 3.14: COMPARISON OF ILLUMINANCE ANALYSIS GRIDS: GOLDEN, LIGHTLOUVER, $\Psi = 0$; DA_{300}
CONTOUR PLOT (1.0 M X 1.0 M GRID AT TOP, 0.5 M X 0.5 M GRID IN MIDDLE) AND DA_{300} X-Y PLOT
(BOTTOM) [%].67

FIGURE 4.1: BASE CASE: GOLDEN, LIGHTLOUVER AND VISION CONTROL BLINDS, $\Psi = 0$; DA_{300} CONTOUR
(TOP, MIDDLE) AND X-Y (BOTTOM) PLOTS [%].71

FIGURE 4.2: BASE BLDG.: ALL LOCATIONS, LOW VLT, LIGHTLOUVER, $\Psi = 0$; DA_{300} CONTOUR (TOP, MIDDLE)
AND X-Y (BOTTOM) PLOTS [%].74

FIGURE 4.3: VISIBLE LIGHT TRANSMITTANCE OF RSF SOUTH DAYLIGHTING WINDOW.....	76
FIGURE 4.4: BASE BLDG.: GOLDEN, LOW AND HIGH VLT, LIGHTLOUVER, $\Psi = 0$; DA ₃₀₀ CONTOUR (TOP, MIDDLE) AND X-Y (BOTTOM) PLOTS [%].....	78
FIGURE 4.5: DIFFERENT BUILDING DEPTHS: GOLDEN, LOW VLT, LIGHTLOUVER, $\Psi = 0$; DA ₃₀₀ CONTOUR PLOTS [%].....	81
FIGURE 4.6: DIFFERENT BUILDING DEPTHS: GOLDEN, LOW VLT, LIGHTLOUVER, $\Psi = 0$; DA ₃₀₀ X-Y PLOT [%]..	82
FIGURE 4.7: SCHEMATIC INTERIOR ELEVATIONS SHOWING FENESTRATION CONFIGURATIONS; DASHED LINE REPRESENTS HEIGHT OF WORKPLANE.....	84
FIGURE 4.8: REPRESENTATIVE CROSS-SECTION UNFOLDED, ITS SURFACES LABELED, AND DIMENSIONED...	85
FIGURE 4.9: BASE CASE AND CONFIGURATION D, GOLDEN, LOW VLT, LIGHTLOUVER, $\Psi = 0$; DA ₃₀₀ CONTOUR (TOP, MIDDLE) AND X-Y (BOTTOM) PLOTS [%].	88
FIGURE 4.10: FENESTRATION CONFIGURATION COMPARISON: GOLDEN, LOW VLT, LIGHTLOUVER, $\Psi = 0$; DA ₃₀₀ CONTOUR (TOP, MIDDLE) AND X-Y (BOTTOM) PLOTS [%].	90
FIGURE 4.11: BASE BLDG. MAXIMUM BUILDING DEPTH FOR NOMINALLY ACCEPTABLE DAYLIGHTING ILLUMINANCE: ALL LOCATIONS, LIGHTLOUVER, $\Psi = 0$; DA ₃₀₀ CONTOUR (TOP, MIDDLE) AND X-Y (BOTTOM) PLOTS [%].	93
FIGURE 4.12: CONFIGURATION E MAXIMUM BUILDING DEPTH FOR NOMINALLY ACCEPTABLE DAYLIGHTING ILLUMINANCE: ALL LOCATIONS, LIGHTLOUVER, $\Psi = 0$; DA ₃₀₀ CONTOUR (TOP, MIDDLE) AND X-Y (BOTTOM) PLOTS [%].	94
FIGURE 5.1: COMPARISON OF THE BASE CASE WITH VISION CONTROL BLINDS ON BOTH DAYLIGHTING AND VIEW WINDOWS: GOLDEN, LIGHTLOUVER AND VISION CONTROL BLINDS, $\Psi = 0$; DA ₃₀₀ CONTOUR (TOP, MIDDLE) AND X-Y (BOTTOM) PLOTS [%].....	100
FIGURE A0.1: ANALYSIS GRID ILLUMINANCE; 12:00, 22 SEPTEMBER; $\Psi = -15^\circ$; LIGHTLOUVER (TOP) AND VISION CONTROL (MIDDLE); ILLUMINANCE PROFILE OF LIGHTLOUVER AND VISION CONTROL ALONG CENTRELINE OF CROSS-SECTION (BOTTOM) [LX].....	126
FIGURE A0.2: ANALYSIS GRID ILLUMINANCE; 12:00, 22 SEPTEMBER; $\Psi = 0$; LIGHTLOUVER (TOP) AND VISION CONTROL (MIDDLE); ILLUMINANCE PROFILE OF LIGHTLOUVER AND VISION CONTROL ALONG CENTRELINE OF CROSS-SECTION (BOTTOM) [LX].....	127
FIGURE A0.3: COMPARISON OF ILLUMINANCE ANALYSIS GRIDS: GOLDEN, LIGHTLOUVER BLIND, $\Psi = -15^\circ$; DA ₃₀₀ CONTOUR PLOT (1.0 M X 1.0 M GRID AT TOP, 0.5 M X 0.5 M GRID IN MIDDLE) AND DA ₃₀₀ X-Y PLOT (BOTTOM) [%].	128
FIGURE A0.4: COMPARISON OF ILLUMINANCE ANALYSIS GRIDS: GOLDEN, LIGHTLOUVER BLIND, $\Psi = 0$; DA ₃₀₀ CONTOUR PLOT (1.0 M X 1.0 M GRID AT TOP, 0.5 M X 0.5 M GRID IN MIDDLE) AND DA ₃₀₀ X-Y PLOT (BOTTOM) [%].	129

FIGURE A0.5: COMPARISON OF ILLUMINANCE ANALYSIS GRIDS: GOLDEN, VISION CONTROL BLIND, $\Psi = -15^\circ$;
 DA_{300} CONTOUR PLOT (1.0 M X 1.0 M GRID AT TOP, 0.5 M X 0.5 M GRID IN MIDDLE) AND DA_{300} X-Y
PLOT (BOTTOM) [%].....129

FIGURE A0.6: COMPARISON OF ILLUMINANCE ANALYSIS GRIDS: GOLDEN, VISION CONTROL BLIND, $\Psi = 0$;
 DA_{300} CONTOUR PLOT (1.0 M X 1.0 M GRID AT TOP, 0.5 M X 0.5 M GRID IN MIDDLE) AND DA_{300} X-Y
PLOT (BOTTOM) [%].....130

FIGURE A0.7: BASE CASE: GOLDEN, LIGHTLOUVER AND VISION CONTROL BLINDS, $\Psi = -15^\circ$; DA_{300} CONTOUR
(TOP, MIDDLE) AND X-Y (BOTTOM) PLOTS [%].....131

FIGURE A0.8: BASE CASE: GOLDEN, LIGHTLOUVER AND VISION CONTROL BLINDS, $\Psi = 0$; DA_{300} CONTOUR
(TOP, MIDDLE) AND X-Y (BOTTOM) PLOTS [%].....131

FIGURE A0.9: BASE BLDG.: GOLDEN AND MONTREAL, LIGHTLOUVER BLIND, $\Psi = -15^\circ$; DA_{300} CONTOUR (TOP,
MIDDLE) AND X-Y (BOTTOM) PLOTS [%].133

FIGURE A0.10: BASE BLDG.: GOLDEN AND MONTREAL, LIGHTLOUVER BLIND, $\Psi = 0$; DA_{300} CONTOUR (TOP,
MIDDLE) AND X-Y (BOTTOM) PLOTS [%].134

FIGURE A0.11: BASE BLDG.: GOLDEN AND PHOENIX, LIGHTLOUVER BLIND, $\Psi = -15^\circ$; DA_{300} CONTOUR (TOP,
MIDDLE) AND X-Y (BOTTOM) PLOTS [%].135

FIGURE A0.12: BASE BLDG.: GOLDEN AND PHOENIX, LIGHTLOUVER BLIND, $\Psi = 0$; DA_{300} CONTOUR (TOP,
MIDDLE) AND X-Y (BOTTOM) PLOTS [%].135

FIGURE A0.13: BASE BLDG.: GOLDEN, LOW VLT, LIGHTLOUVER BLIND, $\Psi = -45^\circ$ TO 45° ; DA_{300} CONTOUR
(TOP, MIDDLE) AND X-Y (BOTTOM) PLOTS [%].....137

FIGURE A0.14: BASE BLDG.: GOLDEN, LOW VLT, LIGHTLOUVER BLIND, $\Psi = -45^\circ$ TO 45° ; DA_{300} CONTOUR
(TOP, MIDDLE) AND X-Y (BOTTOM) PLOTS [%].....138

FIGURE A0.15: BASE BLDG.: GOLDEN, LOW AND HIGH VLT, LIGHTLOUVER BLIND, $\Psi = -15^\circ$; DA_{300} CONTOUR
(TOP, MIDDLE) AND X-Y (BOTTOM) PLOTS [%].....139

FIGURE A0.16: BASE BLDG.: GOLDEN, LOW AND HIGH VLT, LIGHTLOUVER BLIND, $\Psi = 0$; DA_{300} CONTOUR
(TOP, MIDDLE) AND X-Y (BOTTOM) PLOTS [%].....139

FIGURE A0.17: BASE BLDG. AND CONFIGURATION A, GOLDEN, LOW VLT, LIGHTLOUVER BLIND, $\Psi = -15^\circ$;
 DA_{300} CONTOUR (TOP, MIDDLE) AND X-Y (BOTTOM) PLOTS [%].....141

FIGURE A0.18: BASE BLDG. AND CONFIGURATION A, GOLDEN, LOW VLT, LIGHTLOUVER BLIND, $\Psi = 0$; DA_{300}
CONTOUR (TOP, MIDDLE) AND X-Y (BOTTOM) PLOTS [%].141

FIGURE A0.19: BASE BLDG. AND CONFIGURATION B, GOLDEN, LOW VLT, LIGHTLOUVER BLIND, $\Psi = -15^\circ$;
 DA_{300} CONTOUR (TOP, MIDDLE) AND X-Y (BOTTOM) PLOTS [%].....143

FIGURE A0.20: BASE BLDG. AND CONFIGURATION B, GOLDEN, LOW VLT, LIGHTLOUVER BLIND, $\Psi = 0$; DA_{300}
CONTOUR (TOP, MIDDLE) AND X-Y (BOTTOM) PLOTS [%].143

FIGURE A0.21: BASE BLDG. AND CONFIGURATION C, GOLDEN, LOW VLT, LIGHTLOUVER BLIND, $\Psi = -15^\circ$; DA ₃₀₀ CONTOUR (TOP, MIDDLE) AND X-Y (BOTTOM) PLOTS [%].	145
FIGURE A0.22: BASE BLDG. AND CONFIGURATION C, GOLDEN, LOW VLT, LIGHTLOUVER BLIND, $\Psi = 0$; DA ₃₀₀ CONTOUR (TOP, MIDDLE) AND X-Y (BOTTOM) PLOTS [%].	145
FIGURE A0.23: BASE BLDG. AND CONFIGURATION D, GOLDEN, LOW VLT, LIGHTLOUVER BLIND, $\Psi = -15^\circ$; DA ₃₀₀ CONTOUR (TOP, MIDDLE) AND X-Y (BOTTOM) PLOTS [%].	147
FIGURE A0.24: BASE BLDG. AND CONFIGURATION D, GOLDEN, LOW VLT, LIGHTLOUVER BLIND, $\Psi = 0$; DA ₃₀₀ CONTOUR (TOP, MIDDLE) AND X-Y (BOTTOM) PLOTS [%].	147
FIGURE A0.25: BASE BLDG. AND CONFIGURATION E, GOLDEN, LOW VLT, LIGHTLOUVER BLIND, $\Psi = -15^\circ$; DA ₃₀₀ CONTOUR (TOP, MIDDLE) AND X-Y (BOTTOM) PLOTS [%].	148
FIGURE A0.26: BASE BLDG. AND CONFIGURATION E, GOLDEN, LOW VLT, LIGHTLOUVER BLIND, $\Psi = 0$; DA ₃₀₀ CONTOUR (TOP, MIDDLE) AND X-Y (BOTTOM) PLOTS [%].	149
FIGURE A0.27: BASE BLDG. AND CONFIGURATION F, GOLDEN, LOW VLT, LIGHTLOUVER BLIND, $\Psi = -15^\circ$; DA ₃₀₀ CONTOUR (TOP, MIDDLE) AND X-Y (BOTTOM) PLOTS [%].	150
FIGURE A0.28: BASE BLDG. AND CONFIGURATION F, GOLDEN, LOW VLT, LIGHTLOUVER BLIND, $\Psi = 0$; DA ₃₀₀ CONTOUR (TOP, MIDDLE) AND X-Y (BOTTOM) PLOTS [%].	151
FIGURE A0.29: FENESTRATION CONFIGURATION COMPARISON: GOLDEN, LOW VLT, LIGHTLOUVER BLIND, Ψ $= -15^\circ$; DA ₃₀₀ CONTOUR (TOP, MIDDLE) AND X-Y (BOTTOM) PLOTS [%].	153
FIGURE A0.30: FENESTRATION CONFIGURATION COMPARISON: GOLDEN, LOW VLT, LIGHTLOUVER BLIND, Ψ $= 0$; DA ₃₀₀ CONTOUR (TOP, MIDDLE) AND X-Y (BOTTOM) PLOTS [%].	154
FIGURE A0.31: BASE BLDG. MAXIMUM BUILDING DEPTH FOR NOMINALLY ACCEPTABLE DAYLIGHTING ILLUMINANCE: ALL LOCATIONS, LIGHTLOUVER BLIND, $\Psi = 0$; DA ₃₀₀ CONTOUR (TOP, MIDDLE) AND X-Y (BOTTOM) PLOTS [%].	155
FIGURE A0.32: BASE BLDG. MAXIMUM BUILDING DEPTH FOR NOMINALLY ACCEPTABLE DAYLIGHTING ILLUMINANCE: ALL LOCATIONS, VISION CONTROL BLIND, $\Psi = 0$; DA ₃₀₀ CONTOUR (TOP, MIDDLE) AND X-Y (BOTTOM) PLOTS [%].	156
FIGURE A0.33: CONFIGURATION E: MAXIMUM BUILDING DEPTH FOR NOMINALLY ACCEPTABLE DAYLIGHTING ILLUMINANCE: ALL LOCATIONS, LIGHTLOUVER BLIND, $\Psi = 0$; DA ₃₀₀ CONTOUR (TOP, MIDDLE) AND X-Y (BOTTOM) PLOTS [%].	157
FIGURE A0.34: CONFIGURATION E: MAXIMUM BUILDING DEPTH FOR NOMINALLY ACCEPTABLE DAYLIGHTING ILLUMINANCE: ALL LOCATIONS, VISION CONTROL BLIND, $\Psi = 0$; DA ₃₀₀ CONTOUR (TOP, MIDDLE) AND X-Y (BOTTOM) PLOTS [%].	158

List of Tables

TABLE 1.1: OFFICE BUILDING ENERGY USE IN CANADA AND THE USA.	2
TABLE 1.2: TASKS RELATED TO DAYLIGHT DESIGN IN THE BUILDING DESIGN PROCESS.....	7
TABLE 2.1: SELECTED LIST OF CURRENTLY AVAILABLE DAYLIGHT REDIRECTING DEVICES.....	17
TABLE 3.1: DIMENSIONS OF THE REPRESENTATIVE CROSS-SECTION.	51
TABLE 3.2: EFFECTIVE VISIBLE REFLECTANCES OF SURFACES.	52
TABLE 3.3: WINDOW SPECIFICATIONS.	55
TABLE 3.4: WINDOW ASSIGNMENTS TO SURFACES IN THE SIMULATION MODEL.	55
TABLE 3.5: LIGHTLOUVER VISIBLE TRANSMITTANCE.	56
TABLE 3.6: MODEL CALIBRATION DATA AND RELATIVE ERROR.....	59
TABLE 3.7: MODEL CALIBRATION, CVRMSE AND NMBE.	59
TABLE 3.8: COMPARISON OF ILLUMINANCE ANALYSIS GRIDS: GOLDEN, LIGHTLOUVER AND VISION CONTROL BLIND, 1.0 M X 1.0 M AND 0.5 M X 0.5 M GRID, SDA _{300/50} [%].	67
TABLE 4.1: SIMULATION PARAMETERS: COMPARISON OF LIGHTLOUVER AND VISION CONTROL BLINDS.....	69
TABLE 4.2: BASE CASE: GOLDEN, LIGHTLOUVER AND VISION CONTROL BLIND, SDA _{300/50} [%].	70
TABLE 4.3: SIMULATION PARAMETERS – BASE BUILDING EXTENDED STUDY.	72
TABLE 4.4: ANNUAL NUMBER OF SUNSHINE HOURS BY LOCATION.....	73
TABLE 4.5: BASE BLDG. RESULTS BY LOCATION, LOW VLT, DAYLIGHT REDIRECTING BLIND, ORIENTATION; SDA _{300/50} [%].....	73
TABLE 4.6: AVERAGE ANNUAL INSOLATION ON A VERTICAL SOUTH FACADE [KWH/M ²].	76
TABLE 4.7: GOLDEN, LIGHTLOUVER AND VISION CONTROL BLINDS, WINDOW VLT COMPARISON; SDA _{300/50} [%].....	77
TABLE 4.8: GOLDEN; LIGHTLOUVER AND VISION CONTROL BLIND COMPARISON, SDA _{300/50} [%].....	78
TABLE 4.9: SUMMARY OF SIMULATION PARAMETERS – BUILDING DEPTH STUDY.	79
TABLE 4.10: BUILDING DEPTH: GOLDEN, LOW AND HIGH VLT, LIGHTLOUVER AND VISION CONTROL BLIND, ORIENTATION; SDA _{300/50} [%].	80
TABLE 4.11: WINDOW TO WALL RATIO AND WINDOW HEAD HEIGHT CONFIGURATIONS STUDIED.	83
TABLE 4.12: COMPARISON OF FENESTRATION CONFIGURATIONS FOR GOLDEN; SDA _{300/50} [%].	86
TABLE 4.13: CONFIGURATION D, GOLDEN, LOW AND HIGH VLT, LIGHTLOUVER AND VISION CONTROL BLIND, ORIENTATION; SDA _{300/50} [%].	87
TABLE 4.14: BASE BLDG. AND CONFIGURATION E, GOLDEN, LOW VLT, LIGHTLOUVER, ORIENTATION; SDA _{300/50} [%].....	88
TABLE 4.15: BASE BLDG. AND CONFIGURATION D: MAXIMUM BUILDING DEPTH AT WHICH DAYLIGHTING ILLUMINANCE IS NOMINALLY ACCEPTABLE (ALL Ψ ANGLES).	92

TABLE 4.16: BASE BUILDING AND CONFIGURATION E: MAXIMUM BUILDING DEPTH AT WHICH DAYLIGHTING ILLUMINANCE IS NOMINALLY ACCEPTABLE ($\Psi = 0$).....	92
TABLE 5.1: COMPARISON OF VISION CONTROL BLIND ON DAYLIGHTING AND VIEWING WINDOW WITH THE BASE CASE.	100
TABLE A0.1: EXCERPT FROM RSF WEATHER STATION IRRADIANCE DATA.	124
TABLE A0.2: ANALYSIS GRID ILLUMINANCE FOR LEED V2.2 IEQ8.1; 12:00, 22 SEPTEMBER; LIGHTLOUVER; $\Psi = -15^\circ$ [LX].....	125
TABLE A0.3: ANALYSIS GRID ILLUMINANCE FOR LEED V2.2 IEQ8.1; 12:00, 22 SEPTEMBER; LIGHTLOUVER; $\Psi = 0$ [LX].	126
TABLE A0.4: COMPARISON OF ILLUMINANCE ANALYSIS GRIDS: GOLDEN, LIGHTLOUVER AND VISION CONTROL BLIND, 1.0 M X 1.0 M AND 0.5 M X 0.5 M GRID, $SDA_{300/50}$ [%].....	128
TABLE A0.5: LIGHTLOUVER AND VISION CONTROL BLIND SPATIAL DAYLIGHT AUTONOMY, $SDA_{300/50}$ [%]. .	130
TABLE A0.6: BASE BLDG. RESULTS BY LOCATION, WINDOW PROPERTIES, DAYLIGHT REDIRECTING BLIND, ORIENTATION; $SDA_{300/50}$ [%].....	132
TABLE A0.7: BASE BLDG.: GOLDEN AND MONTREAL, LOW VLT, LIGHTLOUVER PERFORMANCE, $SDA_{300/50}$ [%].	133
TABLE A0.8: BASE BLDG.: GOLDEN AND PHOENIX, LOW VLT, LIGHTLOUVER PERFORMANCE, $SDA_{300/50}$ [%].	134
TABLE A0.9: BASE BLDG. RESULTS BY LOCATION, LOW VLT, DAYLIGHT REDIRECTING BLIND, ORIENTATION; $SDA_{300/50}$ [%].	136
TABLE A0.10: GOLDEN, LIGHTLOUVER AND VISION CONTROL, WINDOW VLT COMPARISON; $SDA_{300/50}$ [%].	138
TABLE A0.11: BASE BLDG. AND CONFIGURATION A, GOLDEN, LOW VLT, LIGHTLOUVER, ORIENTATION; $SDA_{300/50}$ [%].	140
TABLE A0.12: BASE BLDG. AND CONFIGURATION B, GOLDEN, LOW VLT, LIGHTLOUVER, ORIENTATION; $SDA_{300/50}$ [%].	142
TABLE A0.13: BASE BLDG. AND CONFIGURATION C, GOLDEN, LOW VLT, LIGHTLOUVER, ORIENTATION; $SDA_{300/50}$ [%].	144
TABLE A0.14: BASE BUILDING AND CONFIGURATION D, GOLDEN, LOW AND HIGH VLT, LIGHTLOUVER AND VISION CONTROL BLIND, ORIENTATION; $SDA_{300/50}$ [%].	146
TABLE A0.15: BASE BLDG. AND CONFIGURATION E, GOLDEN, LOW VLT, LIGHTLOUVER, ORIENTATION; $SDA_{300/50}$ [%].	148
TABLE A0.16: BASE BLDG. AND CONFIGURATION F, GOLDEN, LOW VLT, LIGHTLOUVER, ORIENTATION; $SDA_{300/50}$ [%].	150
TABLE A0.17: COMPARISON OF FENESTRATION CONFIGURATIONS FOR GOLDEN; $SDA_{300/50}$ [%].	152

Nomenclature

Abbreviations, acronyms, and initialisms

AIA	American Institute of Architects
BRDF	Bidirectional reflectance distribution function
BSDF	Bidirectional scattering distribution function
BTDF	Bidirectional transmittance distribution function
CDA	Continuous daylight autonomy
CFS	Complex fenestration system
CVRMSE	Coefficient of variation of the root mean squared error
CWEC	Canadian Weather for Energy Calculations weather file
DA	Daylight autonomy
DGP	Daylight glare probability
EPW	EnergyPlus Weather file
ID, IDP	Integrative design, integrated design process
IES, IESNA	Illuminating Engineering Society of North America
IGU	Insulated glazing unit
LEED	Leadership in Energy and Environmental Design
LL	LightLouver blind
NMBE	Normalized mean bias error
NOAA	National Oceanic and Atmospheric Administration

NRCAN	Natural Resources Canada
NREL	National Renewable Energy Laboratory
NZEB	Net-zero Energy Building
RAIC	Royal Architectural Institute of Canada
RER	Relative error
RET	Renewable energy technology
RFP	Request for proposals
RSF	Research support facility of NREL
sDA	Spatial daylight autonomy
SHGC	Solar heat gain coefficient
TMY3	Typical Meteorological Year weather file (version 3)
UDI	Useful daylight illuminance
VC	Vision Control window/blind
VLT	Visible light transmittance
WHH	Window head height
WWR	Window to wall ratio

Greek letters

α	Altitude angle
θ	Incidence angle
ρ	Reflectance

ψ Building/surface orientation angle with respect to due South

τ Transmittance

Variables

A_i Area of surface i

$BayMiddle_{dep}$ Depth of middle bay in room

$BayNorth_{dep}$ Depth of North bay in room

$BaySouth_{dep}$ Depth of South bay in room

$BlankNorth_{ht}$ Height of blank wall between windows on North façade

C_{ai} Configuration factor between surface i and point a

DA_{300} Daylight autonomy with threshold illuminance value of 300 lx

$DayWinNorth_{ht}$ Height of daylighting window on North façade

$DayWinSouth_{ht}$ Height of daylighting window on South façade

D_{rm} Depth of room

E_a Illuminance at point a

E_{bn} Beam normal illuminance

E_{dh} Diffuse horizontal illuminance

E_{ds} Total diffuse illuminance

F_{ij} View factor from surface i to j

H_{rm} Height of room

I_{bn} Beam normal irradiance

I_{dh}	Diffuse horizontal irradiance
I_{ds}	Total diffuse irradiance
M	Luminous exitance in matrix form
M_{oi}	Initial luminous exitance of surface i
M_i	Luminous exitance of surface i
$OpaqueNorth_{wd}$	Opaque width of wall on either side of North façade windows
$OpaqueSouth_{wd}$	Opaque width of wall on either side of South façade windows
sDA _{300/50}	Spatial daylight autonomy with threshold illuminance of 300 lx; and period of time that this illuminance value is met or exceeded of 50 %
$ViewWinNorth_{ht}$	View window height on North façade
$ViewWinSouth_{ht}$	View window height on South façade
WHH_n	Window head height, North façade
WHH_s	Window head height, South façade
$WinNorth_{wd}$	Width of window on North façade
$WinSouth_{wd}$	Width of window on South façade
W_{rm}	Width of room
WWR_{ds}	Daylighting window to wall ratio, South façade
WWR_n	Overall window to wall ratio, North façade
WWR_s	Overall window to wall ratio, South façade
WWR_{vs}	View window to wall ratio, South façade

Chapter 1 Introduction

Section 1.1 Daylighting renaissance

Daylighting has recently been the subject of renewed interest in the building design community, both in research and practice. It is proposed as a solution to the problem of increasing energy use in the building sector and concern over indoor environmental quality in workplaces and homes. Although daylighting has always been an integral part of buildings, with written daylighting guidelines dating back to Roman architect Vitruvius, it gradually lost favour with building designers and owners in the last century due to relatively inexpensive electricity and the increased use of electric lighting. Lost were the historical building design responses to solar conditions that resulted in distinctive regional architectural vocabularies recognizing the power of natural forces to shape our built environment. However, the current emphasis on energy and environmental design, combined with the accessibility of computing power and new software tools has given new life to this old design element and a new way to harness its power.

Energy use is an important consideration in how a country sustains its socioeconomic development while managing its finite and renewable resources and stewardship of the environment for future generations. In Canada, the building sector is responsible for approximately 30 % of total energy usage¹, according to the most recently published data from NRCAN (2011b). This includes the large sub-sectors of design, construction, operation, and demolition. Similarly, in the United States, residential and commercial buildings accounted for approximately 40 % of total energy usage, based on 2013 figures from the US Energy Information Administration (2013).

¹ NRCAN uses the term secondary energy to describe all end user energy consumption for agriculture, commercial, industrial, residential, and transportation use. The estimate is based on direct energy usage in the residential and commercial/institutional sectors and the industrial (construction subsector).

Within the commercial/institutional sector, the data show that electric lighting is a significant portion of energy use. This energy demand can be reduced with more emphasis on exploiting the freely available energy of the sun for daylighting purposes. In Canada, the portion of energy use for electric lighting in office buildings 45.4 PJ out of a total of 386.2 PJ (Natural Resources Canada 2011a). This represents 12 % of all office space energy use. In the USA, the portion of energy use for electric lighting in office buildings is 295.2 PJ out of a total of 759.6 PJ for all office energy use. This represents 39 % of all office energy use. (U.S. Department of Energy, 2003). The totals for lighting energy use in offices are summarized in Table 1.1.

Table 1.1: Office building energy use in Canada and the USA.

	Lighting Energy Use – Offices (PJ)	Total Energy Use – Offices (PJ)	% Lighting Energy Use – Offices (%)
Canada (2011 data)	45.4	386.2	12 %
USA (2003 data)	295.2	759.6	39 %

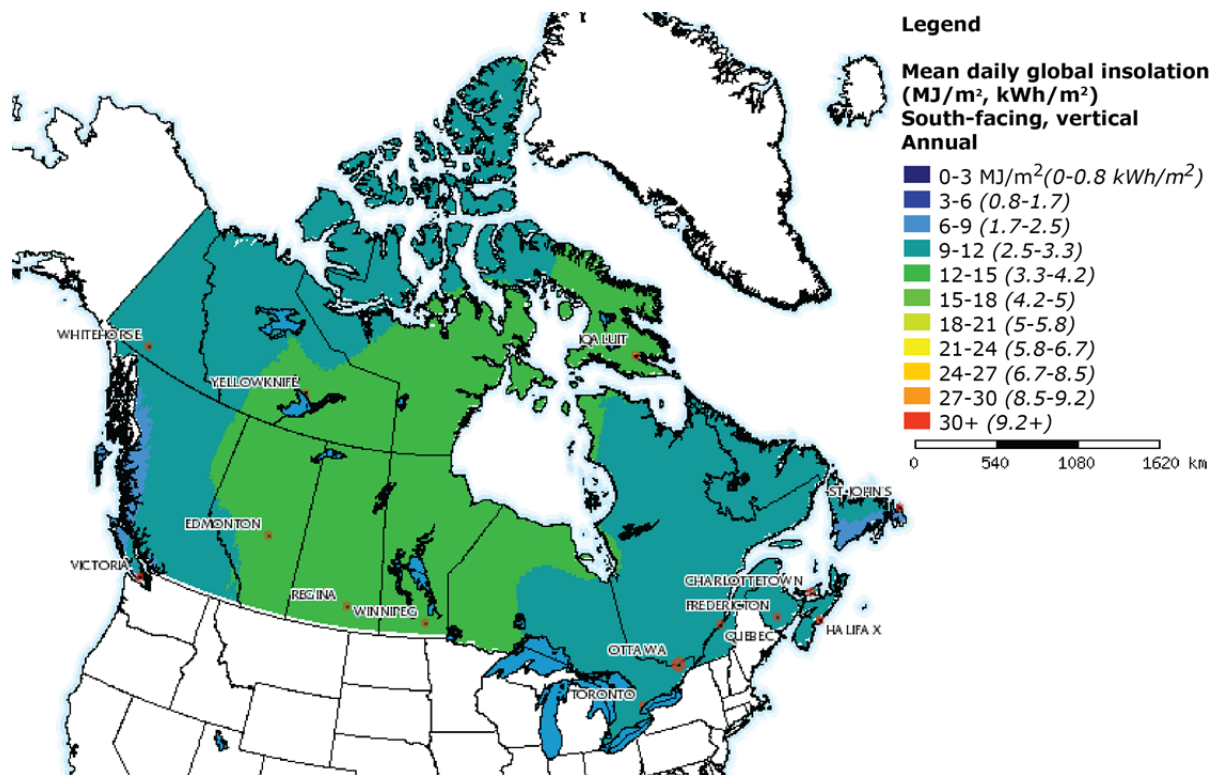


Figure 1.1: Mean daily global insolation (annual) on a South-facing vertical surface (Natural Resources Canada, 2014).

A strong case can be made that lighting energy use can realistically be reduced by using more daylighting, especially considering that sunlight is an abundant renewable energy source. Figure 1.1 shows that most of Canada receives a mean daily global insolation of at least 2.5 – 3.3 kWh/m² for vertical South-facing surfaces, which promotes daylighting use in buildings.

Section 1.2 Importance of daylighting

Beyond the aesthetic appeal that it can lend to buildings, daylighting can offer many benefits from the point of view of energy savings to human health and performance. In terms of reduced energy consumption, simulation studies have shown that office buildings using daylighting with controls like blinds and electric light switching can save from 13 % to over 40 % of total electricity consumption (Li et al., 2002, Bourgeois et al., 2006) and field measurements have shown up to 50 % energy savings in electric lighting for perimeter offices (Li and Lam, 2001). Daylighting can even contribute to reducing HVAC system sizes and peak building power load (Li et al., 2005).

From the perspective of the building occupant, many studies suggest correlations between daylighting and positive effects on occupant behaviour. Heschong conducted a series of studies to examine the daylighting effects on human performance across a range of building occupancies. It was found that for a chain-store retailer with over 100 outlets that are nearly identical in layout and operation, a 40 % increase in sales could be attributed to the use of skylights for daylighting (Heschong Mahone Group, 1999). Similarly, students in classrooms that had large windows and skylights saw an improvement in test scores from 7 to 26 %, while office workers showed a 13 % improvement in mental function and attention when the daylight contribution to illuminance levels were increased from 1 to 20 fc (Heschong, 2002, Heschong Mahone Group, 2003).

Windows and skylights play the important role of admitting daylight into a building. But they also provide a connection to the outside living environment through views and the operability of the units. Research has suggested that there is a human psychological desire to be near windows for the views they provide and the contact with nature, which can affect health, mood and motivation (Menzies and Wherrett, 2005, Ulrich, 1984, Leslie,

2003, Edwards and Torcellini, 2002). Additionally, occupants also respond positively to having the possibility to control their environment such as with operable windows and blinds (Menzies and Wherrett, 2005, Vine et al., 1998), but care must be taken avoid issues of glare (Hygge and Löftberg, 1999)

As the above shows, daylighting holds considerable significance for different aspects of buildings. This multi-faceted nature of daylighting is affirmed in survey data where design professionals offered different definitions of daylighting: as an element that permits the interplay of light and building form to provide stimulating and healthful indoor environments; as a partial replacement for electric lighting that helps promote electric lighting savings; as a resource to reduce building energy consumption, among others (Reinhart et al., 2006). Due to this nature, it is a necessity to understand the preoccupations of each group in order to address them with pertinent design solutions. And because daylighting means different things to architects, lighting engineers, and mechanical engineers, all parties need to pool their tools and knowledge to make the complete decision on daylighting. *Because of this, this thesis identifies a need to develop design guidance aimed at supporting architectural design using techniques that are common to engineering.*

This focus on daylighting as an important design element can be situated within the larger framework of a realistic solution to reducing the energy consumption of buildings: the net-zero energy building (NZEB), a building that over the course of a year consumes as much energy from the grid as it generates to the grid (Marszal et al., 2011). In a NZEB, the integration of energy efficiency measures and renewable energy technologies can contribute to lower overall energy use and increased occupant comfort. A schematic of an archetypal solar net-zero energy building is shown in Figure 1.2. In particular, solar NZEBs can harness the sun's energy to provide daylight (thus decreasing electric lighting energy and associated cooling load), solar radiation for thermal applications, and to generate electricity (Athienitis et al., 2015). For the daylighting component of a NZEB, the daylight redirecting blind is a key solution. But in order to ensure beneficial integration of these elements in a project, the appropriate tools at the appropriate time in the design process are necessary. This starts early with the need to assess advanced daylighting strategies at the beginning of the schematic design phase.

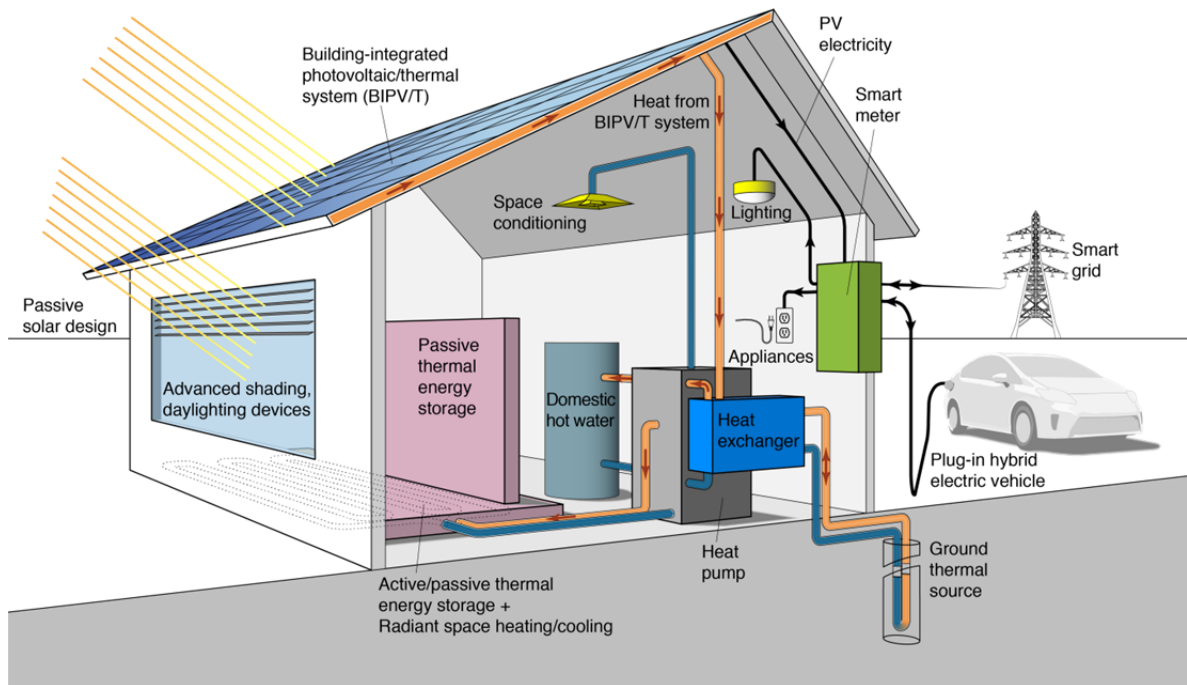


Figure 1.2: Schematic of an archetypal solar net-zero energy building.

Section 1.3 The role of design process

The conventional design process for a building project is based on a linear scheme whereby general, conceptual ideas are detailed and refined over time into a final building design. A series of phases is defined with a set of specific tasks and deliverables required for each. Each phase builds upon the previous one generally without the opportunity to change previous decisions.

A building project usually starts with a pre-design phase which is predominantly an information gathering and analysis period. The functional and technical program along with space relationships is defined, and building site conditions are analyzed. After that, schematic design is usually when the design team starts the building design process. Generally, it is during this phase when the most crucial decisions about the building design are made. Decisions about form (geometry, envelope, orientation) and daylighting are made which can have great consequences on all aspects of the future building, and the well-being, comfort and productivity of its occupants (O'Brien et al., 2015).

The ideal relationships between advanced daylighting design elements (like in a NZEB) and where they are situated in a design timeline to maximize the chances of successful integration are described in Table 1.2. It shows that climate and building orientation through daylighting design are considered as early as possible in a design due to their effects on building geometry (façade, clear heights, and space planning), electric lighting, and HVAC design. Any daylighting strategy must be contemplated right at the beginning of schematic design in order to share timely design information with the connected disciplines and to receive timely feedback from them as well.

Unfortunately, in a conventional design process, the process is highly fragmented, usually characterized by parallel processes whereby each design professional works independently on their portion of the project with little interaction with the other professionals and only meet occasionally to exchange information (AIA 2008, RAIC 2009). It can hinder the integration of design ideas across the disciplines. For example, the electrical lighting systems may be optimized for electrical considerations without any regard to the daylighting design. Windows and blinds are usually specified by the architect but it is the mechanical engineer who is responsible for the energy considerations. At worst, it leads to inappropriate design choices for the most crucial parts of a building that are difficult to change or overcome later on. This is a barrier to design innovation like incorporating advanced daylighting technologies in high-performance buildings such as NZEBs where building systems are complex and collaboration is necessary to ensure anticipated performance.

Building design teams have started using the Integrated Design Process (IDP) (Löhnert et al., 2003, AIA 2008) or Integrative Design (ID) (ANSI 2012) as a way to address these inadequacies of the conventional process, and encourage collaboration and the integration of design ideas across the disciplines in a non-linear process. IDP shifts the phasing of a project to put more emphasis and weight on design at the start of a project and it allows more time for feedback loops to improve design. This results in more opportunities at the beginning of the project to test different ideas and receive feedback.

Table 1.2: Tasks related to daylight design in the building design process.

Pre-design	Schematic Design	Design Development	Construction Documents
General schedule of design activities relevant to daylighting			
Functional and technical programming (including daylit or non-daylit spaces)	Review of alternative Design Approaches	Design coordination	Project coordination
Space Relationships / Flow diagrams (including daylit or non-daylit spaces)	Special studies (e.g. for high performance building, NZEB, etc.)	Project design development	Construction Documents (Working drawings, specifications)
Site selection / Analysis utilization (including building orientation and volumetric studies)	Architectural concept / schematic design (including daylighting and lighting concept; including electrical and mechanical design concept)	Design development drawings and specifications	Construction cost estimation (detailed)
Environmental Studies (including climate analysis)	Schematic design drawings and specifications	Construction cost estimation (some details)	Interiors Construction documents
Energy Studies	Interior design concept(s)	Interior design development	Special bid documents
Special studies (e.g. for high performance building, NZEB, etc.)	Construction cost estimation (preliminary)	Special Studies (e.g. for high performance building, NZEB, etc.)	
Project Budgeting and Economic feasibility studies	Program and Budget Evaluation		
Specific daylighting design tasks			
Program and space relationships will determine which spaces require / accept /tolerate daylight and which ones cannot use daylight	Initial daylighting and solar shading concept based on pre-design studies of program/space relationships and climate and site analysis	Design refinements to daylighting and solar control design; introduce electric lighting design; surface finishes; glare control;	Performance and product specifications for all daylighting and lighting design.
Climate analysis to determine annual sun characteristics (sunny, cloudy, partly cloudy) for daylighting and solar heat shading	General parameters include net floor area; window to wall ratio; floor height; window visible light transmittance; illuminance levels and lighting power densities; passive or active strategies	Detailed coordination of daylighting / solar shading with electric lighting and HVAC control strategies	
Site analysis to determine solar availability (obstructions, orientations, photovoltaic and solar thermal potential)	Once initial daylighting concept(s) have been decided, use simulation or other detailed tools to evaluate effectiveness.	Detailed daylighting and energy simulations to fine-tune all design parameters	
	Begin coordination of daylighting / solar shading with dimmable electric lighting and (lighting and HVAC controls)		

However, not every project will use an IDP. And even the ones that do will still face the fact that at the start of schematic design, building designers need tools to be simple enough to use to support design decisions with few inputs and accurate enough output to guide them in the right general direction before developing their ideas with more complex tools that require more inputs.

Regardless of the design process selected, it is imperative that the building *design team be equipped with very simple, quickly-applied, and appropriately accurate tools to be able to keep up with the rapid pace of the early schematic design phase.*

Section 1.4 Motivation and goals

There are now numerous daylight redirecting blinds on the market that aim to address the issue of energy savings, along with daylighting performance and occupant comfort.

Because they rely on many parameters such as complex geometry and may require automated controls to achieve their high illuminance performance, their angle-dependent optical characteristics cannot be represented or simulated accurately using the simple tools that are normally used at the beginning of schematic design when rapid assessments of design possibilities are needed.

It often requires complex experiments or calculations to characterize the optical properties of the blinds (Andersen and de Boer, 2006). Even though recent research has progressed with newer methods to characterize such blinds and has distilled this information into a proposed extensive markup language (XML) file format standard (McNeil et al., 2013), there are few daylight simulation software programs capable of reading this information as input in order to assess the blinds' illuminance performance in a building situation.

Another hurdle is the requirement to evaluate daylighting performance at short time steps for an entire year to properly aggregate this performance information over time-varying solar conditions at any building location.

Presently, a promising workflow to obtain annual climate-based daylight illuminance performance simulations of interior spaces with daylight redirecting blinds is centered on the Radiance lighting software (Larson and Shakespeare, 1998). The daylight redirecting blind optical characteristics are obtained (e.g. from product manufacturers) or generated in the abovementioned XML format. If the blind is separate from the window, an extra step is required to add the window optical information in the WINDOW 6/7 software (Mitchell et al., 2008) before the ensemble is input into Radiance to execute the daylighting simulations for an interior space using the Radiance three-phase or five-phase method (Ward et al., 2011, McNeil, 2013). This level of complexity is too demanding for inclusion at the

beginning of schematic design, especially since Radiance requires an entire set of building inputs – including all 3d geometry – many elements of which are not yet known.

From a design point of view, the first 3d models in any building design process are exploratory, subject to frequent modification, and are normally made using architectural design software. They are often incomplete, focusing on just one aspect of a building design such as massing or façade design. Radiance, like other daylight simulation software, is not fully interoperable with 3d architectural design software. A 3d architectural model needs to be specially prepared and exported in a Radiance-compatible format before it can be evaluated for daylighting (Petinelli and Reinhart, 2006). Radiance is not design software: it can analyze the daylighting of the 3d model, but it cannot edit the 3d geometry. Therefore, geometry changes need to be made to the 3d architectural model in its native software program, and then exported again to Radiance for daylight re-evaluation. The entire process for geometry-related input is resource-intensive and the Radiance software is computationally demanding, requiring hours or even days to complete the annual parametric-type simulations useful at schematic design (Zuo et al., 2014). Even a single iteration of this *model first, then simulate* workflow can be a costly proposition. At the speed at which design options are explored and evaluated at schematic design, this does not integrate well with most building design workflows (Horvat and Wall, 2012). There needs to be a fast and simple way to compare the performance of these daylight redirecting products and integrate them into the design process at the beginning of the schematic design phase with some level of certainty that they will contribute to good daylighting design before committing resources on further design exploration.

Furthermore, due to the typical way professional fees are broken down within a design contract based on the amount of effort and resources expended in each design phase, schematic design usually represents 12 – 18 % of the total fees allotted to a project (RAIC 2009). This makes schematic design a relatively short phase during which the most important design decisions about the building have to be made. As studies show, architects place a high importance on rules of thumb, simple calculations, and simple, easy to learn and use simulation software that supports them in decision making (Attia et al., 2012,

Galasiu and Reinhart, 2008). The short duration of schematic design has an influence on this.

Nor is it desirable to have a lot of detailed analyses or results at the beginning of schematic design. The details are illusory at best and a waste of time at worst since at such an early stage of design, design options can change very rapidly. (For example, typical design Charrettes² last one or two days. During this time, major decisions about all aspects of a building are explored and design directions are established). Whether in the form of design guidance or software, the tools that can support this process must be simple to use and provide fast, relatively accurate assessments.

Based on this analysis of building design workflows and the state of daylight simulation tools supporting daylight redirecting blinds, this thesis proposes a tool in the form of design guidance for good points of departure for possible design options. The design guidance will concentrate on the elements needed to start integrating daylight redirecting blinds into the design workflow. These are related to building site (climate, building orientation), building geometry (window to wall ratio; window head height; clear floor height; and building depth) and fenestration optical properties (visible light transmittance of windows and blinds). Following this design guidance, a process of iteration and feedback can escalate a design to the level where existing sophisticated simulation tools like Radiance can be introduced effectively to analyze the design and provide more accurate daylighting assessments leading to further design development or design changes.

To be able to create this design guidance, this thesis has a series of well-defined objectives.

² A Charrette in contemporary building design practice refers to either 1) a short collaborative session during which project stakeholders such as client, architect, and engineer work together to draft potential design solutions to a design problem; or 2) an intensive work session before a deadline. A good background reference for the first definition is *A Handbook for Planning and Conducting Charrettes for High-Performance Projects, 2nd Edition*, NREL: www.nrel.gov/docs/fy09osti/44051.pdf

Section 1.5 Thesis objectives

1. Create a simplified mathematical daylighting model, at an appropriate level of accuracy for early schematic design, which can be used to predict annual daylighting performance in an open-plan office space incorporating advanced passive and active daylight redirecting devices.
2. Compare the annual daylighting performance of a representative blind from each of the two classes (passive and active) through the use of a case study. The passive and active blinds selected are the LightLouver and the Vision Control blinds, respectively.
3. Examine the influence of different design parameters and locations on the annual daylighting performance of a daylight redirecting blind in an open-plan office space and identify the most important ones.
4. Derive a general relation that can be used as an early schematic design tool for incorporating daylight redirecting blinds, between the most important identified design parameters and the maximum building depth for a “nominally” daylit open-plan office space.

There are certain limitations to the scope of this thesis. While the simplified model must be able to perform integrated daylighting and thermal simulations, this thesis is only concerned with the daylighting aspect. Explicit energy considerations are addressed in a larger case study by Chen, Yip and Athienitis (2014b, 2014a).

Section 1.6 Thesis overview

Chapter 2 presents literature review with emphasis on sun shading devices, daylight redirecting blinds, the tools that exist to integrate them into simulation programs, and the metrics that will be used to develop a daylighting model and to evaluate daylighting performance.

Chapter 3 describes the thesis methodology that includes the development of the model and where it is situated with respect to the tools in the literature and its application to a case study building. It describes the reasoning behind the choices made and is supported

with evidence from the simulation model calibration process and comparison to existing metrics. The simulation model is verified to produce predictions for the intended resolution required for schematic design.

Chapter 4 presents the essential design parameters for the simulation study along with the results comparing the LightLouver and the Vision Control blinds grouped into three major themes: 1) the direct comparison of the Vision Control blind with the LightLouver in the existing building; 2) parametric studies based on location, orientation, window transmittance properties, and daylight redirecting blinds; and 3) parametric studies based on fenestration geometry and building depth.

Chapter 5 starts with a discussion of the most important findings from the simulations, draws conclusions illustrating their relevance in the early schematic design process; and offers suggestions for further research needs.

Chapter 2 Literature review

Section 2.1 Introduction

This literature review is divided into two main sections. The first one broadly groups together all the physical building elements that are involved when using daylight redirecting blinds to increase daylight illuminance in open-plan office spaces. It focuses on their important physical characteristics, functions, and their effects on a building's occupants. The second section concentrates on the building design processes needed to incorporate daylight redirecting blinds into a design project, including daylighting design tools and ways to evaluate the success of design options such as daylighting metrics.

Section 2.2 Building fenestration elements

1. Window properties

Windows are an important multi-functional component of the building envelope. They play a role in regulating the interactions between the outdoor and interior environments. Aside from their roles of protection, ventilation, and views, their most important role in concert with daylight redirecting blinds is sun control. Windows admit daylight and solar heat energy into a building interior. The characteristics of the glazing, the number of glazings, the gas contained within the glazings, and the coatings applied to the glazings have an effect on the transmittance of the window. This directly affects the visual and thermal comfort of the building occupants. Window glazing reacts differently to the different parts of the solar energy spectrum. The spectrum can be divided into three broad ranges based on wavelength.

- **UV light:** 300 – 380 nm, causes interior materials like fabric and finishes to fade. UV transmittance refers to the percentage of UV light transmitted.
- **Visible light:** 380 – 780 nm: the range that is visible to the human eye. The visible light transmittance (VLT) of an IGU needs to be very high to admit high levels of daylight into a space.

- **Infrared light:** 780 nm and above: This range can be further subdivided into near infrared (short-wave) light which is the heat energy that sunlight transmits into a building; and long-wave infrared which refers to wavelengths longer than those from the sun and is the heat that radiates from materials such as those in a building. The amount of radiation from the entire solar spectrum that is transmitted is referred to as solar transmittance.

However, there are other factors that can reduce the amount of VLT in a window. These are principally coatings that are applied to the glazing. There are electrochromic windows which change their sun control properties through a voltage-dependent coating, and thermochromic windows which change sunlight transmission properties based on dynamic solar radiation intensity. But, the most common are the low emissivity (low-e) coatings that are used to block the transmission of long-wave infrared radiation. They typically reduce the VLT of clear glass by approximately 10 %. (ASHRAE 2013).

The window glazing material is tuned for the different wavelengths for sunlight control to admit more or less daylight and solar heat depending on the building design intent and climate. For example, O'Connor, Lee et al. (1997) suggest using clearer glass combined with sun control for high windows for high daylight transmission and tinted glass below for glare control: *To optimize the performance of daylight redirecting blinds, they should be paired with windows with a very high visible light transmittance (over 65 %).*

2. Sun control devices: blinds, louvers, and daylight redirection

Sun control devices are considered essential in office buildings to assist windows in controlling the amount of daylight and solar gain within a workspace since tuning glazing properties and applying coatings are usually not enough to achieve this goal.

In addition to meeting the base requirements of the windows they are associated with (protection, aesthetics, cost, sun control), sun control devices must also be available in sizes and configurations that can accommodate the widest range of design possibilities, and must use installation methods and sequences that are common or easily integrated in usual

construction practice. Their main function is to provide visual and thermal comfort through sun control (Johnsen and Watkins, 2010, Carmody et al., 2004, Kuhn et al., 2000).

- **Visual comfort:** A sun control device must transmit a sufficient amount of daylight, in a uniform manner to provide even illumination while reducing glare from excessive sky luminance. It should allow views to the exterior and have good colour rendering of transmitted light. And it should provide an option for privacy or for blocking out all daylight into a space.
- **Thermal comfort:** Offer shading from direct sun when required such as during the summer, but allow high solar gains in the winter when the solar heat is useful.

The daylighting control for visual comfort and the solar heat control for thermal comfort may be provided by separate devices (Johnsen and Watkins, 2010). For daylight transmission, ordinary windows are usually sufficient to admit daylight into the building perimeter, but sun control devices can extend this performance in other cases such as supplying daylight to spaces further away from the window location; to spaces that have obstructed views of the sky; or to buildings in locations that are predominately cloudy or excessively sunny. The devices usually use reflective or refractive components to achieve this. Examples of this include anidolic systems and light pipes that collect daylight along the building envelope and transport it to spaces far from or without fenestration. (See, for example, Parans Solar Lighting, www.parans.com). Such devices only require small apertures; but usually do not provide a view.

The simplest sun control devices are fixed devices like light shelves and fins. The horizontal light shelves work best on equator-facing orientations where the sun's altitude angle is usually high. They provide shade and redirect daylight deeper into the interior space. Vertical elements like fins work best on East and West orientations when the sun is low in the sky. In all cases, the fixed devices cannot adjust to the seasonal changes in the sun's path.

Among the most common sun control devices that do allow for adjustments are roller shades, louvers, and blinds. Roller shades control the amount of sun that enters a space and

the views and privacy of the occupants through the weave and perforation design of the shade material but they do not redirect daylight to any advantageous use. Louvers and blinds can provide shade, reduce glare, and redirect daylight into the interior. They can be installed on the exterior part of the façade, within the glazing panes of windows, or on the interior. The advantage of exterior devices is more solar heat can be rejected. Fixed louvers, like light shelves, have the advantage of simplicity, requiring minimal maintenance. However, adjustable louvers can be more effective, offering a range of positions to adapt to changing sun angles.

3. Advanced sun control devices

With the renewed interest in daylighting, there are now advanced sun control devices that emphasize daylight redirection. Like conventional sun control devices, they are either passive or active, and can be installed on the exterior, interior, or within the glazings of windows. They all offer design features that increase the performance or versatility of these devices. Reflector spacing in blinds can be optimized to minimize the obstruction of view to the outside while maintaining daylighting performance. Or, reflectors can retract or change position dynamically to increase the amount of unobstructed view to the outside. To accommodate a larger range of use configurations, different profile depths and assemblies are offered. And window customization options like double- or triple-glazing can be offered if the reflector blinds are an integral part of a window assembly. See Table 2.1 for a summary of some current products on the market, with photos and images in Figure 2.1.

Passive daylight redirecting blinds

These devices rely on specially shaped profiles designed to redirect daylight from many different incidence angles upwards to the ceiling or further into the space above the line of sight of occupants. The profiles reflect back to the exterior any daylight at sun angles that would normally cause glare. They are simple to install and maintenance is minimal, but their performance depends on how well the blade profiles are matched with the local seasonal sun conditions to redirect or reject the sun. The 3M Daylight Redirecting Film and SerraGlaze Daylight Redirecting Film use this same concept except that their daylight

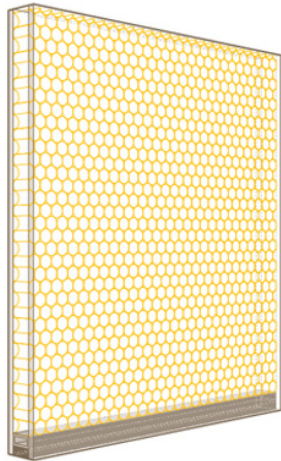
redirecting “blades” consist of a micro-sized prismatic structure or micro-sized blades that are thin enough to apply as a film on the interior side of any conventional window.

Active daylight redirecting blinds

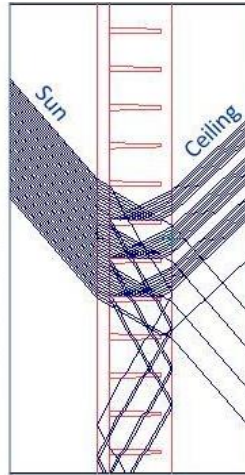
Active daylight redirecting blinds track sky conditions to optimize the amount of daylight that is redirected or rejected from the interior. When connected to a building’s control system and used in conjunction with electric lighting controls, they permit energy savings by dimming or turning off electric lighting when sufficient daylight is available, reducing the cooling load from the electric lights as well. (Lee et al., 1998, Tzempelikos and Athienitis, 2007).

Table 2.1: Selected list of currently available daylight redirecting devices.

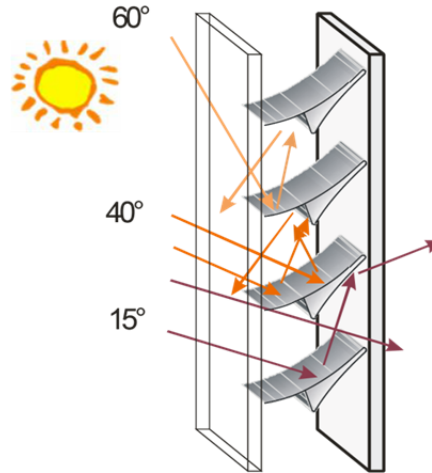
Product / Company	Louvers: f=fixed; r=rotate; u=up / down	Facade (vertical) / roof (horizontal) application	Louver control: auto; manual	1 or 2 sections	Different louver depths and profiles	Blind location: e=exterior side; i=indoor side; b=between glazing; 2x=double glazing; 3x=triple glazing	Minimize obstruction to view
		v=vert.; h=hor.					
LightLouver / LightLouver LLC	f	v	n. a.	1	no	i	no
Vision Control / Unicel Architectural	r	v, h	auto	1	yes	b 2x	yes, rotatable flat blades
Clearshade IGU / Panelite	f	v	n. a.	1	no	b, 2x, 3x	three levels of view transparency
Controlite / Danpalon	r	v, h	auto	1	no	b 2x	yes
Daylight Redirecting Film / 3M	f	v	n. a.	1	no	i	translucent
DLS Ecklite Evolution / Glassolutions	r, u	v	auto / man	2	yes	b 2x, 3x	yes, can fully open
DLS Ecklite SC / Glassolutions	r, u	v	auto / man	1	no	b 2x, 3x	yes, can fully open
Okasolar F / Okalux	f	v	n. a.	1, 2	yes	b 2x, 3x	blade spacing permits view
Okasolar S / Okalux	f	h	n. a.	1	no	b 2x	Partial vision
Okasolar W / Okalux	f	v	n. a.			b 2x, 3x	Blade spacing permits view
RETROLux / Retrosolar	r, u	v, h	auto / man	2	yes	e, i, b 2x	blade spacing permits view
RETROFlex / Retrosolar	r, u	v, h	auto / man	2	yes	e, i, b 2x	yes
SerraGlaze Daylight Redirecting Film / SerraLux Inc.	f	v	n. a.	1	no	i	transparent acrylic film



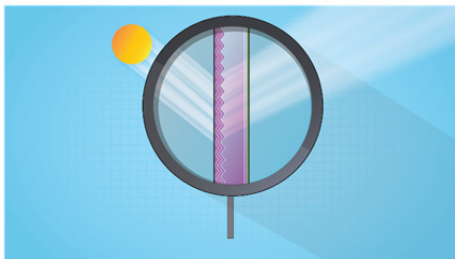
Source: www.panelite.us



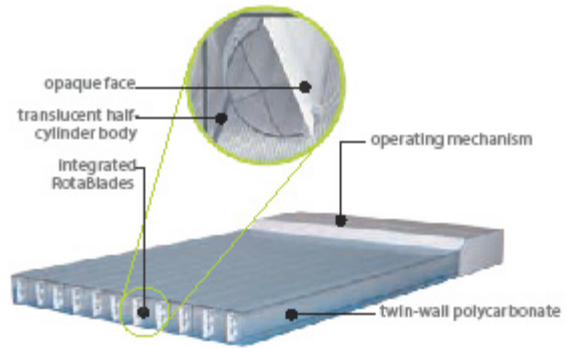
Source: www.serraluxinc.com



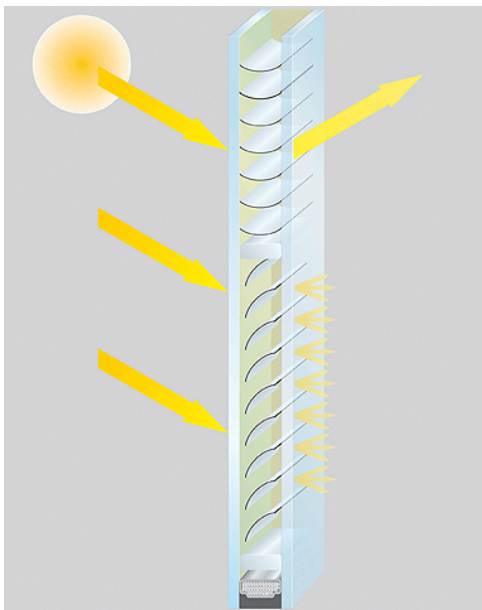
Source: www.okalux.de



Source: solutions.3m.com



Source: www.danpalon.info



Source: www.glassolutions.at



Source: www.retrosolar.de

Figure 2.1: Selected daylight redirecting blinds, left to right, top to bottom: Clearshade, SerraGlaze Daylight Redirecting Film, Okasolar W, 3M Daylight Redirecting Film, Controlite, DLS Ecklite Evolution, RetroLuxTherm.

4. Sun control devices selected for investigation

LightLouver shading system

This is a passive system with specially designed louver profiles optimized to reflect incident sunlight at many different angles into the interior space further than ordinary venetian blinds with a simpler slat-type cross-section (Figure 2.2). It is installed on the indoor side of any window. The LightLouver reflects daylight at an incidence angle of 5 °degrees or higher and therefore can be used on East and West orientations where low sun angles are prevalent at sunrise and sunset but can cause glare. Since the LightLouver profile design does not permit a direct view through the louvers, low sun angle glare is not a concern. Transmittance characteristics for this louver were obtained from the LightLouver company (Rogers, 2013) for use in the daylighting model in this thesis.

Because it is a passive design, there is no interaction with building operations or occupant behaviour and the maintenance required is minimal.



Figure 2.2: LightLouver (Photo: Dennis Schroeder, NREL).

Vision Control window system

This is a mechanical, automatically controlled daylight redirecting system. There is a blind with a slat-type cross-section that is installed in the cavity between the two glazing surfaces in a double-glazed window (Figure 2.3). The louvers have a full range of rotation but they do not retract. This window was previously characterized experimentally by Peng (2009) who also suggested two examples of control strategies for either maximizing view or daylight illuminance through redirection. The Vision Control characteristics have been incorporated in the daylighting model for this thesis study and the control strategies have been modified as necessary.



Figure 2.3: Vision Control window (Photo: Qian Peng).

5. Three-section façade

The concept of the three-section façade (Tzempelikos et al., 2007) formally codifies in a systematic way certain solar design practices known from design experience and historical architectural building types. The three sections, as illustrated in Figure 2.4 serve different functions in a building and are stratified vertically to respond to the sun. The bottom section that rises up to the level of the workplane (the imaginary horizontal plane that defines the level of focus or interest for seated occupants, such as at a desk or a table), at approximately 0.9 m above the finish floor, is the opaque section since daylight that enters a space lower than the height of the workplane does not significantly contribute to overall horizontal illuminance on the workplane (Reinhart, 2005). The middle section is the viewing section and features clear glazing to capture the best views for the building

occupants in seated and standing positions. The top section is the daylighting section which is a modern interpretation of the clerestory – the upper level of a Roman basilica whose walls are punched with windows to allow daylight to illuminate the lower floor (Fletcher and Musgrove, 1987).

Although the principal location for the installation of the advanced daylight redirecting blinds is in the daylighting section of a building façade, a few of the blind manufacturers propose installing their products in the view sections as well. This is the case when the louvers have very low vertical profiles and are sufficiently distanced from each other to minimize view obstructions. These low vertical profile blinds can be installed as two distinct units, one in each of the view and daylighting windows and with separate angle settings for sun control (e.g. Vision Control); or as one unit that spans the combined height of the view and daylighting windows (sometimes called a *split blind*) but that use separate louver profiles to either maximize view or daylight redirection (e.g., RetroLux, RetroFlex, DLS Ecklite Evolution, Okasolar F) while offering independent adjustment of each section (e.g. RetroLux, RetroFlex, DLS Ecklite Evolution).

For this thesis, the distinction between the two different window sections is important since the proposed design guidance for optimizing daylighting through blind redirection is predicated on this separation of window functions.

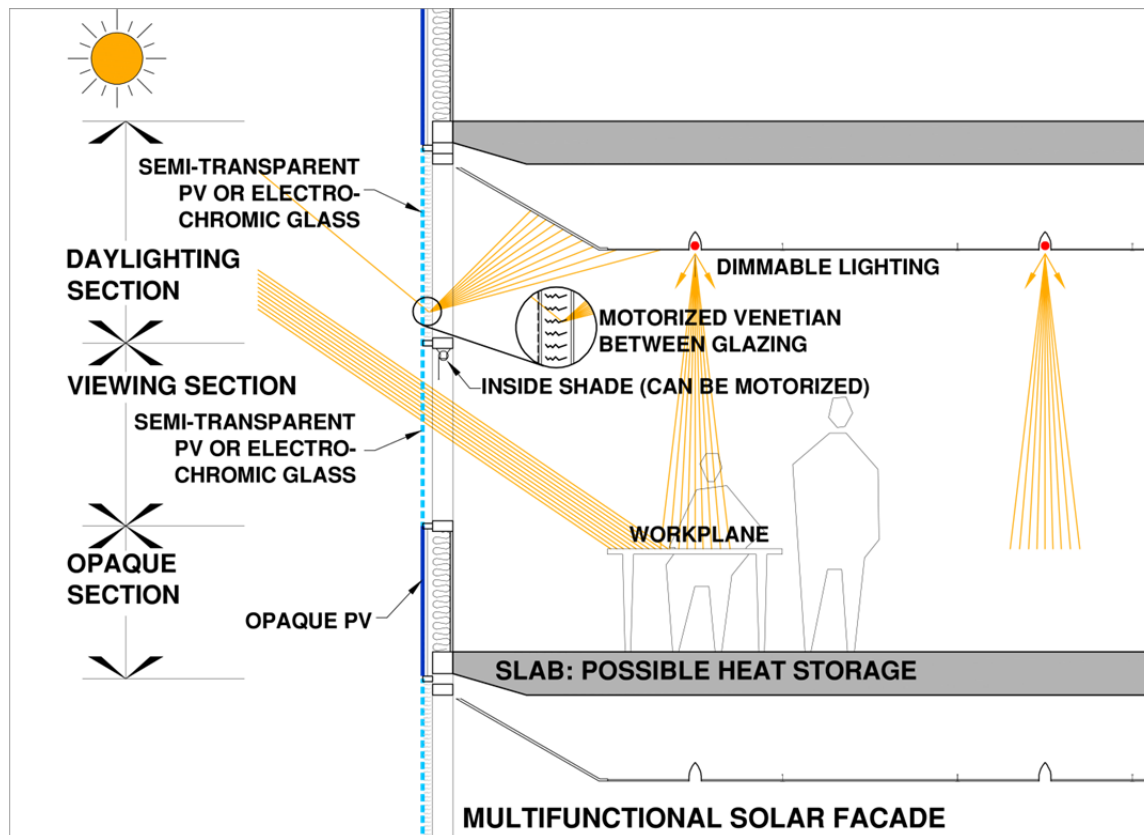


Figure 2.4: Multifunctional solar façade.

6. Occupant behaviour and blinds

Just as important as the physical aspects of blind design and control are the occupant behavioural dimensions. Van Den Wymelenberg (2012) in his review article on occupant interactions with blinds concludes that there is no comprehensive consensus about the way occupants operate blinds or the motivating factors that influence their decisions. For example, Inkarojrit (2005) found that users usually kept their blinds at fixed positions, mostly closed, and rarely adjusted them during the day. This is similar to Cole and Brown (2009) finding that after users have taken action to alleviate discomfort, they are much slower to respond after the discomfort passes.

Continuing further with subjective issues concerning occupant preferences in daylit offices, (Galasiu and Veitch, 2006) find that there is a low acceptance of automatic controls for both shading devices and electric lighting. To increase acceptance, there need to be manual overrides on the controls and the controls themselves have to be simple and easy to operate.

In short, this is an indication that blind controls are more than just an issue of energy efficiency. One example taken from Bordass et al. (1993): occupants perceived the automatic systems as making “abrupt and seemingly capricious changes,” which caused “considerable occupant hostility to automatically-controlled venetian blinds for this reason.”

Because this is a potential issue with the class of active daylight redirecting blinds, building designers will need to consider this in parallel with the design guidance proposed in this thesis.

7. Open-plan office spaces

The larger setting of the workplace is another area where occupant behaviours need to be addressed to obtain a successful daylighting design. Open-plan offices are a common space type encountered in the workplace. They are often proposed as a solution for collaboration amongst workers. They encourage employees to interact and communicate more, leading to greater productivity and employee satisfaction (Maher and von Hippel, 2005). Open-plan offices are flexible spaces, easy to set up and modify and allow for a denser office worker population which may help reduce building, operations and maintenance costs (Smith-Jackson and Klein, 2009).

In spite of these advantages, studies show they may have negative effects on occupant behaviour. Two big factors that cause a decrease in employee satisfaction are related to building acoustics: sound privacy and noise. Employee satisfaction decreases due to concerns over the perceived possibility that their conversations can be overheard by their coworkers (Smith-Jackson and Klein, 2009, Kim and de Dear, 2013). Workers in open-plan offices experience higher levels of distraction and cognitive stress than those in private offices due to noise (Seddigh et al., 2014).

However, one study found that aside from visual privacy, work spaces with low partitions (5 feet or less) or no partitions were less dissatisfied with their workspaces than with partitions higher than 5 feet (Danielsson and Bodin, 2008). From the standpoint of daylighting, the low partitions will also allow daylight to penetrate further into workspaces.

A common suggestion for worker tasks needing increased sound privacy is to add closed ‘breakout’ rooms where employees can go to hold private meetings and telephone calls without being overheard (Kim and de Dear, 2013).

Low partitions and breakout rooms are design solutions that offer the best compromise between efficient daylighting and occupant satisfaction in open-plan offices. Both are implemented in buildings such as the National Renewable Energy Laboratory’s (NREL) Research Support Facility (RSF) which will be described in Section 3.2.

Section 2.3 Daylighting design and analysis tools

Due to the daily and seasonal movement of the sun relative to a building (or more accurately, the constant movement of the Earth around the Sun), and changing atmospheric conditions, solar radiation received at a building’s envelope is a constantly fluctuating quantity that is complex to track. This survey attests to the vast range of attitudes taken to assess daylighting in the building design process. The tools range from “hand” tools to computer simulation. As explained in Section 1.4, since there is currently no simple software that is able to provide early schematic design guidance for daylight redirecting blinds, the following survey will be helpful in identifying the features and the implementation methods required to produce the design guidance this thesis proposes to create, and avoiding the pitfalls that can hamper it.

1. Charts and graphical methods

Solar charts or sun path diagrams represent the simplest way for designers to track the sun relative to a building site to determine location specific aspects of solar access and solar shading such as building siting, orientation, obstructions, shading design, and seasonal effects (Olgyay and Olgyay, 1963, Mazria, 1979). The sun path diagram takes the sky dome and projects it onto a plane parallel to the horizon plane. The sun’s position can be read off the diagram for any point in time at any location. Also, the sun path diagram can be coupled with a graphic solar radiation calculator to obtain sun position and intensity which can be used to inform design. A contemporary application can be found in Robertson’s daylighting design guide for architects (2005).

These are generally static, point-in-time calculations, with the points chosen to represent typical or extreme seasonal conditions (Olgay and Olgay, 1963). From this, a common design strategy is to calculate shading requirements based on sun geometry at noon on the day when the sun is highest and lowest in the sky. Especially during design Charrettes when design time is very short, the low angle of the winter sun can be calculated quickly and then sketched to identify areas that will be in shade, like in the example in Figure 2.5.

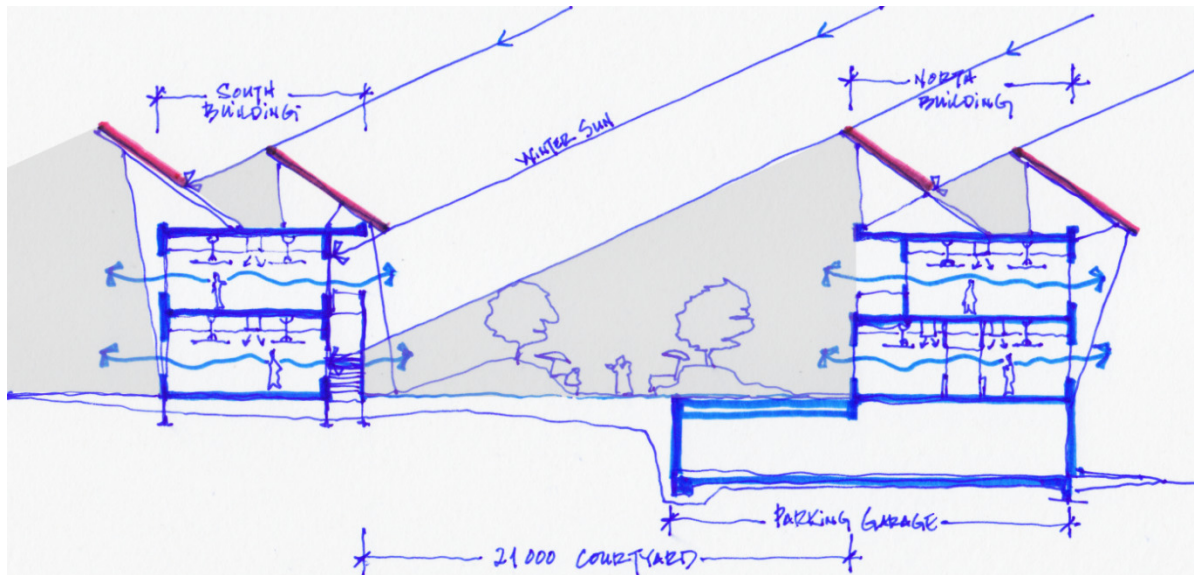


Figure 2.5: Winter sun shading study from Yip and Cory (2013).

These graphical methods have been translated into digital form in most, if not all, architectural 3d modelling software packages such as Rhinoceros 3d, Sketchup, Revit, ArchiCad, Vectorworks, and 3ds Max (the notable exception is AutoCAD). The same point-in-time calculations, based on location, can be made with the same benefits that computers bestow on other information management tasks such as: automation of tedious procedures, easier modifications and tracking of variations, calculation repeatability and comparisons (see for example Climate Consultant (UCLA Energy Design Tools Group, 2014)). However, they do not fundamentally differ from their analogue antecedents. They are useful for general building and site analysis, but cannot assist in designing with daylight redirecting blinds.

2. Rules of thumb: useful daylight building depth calculator

A useful design tool in the pre-design phase (i.e. before schematic design) or during the early days of the schematic design phase is the useful daylight building depth calculator. This rule of thumb provides a very simple way to quickly estimate how deep useful daylight from sidelighting can penetrate into a space. There are many variations in use today (Enermodal 2002, O'Connor et al., 1997, IESNA 2000, Robertson, 2005, ASHRAE 2009, ASHRAE 2013) and all relate the useful daylight penetration depth from sidelighting to the window head height – usually that the useful daylight penetration depth from sidelighting is at most 1.5 (Enermodal) to 2 (IESNA) times the window head height. The daylit area and the quantity of useful daylight are never explicitly defined, and neither is the scope of applicability of the calculation, i.e., climate, latitude, building location or orientation, glazing types, or shading devices (Reinhart, 2005). Light shelves are mentioned in O'Connor et al., (1997), Enermodal, (2002), and Robertson, (2005) as increasing the daylighting penetration depth to 2.5 times the window head height. However, judging from the number of current variations of this simple tool, what it reveals is the design community's preoccupation with a seemingly basic design question: *How deep can a building be daylit by a window?*

More precise definitions have been proposed for “daylit area.” The first describes the daylit area as that which regularly meets target illuminances during occupied hours – with the boundary as the points where the daylight autonomy (see Section 2.310 for definition) falls to half of its maximum value (Reinhart, 2005). From this, it states that the depth of the daylit area is between 1 and 2 times the height of the window head height, and factors in venetian blinds; or up to 2.5 times if shading devices are not needed.

Recently, in the IES LM-83 standard, the IESNA (2012) has updated the daylit area boundary definition (for common workspaces such as open-plan offices) to be the points where the daylight autonomy falls to 300 lx for at least 50 % of the time between 8 AM and 6 PM (see Section 2.310 for more details). A further evolution is the definition of a partially daylit area whose boundary is the points where the daylight autonomy falls to 150 lx for at least 50 % of the time between 8 AM and 6 PM (Reinhart et al., 2014).

These building depth calculators are good examples of initial design guidance for building design. They provide a good starting point for an initial design idea before validation with more accurate tools. One of the outputs from this thesis will be an extension of this simple building depth calculator to include cases of daylight redirecting blinds.

3. Scale models

Instruments such as heliodons (Olgyay and Olgyay, 1963) are the 3-dimensional extension to the sun-path diagrams that describe the sun's position in time. Such instruments use an adjustable light source to study the sun's effects on vastly reduced-scale models. The main advantage of such instruments is the physical visualization of sun conditions on an easily-manipulated physical model. Although useful for qualitative evaluations of design options, they present limitations. The light sources cause diverging rays, leading to distortions for bigger models and erroneous measurements. For the most part, these have been replaced by 3d computer models that perform the same calculations.

In exceptional cases, full-size models, or mock-ups are produced to test particularly innovative design configurations that are prohibitively difficult to impossible to evaluate through conventional means such as simple design tools or simulation. Such mock-ups in the service of design are generally expensive and time-consuming to produce. One recent case is a dynamic shading and lighting control design for new New York Times office building (Lee and Selkowitz, 2006). This is a realistic option only on very special projects and even then, does not help initiate the design process at schematic design.

4. Optical characterization of blinds

The major obstacle to using the design and analysis tools described so far in Section 2.3 is in the physical property descriptions of window blinds. Although blinds are a common feature in workplaces (e.g., there were operable blinds or shades in 84 % of the 61 spaces (Heschong, 2012) that were part of the field data in support of the new Illuminating Engineering Society (IES) spatial Daylight Autonomy (sDA) standard), they have complex light-scattering behaviours that are difficult to optically characterize due to the different shade fabrics and weave densities; louver shapes, profiles, thicknesses, and spacing; curvature; adjustable slat angles and heights; material reflectances and specularities; and

their dependence on sky conditions and incidence angles of the sun (Tzempelikos, 2008, Molina et al., 2014). They are elements in a so-called complex fenestration system (CFS), which refers to any fenestration system that contains components or layers that provide shade or that improve interior daylighting. All the previously mentioned sun control devices in Section 2.2 fall into this category. Other examples include meshes, and prismatic films.

A theoretical framework for describing the behaviour of a material (such as a component of a complex fenestration system or even an entire complex fenestration system as a unit) to light is the bidirectional scattering distribution function (BSDF). It describes the distribution of the outgoing light transmitted (bidirectional transmittance distribution function, BTDF) or reflected (bidirectional reflectance distribution function, BRDF) from many incident directions.

There have been many approaches taken to obtain these BSDFs. Some use physical measurement of samples in specialized scanning instruments, so-called goniophotometers, (Papamichael et al., 1988) to (Andersen and de Boer, 2006) and more recent digital video based ones (Andersen et al., 2010). For large, or macro-structured, devices, such as blinds, another common technique has been to build mock-up spaces with the sun control devices, measure the illuminance levels in the mock-up spaces and compare analytical models or derive mathematical transmittance relationships from the experimental data (Athienitis and Tzempelikos, 2002, Gomes et al., 2014, Peng, 2009). The advantage of this approach is that a physical setup and measurement can capture the variations, imprecisions, or limitations in real manufactured objects and rooms/spaces as opposed to their theoretical design or specifications. However, the measurement process is very time-consuming and often expensive. Additionally, new measurements need to be made for each configuration or variation of a product such as for different finishes, colours, weave densities, etc. Finally, for the more detailed measurements from scanners, there are size limitations to the samples that can be scanned. Goniophotometers are ideal for homogenous micro-structured blinds. Macro-structured blinds such as venetians have discontinuous characteristics such as the space between louvers that take them out of the range of the scanners' incident light source.

There are models for venetian blinds based on analytical geometry (Tzempelikos, 2008), radiosity methods (Carli, 2006, Gomes et al., 2014) or hybrid (radiosity/raytracing) methods (Chan and Tzempelikos, 2012). Their specificity is an advantage, but also a disadvantage in that they cannot be applied or easily adapted to other classes of sun control devices (such as roller shades). Moreover, the radiosity methods make certain assumptions about the sun control materials such as the materials 1) are perfect diffusers; 2) have no thickness; and 3) do not exhibit edge effects.

Another class of models simulates the physical experiments. For this, forward raytracing software that emits rays from the light source to the specimen is typically used to generate analytical solutions (Andersen and de Boer, 2006, Andersen et al., 2005). These raytracing methods are much more flexible and are well suited to testing many variations of a single product, such as for daylight optimization during a product's design phase. They can eliminate the need for making physical product prototypes for testing. Raytracing is not limited to perfectly diffusing materials nor by the geometry assumptions of the radiosity models – it can handle extremely complex geometry and can assess the optical light scattering distribution of *any* material. Practically, though, the simplifying assumptions in radiosity models have been shown to have little adverse effect except in the case of specular properties (Rubin et al., 2007).

A distinction must be made between these forward raytracing software programs and the more common backwards raytracing software such as the open-source Radiance (Larson and Shakespeare, 1998) . Because forward raytracers emit rays from a light source to a receiver, there are a large percentage of the rays that never reach the receiver and therefore do not contribute to the illuminance of the receiver. To make raytracing more efficient, a backwards raytracer emits rays from the receiver and scatters them backwards through probabilistic sampling methods to find the light source. Unfortunately in the case of complex fenestration systems, a backwards raytracer is normally inaccurate due to the large number of inter-reflections a ray is subjected to resulting in a low probability that it finds its way to the light source. A prohibitive large number of samples would be required to obtain an accurate result.

There have been recent advances in research to overcome these limitations. A newly developed software program called *genBSDF* has been added to Radiance which reverses the way Radiance considers the source and the receiver, effectively using Radiance like a forward raytracer (McNeil and Lee, 2013, McNeil et al., 2013). The *genBSDF* output format for a BSDF is an extensible markup language (XML) file that is compatible with WINDOW 6/7 (Mitchell et al., 2008) which is a research-grade window design software application that is compatible with Radiance. Coupled with a new Radiance simulation method, called the three-phase method (and more recently the five-phase method) (McNeil, 2013), this new development shows promise in being able to simplify the process of obtaining accurate BSDFs and using them in daylighting simulations of interior spaces.

Some hurdles still remain. The current software methods to obtain BSDFs are well adapted to researchers and product developers (for example, in the early stages of product design), but have yet to attain a level of ease of use, availability of BSDF data, integration with other software, and integration with existing design workflows that building designers are accustomed to. Raytracing programs still hinge on needing accurate model descriptions – such as material geometry and reflectance and specular properties – to produce accurate BSDFs (Nilsson and Jonsson, 2010) and also assume ideal manufacturing tolerances and quality control. In the case of an existing product, this information may be difficult to obtain or measure depending on the particular building design situation. *Due to these issues, a simplified approach to modelling the daylight redirecting blinds will be sought.*

5. Daylighting simulation software

A practical alternative to physical models is to use daylight simulation software to provide the tools needed to begin the building design process. The simple point-in-time calculations built into most 3d architectural modelling software mentioned previously are useful for *qualitative* assessments of design options, but specialized daylighting software is able to provide *quantitative* output. Based on the information in Section 1.4 and Section 2.2, the following criteria are identified as essential for an ideal daylighting simulation program:

- Support for different kinds of passive and active daylight redirecting blinds. This includes complex profile shapes and control strategies for active blinds.
- Support for different climates. This usually takes the form of typical meteorological year (TMY) weather files.
- Can generate predictions at one hour time steps for an entire year.
- Support for large, open-plan spaces.
- Support for multiple windows.
- Can generate illuminance values for daylight sufficiency analysis.

Robinson and Stone (2006) use a radiosity model for computational efficiency, but the split-flux method employed tends to under predict interior illuminances in deep spaces (O'Brien et al., 2015) like open-plan offices. Other studies using simplified radiosity or raytracing models with support for blind movements and controls (Nielsen et al., 2011, Hviid et al., 2008) are intended for modelling small private offices with support for only one window, or are incompatible with blinds with complex profile shapes like the LightLouver (Athienitis and Tzempelikos, 2002).

One promising research project called LightSolve (Kleindienst et al., 2008, Andersen et al., 2008) that supports both complex building geometry and daylight redirecting blinds, is aimed at building designers for use in schematic design and offers interactive ways to visually represent daylighting data to help in making design decisions. However, the software requires an externally constructed 3d model as input and does not have the ability to make modifications to the geometry for interactive parametric studies. This makes it more suited to the end of schematic design or the beginning of design development. Although there is a prototype plug-in for SketchUp which couples the interactive calculation engine of LightSolve with the native modelling abilities of SketchUp, there are presently limitations related to climate and geometry that make it unsuitable for general design use (Gagne et al., 2011).

As previously mentioned in Section 1.4, the current state-of-the-art in accurate annual climate-based daylight simulations of spaces using daylight redirecting blinds is based on the Radiance three- or five-phase method. Aside from executing these simulations at the

Radiance command-line, currently the only graphical front-end compatible with the three- or five-phase method is OpenStudio (NREL, 2015). The time and energy resources needed to setup and execute these Radiance simulations are acceptable for the end of schematic design or for design development, but are too demanding when initiating the design process.

Based on the abovementioned research, the computationally efficient radiosity method will be used for the daylighting evaluations in this study and will include extended 3d geometry support for the three-section façade.

6. Radiosity model

The radiosity method of calculating luminous quantities in a space is based on the principle of an energy balance. It was first used in radiation heat transfer calculations to determine the energy balance of a set of surfaces in a closed space exchanging radiant energy and then applied to lighting calculations by Goral, Torrance et al. (1984). The method considers all light interaction between the surfaces in a space. But the surfaces must exhibit constant physical properties, that is, be ideal diffusers (Lambertian surfaces) and the energy transferred between two surfaces is constant. The surfaces are discretized into sub-surfaces small enough to be considered planar with uniform properties. From this definition, we can note that radiosity cannot model specular light interactions. Any light reaching a surface is either absorbed or re-radiated uniformly to the other surfaces in the space.

A light energy balance calculation is made for each surface in the space. The luminous flux, or luminous exitance, M_i , leaving a surface i is equal to its initial luminous exitance, M_{oi} , and the luminous flux that it receives from all other surfaces and scatters back to the space. The amount of luminous flux that is scattered by surface i is determined by the reflectance of the surface, ρ_i . And the amount of luminous flux surface i receives is determined by the sum over all other surfaces of the fraction of their luminous flux which reaches surface i .

$$M_i = M_{oi} + \rho_i \sum_j M_j F_{ij} \quad (2.1)$$

where F_{ij} is the view factor denoting the fraction of the flux radiating from surface i with surface area A_i that is received by a second surface j with surface area A_j . The view factor accounts for all the inter-reflections between surfaces and is a strictly geometrical quantity. The most general form, as shown in Figure 2.6 with \mathbf{n}_i and \mathbf{n}_j representing unit normal vectors, is denoted by

$$F_{ij} = \frac{1}{A_i} \iint_{A_i A_j} \frac{\cos \theta_i \cos \theta_j}{\pi r^2} dA_j dA_i \quad (2.2)$$

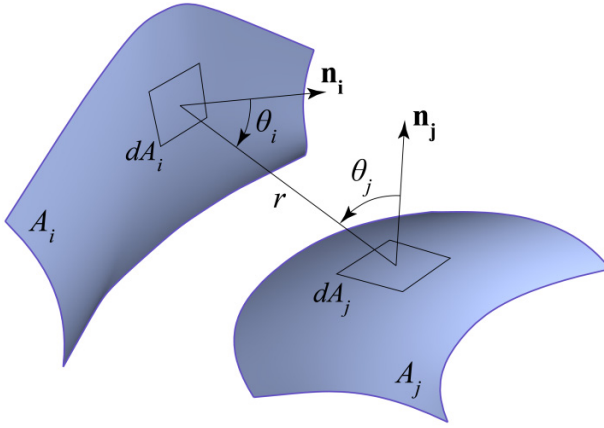


Figure 2.6: View factor between two arbitrary surfaces.

See Appendix A1.6 for view factor calculations. Once all the view factors of the interior space are known, the final luminous exitance, M_i , of surface i can be determined.

For a space with n surfaces, the above equation can be expanded and rearranged to produce

$$\begin{aligned} M_{o1} &= M_1 - (\rho_1 M_1 F_{11} + \dots + \rho_1 M_n F_{1n}) \\ M_{o2} &= M_2 - (\rho_2 M_1 F_{21} + \dots + \rho_2 M_n F_{2n}) \\ \vdots &= \vdots \qquad \qquad \qquad \vdots \qquad \qquad \qquad \vdots \\ M_{on} &= M_n - (\rho_n M_1 F_{n1} + \dots + \rho_n M_n F_{nn}) \end{aligned} \quad (2.3)$$

which can be expressed as an $(n \times n)$ matrix:

$$\mathbf{M}_o = (\mathbf{I} - \mathbf{T}) \cdot \mathbf{M} \quad (2.4)$$

where \mathbf{I} is the $(n \times n)$ identity matrix and \mathbf{T} is an $(n \times n)$ matrix whose elements are equal to $T_{ij} = \rho_i \cdot F_{ij}$

Solving for M gives

$$\mathbf{M} = (\mathbf{I} - \mathbf{T})^{-1} \cdot \mathbf{M}_0 \quad (2.5)$$

The illuminance at any point a can be obtained by summing up the contribution of the luminous exitance of each surface to the point a .

$$E_a = \sum_i M_i \cdot C_{ai} \quad (2.6)$$

where C_{ai} is the configuration factor between surface i and point a , which represents the fraction of the flux that radiates from surface i and is received at point a . See Appendix A1.7 for configuration factor calculations.

An important factor to consider is that discretizing surfaces into smaller sub-surfaces produces finer results at the cost of increased computational time.

The radiosity method requires input of the sky illuminance that describes the quantity of daylight from the sun and the sky that reaches the exterior face of the windows in the building of interest. This is obtained from the sky model.

7. Sky models for daylighting

The luminous nature of the sky makes it a complex phenomenon to model accurately. Many sky luminous distribution models exist and have been used through the years. Some common ones used today include the Commission internationale de l'éclairage (CIE) models. The CIE overcast sky model has a regular distribution of luminance from horizon to zenith with the zenith three times as bright as the horizon. The CIE clear sky model is brightest at the sun position, darkest opposite the sun position, with horizon brightness between the two extremes. (Reinhart, 2006).

The most widely used of the partly cloudy sky models is the Perez model in which the sky luminance is modelled as a function of sky clearness, brightness, and solar altitude (Perez et al., 1990, Perez et al., 1993). It is a series of statistically derived models that generate specific solar radiation components that are useful for monitoring or simulation applications. They all share a common set of inputs, namely, global horizontal irradiance,

direct (beam) irradiance, dew point temperature, and solar geometry. The solar geometry is calculated as described in Appendix A1.4. All the other inputs are obtained from weather station data.

The three particular models useful for the daylighting simulations in this study are:

1. **The diffuse irradiance model.** It consists of three components: the isotropic part, which is the solar radiation received uniformly from the entire sky dome; the circumsolar diffuse, which is the result of scattering of solar radiation and is concentrated in the part of the sky around the sun; and the horizon brightening, which is concentrated near the horizon and is most pronounced in clear skies. The output from this model is I_{ds} , the total diffuse irradiance on any tilted surface. The inputs are the solar constant, I_{sc} (Kopp and Lean, 2011); the diffuse horizontal irradiance, I_{dh} ; the beam normal irradiance, I_{bn} ; the altitude angle, α ; and the incidence angle, θ .
2. **The luminous efficacy model.** This relates direct, global, and diffuse irradiance to direct, global, and diffuse illuminance (where the efficacy refers to the yield of the light source with respect to the human eye).
3. **The diffuse illuminance model.** This model predicts the total diffuse illuminance, E_{ds} , on any tilted surface. Its calculations use statistically derived coefficients of the same form as those used in the diffuse irradiance model.

Finally, the total illuminance at any surface on the Earth is composed of the three components: the direct sunlight, the diffuse daylight coming from the sky, and the diffuse reflected light coming from the ground or other surrounding surfaces.

8. Contingency at schematic design and model resolution

To put into perspective the accuracy that is required of a daylighting model to inform initial design decisions, it's useful to look at the quantity of information available about the building design as it progresses to the final design.

Regardless of whether a conventional, linear design process or an integrated design process is used in a project, milestones with deliverables are usually set at the end of each of the

three general design phases (schematic, design development, and construction documentation) to formally evaluate the work to determine how the project is meeting its program goals and objectives. Opportunity to make changes or adjustments is available. Typically the deliverables include drawings, specifications, a work schedule, and a construction budget cost estimate.

At the first of these milestones, at the end of the schematic design stage, many major design decisions have been made, but the building design is *still incomplete* and there may exist unforeseen or unpredictable conditions such as how specific implementations of theoretical systems may cause conflicts or incompatibilities and uncertainties concerning project scope and budget. (Unless a design concept hinges on a specific product or system, the selection of products available in the marketplace is typically not made until the next phase, design development). At the end of schematic design, the design is at most 5 % – 25 % complete (Canadian Institute of Quantity Surveyors, 2012). This incompleteness or lack of detail is captured in the construction budget cost estimate in a design contingency line item. *This design contingency is usually between 10 % – 15 %* (U.S. General Services Administration, 2007, Government of Quebec, 2005) depending on design and delivery methods as well as the complexity of the project. There is a separate line item for construction contingency which is a measure of construction-related uncertainties such as unexpected labour market and materials issues.

Additionally, a recent Joint Federal Government/Industry Cost Predictability Taskforce (2012) has found that the overall construction budget cost estimate at the schematic design stage can have a variance of $\pm 20\% - 30\%$ underscoring the *significant number of unknowns at this stage of the design process*.

This information helps put into context the problem of *too* much resolution or information in simulation models. There are diminishing returns on model accuracy with higher model resolution. Just how accurate does a simulation model need to be to commit to a design? Simple models may be sufficient early in the design process. Key general questions that require quick, order of magnitude answers are posed. Is a passive or active daylighting system better? How much better? Why is that? What are the effects of climate, building

orientation, window heights, window to wall ratios, building depth? How much daylighting can we obtain? Because of this, it is justifiable to avoid high resolution models.

In order to answer these questions, some recommendations and metrics are required to interpret any output from simulation models.

9. Recommended illuminance levels

Recommended threshold illuminance levels are determined by task requirements. This can range from 100 lx for corridor lighting to 500 lx for general office tasks to over 1000 lx for precision work (Canada Labour Code, 2014, IESNA 2000). Although these codes and handbooks recommend 500 lx for general office work, recent research suggests that lighting levels below 500 lx may still be considered useful in an office environment (Reinhart and Voss, 2003). In fact, 300 lx is used as the threshold illuminance for common workplace environments (such as open-plan offices) in the sDA_{300/50} standard (IESNA, 2012). An influencing factor for these lower illuminance thresholds is the prevalent use of computer monitors, or video display terminals (VDT), and the shift away from office work involving paper documents on the horizontal workplane and more towards the vertical workplane of the VDT (IESNA 2000).

10. Metrics for daylighting design

What is good daylighting? The answer to that seemingly simple question still eludes us. Due to the neglect of daylighting in buildings in the last century leading up to the 1970s oil crisis, the advancement in daylighting metrics suffered as well.

The oldest metric still currently used to quantitatively judge what good daylighting is, is the **daylight factor**. It is defined as the ratio of the illuminance at an interior point to the illuminance on an external, unobstructed horizontal surface under a CIE overcast sky (Hopkinson, 1963). Ironically, its original purpose was not to evaluate daylighting levels inside a space, but rather in legal disputes to demonstrate lines of sight for window solar access and limits of neighbouring buildings' obstructions. (Reinhart et al., 2006). Its advantages are that it is affected by building geometry, interior surface properties, and exterior surroundings, making it a useful metric by which to evaluate design options.

However, it suffers from many shortcomings that make it obsolete for many of the demands of daylighting design today. Because the daylight factor uses an overcast sky model at no time is direct sun considered in any of the calculations. Therefore daylight factor cannot distinguish between building orientation, season, time of day, nor building location (latitude) among other things. Also, as a ratio, it does not provide absolute illuminance values which are helpful in predicting glare probability.

In contrast to the daylight factor's immutability to real sky conditions, recent years have seen the development of *dynamic daylighting metrics*, or *climate-based daylighting metrics*, that address many of the issues that are inadequate with the daylight factor. In addition to diffuse skylight, a dynamic daylighting metric must *also* account for diffuse ground-reflected light and direct sunlight. The calculation period must be over the period of a year to capture climatic and seasonal changes. And it must be able to establish a range of daylighting considered useable and determine unsuitable ranges when conditions fall below or above these thresholds. Also important is the daily time period for evaluation, whether it is from sunrise to sunset, only the normally occupied hours of the day, or some other justifiably defined period. All these factors will lead to enormous amounts of data. How this data is represented in an easy to follow manner is paramount: is it best visualized temporally or spatially?

The **daylight autonomy** (DA) of a point on a horizontal plane is the percentage of the annual occupied hours that a point on a horizontal plane meets or exceeds a threshold illuminance level at that point by daylight alone (Reinhart et al., 2006, Reinhart and Walkenhorst, 2001). The evaluations take place over regular time steps, usually hourly or shorter. DA can be used in conjunction with non-dimmable electric lighting controlled by occupancy or daylight sensor to predict potential energy savings (Carlucci et al., 2015).

Over time, DA was refined to account for new research that further refines the range of acceptable illuminance for the workplace. **Continuous daylight autonomy** (CDA) is the percentage of the annual occupied hours that a point fully *or partially* meets or exceeds a threshold illuminance level. Unlike with DA which makes an all-or-nothing evaluation of a point in time's contribution to daylighting, CDA allows for partial fulfillment of a

threshold illuminance (Rogers, 2006), acknowledging that *any* daylight is beneficial. It is particularly useful in combination with estimating energy savings when using automatically dimmable electric lighting. (Carlucci et al., 2015).

Useful daylight illuminance (UDI) is another recent dynamic daylighting metric for evaluating horizontal workplane illuminance for office spaces due to daylight alone. It subdivides the range of illuminances into three bins: illuminance under 100 lx, between 100 lx and 2000 lx, and over 2000 lx. These three categories correspond to illuminance levels when daylighting alone is inadequate, adequate, and excessive for workplane sufficiency (Nabil and Mardaljevic, 2005, Nabil and Mardaljevic, 2006). One of the improvements that UDI brings to illuminance metrics is the acknowledgment that excessively high daylight illuminance values are not useful, but instead can be signs of potential visual discomfort and glare. Outside of workplace settings, other research has suggested the thresholds for the UDI bins may need to be adjusted to accommodate the more tolerant requirements of the residential environment (Mardaljevic et al., 2009).

There are also luminance metrics which approach the problem from the point of view of glare and venture away from using the horizontal workplane as the plane of reference for daylighting measurements. One example is **Daylight Glare Probability (DGP)** (Wienold and Christoffersen, 2006) which takes into account daylight source luminance, viewer position and orientation relative to the window. DGP calculations are sorted into three bins of less than 0.30 (barely perceptible), between 0.30 and 0.45 (disturbing), and over 0.45 (intolerable).

All of the aforementioned *dynamic daylighting metrics* or *climate-based metrics* characterize a space discretely at various *points* in the space. And they all establish some threshold illuminance levels that purport to be sufficient for daylighting. This presents some problems. There are no common guidelines as to how many points to evaluate and where those points should be located in the space. Also, there are disagreements as to the appropriate threshold levels or bins used to evaluate the analysis points. And, although the dynamic daylighting metrics were created from supporting data of existing spaces, there aren't any studies to verify if the proposed metrics do indeed predict correctly the

daylighting quality of future spaces. Furthermore, since these are all annual metrics calculated usually at 1 hour time steps, they generate a lot of data that becomes unwieldy. Therefore, to obtain an *overall* evaluation of a floor area, instead of point by point evaluations, another metric is still required to consider all the data points as a whole and distill them into a simpler to use quantity.

Most recently, another variation on daylight autonomy was proposed by the Illuminating Engineering Society (IES) called **Spatial Daylight Autonomy** (sDA) that is applicable to common workspaces such as open-plan offices, classrooms, meeting rooms, multi-purpose rooms, and other areas with similar task illuminance requirements (IESNA, 2012). It is defined as the fraction of an analysis area that meets a minimum daylight illuminance level for a specified portion of the occupied hours per year. Spatial daylight autonomy takes the idea of daylight autonomy and weights the values of the individual illuminance points over the entire area of a space. What this achieves which is different from the other dynamic daylighting metrics is that it proposes to characterize a space with a *single* number instead of the matrix of numbers that results from a daylight autonomy analysis. And, it is a simpler metric to use at the beginning of schematic design since it describes an *area* that satisfies illumination sufficiency. It makes explicit the link between the illuminance distribution and the geometry of a space.

The IES has standardized the parameters used for the sDA metric to facilitate uniform application and permit comparisons across different projects and design teams. The IES recommendation for sDA to measure daylight sufficiency is to use for each analysis point an illuminance analysis threshold of 300 lx on the horizontal workplane and a temporal threshold of 50 % of the period of analysis. Among the other parameters: the period of analysis is from 8 AM to 6 PM local time, hourly (for 10 evaluations per day); the daylight conditions are to be obtained from TMY weather files; the analysis points are to be on a regular grid of at most 24 inches x 24 inches, 30 inches above the finish floor, and between 12 – 24 inches from the walls; radiosity surfaces preferably no larger than 1 ft. x 1 ft.

Taken together, the analysis results in a quantity denoted by $sDA_{300/50}$ that represents the fraction of analysis points over the entire analysis area that meet or exceed 300 lx for at

least 50 % of the analysis period. The performance criteria used to qualify an analyzed space for daylight sufficiency are:

- For “Preferred Daylight Sufficiency,” the $sDA_{300/50}$ values for an analysed space must meet or exceed 75 % ($sDA_{300/50} \geq 75 \%$);
- For “Nominally Accepted Daylight Sufficiency,” the $sDA_{300/50}$ values for an analyzed space must meet or exceed 55 % ($55 \% \leq sDA_{300/50} < 75 \%$).

A complementary metric to sDA to address issues of possible visual discomfort is the Annual Sunlight Exposure (ASE) metric (IESNA, 2012). ASE measures the annual amount of direct sun impinging on a space. The ASE uses many of the same recommended parameters as the sDA in its application

One shortcoming of sDA that it shares with both DA and UDI is that it sacrifices information in favour of retaining spatial relationships. For example, it does not evaluate daylight illuminance uniformity, since it averages out all the analysis point illuminance values over an entire floor area. There may be points in a floor area that seldom, or never, reach 300 lx over the course of a year yet the overall floor area may be deemed “daylit.” This eliminates any sense of the annual variations in performance of any particular point. For this, other researchers have proposed temporal maps of illuminance distribution (Kleindienst et al., 2008), however, this may be a concept best used in design development to fine-tune a design rather than at the beginning of the design process when overall design decisions need to be made.

The $sDA_{300/50}$ metric is proposed for this thesis study since the building types where its supporting data was collected (Saxena et al., 2010) and its field of applicability – common workplace environments – is exactly the space type that this thesis seeks to provide daylighting design guidance for. It will also provide an opportunity to test the validity of the sDA metric.

Section 2.4 Summary

1. Daylight redirecting blinds hold great potential as a solution to increasing daylighting in deep floor plans. There are two classes of devices: passive, which depends entirely on blind shape for its year-round performance; and active, which utilizes adjustable blind angles to respond to sun conditions. Most products in both classes are installed either on the indoor side of a window or between the glazing of a window.
2. Windows, views, and daylight provide benefits to building occupants but care must be taken to ensure occupant comfort. Occupants who are aware of their surroundings and perceive that they have control over their environment are less dissatisfied with their work environments.
3. Current daylighting software tools that support daylight redirecting blinds are best suited for analysis tasks. Simple, computationally efficient simulation models geared towards initial design and based on the radiosity method lack support for some of the essential features required in this study. There is a lack of simple, easy to use design tools incorporating accessible blind information to help integrate daylight redirecting blinds into early schematic stage design.
4. Daylighting metrics that address daylight sufficiency in workplaces are still evolving. The recent spatial daylight autonomy (sDA) metric is the first to link annual daylight illuminance levels with the floor plan geometry of a space, providing building designers design guidance.
5. An appropriate level of effort must match the intent in any design situation. The design process usually starts at schematic design. It is during this phase that the most crucial design decisions such as daylighting and solar control strategies are made. However, the building design will be at most 25 % complete at the end of the schematic design phase. Because there are still so many unknowns at this stage, building professionals usually factor in a design contingency of up to 15 % on the total construction cost to realize the design. Any early schematic design tool (whether for daylighting, thermal, etc.) must take these uncertainties into account and predict within a similar accuracy.

Chapter 3 Methodology part 1: simulation model

Section 3.1 Introduction

The literature review shows that the currently available daylighting software that supports annual climate-based simulations of daylight redirecting blinds are resource-intensive, involving a lot of user input such as complete geometry and physical properties descriptions of all the building design elements in a space; and are computationally-intensive. On the other end of the spectrum, there is simpler, faster computing daylighting software, but each lacks one or many of the essential features needed to conduct this investigation. Some simulate small private offices, with only one window on the equator-facing façade with no support for the three-section façade concept; some support venetian-type blinds, but not the LightLouver; some support more complex fenestration systems, but cannot run annual simulations.

Based on the above, this thesis proposes to create a simplified simulation model using the radiosity method that is computationally efficient and can support annual climate-based daylighting simulations of daylight redirecting blinds. The simplified model is validated through the use of a case study of a high-performance multi-storey open-plan double-perimeter zone office building in Golden, USA (40°N, 105°W). The daylighting illuminance performance of two classes of blinds, passive and active, is investigated. The representative models for the passive and active classes are the LightLouver and the Vision Control blinds, respectively. The study is then extended to encompass a variety of parameters that are important at the beginning of the schematic design phase. Analyses are made using the new spatial daylight autonomy (sDA) metric. The results are correlated and generalized as design guidance intended to provide building designers with support at the beginning of the schematic design phase.

This chapter, Methodology part 1, describes the development and validation of the simulation model. The next chapter, Methodology part 2, describes the parametric investigation of the passive and active daylight redirecting blinds using the simulation model.

Because the building is very modular, only one representative bay is analyzed in this study. Results can then be propagated to the total number of bays in each of the building wings. One obvious limitation is that the model does not account for special spaces such as the main entrance lobby and the various rooms in the spine that bridges the long wings (see Figure 3.2). Nor does the model properly represent the topmost floor which has increased interior ceiling height due to the sloped roof.

Once the initial comparison of the two daylight redirecting blinds' daylighting performance is completed, further simulations are carried out to examine the effects of various parameters on the daylighting illuminance of the space. These simulations may suggest relationships that can be identified as design guides for use during the early schematic design phase of a building project.

The main daylighting model used in this case study was developed using the radiosity method in the Mathcad calculation software program (PTC, 2010). A supplementary 3d model was made using Rhinoceros 3d (McNeel North America, 2014) and Ecotect (Autodesk, 2011) programs for the point-in-time self-shading analysis. Although Ecotect is not BESTEST (Judkoff and Neymark, 1995) certified, the self-shading analysis is a simple qualitative geometry test based on solar angle calculations and building massing.

Section 3.2 Case study building



Figure 3.1: Main entrance of the RSF (Photo: Dennis Schroeder, NREL).

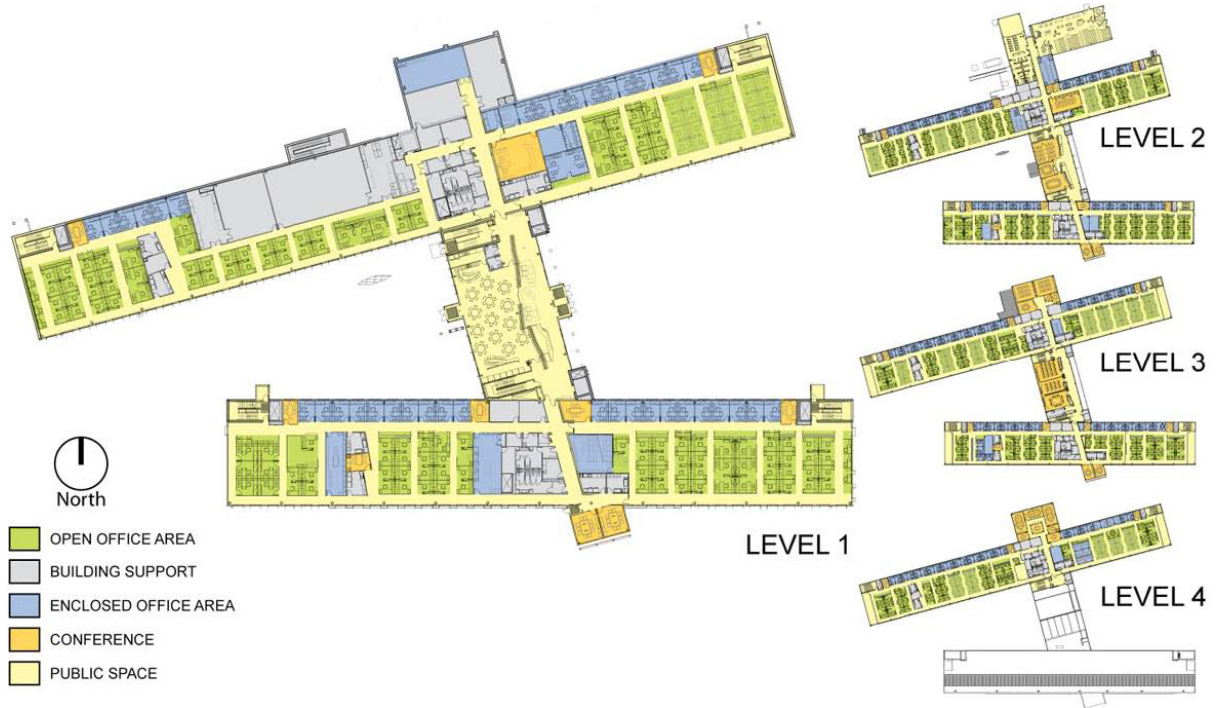


Figure 3.2: General floor plans of Phase I of the RSF (Drawings courtesy of RNL Design).

The case study building selected for this study is the National Renewable Energy Laboratory (NREL) Research Support Facility (RSF) (Figure 3.1). It is located on the NREL campus in Golden, Colorado (39.7°N, 105.2°W, 1829 m above sea level). The local climate is heating dominated and most days of the year are sunny. The RSF is an office building that was constructed in two phases. Phase I, at 20 400 m², accommodates 822 occupants and comprises two East-West oriented wings that are connected by a North-South spine. The Phase I building design-build contract price was US \$64.3 million. A subsequent extension to the building, Phase II, added 13 000m² for 500 additional occupants in another East-West oriented wing directly north of Phase I and connects along the North-South spine of the complex. Phase II’s design-build contract price was US \$27.1 million. See Figure 3.2 for a general plan of the Phase I building. Phase II is not shown illustrated nor discussed in this thesis.

The RSF is a high profile office building designed to showcase sustainable design with particular emphasis on energy efficiency and renewable energy technologies (RET). The most important RET is the roof-mounted photovoltaic system which is designed to

generate as much energy as the building consumes on an annual basis. A building energy use intensity (EUI) target of 110.7 kWh/m²/yr, including data centre energy use, was calculated using extensive building simulation prior to the posting of the request for proposals (RFP). To ensure that this energy target was met, NREL included it as a requirement in the design-build contract agreement. The monitored EUI for the first year of building occupation is 111.7 kWh/m²/yr (Hootman, 2013). Figure 3.3 shows the breakdown of the RSF’s total annual measured energy consumption. Hirsch, Okada et al., (2011) provide a detailed account of the different building simulation programs that were instrumental in supporting the design process through the different stages of the project.

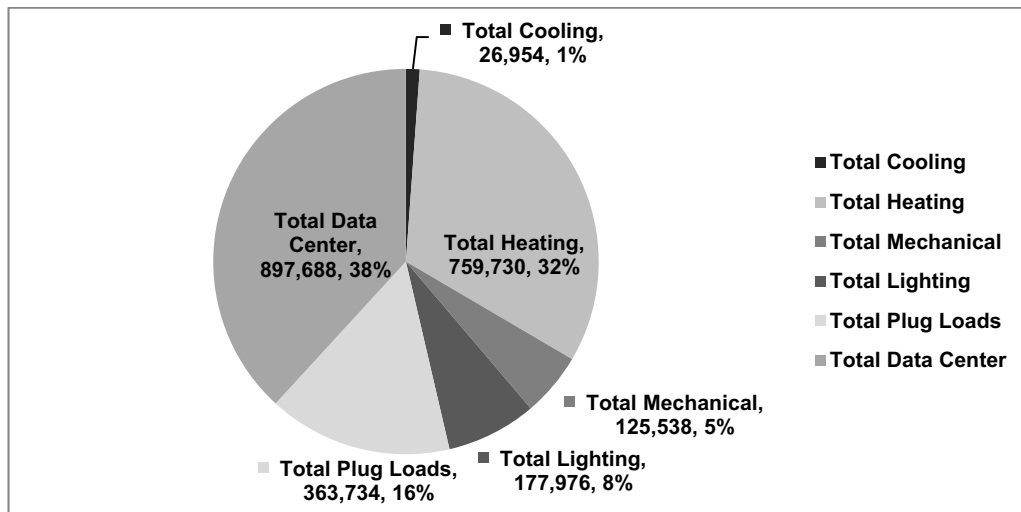


Figure 3.3: Energy use breakdown of the RSF.

There are many other exceptional features of the RSF as a demonstration project of leading-edge research in energy efficiency and renewable energy technologies translated into a real world project that is market-competitive (Hootman, 2013). These features are extensively documented on the RSF website.

To achieve such ambitious objectives, NREL decided at the project planning stage that the project would use innovative design methods such as an IDP, a design-build project delivery method, and detailed building performance specifications (including overall energy use intensity targets) to integrate the innovative technologies. These requirements were formalized in the RFP along with budget ceilings. Thus, all design and construction

teams wishing to bid on the project had to accept these conditions. The project risk was shifted to them from NREL, the building owner. This provided the motivation for them to work together in the IDP, drawing upon each team member's strengths to seek out innovative solutions. This integration happens right from the start of the design project. Traditional adversarial relationships that pitted design professionals (architect and engineer) versus building constructor and architect versus engineer are eliminated, allowing synergies such as constructor input at the schematic design phase and tighter coordination between architectural and engineering systems.

The building façade is constructed with modular 11 in thick precast concrete sandwich panels, which are 3 m wide and designed so that three fit exactly in one structural bay. The roof is composed of a 76 mm concrete slab on steel decking with insulation on the exterior side. The vertical structure for each of the long wings is along the perimeter, leaving the open-plan office free of columns or other obstructions to maximize views, daylight penetration, and natural ventilation. Long-span open-web steel joists support the floor and roof assemblies. The overall window to wall ratio for each façade is: South, 30 %; East 32 %; West, 31 %; North, 21 %. A daylighting window and a view window are stacked vertically and centred from side to side within each precast façade panel. On the South façade, the view window has a fixed exterior shading device to prevent direct sunlight from entering the space. The South façade daylighting window has the LightLouver daylight redirecting blind installed on its inside face. See window section, Figure 3.4.

The daylighting design of the RSF was a particularly difficult challenge. NREL specified in the RFP that obtaining the LEED v2.2 IEQ 8.2 point for daylighting was a requirement, thus making it very influential in the building design. For an open-plan office building, the daylighting metric becomes the factor that determines the depth of the main wings of the building. The design team made extensive point-in-time (noon, on the equinox, under clear skies) daylighting simulations using the Radiance lighting software for a set of design parameters including window to wall ratios, window head heights, glazing transmittance, and different interior finishes. From these simulations the building depth was determined to be 18 m. At the time the RSF was being designed, Radiance was not yet capable of supporting annual climate-based simulations with complex daylight redirecting blinds such

as the LightLouver. Therefore, as the design project progressed into design development, exceptional techniques were used to predict the annual daylighting behaviour of the building using the LightLouver for the purposes of coordinating with the electric light dimming design and estimating total building energy usage. These included using highly detailed 3d models of the LightLouver with aggressive simulation parameters and custom manipulation of other daylighting tools such as Radmap and SPOT (Guglielmetti et al., 2010).

The result is a tightly integrated daylighting and electric lighting control system. The RSF lighting load is 8 % of total energy usage. This compares very favourably to the American average for commercial and institutional buildings of 39 % (Table 1.1). This shows that the RSF already has exceptionally low lighting energy consumption.

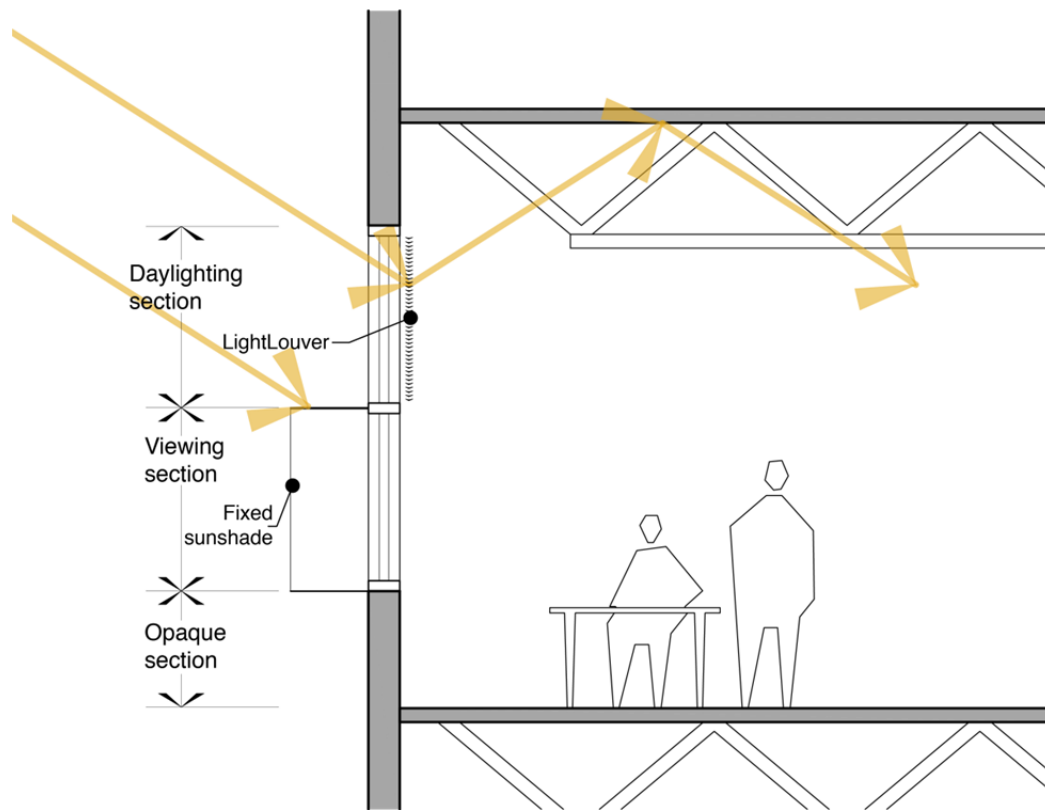


Figure 3.4: Schematic cross-section showing window design for daylighting system.

Section 3.3 Radiosity model

The radiosity method was selected for the daylighting model since *it represents a good match between the level of effort and computational efficiency with the level of detail required for its intended purpose*. Simplified flowcharts of the daylighting model and the active blind control strategy are shown below in Figure 3.5. The sub-sections below describe the specific components of the model. (Refer to Appendix A1 for modelling details and detailed flowcharts).

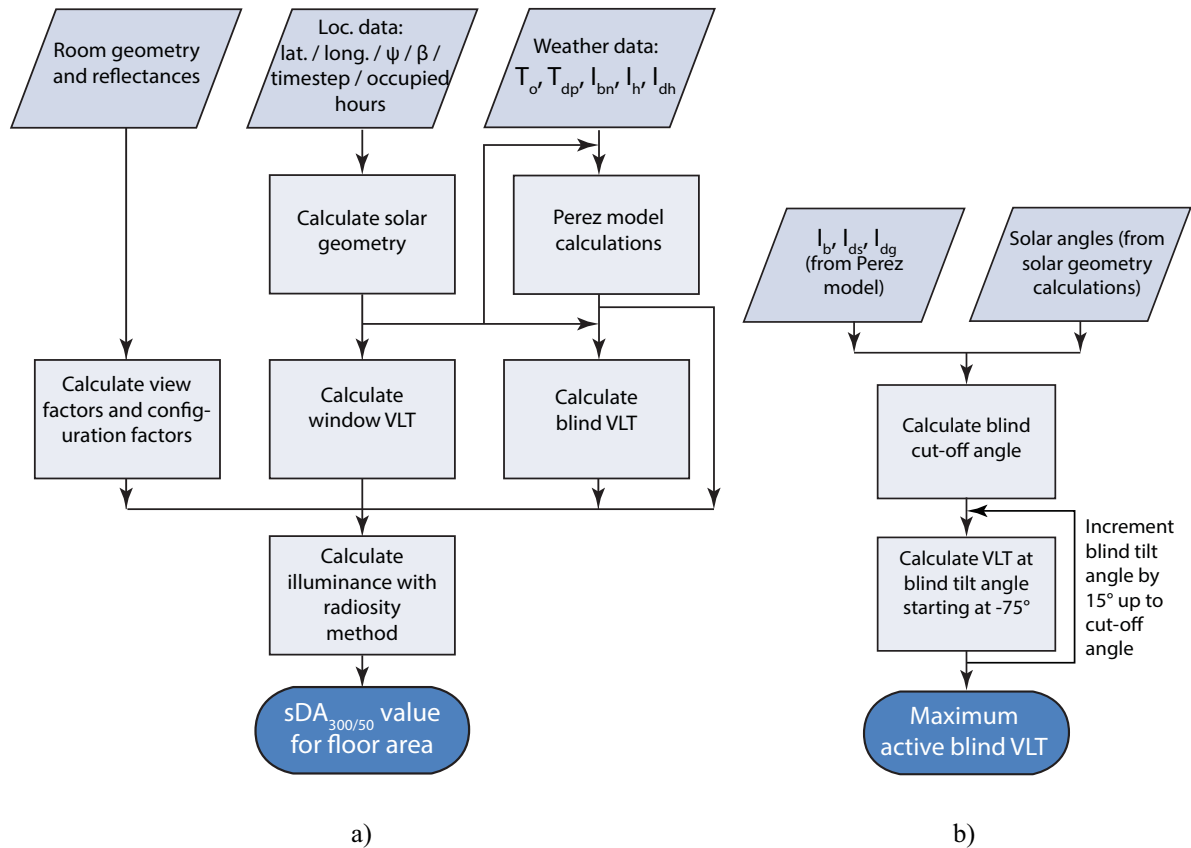


Figure 3.5: Simplified flowchart of a) daylighting model, b) active blind control strategy.

1. Room geometry

A representative cross-section on an intermediate floor of the North wing of the RSF is selected for the case study, as shown in the key plan in Figure 3.6. In Figure 3.7 the cross-section is unfolded to identify each interior surface by number and to locate all pertinent dimensions that are listed in Table 3.1. Of particular note are surfaces 9, 10, 11, and 12 which represent the windows. The overall dimensions of the representative cross-section

are 3.048 m wide, 3.963 m tall, and 18.000 m deep. The illuminance workplane is at 0.914 m and is used as the bottom surface of the representative cross-section (see Section 3.34 on modelling assumptions for an explanation of this). The ceiling geometry and interior furniture has been simplified in the 19-surface model. Since the building section is very deep, it has been subdivided into a South zone, interior zone, and North zone, referred to in the model as BaySouth_{dep}, BayMiddle_{dep}, and BayNorth_{dep}.

*This representative cross-section, with the aforementioned dimensions will be referred to as the reference, or **base building** in the rest of this document. The base building in the existing location of Golden, CO will be referred to as the **base case**.*

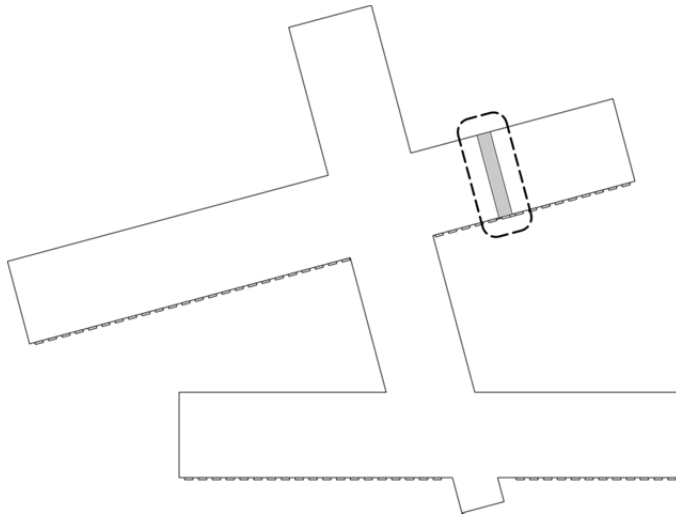


Figure 3.6: Key plan of RSF showing location of representative cross-section.

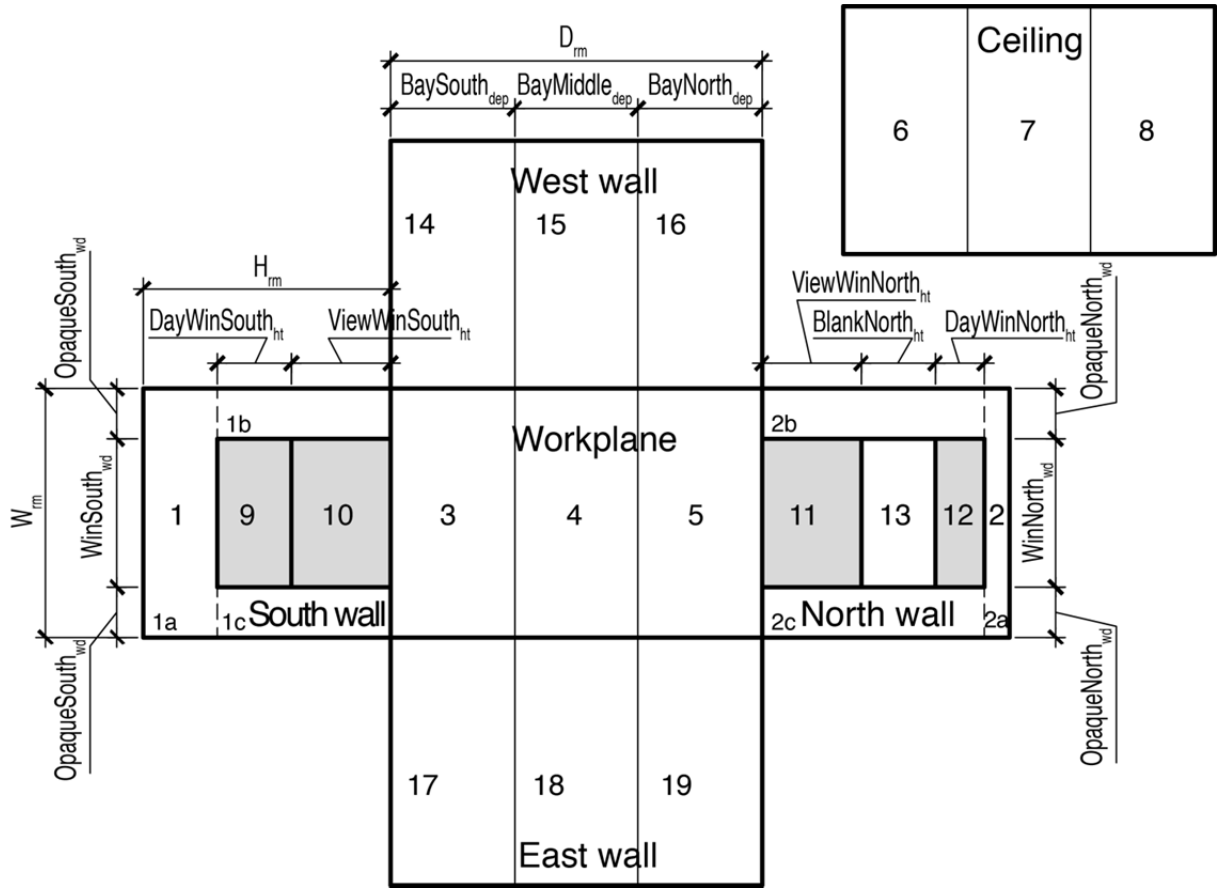


Figure 3.7: Representative cross-section unfolded, its surfaces labeled, and dimensioned.

Table 3.1: Dimensions of the representative cross-section.

Variable	Value (m)
D_{rm}	18.0
W_{rm}	3.0
H_{rm}	3.048
$WinSouth_{wd}$	1.8288
$DayWinSouth_{ht}$	0.9144
$ViewWinSouth_{ht}$	1.2192
$WinNorth_{wd}$	1.8288
$DayWinNorth_{ht}$	0.762
$ViewWinNorth_{ht}$	1.2192
$BlankNorth_{ht}$	0.9144
$BaySouth_{dep}$	8.55
$BayMiddle_{dep}$	3.075
$BayNorth_{dep}$	6.375
$OpaqueSouth_{wd}$	0.586
$OpaqueNorth_{wd}$	0.586

2. Effective visible reflectances of surfaces

The effective visible reflectances of the model surfaces, shown in Table 3.2, were determined through the calibration of the mathematical model. For more information about the visible reflectance values, see Section 3.5 on model calibration.

Table 3.2: Effective visible reflectances of surfaces.

Surface number																		
1	2	3	4	5	6	7	8	9	10	11	12	13	14	15	16	17	18	19
Reflectance																		
0.4	0.4	0.4	0.2	0.2	0.5	0.6	0.4	0.2	0.2	0.2	0.2	0.4	0.5	0.54	0.1	0.5	0.54	0.1

3. Simulation time step and length of simulation

All simulations are performed at a time step of 1 hour as specified by the sDA_{300/50} standard. Since the simulations are for an office building, only the time when the building is normally occupied is simulated. This is weekdays from 08:00 to 17:00, for a total of ten simulations a day and a total of 2610 time steps evaluated for the year.

4. Modeling assumptions

Because the results from the simulations are intended to assist in making design choices at early schematic design, there are some simplifications and assumptions made in the modelling process that reflect this.

1. Except for the instance of the model calibration, building models are simulated without external obstructions such as other buildings or landscaping.
2. The LightLouver is assumed to be 100 % effective at blocking direct sunlight into the space.
3. The reflections from the LightLouver, Vision Control blind, and the interior finishes do not contain a specular component (i.e. all reflections are uniformly diffuse).
4. The fixed exterior sun shading device over the South view window blocks all the direct solar radiation and 60 % of the diffuse solar radiation from entering the building.

5. Because all direct solar radiation is assumed to be blocked by the LightLouver, the Vision Control blind, and the fixed exterior sun shading device from entering the building, a daylight glare analysis was not performed.
6. The workplane is defined at a height of 0.914 m to align it with the height of the window sill. Thus, the floor cavity below the window sill coincides with the floor cavity below the workplane. This allows us to represent the reflectance of the floor cavity below the window sill by an effective reflectance for a horizontal surface (Murdoch, 2003) that also represents the reflectance of the floor cavity below the workplane. The $sDA_{300/50}$ metric uses 0.8 m for workplane height.
7. The visible reflectance values of the interior furnishings have been subsumed into the visible reflectance values of the interior surfaces in the model.
8. The $sDA_{300/50}$ metric was established using research conducted between latitudes $37^{\circ}N$ and $48^{\circ}N$ in North America and is applicable within this range. It is assumed that $sDA_{300/50}$ is applicable to Phoenix ($33^{\circ}N$) and Vancouver ($49^{\circ}N$).

5. Weather data

There are two sources of weather data used in the case study. The weather data for the model calibration were sourced from the NREL weather station that is located on the campus of the RSF building (NREL 2014). A sample is shown in Appendix A2.1. The weather data for the annual simulations were sourced from EnergyPlus-formatted weather (EPW) files. For these EPW files, the American cities' data were sourced from Typical Meteorological Year 3 (TMY3) data and the Canadian cities' data were sourced from Canadian Weather for Energy Calculations (CWEC) data (U.S. Department of Energy, 2013).

The source weather data from both the NREL onsite weather station and the TMY3/CWEC data are recorded at one minute intervals and are presented ordinarily in an hourly format where the minute by minute data from the 60 minutes up to and including the timestamp are averaged and attributed to the timestamp (Wilcox and Marion, 2008). This means that

each average hourly data point is temporally centered on the half-hour previous to the timestamp.

In the daylighting simulations, the time steps are also hourly, but the sun's position in the sky is ordinarily calculated hourly on the hour in the model, hence creating a half-hour offset between the solar position and the irradiance information from the weather data. This is not an issue with the NREL weather station weather data used for the model calibration since the illuminance data collected on site was collected at every hour on the hour.

For the annual daylighting simulations, the mathematical model's algorithm was reprogrammed to calculate the sun position at the half-hour preceding each time step to synchronize with the EPW hourly data. The alternative to repack each of the 8760 time steps in each relevant EPW file was judged to be too time consuming and prone to error since each additional future location that can potentially be simulated will have to have its EPW weather file repacked before use in the simulation model.

Furthermore, the EPW weather data is presented in the format of hour of the year, that is, from one to 8760. This had to be converted to the day, and hour of the day format, that is, from one to 365 and from one to twenty-four, that the solar position calculations use in the model. This weather data conversion algorithm was adapted from Tzempelikos (2005).

6. Solar geometry calculations

The sun's location in the sky relative to the building is determined for each time step (time, date, location). This information is needed as input for the Perez sky model as well as for determining the visible transmittance of the windows and the daylight redirecting blinds. Notable quantities are the incidence angle, altitude angle used in the Perez model, and the incidence and profile angles used for the glazing and daylight redirecting blinds. See Appendix A1.4 for all solar geometry equations used.

7. Window data

The following window specifications in Table 3.3, taken from the ASHRAE Handbook (ASHRAE 2009) are used in the mathematical model. Curve fitting was used to generate

mathematical expressions that are incorporated in the mathematical model. See Table 3.4 for the window assignments in the simulations. Note that the designations “low” and “high” visible light transmittance (VLT) are relative distinctions within the simulations. By design, the glazing for the daylighting windows must have high VLT to fulfill their task as part of the daylight redirecting system. As an example, in the LightLouver company’s planning guide, a minimum recommended VLT for the daylighting window is 65 %³.

Table 3.3: Window specifications.

	Window description	Multi-glazing	SHGC		Visible Transmittance	
			Normal incidence	Diffuse	Normal incidence	Diffuse
A	Low SHGC / VLT (RSF daylighting window)	Double-glazed	0.37	0.32	0.70	0.58
B	High SHGC / VLT	Double-glazed	0.70	0.61	0.76	0.64
C	Low SHGC / VLT (RSF view window)	Triple-glazed	0.36	0.30	0.59	0.44
D	High SHGC / VLT	Triple-glazed	0.62	0.52	0.68	0.56

Table 3.4: Window assignments to surfaces in the simulation model.

	surface number	Low VLT (c1)	High VLT (c2)
DayWinSouth	9	A	B
ViewWinSouth	10	C	D
ViewWinNorth	11	C	D
DayWinNorth	12	C	D

8. LightLouver visible light transmittance

The visible light transmittance data in Table 3.5 was obtained from the LightLouver company (Rogers, 2013). Like with the window data, curve fitting was used to generate a mathematical expression for the visible transmittance (Figure 3.8) to be used in the mathematical model.

³ See http://lightlouver.com/uploads/LL_Guidelines_NEW_8_29_13.pdf

Table 3.5: LightLouver visible transmittance.

Angle of incidence (°)	Visible transmittance (%)
25	35
50	55
75	77
	Diffuse visible transmittance
All angles	57

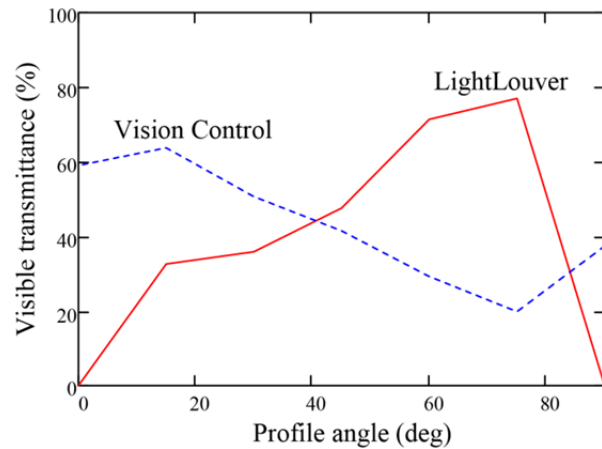


Figure 3.8: Visible light transmittance of LightLouver and Vision Control blinds.

9. Vision Control visible light transmittance and control strategy

The Vision Control system visible light transmittances (Figure 3.8) and control strategy were obtained from a previous study by Peng (2009). The visible light transmittances were modified to include an adjustment factor to reduce visible transmittance when incidence angles occur at large solar-surface azimuth angles. The control strategy was and modified to change the base angle from which the control strategy increments the blind tilt angles. The blind control is optimized for maximum effective transmittance since view to the outside is not essential because the daylighting window is above the line of sight of a standing adult.

There are two conditions that the blinds are programmed for.

1. For clear skies, the blinds are tilted to the blind angle at which beam radiation is blocked from entering the room and for which the visible transmittance is a maximum. The maximum visible transmittance is determined at each time step using a lookup table pairing solar profile angles with blind tilt angles (Peng, 2009).

2. For overcast skies, a solar radiation maximum of 100 W/m^2 was used to determine this condition. The blinds are open to the tilt angle of maximum transmittance. This turns out to be 15° (as measured clockwise from the vector normal to the window surface, pointing towards the exterior).

Section 3.4 Daylighting metrics

$sDA_{300/50}$ is used as the metric to evaluate the daylighting performance of the different model options. $sDA_{300/50}$ is suited to this study since the metric was based on an analysis of 61 daylit common workplace environments in the United States by daylighting experts and building occupants (Saxena et al., 2010). This consisted of open offices, classrooms, meeting rooms, etc. The metric is a good compromise between detailed single point-in-space metrics such as daylight autonomy which provide excessive information and accuracy especially in a simplified model; and single point-in-time daylighting simulations which are too simplified and do not provide a performance picture of the entire year. Another advantage of $sDA_{300/50}$ is that it is a spatially weighted application of daylight autonomy that relates the values to a percentage of building area (IESNA, 2012) which is easier to visualize in terms of impact on the building form than other metrics which remain abstract and have no direct relationship to building form as understood by designers at the schematic design stage. An illuminance quantity was used to evaluate the daylighting performance of the space. In future work, a luminance metric can also be applied to determine if there are any potential glare issues in the space.

Section 3.5 Model calibration

Interior horizontal illuminance measurements were taken at the RSF on 16 January 2013, a clear sunny day, in a typical office bay on an intermediate floor during daylight hours at locations of 3.66 m (12 ft.), 9.14 m (30 ft.), 12.19 m (40 ft.), and 16.46 m (54 ft.) from the South façade. The measurements were taken at a distance of 0.84 m (33 in.) from the finish floor. See Table 3.6. The model was calibrated to within a relative error (RER) of $\pm 15\%$

on all but two measurements which are within +20 % RER. For all points, the coefficient of variation of the root-mean-square error (CVRMSE)⁴ is below 13 % and the normalized mean bias error (NMBE)⁴ is between -1.4 % and 4 %. See Table 3.6, Table 3.7, and Figure 3.9. This accuracy is considered acceptable for the intended use of the model as a support tool for decision-making at the start of the schematic design phase. The variance with which the model can predict interior horizontal illuminance is in line with the level of design contingency at the end of the schematic design phase of up to 15 %. In this context, even if the model were more accurate in its ability to predict illuminance values, that accuracy would be lost on the overall design process since the building design is only at best 25 % complete at this point in the project.

Nevertheless, it is instructive to examine the error results for possible improvement for future work. First and foremost, the building geometry was simplified to just 19 surfaces to represent the entire space. The effects on the interior illuminance of many of the physical features of the space were subsumed into the reflectance values of the room surfaces. Examples are the window depth and framing and the open web steel joints in the ceiling cavity.

Likewise, the interior furnishings have an influence on the light distribution in the space. They reflect and absorb light depending on their geometries, locations, and material properties such as reflectance and absorptance. These, too, are represented in the room surface reflectance values.

The interior horizontal illuminance measurements were taken at a workplane height of 0.84 m (33 in) whereas the workplane height was modelled at 0.91 m (36 in.) to align it with the height of the window sill in order to reduce the number of surfaces in the radiosity model. Since the windows are the source of the daylight, and the measurements were taken

⁴ $CVRMSE = \frac{\sqrt{\frac{1}{n} \sum_i^n (\hat{y}_i - y_i)^2}}{\bar{y}} \times 100\%$, and $NMBE = \frac{\frac{1}{n} \sum_i^n (\hat{y}_i - y_i)}{\bar{y}} \times 100\%$, where \hat{y}_i is the simulated value; y_i is the measured value; \bar{y} is the mean measured value; and n is the number of measurements.

Table 3.6: Model calibration data and relative error.

Time hour	Simulated				Measured data				Relative error, RER			
	Pt 1 (12 ft) lux	Pt 2 (30 ft) lux	Pt 3 (40 ft) lux	Pt 4 (54 ft) lux	Pt 1 lux	Pt 2 lux	Pt 3 lux	Pt 4 lux	Pt 1 %	Pt 2 %	Pt 3 %	Pt 4 %
9	718	221	92	141	700	210	90	150	2.6	5.4	2.6	-5.9
10	854	265	113	181	810	230	100	170	5.4	15.1	13.4	6.8
11	919	283	117	174	950	260	110	200	-3.2	8.9	5.9	-12.8
12	929	285	117	172	980	330	130	150	-5.2	-13.5	-10.2	15.0
13	872	268	110	164	790	310	130	150	10.3	-13.6	-15.3	9.5
14	706	218	92	144	590	220	90	120	19.7	-1.0	2.2	19.6

Table 3.7: Model calibration, CVRMSE and NMBE.

	Pt 1	Pt 2	Pt 3	Pt 4
	%	%	%	%
CVRMSE	8.0	12.8	11.6	12.4
NMBE	3.7	-1.3	-1.4	4.0

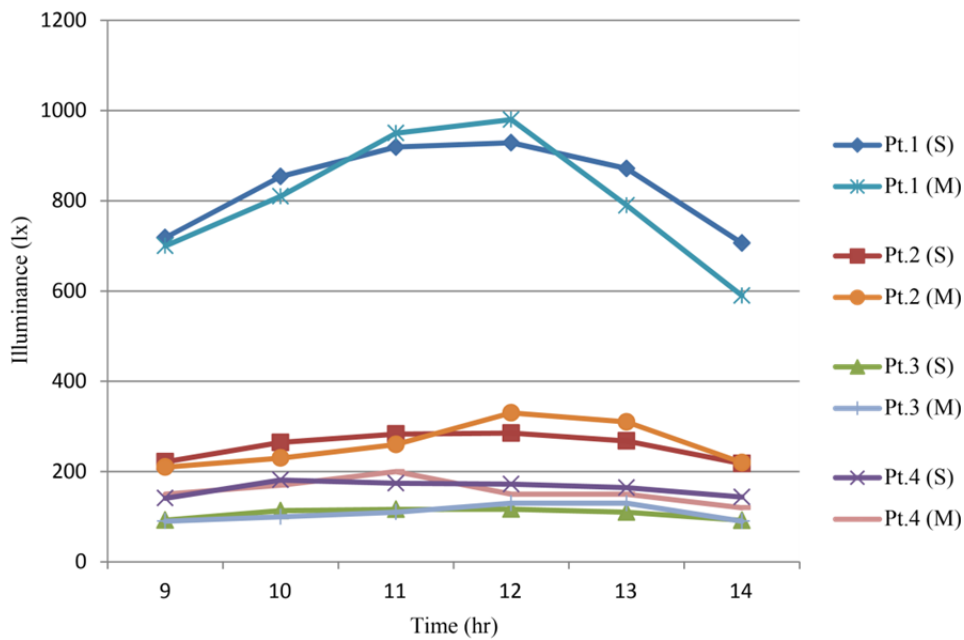


Figure 3.9: Simulated (S) and measured (M) illuminance values for model calibration.

at a height inferior to that of the window sill, the model simplification may be causing the model to slightly *under-predict* the illuminance of the workplane by attributing values to points that are 75 mm lower in real life than in the model (i.e. 75 mm lower from the light source in real life than in the model). However, it can be concluded that this assumption is not greatly skewing the results since the model calibration shows that each sensor point both under-predicts and over-predicts illuminance over the course of the day, and that at each time step the sensor points both under-predict and over-predict.

Furthermore, at each of the measurement times except for 10:00, the four sensor points have both positive and negative RER, suggesting that the fluctuations may be caused by inaccurate representation of the space geometry and physical properties. It may be that the simplification of the geometry ends up averaging the space properties uniformly when they should not be. For example, the furniture layout of the space is not symmetrical along an East-West axis; that is, the South side of the office is very open with low furniture partitions while the North side of the office has partitions that reach a height of 2 m. Although there is a distinction made in the model with surfaces subdivided for the South, middle, and North zones, this may not have been fine enough. A finer discretization may solve this problem at the cost of longer simulation calculation times.

Then, at each of the four sensor points, the RER is both positive and negative for different times of the day, suggesting that the fluctuations are caused by the averaging of the weather data or inaccurate modelling of the window optical response to the weather data or sun position.

The biggest source for error may be in the use of average hourly irradiance values. It was not possible to synchronize (to the minute) the exterior irradiance measurements with the interior illuminance measurements. This is due to the fact that the building is not an experimental laboratory or mock-up office, but a fully occupied and functioning office building with security and access restrictions. Sky conditions may vary from one instant to the next and choosing a value at a time step that is *just* one minute later than the actual one required may lead to errors. See for example, in Appendix A2.1, the irradiance data centred on 09:00. In a span of three minutes, from 08:59 to 09:01, the direct normal

irradiance – the largest component of solar radiation at that time – varies from 810.06 W/m² to 725.16 W/m² to 588.50 W/m². Irradiance input data that is too low or too high may explain why the illuminance predictions at each sensor point fluctuate between underestimating and overestimating.

The Mathcad model does not account for daylight obstructions due to objects in the building's immediate surroundings. The RSF's Phase I North Wing, from where the interior illuminance measurements were taken, experiences self-shading for certain periods of the day. To examine the extent to which self-shading may be a factor in the model calibration, a Rhinoceros 3d (McNeel North America, 2014) massing model was constructed using dimensions from building plans and then exported into Ecotect (Autodesk, 2011). Figure 3.11 and Figure 3.12 show the result of the Ecotect sun shading analysis of the RSF for 14:00 on 16 January. Although care was taken to model the building accurately in Rhinoceros, there was no on-site verification of the building dimensions. Taking this into account, it does appear that the bay in which the illuminance measurements were taken is *partially* in the shade at 14:00. Thus self-shading may account for why the Mathcad model's illuminance prediction at 14:00, 706.27 lx, is much higher than the measured value, 590 lx, accounting for the 19.7 % RER. Interestingly, it is at the same time step that the northernmost sensor point exhibits its highest calibration error. The Mathcad model predicts an illuminance of 143.53 lx while the measured value is 120 lx. In this case, although the error is high at 19.6 % RER, the quantities being measured are very small. The absolute difference between the predicted and measured values is only 23.52 lx, making the RER perhaps not a useful measure of the model's accuracy in this case. A global view of the point 4 calibration is that the CVRMSE is 12.4 %, considered acceptable.

Another assumption that may lead to errors is that all daylight entering the building is 100 % diffuse. This assumption was made to facilitate illuminance computation using a radiosity method. In reality, the exterior sunshades do not block 100 % of the direct sunlight into the building. In fact, Figure 3.10 shows direct sun entering the space and a user's makeshift sunshade installed at their workstation.



Figure 3.10: Makeshift sunshade installed at a workstation.

Additionally, the LightLouver's reflections exhibit some specularity. Since the radiosity method does not take this into account, it may be that the Mathcad model under predicts interior illuminance in the presence of strong direct sun.

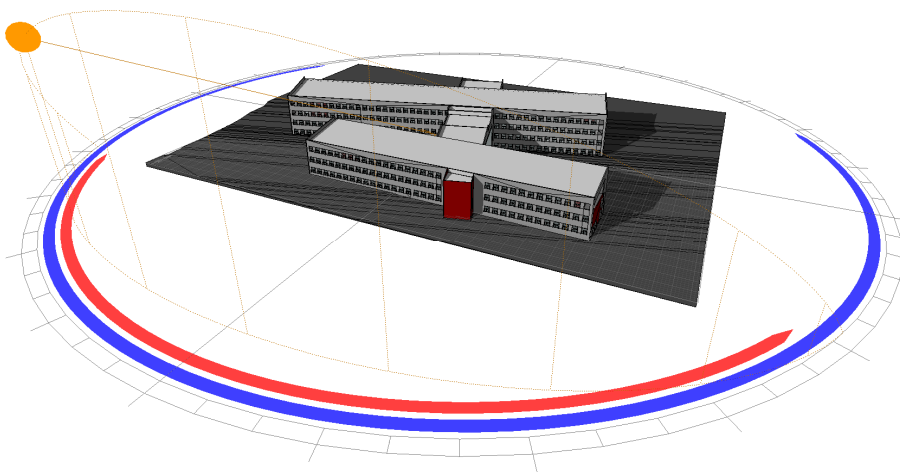


Figure 3.11: Ecotect sun shading analysis of the RSF for 14:00 on 16 January.

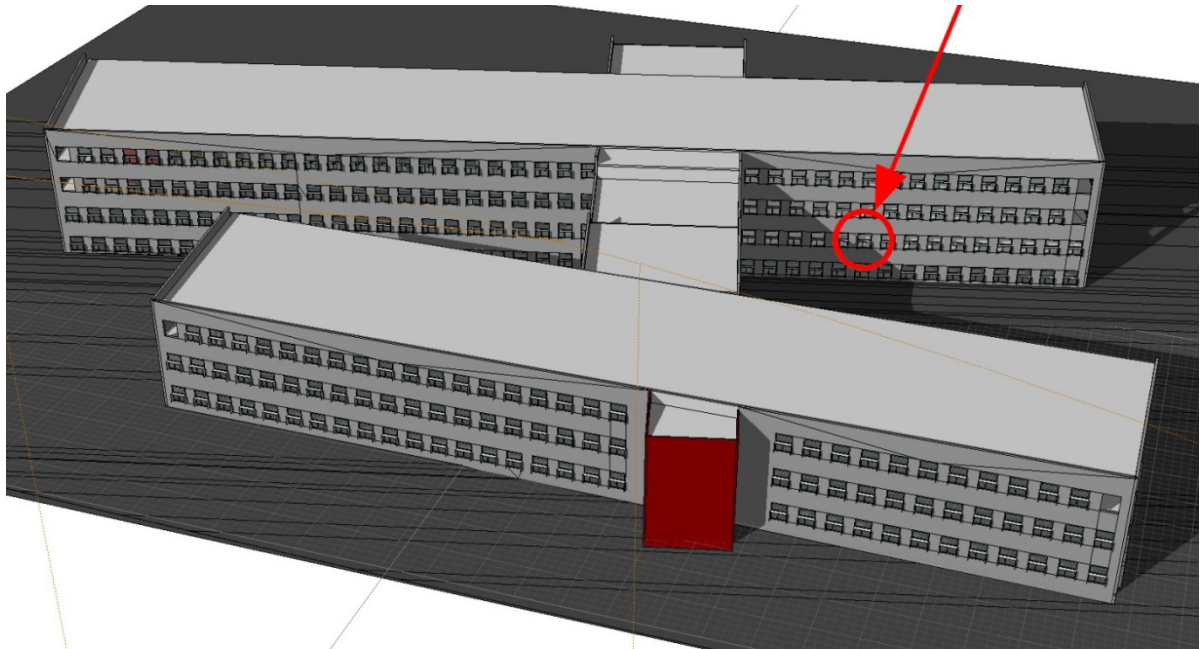


Figure 3.12: Ecotect sun shading analysis of the RSF for 14:00 on 16 January; closer view showing self-shading.

Section 3.6 Model verification for LEED v2.2

As part of the RSF’s original project objectives, as outlined in NREL’s RFP documents⁵, a very high priority agenda item was for the building to attain LEED v2.2 Platinum status in the category of New Construction and Major Renovation. This is the highest LEED performance rating attainable. This desire can be seen as a natural extension of the principles of the integrated design process (IDP) and enhanced project delivery methods that were emphasized as the best way to design and construct an exemplary net-zero energy building. The RFP documents further codify this and serve as the framework for the collaborative process (RFP Part 1 § 8.1) (NREL 2008a). It must be mentioned that NREL can be considered a “sophisticated client” (RAIC 2009). Typically, this is not a single person, but an organization with in-house expertise of the building industry (like architects or engineers) who can understand the building and construction process without reliance

⁵ The set of RFP documents are available at http://www.nrel.gov/sustainable_nrel/rsf.html

on third parties to make informed decisions on the building's design brief, construction budget, and future operation. This expertise is evidenced by the way they used the RFP to detail the performance specifications that the building design must meet.

In the performance specifications (See Question 11 of Amendment 5) (NREL 2008b), it is stipulated that the building is to satisfy the requirements for the LEED v2.2 IEQ 8.1 – Daylighting credit. The aim of this credit is to enhance indoor environmental quality by the use of daylighting for a substantial portion of the regularly occupied area of the building during regularly occupied hours. The compliance path chosen for the credit was option 2, which was the one using a daylight simulation model. In option 2, the simulation model has to demonstrate a minimum daylight illuminance of 250 lx (25 fc) on a horizontal plane 0.76 m (30 in) above the floor in 75 % of all regularly occupied spaces under clear sky conditions at noon at the equinox. (U.S. Green Building Council, 2005).

As a verification of the Mathcad model's daylight performance prediction abilities, a simulation was run for each wing (i.e. with $\psi = 0$ and $\psi = -15^\circ$) with the parameters for the abovementioned LEED v2.2 IEQ 8.1 daylighting credit. A 0.5 m x 0.5 m illuminance calculation point grid, or analysis grid, was used at 0.92 m above the finish floor level, with a maximum offset of 0.5 m from any wall. The Mathcad simulation calculated a minimum of 250 lx in 75 % and 78 % of the floor area in the North wing ($\psi = -15\text{deg}$) and South wing ($\psi = 0$) respectively, both meeting the threshold required by the LEED credit. See Figure 3.13 and Figure A0.1 for falsecoloured illuminance maps of the model and an illuminance graph taken along the centreline of the model. As previously discussed, due to reasons of modelling simplification, the workplane was taken at a height of 0.914 m even though the four sensor points were at 0.84 m above the finish floor. Thus, it can be inferred that the illuminance levels predicted at 0.76 m, the height stipulated in the LEED v2.2 IEQ 8.1 credit, would be slightly *higher*, resulting in the calculation for the LEED credit to be *greater* than the required 75 % minimum. Although this LEED v2.2 simulation is a static, single point-in-time calculation, it nevertheless shows that the Mathcad model is capable of correctly predicting that this building design earned the LEED daylighting credit IEQ 8.1. Also see Appendix A2.2 for more data and graphs.

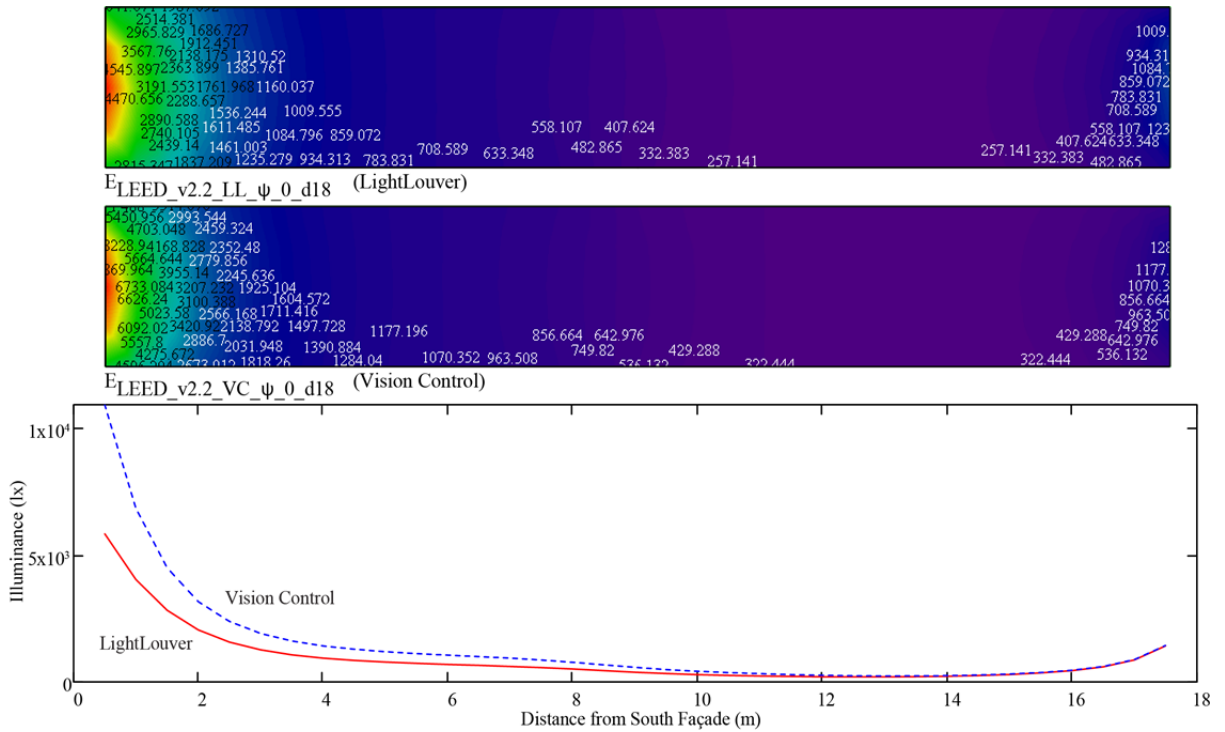


Figure 3.13: Analysis Grid Illuminance; 12:00, 22 September; $\psi=0$; LightLouver (top) and Vision Control (middle); illuminance X-Y plot (bottom) [lx].

Section 3.7 Illuminance analysis grid resolution

The horizontal workplane for this case study was defined at 0.915 m above the finish floor. A horizontal illuminance analysis grid, facing upwards, was placed on the horizontal workplane to measure the illuminance distribution of the interior space. There are two densities of analysis grids defined in the mathematical model, one at 1.0 m x 1.0 m between analysis points, and the other at 0.5 m x 0.5 m. 0.6 m x 0.6m represents the coarsest analysis grid recommended by the IESNA (2012). Full annual time-series illuminance simulations were performed using both analysis grids to observe the effects of the analysis grid resolution on the simulation results. Table 3.8 shows the $sDA_{300/50}$ simulation results from the two model resolutions across the range of orientations, daylight redirecting systems, and window types. At the bottom of the table is the relative error (RER) calculated with the assumption that the $sDA_{300/50}$ values for the 0.5 m x 0.5 m grid are the “correct” ones. The coarser model under predicts with a minimum of -9.1 % RER for the case of the Vision Control, $\psi = -15^\circ$ orientation, using the high visible light transmittance (VLT) glazing; and it under predicts with a minimum of -6.0 % RER for the

case of the LightLouver, $\psi = -30^\circ$ orientation, using the high VLT glazing. The coarser model over predicts with a maximum of 9.6 % RER for the case of the Vision Control, $\psi = -15^\circ$ orientation, using the low VLT glazing, and over predicts with a maximum of 11.1 % RER for the case of the LightLouver, $\psi = -15^\circ$, 0 orientation, using the low VLT glazing. The coarser model under predicts by a maximum of -9.1 % and over predicts by a maximum of 11.1 %. Overall, it appears that the coarser model under- and over predicts at a similar frequency.

Figure 3.14 shows another comparison between the 0.5 m x 0.5 m analysis grid model and the 1.0 m x 1.0 m analysis grid model. It shows the DA_{300} values of the analysis grid taken at a section along the central axis of the model. The condition for South orientation ($\psi = 0$), LightLouver, and low VLT is shown. It is representative of the other orientations and the Vision Control blind. The biggest divergence of the two graphs occurs at two conditions: 1) at very low DA_{300} values, which corresponds to the middle zone of the space; and 2) near the North façade, which corresponds to a zone with a large illuminance gradient (falloff) in a short horizontal distance perpendicular to the window (i.e. light source). This can explain why the coarser model has difficulty resolving the illuminance patterns in these areas. However, since the illuminance levels in the middle zone are much lower than the DA_{300} threshold of 50 % required for the $sDA_{300/50}$ metric, the points in the middle zone would not contribute to the $sDA_{300/50}$ total regardless if the model had a higher resolution to resolve more accurately their illuminance values or not. As for the North zone, the horizontal depth of the zone through which the illuminance gradient drops precipitously is so shallow as to limit its impact on the overall $sDA_{300/50}$ value for the space. In spite of these differences, the overall DA_{300} profile of the lower resolution analysis grid tracks very closely to the higher resolution analysis grid. See Appendix A2.3 for more detailed results.

Table 3.8: Comparison of illuminance analysis grids: Golden, LightLouver and Vision Control blind, 1.0 m x 1.0 m and 0.5 m x 0.5 m grid, sDA_{300/50} [%].

sDA _{300/50}	Orientation ψ													
	-45°		-30°		-15°		0		15°		30°		45°	
Golden	low VLT	high VLT	low VLT	high VLT	low VLT	high VLT	low VLT	high VLT	low VLT	high VLT	low VLT	high VLT	low VLT	high VLT
1.0 m x 1.0 m grid														
LightLouver	28	35	33	41	39	44	39	44	33	44	33	41	28	35
Vision Control	33	35	39	41	44	44	39	44	39	46	33	41	30	35
0.5 m x 0.5 m grid														
LightLouver	29	36	34	43	35	46	35	46	35	43	32	39	29	35
Vision Control	31	36	37	43	41	49	41	47	38	43	32	38	31	35
RER *														
LightLouver	-5.7	-2.6	-1.6	-6.0	11.1	-3.6	11.1	-3.6	-4.8	2.6	3.4	3.3	-5.7	0.5
Vision Control	9.1	-2.6	6.1	-6.0	9.6	-9.1	-4.1	-5.9	2.9	6.8	3.4	7.8	-3.0	0.5

* The 0.5 m x 0.5 m grid is the reference

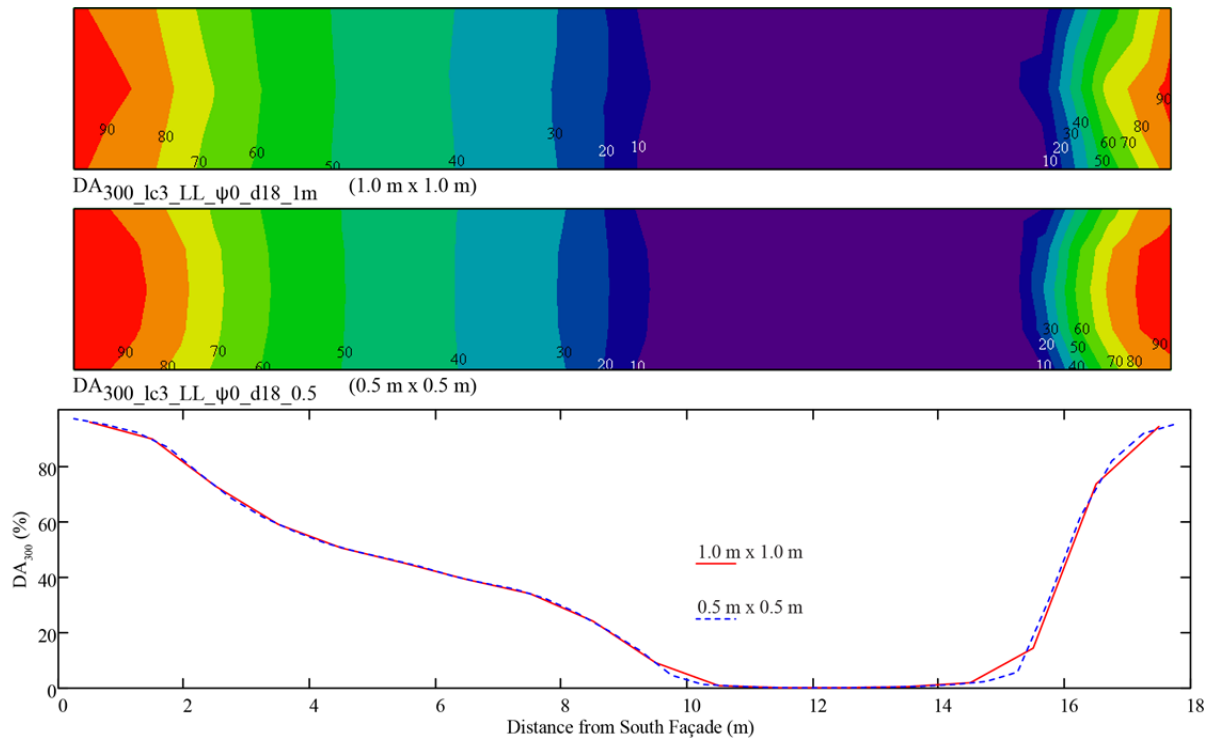


Figure 3.14: Comparison of illuminance analysis grids: Golden, LightLouver, $\psi = 0$; DA₃₀₀ contour plot (1.0 m x 1.0 m grid at top, 0.5 m x 0.5 m grid in middle) and DA₃₀₀ X-Y plot (bottom) [%].

Another issue of model resolution is in the geometric description of the office space. As previously stated, the effects of the furniture geometry and physical properties on the reflectances of the room are represented by the 19 surfaces in the model. Because surfaces 3, 4, 5 (workplane); 6, 7, 8 (ceiling); 14, 15, 16 (West wall); and 17, 18, 19 (East wall) represent a coarse subdivision of continuous, planar surfaces, the edges at their intersections register as “bumps” in the illuminance graphs. The “bumps” represent the transitional effects of the model resolution from one zone and the next and is most prominent in the lower, X-Y plot in Figure 3.14 at the transition from the South bay to the middle bay, at approximately 8 m from the South facade. This artifact is attenuated with denser subdivisions of the model surfaces. But, since the final metric used in the case study is $sDA_{300/50}$, its averaging of the illuminance in the room prevents the “bumps” from having a disproportionate effect on the predicted results. *Thus, a case can be made that the lower resolution 1.0 m x 1.0 m sensor grid is sufficient for use in support of design decisions made at the beginning of schematic design.*

Note that simulations with the 0.5 m x 0.5 m grid were only performed for the existing building in the Golden climate. All other simulations are with the 1.0 m x 1.0 m analysis grid. Performance comparisons are never made between simulations with the 0.5 m x 0.5 m analysis grid and the 1.0 m x 1.0 m analysis grid except for the purpose of measuring the effects of grid resolution on DA_{300} and $sDA_{300/50}$ as described above.

Chapter 4 Methodology part 2: building design parameters

Section 4.1 Base case: comparative analysis of the LightLouver and the Vision Control blind (existing location)

After model calibration, the preliminary simulations are to compare the daylighting performance of the LightLouver passive daylight redirecting blind with the Vision Control active daylight redirecting blind in the RSF's existing location of Golden. Table 4.1 shows the parameters of importance in this comparison. Annual simulations are run for both daylight redirecting blinds and for both the South wing, which faces directly south ($\psi = 0$), and the North wing which is oriented 15° East of South ($\psi = -15^\circ$). Other than changing the daylight redirecting blind on the South daylighting window, all other parameters are the same as in the existing building.

Table 4.1: Simulation parameters: comparison of LightLouver and Vision Control blinds.

Parameter	Symbol in simulation	Values tested
Location (Climate)	lc	lc3 = Golden, CO (40°N, 105°W)
Building orientation	ψ ($\psi = -90^\circ$ is due East; $\psi = 0^\circ$ is due South; $\psi = 90^\circ$ is due West)	$-15^\circ, 0$
Daylight redirecting blind	cfs	LightLouver (cfs1) Vision Control (cfs2)
Visible light transmittance	VLT	* 59 % and 70 % (c1)
Window to Wall Ratio (South façade)	WWR _s	33 %
Window Head Height (South façade)	WHH _s	3.048 m
Building depth	D	18.000 m

* The pair of VLT values are used together since one is used by the view window and the other by the daylighting window

The results show that the LightLouver and Vision Control blinds obtain $sDA_{300/50}$ values of 35 % and 41 %, respectively (Table 4.2). This is the same result for both building wings. Based on these results, this building's daylighting performance would not meet the $sDA_{300/50}$ requirement of 55 % to be considered "nominally acceptable." Figure 4.1 shows

the results in a DA_{300} colour contour plot and X-Y plot for the South wing ($\psi = 0$). The colour contour plots are all oriented with the South façade on the left side of the page. The X-Y plots for this study all represent the row of illuminance analysis points going through the central axis in the building cross-section.

The X-Y plot shows clearly that the majority of the Vision Control blind’s illuminance performance gain occurs in the area that is between 4 m and 11 m from the South façade. Also, the simulations confirm, as normally expected, that the daylighting performance in the space near the North façade is virtually identical for the LightLouver and the Vision Control since the daylight redirecting blind is installed on the South façade daylighting window and has insignificant influence on the North zone illuminance. This can best be seen in the X-Y plot in Figure 4.1, as well. More results can be found in Appendix A3.1.

From this it is concluded that the Vision Control blind achieves a 17 % better illuminance performance relative to the LightLouver; all other conditions being equal.

Table 4.2: Base case: Golden, LightLouver and Vision Control blind, $sDA_{300/50}$ [%].

0.5 m x 0.5 m	$\psi = -15^\circ$ (15E) North wing	$\psi = 0$ South wing
LightLouver	35	35
Vision Control	41	41

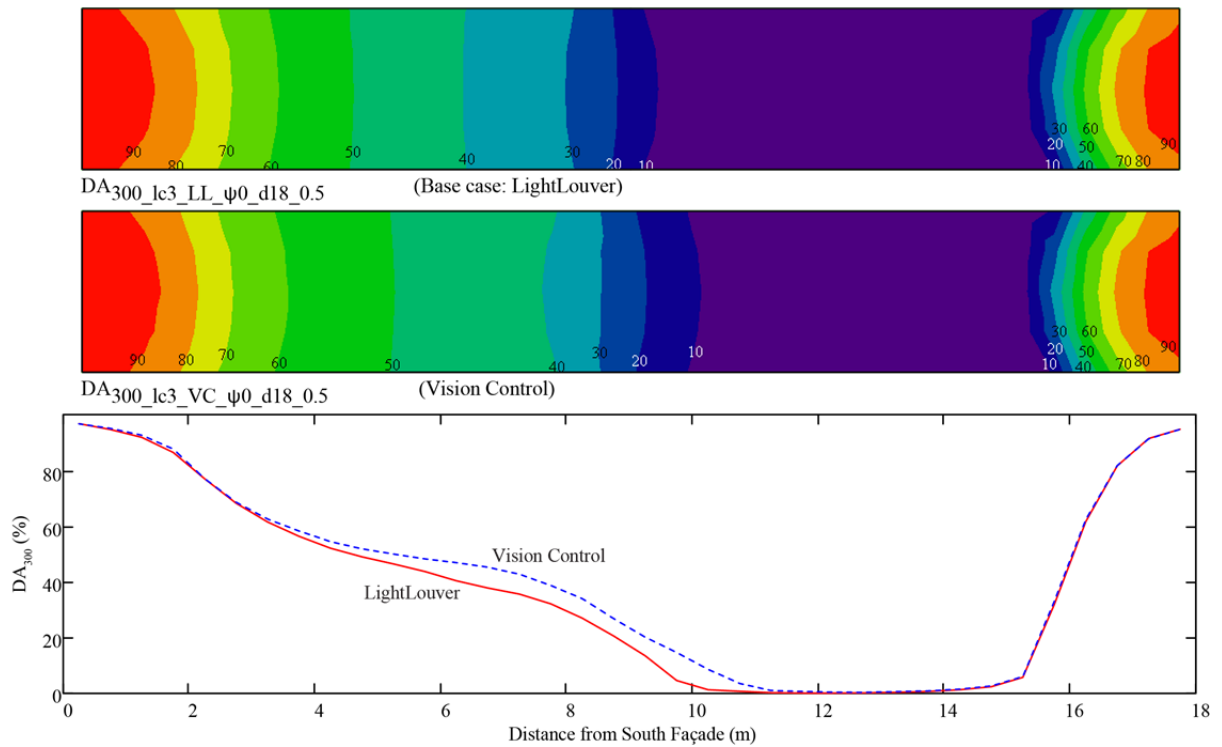


Figure 4.1: Base case: Golden, LightLouver and Vision Control blinds, $\psi = 0$; DA_{300} contour (top, middle) and X-Y (bottom) plots [%].

Section 4.2 Base building: extended daylighting study (effect of climate, building orientations, window properties)

With the daylight illuminance performance comparison of the LightLouver and Vision Control blinds in the RSF’s existing location complete, a second extended exercise is undertaken to determine if the illuminance performance of the two daylight redirecting blinds in the archetypal open-plan cross-section can be generalized to other locations and building parameters. The parameters that may have significant impact on early schematic design decisions are examined. These are summarized in Table 4.3 and described below. The DA_{300} and $sDA_{300/50}$ metrics will continue to be used to assess the daylight sufficiency of the building. Representative findings are shown; more results can be found in Appendix A3.2 to A3.6. The parameters describing the building depth and the geometry of the façade elements (window to wall ratio, window head height) will be discussed in succeeding sections.

Table 4.3: Simulation parameters – base building extended study.

Parameter	Symbol in simulations	Values tested
Location (Climate)	lc	Golden, CO (40°N, 105°W) (lc3) Montreal, QC (45°N, 74°W) (lc2) Vancouver, BC (49°N, 123°W) (lc4) St. John’s, NL (48°N, 53°W) (lc5) Phoenix, AZ (33°N, 112°W) (lc6)
Building orientation	ψ ($\psi = -90^\circ$ is due East; $\psi = 0^\circ$ is due South; $\psi = 90^\circ$ is due West)	-45°, -30°, -15°, 0, 15°, 30°, 45°
Daylight redirecting blind	cfs	LightLouver (cfs1) Vision Control (cfs2)
Window Visible Light Transmittance	VLT	* 59 % and 70 % (c1) * 68 % and 76 % (c2)
Window to Wall Ratio (South façade)	WWR_s	33 %
Window to Wall Ratio (North façade)	WWR_n	31 %
Window Head Height (South façade)	WHH_s	3.048 m
Window Head Height (North façade)	WHH_n	3.810 m
Building depth	D_{rm}	18 m

* Each pair of VLT values is used as a set since one is used by the view window and the other by the daylighting window

Location: Aside from Golden, CO, a range of locations across North America is chosen to examine the influence of geography and yearly insolation on the performance of the daylight redirecting blinds in the archetypal cross-section. Phoenix, AZ, is the southernmost and sunniest of the locations. St. John’s, NL, is the cloudiest. Table 4.4 shows the total annual sunshine hours at each location. The results across all locations are shown in Table 4.5. Figure 4.2 shows DA_{300} contour plots and X-Y plots comparing daylighting performance in all locations for $\psi = 0$. Phoenix has the best $sDA_{300/50}$ performance of all the locations, for all orientations, for the LightLouver and the Vision Control blind. With all other parameters being equal, we see that the area corresponding to $DA_{300} = 50 \%$, the daylit zone, for Phoenix is roughly twice as deep as for St. John’s. Golden is not far behind Phoenix in depth of daylit zone, followed by Montreal, Vancouver, and St. John’s. One interesting note is that the $sDA_{300/50}$ performance of

Phoenix is not a maximum at the South façade orientation as one normally expects. At $\psi = -15^\circ$ and $\psi = 0$, the daylighting performance in Phoenix is no better than that of Golden. It is only when moving the facade orientation away from due South that the daylighting performance gains in Phoenix are realized – as much as 57 % in the case of $\psi = -45^\circ$ as compared to Golden. See the next subsection on building orientation and latitude for possible explanations for these results.

Table 4.4: Annual number of sunshine hours by location.

Location	Annual sunshine hours
Montreal	2051
Golden	*
Vancouver	1938
St. John's	1497
Phoenix	3872

Canadian data from Environment Canada,

Phoenix data from the National Oceanic and Atmospheric Administration (NOAA).

* Data unavailable

Table 4.5: Base bldg. results by location, low VLT, daylight redirecting blind, orientation; $sDA_{300/50}$ [%].

$sDA_{300/50}$, low VLT, 1.0m x 1.0m	Orientation ψ						
	-45°	-30°	-15°	0	15°	30°	45°
Golden							
LightLouver (cfs1)	28	33	39	39	33	33	28
Vision Control (cfs2)	33	39	44	39	39	33	30
Montreal							
LightLouver (cfs1)	28	33	33	30	33	33	28
Vision Control (cfs2)	30	35	39	39	39	39	33
Vancouver							
LightLouver (cfs1)	19	20	24	24	24	20	19
Vision Control (cfs2)	20	24	24	24	24	24	20
St. John's							
LightLouver (cfs1)	24	20	24	24	24	24	20
Vision Control (cfs2)	28	24	24	24	24	24	28
Phoenix							
LightLouver (cfs1)	44	44	39	39	39	44	33
Vision Control (cfs2)	44	44	44	41	44	44	33

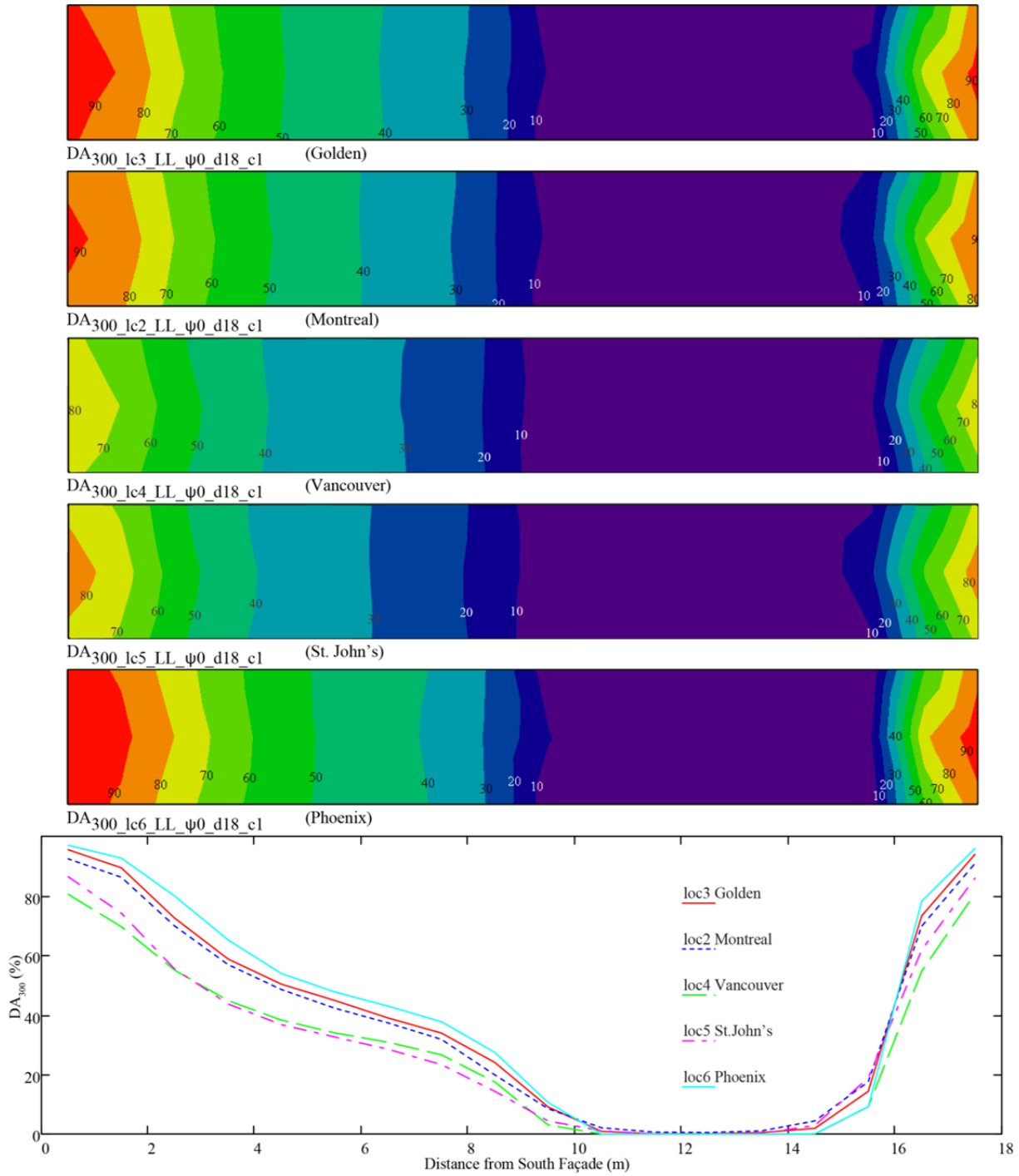


Figure 4.2: Base bldg.: all locations, low VLT, LightLouver, $\psi = 0$; DA_{300} contour (top, middle) and X-Y (bottom) plots [%].

Building orientation and latitude: Simulations are carried out to evaluate the daylight redirecting blinds' performance for a range of building orientations (ψ) from 45° West of South to 45° East of South. These angle limits were set based on the fact that incident solar radiation on façades with Eastern and Western orientations is very low on the horizon and horizontal louvers on such façades are typically not effective for solar control. Vertical louvers are best applied in such conditions.

From Table 4.5 we can observe that the best daylighting performance by façade orientation is not always at the South-facing façade. Because Phoenix is the location nearest to the equator in this study, it will be used to examine the effect of orientation and latitude on the amount of daylight that is transmitted through the equator-facing facade. A directly South-facing vertical surface in Phoenix does not have as much daylight transmitted through façade glazing due to large incidence angles and the incidence angle dependence of glazing transmittance. For example, at 12:30 on the summer solstice, 21 June, when the sun is at its highest point in the sky, the sun's altitude angle is approximately 80° which, in this case, is the same as the incidence angle since the solar-surface azimuth is zero. From the visible light transmittance graph of the RSF daylighting window in Figure 4.3, we see that visible light transmittance is approximately 70 % between incidence angles of zero to 50°. At larger incidence angles the visible light transmittance drops off precipitously. At an incidence angle of 80° the visible light transmittance is only approximately 20 %. Façade orientations farther away from due South will have their surface-solar azimuth equal to zero more often when the sun is lower in the sky, thus allowing more daylight transmission through the glazing.

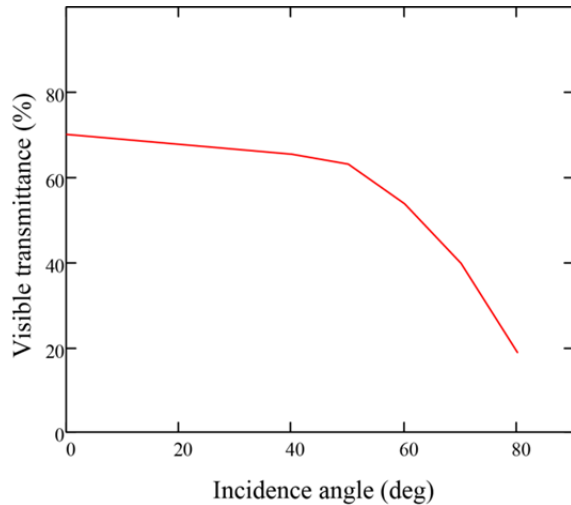


Figure 4.3: Visible light transmittance of RSF South daylighting window.

An analysis of the EnergyPlus Weather (EPW) files can offer another explanation why the best daylighting performance is not necessarily at a façade oriented due South. Table 4.6 shows the average annual insolation on a vertical façade for various orientations and locations calculated from the respective locations’ EPW files. From this we see that it is not always the South-facing façade that receives the most annual insolation. Montreal and Vancouver receive their maximum insolation at $\psi = 15^\circ$. For Phoenix, a vertical surface at $\psi = 15^\circ$ receives *almost* the same insolation as one facing due South. One last point that Table 4.6 may offer to help in understanding the sDA_{300/50} results across different orientations: insolation values are not symmetrical about the South axis. The EPW files capture local climate conditions such as mornings being sunnier than afternoons or vice versa.

Table 4.6: Average annual insolation on a vertical South facade [kWh/m²].

Location	ψ Orientation												
	-90°	-75°	-60°	-45°	-30°	-15°	0	15°	30°	45°	60°	75°	90°
Montreal	558	630	700	761	814	854	876	880	862	826	777	714	642
Golden	631	711	785	846	897	931	941	929	897	848	788	717	640
Vancouver	428	483	536	585	627	659	680	686	676	649	609	557	499
St. John's	453	504	554	597	632	654	662	653	629	594	554	508	461
Phoenix	763	853	923	975	1012	1032	1036	1035	1017	982	931	861	771

Window Visible Light Transmittance (VLT): There are four window types used. The windows represent typical choices for cooling and heating dominated North American climates. The low SHGC windows with VLT = 59 % and 70 % for the view and daylighting window, respectively, are used for the American locations; the high SHGC windows with VLT = 68 % and 76 %, respectively, for the Canadian locations⁶. The two windows in each set are always simulated together since one is for the daylighting window, the other for the view window. The high VLT windows offer better sDA_{300/50} performance by 13 % to 25 % for the case of the LightLouver and 0 to 24 % for the Vision Control, both for Golden (Table 4.7). An example contour plot and X-Y plot is shown in Figure 4.4.

Table 4.7: Golden, LightLouver and Vision Control blinds, window VLT comparison; sDA_{300/50} [%].

Golden, 1.0x1.0	ψ Orientation						
	-45°	-30°	-15°	0	15°	30°	45°
LightLouver							
Low VLT	28	33	39	39	33	33	28
High VLT	35	41	44	44	44	41	35
Vision Control							
Low VLT	33	39	44	39	39	33	30
High VLT	35	41	44	44	46	41	35

⁶ The descriptions “low” and “high” for SHGC and VLT are used relatively since the daylighting windows need to have a VLT of at least 65 % for useful daylight redirection.

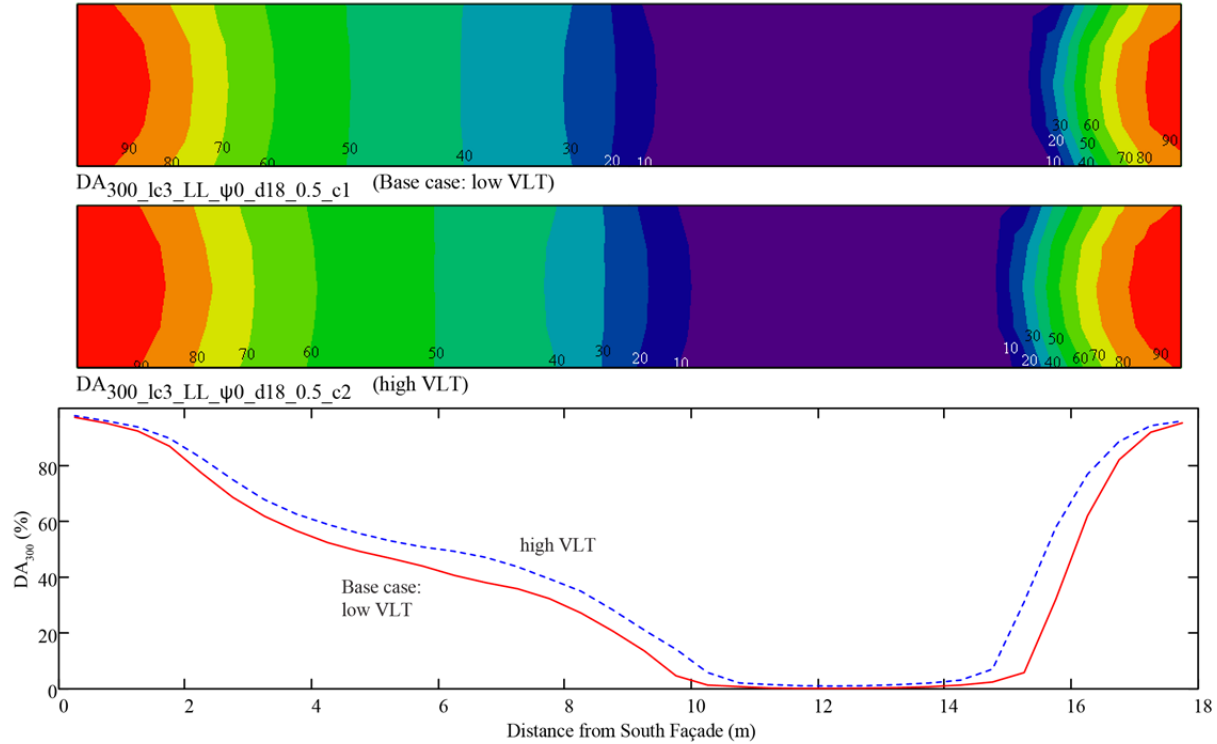


Figure 4.4: Base bldg.: Golden, low and high VLT, LightLouver, $\psi = 0$; DA_{300} contour (top, middle) and X-Y (bottom) plots [%].

Daylight redirecting blind: Referring to Table 4.8, for Golden, we see that at each façade orientation tested, the Vision Control blind daylighting performance is equal or better than the LightLouver except at $\psi = 30^\circ$ for high VLT windows. The Vision Control blind daylighting performance increase is as much as 17 % depending on façade orientation. *It can be concluded that in Golden, for most orientations, the Vision Control blind will improve $sDA_{300/50}$ daylighting performance by as much as 17 % compared to the LightLouver.* A similar result is found for the other locations.

Table 4.8: Golden; LightLouver and Vision Control blind comparison, $sDA_{300/50}$ [%].

sDA _{300/50} 0.5x0.5	Orientation ψ													
	-45°		-30°		-15°		0		15°		30°		45°	
Golden	low VLT	high VLT	low VLT	high VLT	low VLT	high VLT	low VLT	high VLT	low VLT	high VLT	low VLT	high VLT	low VLT	high VLT
LightLouver	29	36	34	43	35	46	35	46	35	43	32	39	29	35
Vision Control	31	36	37	43	41	49	41	47	38	43	32	38	31	35

Section 4.3 Effect of building depth on $sDA_{300/50}$

The effect of building depth on daylight illuminance is studied using the parameters described in Table 4.9. For the location of Golden, the building depth was varied from 11 m to 17 m and compared to the 18 m depth of the base building. Table 4.10 shows the complete results for the LightLouver and Vision Control blind with the low VLT and high VLT window options. For example, it shows that the **base building ($\psi = 0$, low VLT, LightLouver) achieves a daylighting illuminance performance that is “nominally acceptable” (i.e. $sDA_{300/50} = 55\%$) at a maximum building depth of 14 m. The further away from due South, the base building has to be shallower to achieve the same nominally acceptable daylighting performance. For $\psi = -15^\circ$, this depth is between 13 m and 14 m. At the furthest from due South, $\psi = -45^\circ$ and 45° , this building depth is between 12 m and 13 m.**

Table 4.9: Summary of simulation parameters – building depth study.

Parameter	Symbol in simulations	Values tested
Location (Climate)	lc	Golden, CO (40°N, 105°W) (lc3) Montreal, QC (45°N, 74°W) (lc2) Vancouver, BC (49°N, 123°W) (lc4) St. John’s, NL (48°N, 53°W) (lc5) Phoenix, AZ (33°N, 112°W) (lc6)
Building orientation	ψ	-45°, -30°, -15°, 0, 15°, 30°, 45°
Daylight redirecting blind	cfs	LightLouver (cfs1) Vision Control (cfs2)
Window Visible Light Transmittance	VLT	* 59 % and 70 % (c1) * 68 % and 76 % (c2)
Window to Wall Ratio (South façade)	WWR_s	33 %
Window to Wall Ratio (North façade)	WWR_n	31 %
Window Head Height (South façade)	WHH_s	3.048 m
Window Head Height (North façade)	WHH_n	3.810 m
Building depth	D_{rm}	11 m, 12 m, 13 m, 14 m, 15 m, 16 m, 17 m, 18 m

* Each pair of VLT values is used as a set since one is used by the view window and the other by the daylighting window

The Vision Control blind's sDA_{300/50} performance is equal to or better than the LightLouver's except for a handful of cases. The relative improvement is up to 22 % for low VLT windows and 12 % for the high VLT windows.

Figure 4.5 and Figure 4.6 offer graphical comparisons. From the contour plots in Figure 4.5 we can see that between a depth of 18 m and 15 m, the inadequately daylit area (dark colour in the contour plots) contracts until the 14 m depth when interzonal reflections start affecting the illuminance patterns in the building.

Table 4.10: Building depth: Golden, low and high VLT, LightLouver and Vision Control blind, orientation; sDA_{300/50} [%].

Golden		ψ orientation													
		-45°		-30°		-15°		0		15°		30°		45°	
Bldg. depth (m) blind		low VLT	high VLT	low VLT	high VLT	low VLT	high VLT	low VLT	high VLT	low VLT	high VLT	low VLT	high VLT	low VLT	high VLT
11	LightLouver (cfs1)	67	100	70	100	70	94	70	94	67	94	67	100	67	100
	Vision Control (cfs2)	82	100	76	100	76	94	76	94	76	94	70	100	82	100
12	LightLouver (cfs1)	61	81	61	78	64	75	67	75	58	75	61	78	61	81
	Vision Control (cfs2)	61	78	69	81	69	78	67	78	69	75	61	78	61	81
13	LightLouver (cfs1)	46	69	54	69	59	69	59	64	54	69	54	69	46	69
	Vision Control (cfs2)	54	69	62	69	62	69	62	69	62	69	54	69	49	69
14	LightLouver (cfs1)	43	57	50	60	50	60	55	60	50	60	50	64	43	57
	Vision Control (cfs2)	43	57	55	64	57	64	57	60	57	60	50	64	43	57
15	LightLouver (cfs1)	40	49	47	56	47	60	47	60	47	56	40	53	36	42
	Vision Control (cfs2)	40	49	47	56	53	62	53	60	53	56	47	49	40	42
16	LightLouver (cfs1)	38	42	44	52	44	52	44	54	44	52	38	46	31	40
	Vision Control (cfs2)	38	40	44	52	50	58	50	56	44	52	40	46	38	40
17	LightLouver (cfs1)	31	37	35	49	41	49	41	47	37	49	35	43	29	37
	Vision Control (cfs2)	35	37	41	49	47	53	47	51	41	49	35	43	31	37
18	LightLouver (cfs1)	28	35	33	41	39	44	39	44	33	44	33	41	28	35
	Vision Control (cfs2)	33	35	39	41	44	44	39	44	39	46	33	41	30	35

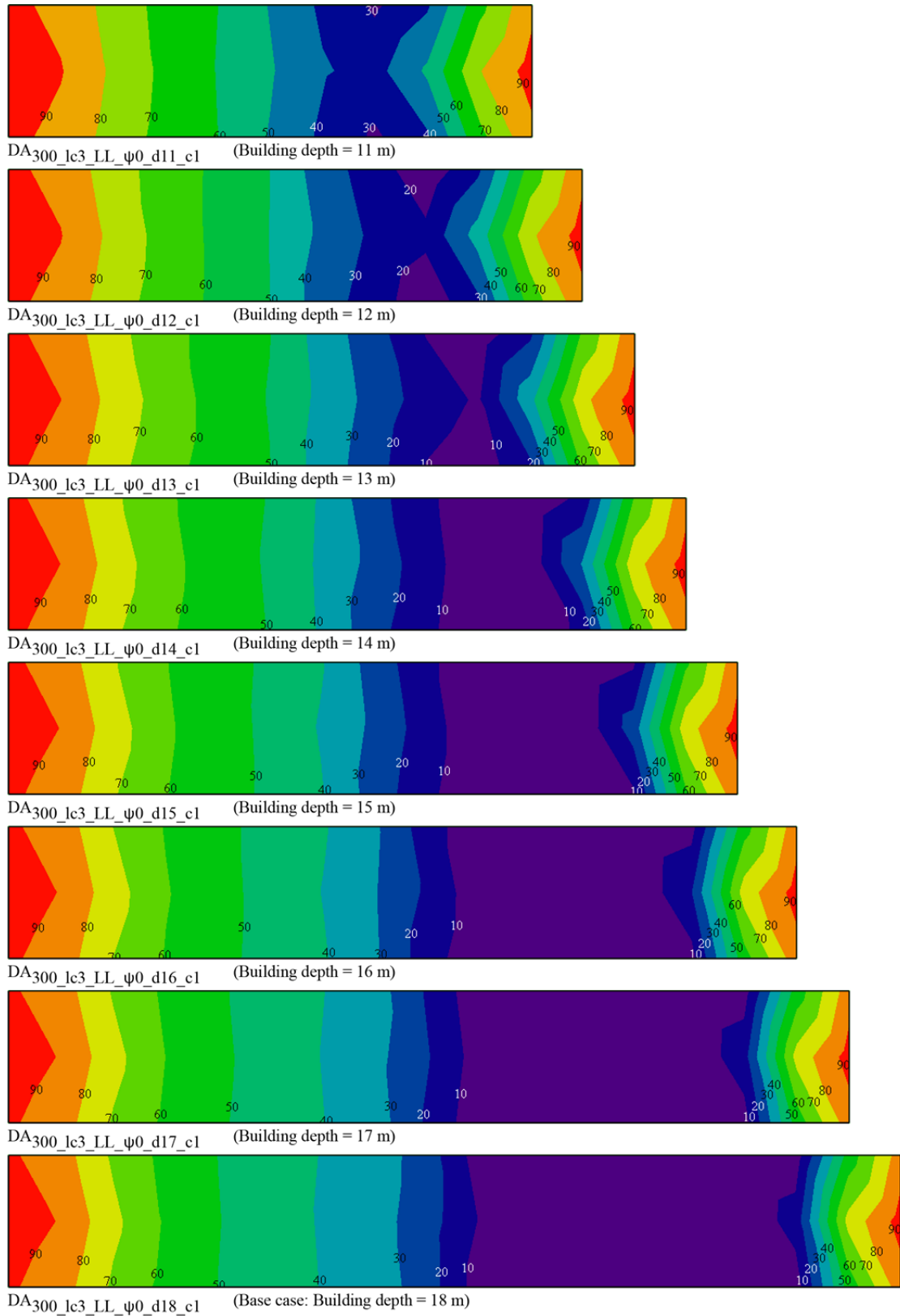


Figure 4.5: Different building depths: Golden, low VLT, LightLouver, $\psi = 0$; DA₃₀₀ contour plots [%].

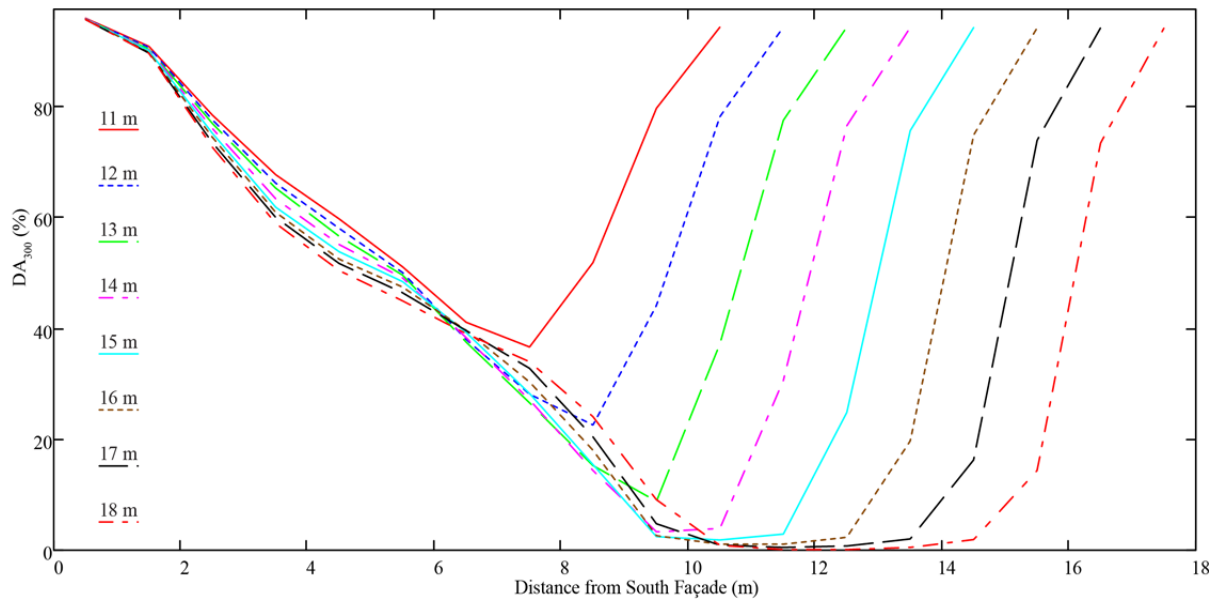


Figure 4.6: Different building depths: Golden, low VLT, LightLouver, $\psi = 0$; DA_{300} X-Y plot [%].

Section 4.4 Window to wall ratio and window head height

The geometry of the fenestration in the equator-facing façade is a very important element not only to the daylighting and thermal design of a building, but to the façade’s architectural character. As such, fenestration is among the key elements that must be addressed by the design team at the start of the schematic design phase. Changes to fenestration geometry late in the design process are costly in terms of budget and time since windows require their own structure which is tightly coordinated with the general structure of the façade.

Various configurations of window to wall ratios and window head heights, labeled **A** to **F** in Table 4.11, and Figure 4.7, are simulated to quantify their influence on daylighting performance with the goal to provide this information to support the schematic design process. The unfolded building section is repeated in Figure 4.8 below for reference. Results for Golden are in Table 4.12. Complete descriptions for the configurations are presented in Appendix A3.7 to A3.13. Complete results for all locations are contained in Appendix A4.

Table 4.11: Window to wall ratio and window head height configurations studied.

Parameter	Fenestration configurations						
	Base bldg.	A	B	C	D	E	F
Refer to Figure 4.8 for definitions							
D_{rm} (m)	18.000	18.000	18.000	18.000	18.000	18.000	18.000
W_{rm} (m)	3.000	3.000	3.000	3.000	3.000	3.000	3.000
H_{rm} (m)	3.048	3.048	3.048	3.048	3.048	3.048	3.048
WinSouth _{wd} (m)	1.829	1.829	1.829	2.100	2.500	1.400	1.829
DayWinSouth _{ht} (m)	0.914	1.650	1.800	1.650	1.900	1.195	0.914
ViewWinSouth _{ht} (m)	1.219	1.219	1.219	1.219	0.900	1.593	1.219
WinNorth _{wd} (m)	1.829	1.829	1.829	1.829	1.829	1.829	1.829
DayWinNorth _{ht} (m)	0.762	0.762	0.762	0.762	0.762	0.762	0.762
ViewWinNorth _{ht} (m)	1.219	1.219	1.219	1.219	1.219	1.219	1.219
BlankNorth _{ht} (m)	0.914	0.914	0.914	0.914	0.914	0.914	0.153
Window to wall ratio, South façade, WWR_s	0.328	0.441	0.465	0.507	0.589	0.328	0.328
Window to wall ratio, North façade, WWR_n	0.305	0.305	0.305	0.305	0.305	0.305	0.305
Window to wall ratio, South daylight window, WWR_{ds}	0.141	0.254	0.277	0.292	0.400	0.141	0.141
Window to wall ratio, South view window, WWR_{vs}	0.188	0.188	0.188	0.215	0.189	0.188	0.188
* Window head height, South façade WHH_s (m)	3.048	3.783	3.933	3.783	3.714	3.701	3.048
* Window head height, North façade WHH_n (m)	3.810	3.810	3.810	3.810	3.810	3.810	3.048
Notes:							
	Parameters that have been changed from the base building are highlighted in yellow.						
	* Since the room cavity below the workplane is not modelled, the height of the workplane must be added to the window heights to obtain the room's WHH; (total room height is 3.963 m).						
	Configuration A: increase DayWinSouth _{ht} height to make WHH_s higher; also makes WWR_{ds} bigger.						
	Configuration B: increase just DayWinSouth _{ht} ; makes WWR_{ds} and WHH_s increase; tallest WHH_s in study.						
	Configuration C: increase WinSouth _{wd} which makes WWR_{ds} and WWR_{vs} bigger; overall WWR_s increases and WHH_s increases.						
	Configuration D: increase WWR_{ds} to 40 %.						
	Configuration E: all WWR are same as base bldg.; but DayWinSouth _{ht} is taller; i.e. WHH_s is higher.						
	Configuration F: lowered DayWinNorth window to be at the same WHH as the WHH_s to see if DayWinNorth _{ht} has effect on $sDA_{300/50}$.						
	Configuration E: raising WHH_s but keeping WWR_s constant produces up to 8 % performance gain.						
	Configuration F: lowering DayWinNorth window has little to no effect on overall $sDA_{300/50}$.						

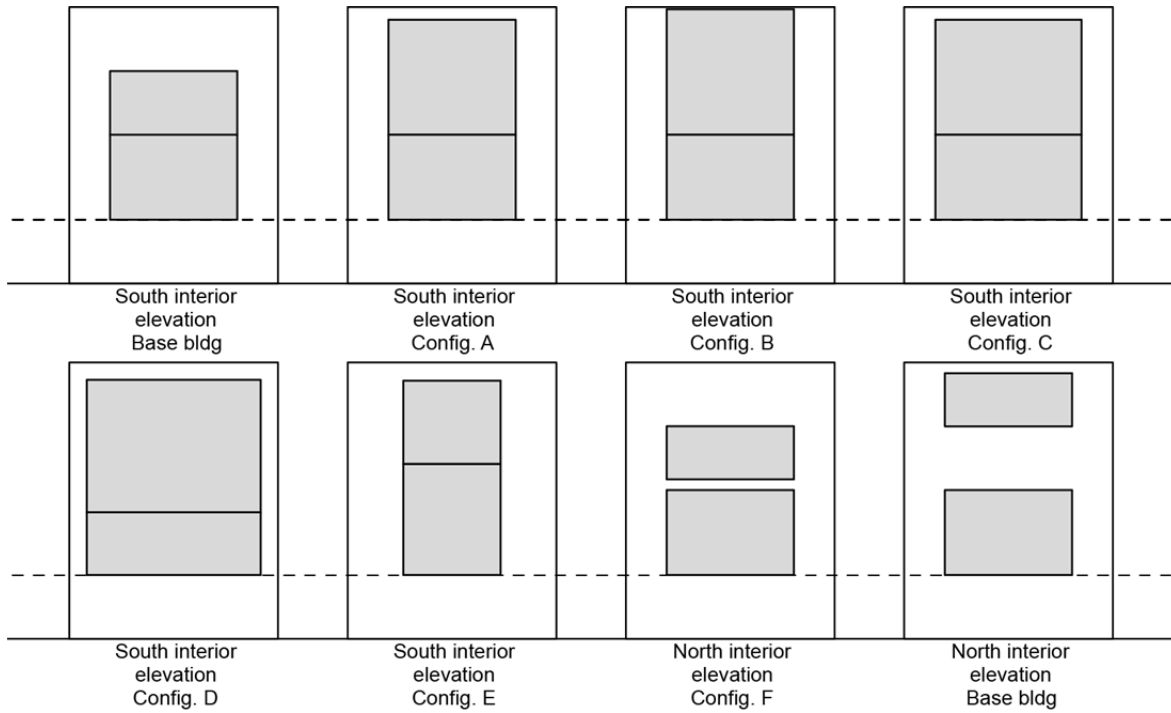


Figure 4.7: Schematic interior elevations showing fenestration configurations; dashed line represents height of workplane.

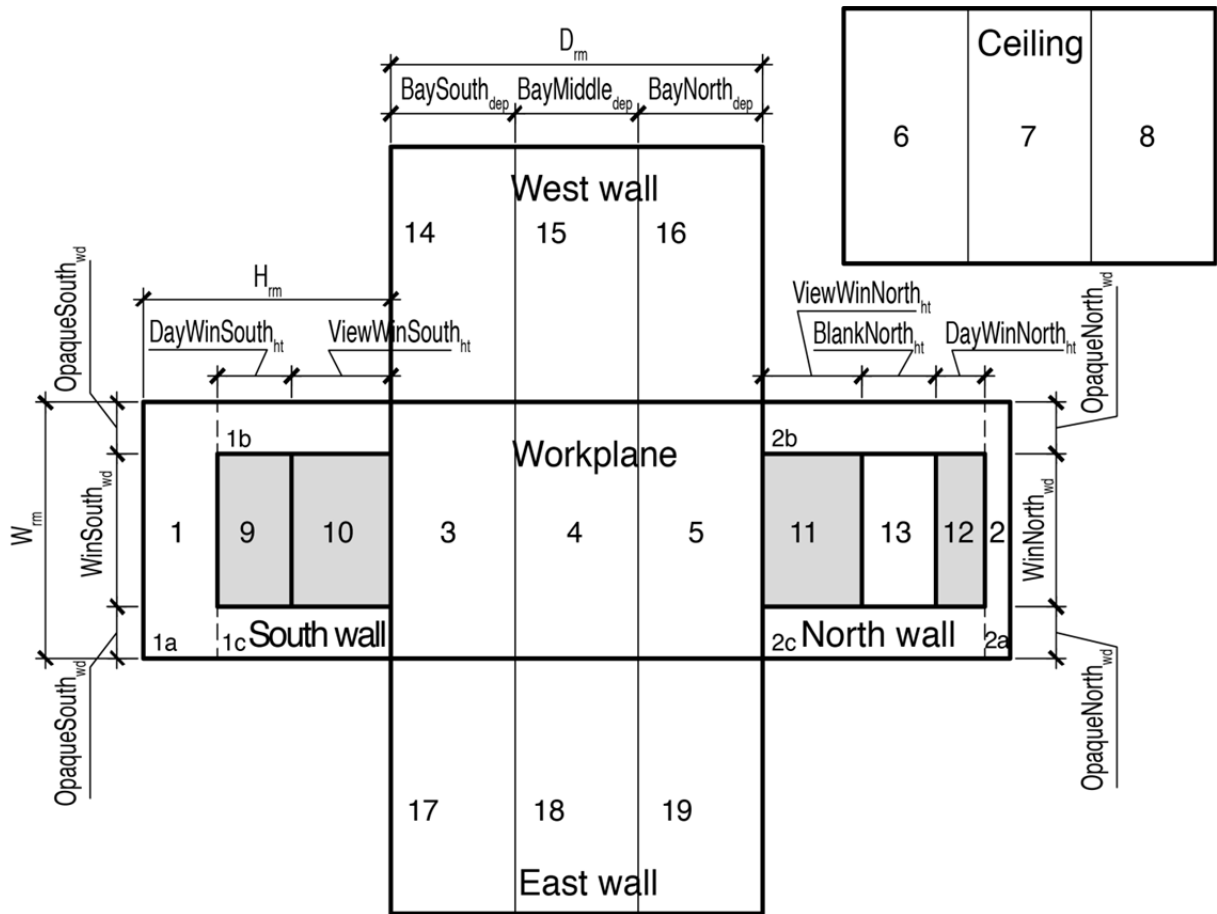


Figure 4.8: Representative cross-section unfolded, its surfaces labeled, and dimensioned.

Results for Golden are shown in Table 4.12. In configurations A to D, the daylighting window is made larger and the window head height is made higher than in the base building. This results in increased $sDA_{300/50}$ performance for all cases. For many of the blind/window VLT/orientation combinations the $sDA_{300/50}$ is over 55 %, making them “nominally acceptable” for daylighting –compared to a best case $sDA_{300/50}$ of 46 % for the base building for Vision Control blind/high VLT windows/ $\psi = 15^\circ$.

Table 4.12: Comparison of fenestration configurations for Golden; $sDA_{300/50}$ [%].

Golden, 1.0 x 1.0, D18		ψ orientation													
		-45°		-30°		-15°		0		15°		30°		45°	
Configuration blind		low VLT	high VLT	low VLT	high VLT	low VLT	high VLT	low VLT	high VLT	low VLT	high VLT	low VLT	high VLT	low VLT	high VLT
base bldg	LightLouver (cfs1)	28	35	33	41	39	44	39	44	33	44	33	41	28	35
	Vision Control (cfs2)	33	35	39	41	44	44	39	44	39	46	33	41	30	35
A	LightLouver (cfs1)	44	52	54	57	56	57	56	56	56	57	50	57	41	52
	Vision Control (cfs2)	50	52	56	57	56	63	56	56	56	57	54	57	44	52
B	LightLouver (cfs1)	50	57	56	57	56	63	56	61	56	57	50	57	44	52
	Vision Control (cfs2)	50	57	56	57	56	63	56	63	56	63	56	57	50	52
C	LightLouver (cfs1)	50	57	56	63	56	63	56	61	56	63	56	57	50	57
	Vision Control (cfs2)	56	57	56	63	61	63	61	63	56	63	56	57	50	57
D	LightLouver (cfs1)	56	63	61	63	61	63	61	63	61	63	56	63	56	57
	Vision Control (cfs2)	56	63	61	63	61	63	61	63	61	63	61	63	56	57
E	LightLouver (cfs1)	30	37	39	46	39	50	39	50	39	44	33	41	28	35
	Vision Control (cfs2)	33	35	39	46	44	50	44	50	39	46	35	41	33	35

In configuration D, the size of the South façade daylighting window is increased from a WWR_{ds} of 14 % to 40 % while keeping the South façade view window (WWR_{vs}) the same as in the base building. In the case of Golden (Table 4.13 and Figure 4.9), the results show that the $sDA_{300/50}$ performance of the LightLouver and the Vision Control blind is virtually identical. Also, the $sDA_{300/50}$ at all façade orientation angles reaches a minimum of 56 % – thereby attaining the “nominally acceptable” level for a daylit space for $sDA_{300/50}$. With the LightLouver, the $sDA_{300/50}$ performance increases by as much as 85 % over the reference case for the low VLT windows (at orientation $\psi = -30^\circ$ and 15°) and as much as 54 % for the high VLT windows (at orientation $\psi = \pm 30^\circ$). With the Vision Control window in Golden, the $sDA_{300/50}$ increase is as much as 87 % for the low VLT windows (at orientation $\psi = 45^\circ$) and 80 % for the high VLT windows (at orientation $\psi = -45^\circ$).

In configuration D, all combinations of blind/window VLT/orientation result in “nominally acceptable” daylighting ($sDA_{300/50}$ over 55 %) for Golden, Montreal, and Phoenix. As well,

a number of the combinations in Vancouver and St. John’s are considered “nominally acceptable” for daylighting.

Furthermore, using the same configuration D, but a different time period of evaluation (August 01 and 02; and February 12 and 13) and time step (15 min), Chen, Yip and Athienitis (2014b, 2014a) show that when thermal performance is taken into account, increasing WWR_{ds} from 14 % to 40 % contributes to a decrease in winter space heating for the Vision Control blind using the high SHGC and high VLT windows (from 9.7 kWh/m facade width to 7.1 kWh/m facade width) while it is practically constant for the LightLouver (from 10.5 kWh/m facade width to 10.1 kWh/m facade width). For space cooling performance, the same increase in WWR_{ds} increases the space cooling load slightly for the Vision Control blind using the low SHGC and low VLT windows (from -1.8 kWh/m facade width to -2.0 kWh/m facade width) and increases it further for the LightLouver (from -1.9 kWh/m facade width to -2.6 kWh/m facade width). Thus, when increasing WWR_{ds} to 40 %, both blinds’ daylighting performance increases equally, but the Vision Control blind has better thermal performance than the LightLouver.

Table 4.13: Configuration D, Golden, low and high VLT, LightLouver and Vision Control blind, orientation; $sDA_{300/50}$ [%].

Golden, 1.0x1.0, D18	ψ Orientation													
	-45°		-30°		-15°		0		15°		30°		45°	
	low VLT	high VLT	low VLT	high VLT	low VLT	high VLT	low VLT	high VLT	low VLT	high VLT	low VLT	high VLT	low VLT	high VLT
Reference (base bldg.)														
LightLouver (cfs1)	28	35	33	41	39	44	39	44	33	44	33	41	28	35
Vision Control (cfs2)	33	35	39	41	44	44	39	44	39	46	33	41	30	35
Configuration D														
LightLouver (cfs1)	56	63	61	63	61	63	61	63	61	63	56	63	56	57
Vision Control (cfs2)	56	63	61	63	61	63	61	63	61	63	61	63	56	57

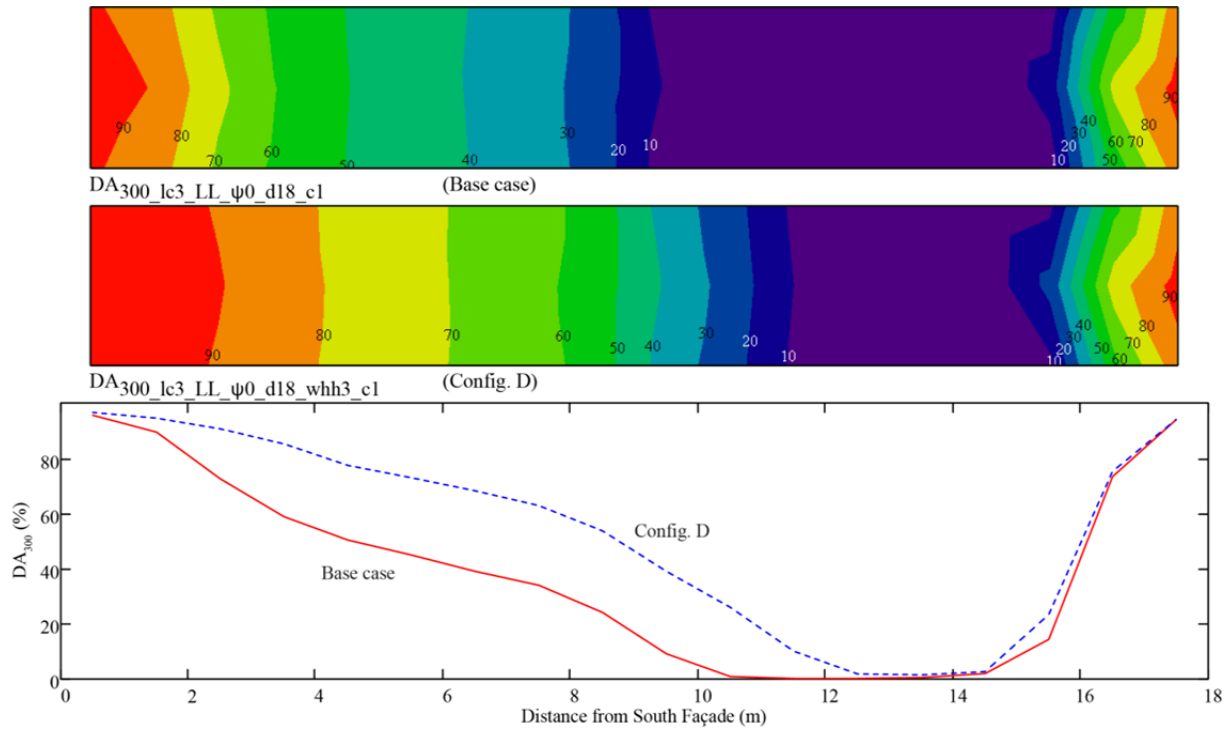


Figure 4.9: Base case and configuration D, Golden, low VLT, LightLouver, $\psi = 0$; DA_{300} contour (top, middle) and X-Y (bottom) plots [%].

In configuration E, the window head height was increased while keeping the window to wall ratio the same as in the base building. For certain combinations of blind/window VLT/orientation, this can increase the $sDA_{300/50}$ performance by as much as 18 % (Golden/LightLouver/low VLT/ $\psi = -30^\circ$ and 15°) (Table 4.14 and Figure 4.10), 13 % (Phoenix/LightLouver/low VLT/ $\psi = -15^\circ, 0, 15^\circ$), 18 % (Vancouver, St. John's), 31 % (Montreal/LightLouver/low VLT/ $\psi = 0$). In no cases does it decrease the $sDA_{300/50}$ performance below that of the base building configuration. Therefore, at the same WWR, a higher WHH is better for daylighting.

Table 4.14: Base bldg. and configuration E, Golden, low VLT, LightLouver, orientation; $sDA_{300/50}$ [%].

Golden, LL, c1, 1.0x1.0 D18	ψ Orientation						
	-45°	-30°	-15°	0	15°	30°	45°
Reference (base bldg.)	28	33	39	39	33	33	28
Configuration E	30	39	39	39	39	33	28

One last parameter tested is the window head height on the North façade. The base building at the North façade positions the North daylighting window higher up than the corresponding daylighting window on the South façade (see Figure 4.7 or Table 4.11). In configuration F, the North daylighting window is lowered to the same height as the South daylighting window. The conclusion is that this configuration has no impact on $sDA_{300/50}$ values. It can be concluded that the North façade window head height is not significant in influencing $sDA_{300/50}$ for the open plan.

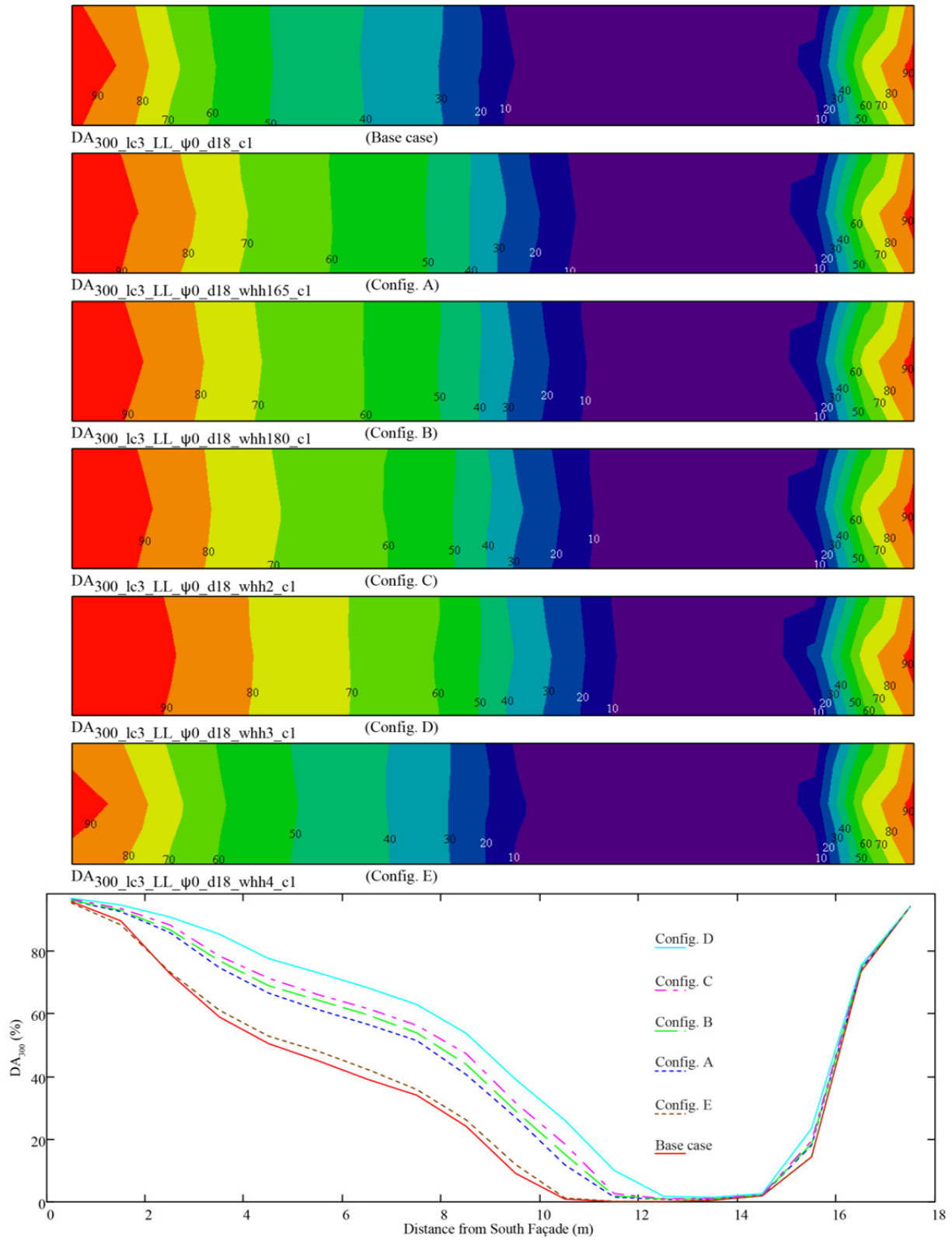


Figure 4.10: Fenestration configuration comparison: Golden, low VLT, LightLouver, $\psi = 0$; DA_{300} contour (top, middle) and X-Y (bottom) plots [%].

Section 4.5 Design inquiry: maximum building depth for daylit open-plan building

The preceding sections have shown that the WWR and WHH on the equator-facing façade improve $sDA_{300/50}$ performance over the base building in varying degrees based on their combinations, and that WHH_n has trivial effect on $sDA_{300/50}$.

The effects of these parameters on improving the daylighting of a building have been calculated *while holding the floor area constant*. This method of analyzing the daylighting design issue assumes that for important design reasons the floor plate dimensions of a building design have to be respected. For example, to maximize site density, a common design solution is to make a floor plate as big as possible. Daylighting will be subordinate to this design directive and the part of the resulting floor area with insufficient daylight will simply rely on electric lighting at all times. For these situations, further simulations can be undertaken to evaluate methodologies for integrating electric lighting controls with daylighting (Athienitis and Tzempelikos, 2002, Rogers, 2011). *Any* daylighting contribution is useful in reaching an overall target illumination level and reducing the electric lighting energy and cooling load.

This thesis argues that an equally common design question is: *How deep can a floor plate be for the entire floor area to be considered nominally daylit?* For this purpose another set of simulations are carried out concentrating on determining this building depth.

Using the base building as a conservative or “worst case” scenario, more simulations are executed to determine the maximum building depth at which the $sDA_{300/50}$ performance attains the level of “nominally acceptable,” i.e. 55 % – the building is considered daylit. For these, the low VLT windows (c1) are assigned to the American locations and the high VLT windows (c2) are assigned to the Canadian locations.

The different climates/locations reach the nominally acceptable level of daylight sufficiency using the $sDA_{300/50}$ metric of 55 % at different building depths depending on the blind used (Table 4.15, and Figure 4.11). For a South orientation ($\psi = 0$), this depth ranges from 11.5 m for Vancouver to 15.0 m for Montreal, with 14.5 m for Golden (Table

4.16). Note that the range in Table 4.15 refers to the maximum building depth taking into account all orientation (ψ) angles.

Table 4.15: Base bldg. and configuration D: maximum building depth at which daylighting illuminance is nominally acceptable (all ψ angles).

	Montreal (lc2) (high VLT)	Golden (lc3) (low VLT)	Vancouver (lc4) (high VLT)	St. John's (lc5) (high VLT)	Phoenix (lc6) (low VLT)
Base building					
LightLouver	13.5 m – 15.0 m	12.2 m – 14.0 m	11.2 m – 11.5 m	11.5 m – 11.8 m	13.4 m – 14.6 m
Vision Control	13.5 m – 15.0 m	12.8 m – 14.5 m	11.2 m – 11.5 m	11.8 m – 12.2 m	13.4 m – 14.7 m
Configuration D					
LightLouver	20.9 m – 22.0 m	18.7 m – 19.3 m	16.7 m – 18.0 m	17.0 m – 18.5 m	19.4 m – 19.7 m
Vision Control	20.7 m – 22.0 m	18.7 m – 19.3 m	16.8 m – 18.0 m	17.0 m – 18.5 m	19.5 m – 19.8 m

Table 4.16: Base building and configuration E: maximum building depth at which daylighting illuminance is nominally acceptable ($\psi = 0$).

$\Psi = 0$	Montreal (lc2) (high VLT)	Golden (lc3) (low VLT)	Vancouver (lc4) (high VLT)	St. John's (lc5) (high VLT)	Phoenix (lc6) (low VLT)
Base building					
LightLouver	15.0 m	14.0 m	11.5 m	11.8 m	14.6 m
Vision Control	15.0 m	14.5 m	11.5 m	12.1 m	14.7 m
Configuration E					
LightLouver	15.0 m	14.4 m	12.3 m	12.4 m	14.7 m
Vision Control	16.0 m	14.5 m	12.3 m	12.6 m	14.7 m

Another set of simulations is executed using configuration E for a South orientation. Recall that configuration E has the same window to wall ratios as the base building but has taller and narrower windows. Results are tabulated in Table 4.16 and plotted in Figure 4.12.

Similar to the results found in Section 4.4, the configuration E daylighting performance – this time measured by maximum building depth for nominally acceptable daylighting – is always equal to or better than that of the base building configuration.

Whereas the base configuration represents the most conservative case for predicting maximum building depth for a “nominally” daylit open-plan building, configuration D represents an optimal case (see Table 4.13, for example). Therefore, a set of simulations using configuration D is executed to establish the upper bound for the maximum building depth for a “nominally” daylit open-plan building. The results are shown in Table 4.15. The range in each cell represents the maximum building depth obtained at the least and most favourable building orientations to daylighting. More plotted results can be found in Appendix A3.14.

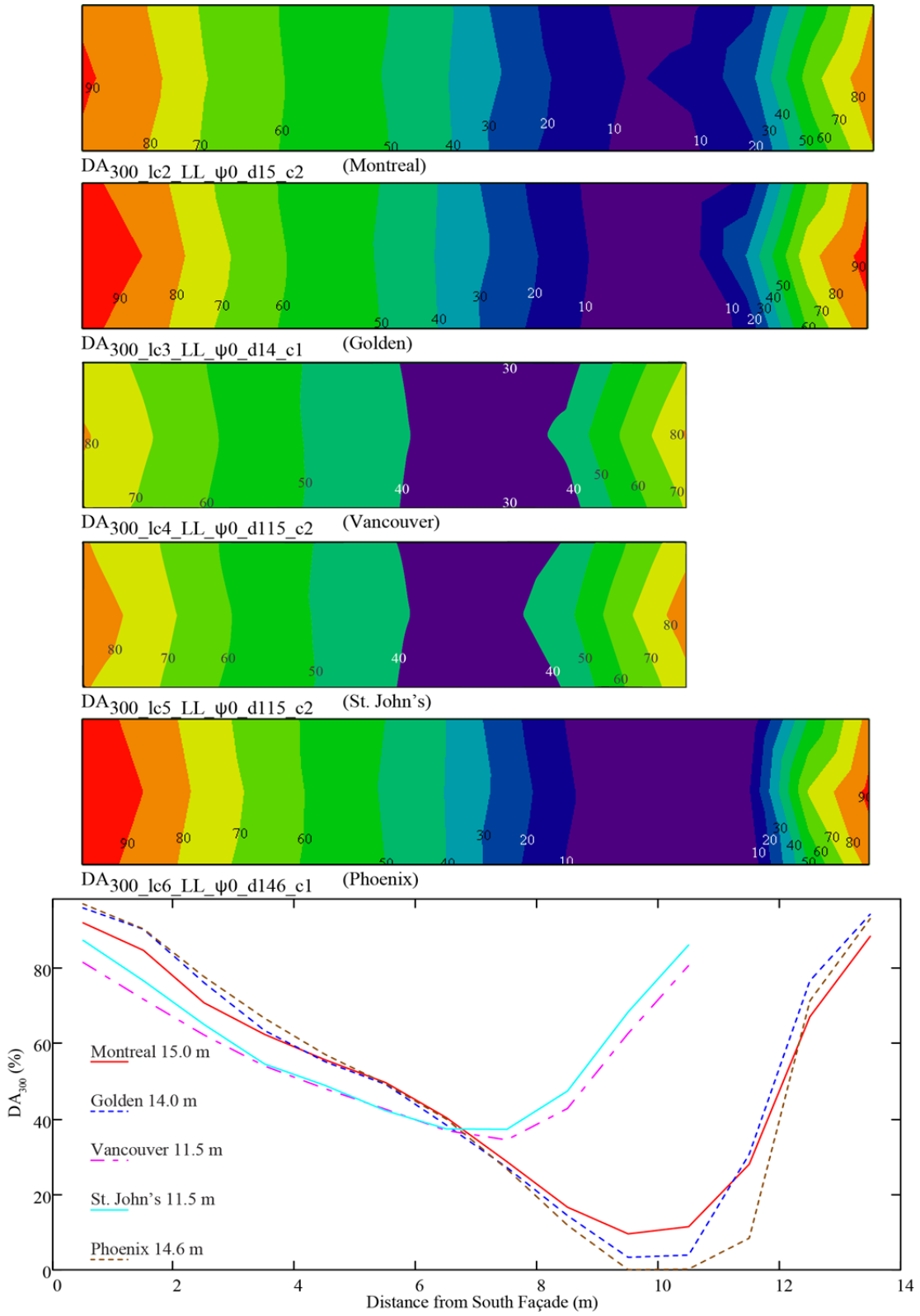
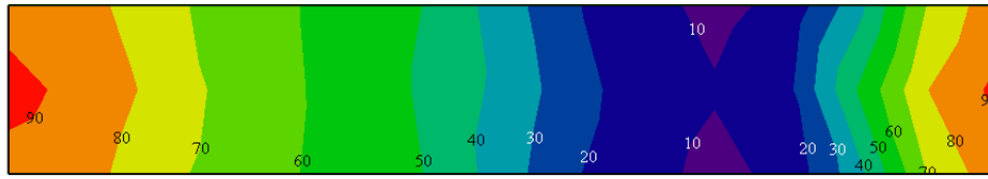
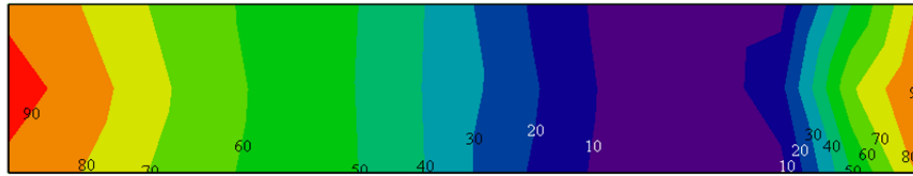


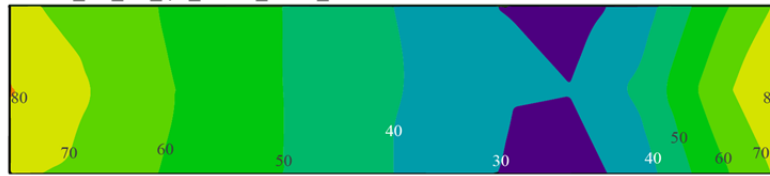
Figure 4.11: Base bldg. maximum building depth for nominally acceptable daylighting illuminance: all locations, LightLouver, $\psi = 0$; DA_{300} contour (top, middle) and X-Y (bottom) plots [%].



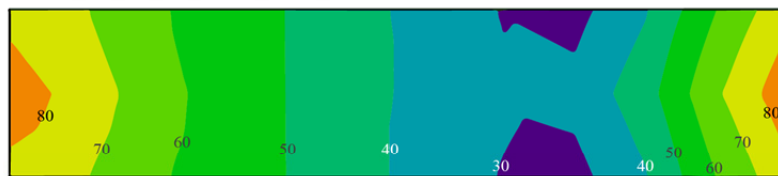
DA₃₀₀_lc2_LL_ψ0_d15_whh4_c2 (Montreal)



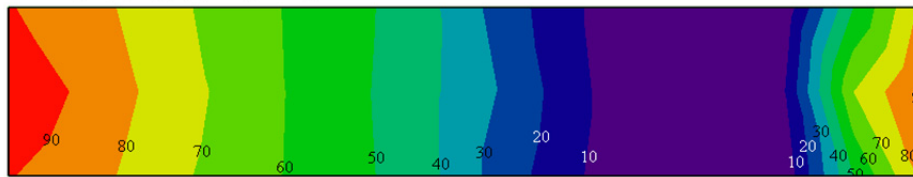
DA₃₀₀_lc3_LL_ψ0_d1441_whh4_c1 (Golden)



DA₃₀₀_lc4_LL_ψ0_d1228_whh4_c2 (Vancouver)



DA₃₀₀_lc5_LL_ψ0_d124_whh4_c2 (St. John's)



DA₃₀₀_lc6_LL_ψ0_d1467_whh4_c1 (Phoenix)

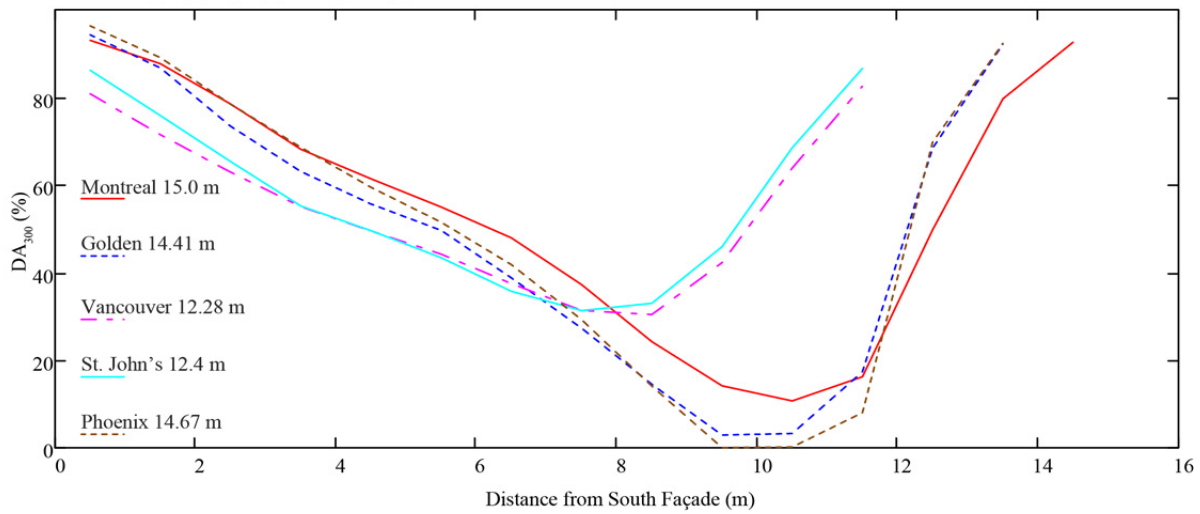


Figure 4.12: Configuration E maximum building depth for nominally acceptable daylighting illuminance: all locations, LightLouver, $\psi = 0$; DA₃₀₀ contour (top, middle) and X-Y (bottom) plots [%].

Chapter 5 Discussion and conclusions

Based on the model calibration and the analysis of the simulation results, this study has shown that the proposed simplified daylighting model using the radiosity method combined with the new spatial daylight autonomy (sDA_{300/50}) metric is reliable, predictable, and is capable of providing the support for design decisions within the expected range of accuracy normally encountered in early schematic design. This level of accuracy is acceptable at this stage, since building form and composition are still indeterminate and having the ability to make *rapid* assessments including *comparative* analyses of available options is paramount. A range of locations, window visible light transmittance values, daylight redirecting blinds, building façade orientations, and fenestration geometry was studied using this approach.

The simulations show that replacing the LightLouver passive daylight-redirecting system as installed in the RSF in its existing location in Golden, Colorado, with the Vision Control active daylight-redirecting system would result in a relative illuminance performance increase of 17 %.

The literature review shows that there is an evolution in the products on the market that purport to offer better sun control performance. Unlike the Vision Control blind, whose profile design was constrained by structural and mechanical performance concerns, other products on the market put an emphasis on refined louver shapes and micro-prismatic materials optimized for daylight redirection. Therefore the results from this thesis are representative of the baseline performance of these two classes of daylight redirecting devices, with better performance anticipated with newer products. Generally, active daylight redirecting blinds will perform as well as or better than passive daylight redirecting blinds for most configurations tested in this case study, across all the different locations and parameters.

The results must be judged with an eye to the larger objective: offer design solutions to address the entire solar energy spectrum. Both classes of daylight redirecting blind – passive and active – achieve good performance under all test scenarios. Therefore, with

daylighting requirements being equal, the final choice of blind must take into consideration the solar heat gain requirements of the building due to climate and orientation. An important factor in this calculation is the installation location of the blind. From a thermal performance point of view, the best location for blinds is on the exterior side of a window. Solar heat is blocked before it enters the space, limiting the amount that is re-radiated into the space as longwave radiation. When this isn't possible due to wind, building height, or other climatic factors, a second-best choice is to locate the blinds between the layers of the window glazing. Unfortunately installing a blind on the indoor side of a window is not effective at reducing solar heat gain.

A passive blind installed on the indoor side of a window may be acceptable for mild, temperate climates – especially with the benefits of simplicity, low maintenance, and convenient retro-fit possibilities – but may cause excessive overheating in climates with high cooling load. In this respect, the greatest flexibility is offered by the class of active blinds installed between the window glazing which can control when daylighting or solar heat is desired in the interior.

The parameters of window to wall ratio (WWR) and window head height (WHH) must be specified together to accurately predict the illuminance performance of a design option at the beginning of the schematic design stage. Specifying only one of the two may lead to a relative difference of up to 8 % in maximum building depth for which the building can be considered nominally daylight. All else being equal, increasing the window head height without increasing the window to wall ratio can increase $sDA_{300/50}$ in some situations.

Simulations show the maximum depth of a double-perimeter open-plan space that is 'nominally acceptable' for daylighting varies with location, orientation, window to wall ratio, window head height, visible transmittance, and model of daylight redirecting blind. Using the window to wall ratio and window head height configuration of the existing RSF, the maximum building depth ranges from 11.5 m if the building is in Vancouver, to 14.5 m in Golden, and 15 m in Montreal. Increasing the window to wall ratio and window head height of the existing RSF will allow it to be nominally daylight at 18 m (its existing depth).

Based on the simulation results varying all parameters, *the maximum building depth for a nominally daylight double-perimeter open-plan office building is equal to 3.7 to 5.9 times the window head height of the equator-facing daylighting window, depending on climate.* This calculation may be used as a first approximation at the beginning of the schematic design phase when quick sketches and hand calculations are still common for design exploration before the building design has taken shape and the design team commits to developing specific design options.

More importantly, this thesis demonstrates a range of choices that reflects the nature of a design project at the beginning of schematic design. There is no *singular best* choice for daylighting design – just like there is no *singular best* design process. Each project will have its own unique set of priorities and design objectives. Sometimes, these can lead to conflicting demands and compromises. Being able to obtain design guidance on what is the *optimal* choice and – in circumstances when the optimal choice is not possible to implement – what are other *near-optimal* choices, is essential for early schematic design. Here are some examples.

Although the active daylighting blind consistently shows better daylighting performance than the passive blind throughout the many sets of simulations, this performance may come at the cost of additional building overhead such as commissioning and maintenance, and possible lost occupant productivity due to the distraction of the frequent movement of the blinds. For all its simplicity, the passive daylighting blind performs almost as well as the active blind, has no moving parts and only requires dusting to maintain performance over the lifetime of the product.

Another issue that may ultimately boil down to a building owner's benefit cost perspective is maximum depth of building for which daylighting is deemed 'nominal.' sDA_{300/50} sets two thresholds for meeting daylight sufficiency: 55 % which is "nominal" and 75 % which is "preferred." The benefit of increasing sDA_{300/50} from 55 % to 75 % is better daylighting for a larger *percentage* of the building's floor area, thus increasing the quality of the indoor environment for the building occupants. To achieve this in a double-perimeter open-plan office requires increasing the daylighting window size and pairing it with a daylight

redirecting blind; or decreasing the depth of the building; or both. As the simulations show, the RSF case study building crosses the $sDA_{300/50}$ 55 % threshold when increasing its daylighting window to wall ratio to 40 % (configuration D) from 14 %. Beyond that, the building depth has to be shortened to 14 m from 18 m before the same fenestration configuration D can attain the $sDA_{300/50}$ 75 % threshold. Therefore, 4 m of building depth, or 12 m² of column-free floor area has to be sacrificed from a total of 54 m² in the typical bay. Considering that the North wing of the RSF is four storeys tall, this means that 48 m² of additional column-free floor area or *almost* the equivalent of another storey is needed to improve the $sDA_{300/50}$ performance to 75 % and maintain the same net floor area.

But making such a drastic design change as reducing the building depth by 4 m may go against one of the tenets of open-plan offices, which is to maximize the number of employee workspaces per useable floor area. It is usually more expensive to build another storey than to add more horizontal floor area. Countervailing arguments include the desire of building occupants to be near windows and their views to provide contact to the outside environment and to enhance productivity.

Furthermore, there is the possible incentive of the CaGBC and USGBC LEED green building rating systems' daylighting credit to consider. For the LEED v4 daylighting credit IEQ 8.1, the normal compliance path is to demonstrate good daylighting using $sDA_{300/50}$ as the performance metric. LEED v4 awards 2 points for achieving an $sDA_{300/50}$ of 55 % and 3 points for achieving 75 %⁷. Real estate research indicates that office buildings with green building certifications such as LEED tend to have higher occupancy rates and charge higher rents (Miller et al., 2008). Simply put, this is a trade-off between a deeper, denser building and increased occupant comfort and productivity: "*How much is $sDA_{300/50}$ 75 %, or 'preferred' daylighting performance, worth to the building owner?*"

⁷ The certification levels are LEED Certified: 40 – 49 points; LEED Silver: 50 – 59 points; LEED Gold: 60 – 79 points; LEED Platinum: 80 + points. See <http://www.usgbc.org/certification>

These examples illustrate the larger context in which this design guidance for daylight redirecting blinds can be situated. At the beginning of any building design process, building owners need to be aware of these issues and clearly state their positions and building designers need the simple design guidance to begin the design process, quickly assess options, and choose the most promising path for further development when more detailed simulation tools can be introduced.

Section 5.1 Further research needs

1. It is useful to determine the depth of the “daylit area” (corresponding to the area where the daylight autonomy attains a threshold illuminance of 300 lx for over 50 % of the occupied hours ($DA_{300} = 50\%$)) even if the overall floor area may not qualify as “nominally daylit.” Such a calculation is useful in space planning to determine where architectural program elements requiring daylight may be placed. The depth of the “daylit area” can be developed as function of the window head height as an extension of the useful daylight building depth calculator supporting daylight redirecting blinds.
2. A second iteration of this design guidance can integrate glare and solar heat gain evaluations since there is a need for simple early schematic design stage guidance that considers all aspects of the sun’s impact on a building. New building parameters can include thermal mass type, size, and location.
3. There are daylight redirecting blinds on the market that provide a high percentage of unobstructed view through their louvers that may be installed in view windows. These need to be investigated to provide design guidance at the early schematic design stage. As an example, if a Vision Control blind is installed in the view window in addition to the daylighting window of the RSF building, the $sDA_{300/50}$ of the space can reach 52 % and 53 % for façade orientation angles of $\psi = 0$ and -15° in Golden. This is just under the $sDA_{300/50}$ “nominally acceptable” daylighting threshold of 55 %. See Table 5.1 and Figure 5.1 for a comparison with the base case.

Table 5.1: Comparison of Vision Control blind on daylighting and viewing window with the base case.

Golden, 0.5x0.5	ψ Orientation													
	-45°		-30°		-15°		0		15°		30°		45°	
	low VLT	high VLT	low VLT	high VLT	low VLT	high VLT	low VLT	high VLT	low VLT	high VLT	low VLT	high VLT	low VLT	high VLT
LightLouver	29	36	34	43	35	46	35	46	35	43	32	39	29	35
Vision Control / Vision Control	38	42	49	52	53	54	52	54	49	53	44	47	36	39

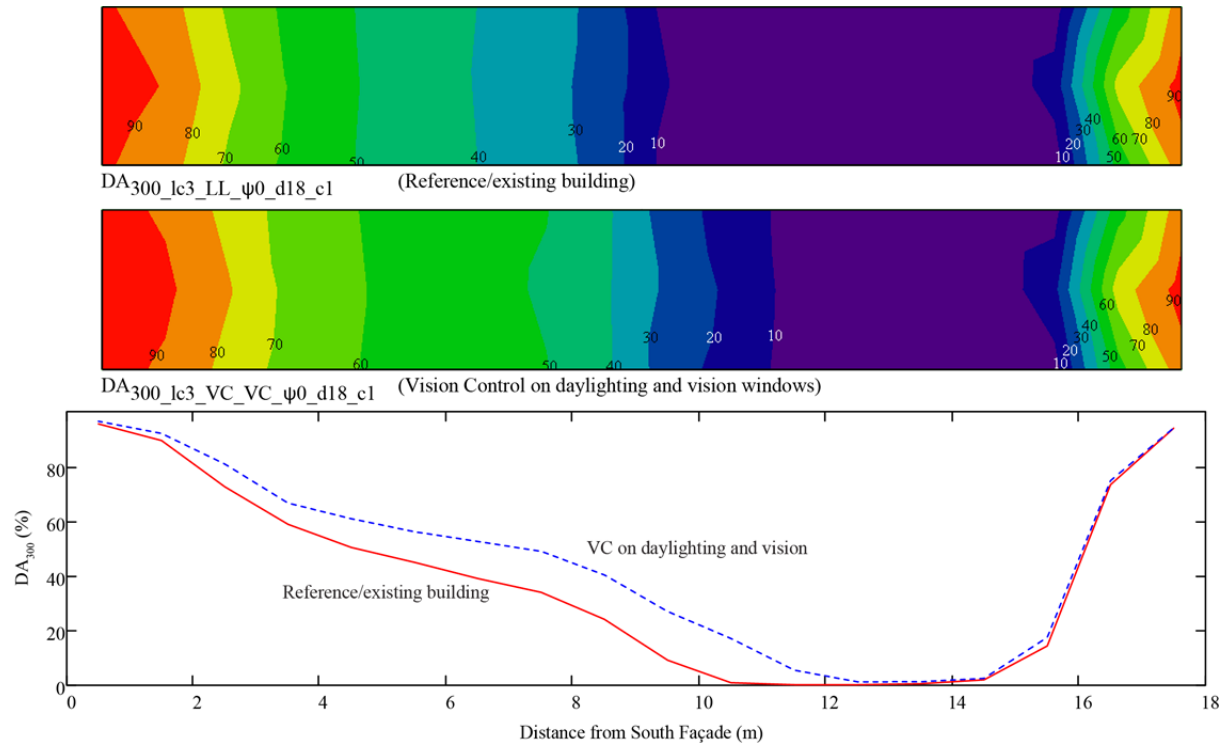


Figure 5.1: Comparison of the base case with Vision Control blinds on both daylighting and view windows: Golden, LightLouver and Vision Control blinds, $\psi = 0$; DA_{300} contour (top, middle) and X-Y (bottom) plots [%].

References

- AMERICAN INSTITUTE OF ARCHITECTS (AIA) 2008. *The Architect's Handbook of Professional Practice*, Hoboken, Wiley.
- AMERICAN NATIONAL STANDARDS INSTITUTE (ANSI) & INSTITUTE FOR MARKET TRANSFORMATION TO SUSTAINABILITY (MTS) 2012. Integrative Process (IP): ANSI Consensus National Standard Guide, Design and Construction of Sustainable Buildings and Communities. Washington, DC: American National Standards Institute, Institute for Market Transformation to Sustainability.
- AMERICAN SOCIETY OF HEATING, REFRIGERATING AND AIR-CONDITIONING ENGINEERS (ASHRAE), 2009. *ASHRAE Handbook - Fundamentals*, Atlanta, GA, USA, American Society of Heating, Refrigerating, and Air-Conditioning Engineers (ASHRAE).
- AMERICAN SOCIETY OF HEATING, REFRIGERATING AND AIR-CONDITIONING ENGINEERS (ASHRAE), 2013. *ASHRAE Handbook - Fundamentals*, Atlanta, GA, USA, American Society of Heating, Refrigerating, and Air-Conditioning Engineers (ASHRAE).
- ANDERSEN, M. & DE BOER, J. 2006. Goniophotometry and assessment of bidirectional photometric properties of complex fenestration systems. *Energy and Buildings*, 38, 836-848.
- ANDERSEN, M., KLEINDIENST, S., YI, L., LEE, J., BODART, M. & CUTLER, B. 2008. An intuitive daylighting performance analysis and optimization approach. *Building Research and Information*, 36, 593-607.
- ANDERSEN, M., RUBIN, M., POWLES, R. & SCARTEZZINI, J. L. 2005. Bi-directional transmission properties of Venetian blinds: Experimental assessment compared to ray-tracing calculations. *Solar Energy*, 78, 187-198.
- ANDERSEN, M., STOKES, E., GAYESKI, N. & BROWNE, C. 2010. Using digital imaging to assess spectral solar-optical properties of complex fenestration materials: A new approach in video-goniophotometry. *Solar Energy*, 84, 549-562.
- ATHIENITIS, A. K., CELLURA, M., CHEN, Y., DELISLE, V., BOURDOUKAN, P. & KAPSIS, K. 2015. Modeling and design of Net ZEBs as integrated energy systems. In: ATHIENITIS, A. K. & O'BRIEN, W. (eds.) *Modeling, Design, and Optimization of Net-Zero Energy Buildings*. Hoboken: Wiley.
- ATHIENITIS, A. K. & TZEMPELIKOS, A. 2002. A methodology for simulation of daylight room illuminance distribution and light dimming for a room with a controlled shading device. *Solar Energy*, 72, 271-281.
- ATTIA, S., HENSEN, J. L. M., BELTRÁN, L. & DE HERDE, A. 2012. Selection criteria for building performance simulation tools: Contrasting architects' and engineers' needs. *Journal of Building Performance Simulation*, 5, 155-169.
- AUTODESK, I. 2011. Ecotect Analysis. v2011 ed. San Rafael, CA: Autodesk, Inc.
- BORDASS, B., BROMLEY, K. & LEAMAN, A. User and occupant controls in office buildings. International conference on building design, technology and occupant well-being in temperate climates, Brussels, Belgium, 1993. 12-5.

- BOURGEOIS, D., REINHART, C. & MACDONALD, I. 2006. Adding advanced behavioural models in whole building energy simulation: A study on the total energy impact of manual and automated lighting control. *Energy and Buildings*, 38, 814-823.
- CANADA LABOUR CODE 2014. Canada Occupational Health and Safety Regulations. *In: CANADA, G. O. (ed.) SOR86-304*. Ottawa: Government of Canada.
- CANADIAN INSTITUTE OF QUANTITY SURVEYORS 2012. Quantity Surveying & Cost Consulting Services: Schedule of Services and Recommended Charges. 6 ed. Markham, ON: Canadian Institute of Quantity Surveyors.
- CARLI, INC., 2006. Calculation of Optical Properties for a Venetian Blind Type of Shading Device. Amherst, MA.
- CARLUCCI, S., PAGLIANO, L., O'BRIEN, W. & KAPSIS, K. 2015. Comfort considerations in Net ZEBs: theory and design. *In: ATHIENITIS, A. K. & O'BRIEN, W. (eds.) Modeling, Design, and Optimization of Net-Zero Energy Buildings*. 1 ed. Berlin: Ernst & Sohn GmbH & Co. KG.
- CARMODY, J., SELKOWITZ, S., LEE, E. S., ARASTEH, D. & WILLMERT, T. 2004. *Window systems for high-performance buildings*, New York, W.W. Norton & Co.
- CHAN, Y. C. & TZEMPELIKOS, A. 2012. A hybrid ray-tracing and radiosity method for calculating radiation transport and illuminance distribution in spaces with venetian blinds. *Solar Energy*, 86, 3109-3124.
- CHEN, Y., YIP, S. & ATHIENITIS, A. 2014a. A Case Study on the Daylighting and Thermal Effects of Fixed and Motorized Light Louvers. *eSim 2014*. Ottawa, On.
- CHEN, Y., YIP, S. & ATHIENITIS, A. 2014b. Effects of Fixed and Motorized Window Louvers on the Daylighting and Thermal Performance of Open-Plan Office Buildings. *3rd International High Performance Buildings Conference*. West Lafayette, Indiana.
- COLE, R. J. & BROWN, Z. 2009. Reconciling human and automated intelligence in the provision of occupant comfort. *Intelligent Buildings International*, 1, 39-55.
- DANIELSSON, B. C. & BODIN, L. 2008. Office type in relation to health, well-being, and job satisfaction among employees. *Environment and Behavior*, 40, 636-668.
- EDWARDS, L. & TORCELLINI, P. 2002. A Literature Review of the Effects of Natural Light on Building Occupants. Golden, Colorado: NREL.
- ENERMODAL ENGINEERING LIMITED FOR PUBLIC WORKS AND GOVERNMENT SERVICES CANADA. 2002. Daylighting Guide for Canadian Commercial Buildings. Available: <http://www.enermodal.com/pdf/DaylightingGuideforCanadianBuildingsFinal6.pdf> [Accessed 01 Aug 2014].
- FLETCHER, B. & MUSGROVE, J. 1987. *Sir Banister Fletcher's A history of architecture*, London; Boston, Butterworths.
- GAGNE, J. M. L., ANDERSEN, M. & NORFORD, L. K. 2011. An interactive expert system for daylighting design exploration. *Building and Environment*, 46, 2351-2364.
- GALASIU, A. D. & REINHART, C. F. 2008. Current daylighting design practice: A survey. *Building Research and Information*, 36, 159-174.

- GALASIU, A. D. & VEITCH, J. A. 2006. Occupant preferences and satisfaction with the luminous environment and control systems in daylit offices: a literature review. *Energy and Buildings*, 38, 728-742.
- GOMES, M. G., SANTOS, A. J. & RODRIGUES, A. M. 2014. Solar and visible optical properties of glazing systems with venetian blinds: Numerical, experimental and blind control study. *Building and Environment*, 71, 47-59.
- GORAL, C. M., TORRANCE, K. E., GREENBERG, D. P. & BATTAILE, B. 1984. Modeling the Interaction of Light Between Diffuse Surfaces. *Computer Graphics (ACM)*, 18, 213-222.
- GOVERNMENT OF QUEBEC 2005. Processus d'élaboration d'un projet de construction : guide à l'intention des professionnels du ministère, responsables des projets d'immobilisation. Québec, QC: Ministère de la culture et communications.
- GUGLIELMETTI, R., PLESS, S. & TORCELLINI, P. On the use of integrated daylighting and energy simulations to drive the design of a large net-zero energy office building. Proc. Fourth National Conference of IBPSA-USA, New York, NY, 2010.
- HESCHONG, L. 2002. Daylighting and human performance. *ASHRAE Journal*, 44, 65-67.
- HESCHONG, L. 2012. Daylight Metrics. Gold River, CA: Heschong Mahone Group, Inc.
- HESCHONG MAHONE GROUP 1999. Skylighting and Retail Sales: An Investigation into the Relationship Between Daylighting and Human Performance. Fair Oaks, CA.
- HESCHONG MAHONE GROUP 2003. Windows and Offices: A Study of Office Worker Performance and the Indoor Environment. Fair Oaks, California.
- HIRSCH, A., OKADA, D., PLESS, S. & ANTIA, P. The role of modeling when designing for absolute energy use intensity requirements in a design-build framework. *ASHRAE Transactions*, 2011. 398-405.
- HOOTMAN, T. 2013. *Net Zero Energy Design: A Guide for Commercial Architecture*, Hoboken, NJ, John Wiley & Sons, Inc.
- HOPKINSON, R. G. 1963. *Architectural Physics: Lighting*, London, UK, H.M. Stationery Off.
- HORVAT, M. & WALL, M. 2012. Solar Design of Buildings for Architects: Review of Solar Design Tools. *Report T.41*. Toronto, Canada; Lund, Sweden: IEA SHC.
- HVIID, C. A., NIELSEN, T. R. & SVENDSEN, S. 2008. Simple tool to evaluate the impact of daylight on building energy consumption. *Solar Energy*, 82, 787-798.
- HYGGE, S. & LÖFTBERG, H. A. 1999. Post Occupancy Evaluation of Daylight in Buildings - A report of IEA SHC Task 21/ ECBCS Annex 29. Gävle, Sweden.
- IESNA, I. 2012. LM-83-12 IES Spatial Daylight Autonomy (sDA) and Annual Sunlight Exposure (ASE). New York, NY, USA: IESNA Lighting Measurement.
- ILLUMINATING ENGINEERING SOCIETY OF NORTH AMERICA 2000. *IESNA Lighting Handbook*, New York, Illuminating Engineering Society of North America.
- INKAROJRIT, V. 2005. *Balancing comfort: Occupants' control of window blinds in private offices*. 3210631 Ph.D., University of California, Berkeley.
- JOHNSON, K. & WATKINS, R. 2010. Daylight in Buildings: ECBCS Annex 29 / SHC Task 21 Project Summary Report. Hertfordshire, UK: AECOM Ltd.

- JOINT FEDERAL GOVERNMENT / INDUSTRY COST PREDICTABILITY
TASKFORCE 2012. Guide to Cost Predictability in Construction: An Analysis of Issues Affecting the Accuracy of Construction Cost Estimates. Ottawa.
- JUDKOFF, R. & NEYMARK, J. 1995. International Energy Agency building energy simulation test (BESTEST) and diagnostic method. National Renewable Energy Lab., Golden, CO (US).
- KIM, J. & DE DEAR, R. 2013. Workspace satisfaction: The privacy-communication trade-off in open-plan offices. *Journal of Environmental Psychology*, 36, 18-26.
- KLEINDIENST, S., BODART, M. & ANDERSEN, M. 2008. Graphical Representation of Climate-Based Daylight Performance to Support Architectural Design. *LEUKOS - Journal of Illuminating Engineering Society of North America*, 5, 39-61.
- KOPP, G. & LEAN, J. L. 2011. A new, lower value of total solar irradiance: Evidence and climate significance. *Geophysical Research Letters*, 38.
- KUHN, T. E., BÜHLER, C. & PLATZER, W. J. 2000. Evaluation of overheating protection with sun-shading systems. *Solar Energy*, 69, 59-74.
- LARSON, G. W. & SHAKESPEARE, R. 1998. *Rendering with Radiance : the art and science of lighting visualization*, San Francisco, Morgan Kaufmann.
- LEE, E. S., DIBARTOLOMEO, D. L. & SELKOWITZ, S. E. 1998. Thermal and daylighting performance of an automated venetian blind and lighting system in a full-scale private office. *Energy and Buildings*, 29, 47-63.
- LEE, E. S. & SELKOWITZ, S. E. 2006. The New York Times Headquarters daylighting mockup: Monitored performance of the daylighting control system. *Energy and Buildings*, 38, 914-929.
- LESLIE, R. P. 2003. Capturing the daylight dividend in buildings: Why and how? *Building and Environment*, 38, 381-385.
- LI, D. H. W. & LAM, J. C. 2001. Evaluation of lighting performance in office buildings with daylighting controls. *Energy and Buildings*, 33, 793-803.
- LI, D. H. W., LAM, J. C. & WONG, S. L. 2002. Daylighting and its implications to overall thermal transfer value (OTTV) determinations. *Energy*, 27, 991-1008.
- LI, D. H. W., LAM, J. C. & WONG, S. L. 2005. Daylighting and its effects on peak load determination. *Energy*, 30, 1817-1831.
- LÖHNERT, G., DALKOWSKI, A. & SUTTER, W. 2003. Integrated Design Process: a guideline for sustainable and solar-optimised building design. *Berlin: IEA International Energy Agency*.
- MAHER, A. & VON HIPPEL, C. 2005. Individual differences in employee reactions to open-plan offices. *Journal of Environmental Psychology*, 25, 219-229.
- MARDALJEVIC, J., HESCHONG, L. & LEE, E. 2009. Daylight metrics and energy savings. *Lighting Research and Technology*, 41, 261-283.
- MARSZAL, A. J., HEISELBERG, P., BOURRELLE, J. S., MUSALL, E., VOSS, K., SARTORI, I. & NAPOLITANO, A. 2011. Zero Energy Building - A review of definitions and calculation methodologies. *Energy and Buildings*, 43, 971-979.
- MAZRIA, E. 1979. *The Passive Solar Energy Book: a Complete Guide to Passive Solar Home, Greenhouse, and Building Design*, Emmaus, PA, Rodale Press.
- MCNEEL NORTH AMERICA 2014. Rhinoceros. v5 ed. Seattle: McNeel North America.
- MCNEIL, A. 2013. The Five-Phase Method for Simulating Complex Fenestration with Radiance. Berkeley, CA: Lawrence Berkeley National Laboratory.

- MCNEIL, A., JONSSON, C. J., APPELFELD, D., WARD, G. & LEE, E. S. 2013. A validation of a ray-tracing tool used to generate bi-directional scattering distribution functions for complex fenestration systems. *Solar Energy*, 98, 404-414.
- MCNEIL, A. & LEE, E. S. 2013. A validation of the Radiance three-phase simulation method for modelling annual daylight performance of optically complex fenestration systems. *Journal of Building Performance Simulation*, 6, 24-37.
- MENZIES, G. F. & WHERRETT, J. R. 2005. Windows in the workplace: Examining issues of environmental sustainability and occupant comfort in the selection of multi-glazed windows. *Energy and Buildings*, 37, 623-630.
- MILLER, N., SPIVEY, J. & FLORANCE, A. 2008. Does green pay off? *Journal of Real Estate Portfolio Management*, 14, 385-399.
- MITCHELL, R., KOHLER, C., KLEMS, J. H., RUBIN, M., ARASTEH, D., HUIZENGA, C., YU, T. & CURCIJA, D. 2008. Window 6.2 / Therm 6.2 Research Version User Manual. Berkeley, CA: Lawrence Berkeley National Laboratory.
- MOLINA, G., BUSTAMANTE, W., RAO, J., FAZIO, P. & VERA, S. 2014. Evaluation of radiance's genBSDF capability to assess solar bidirectional properties of complex fenestration systems. *Journal of Building Performance Simulation*.
- MURDOCH, J. B. 2003. *Illuminating engineering : from Edison's lamp to the LED*, New York, Visions Communications.
- NABIL, A. & MARDALJEVIC, J. 2005. Useful daylight illuminance: A new paradigm for assessing daylight in buildings. *Lighting Research and Technology*, 37, 41-59.
- NABIL, A. & MARDALJEVIC, J. 2006. Useful daylight illuminances: A replacement for daylight factors. *Energy and Buildings*, 38, 905-913.
- NATIONAL RENEWABLE ENERGY LABORATORY 2008a. NREL Research Support Facilities Request for Proposal and Conceptual Documents Appendix A: Conceptual Documents. Golden, CO: National Renewable Energy Laboratory.
- NATIONAL RENEWABLE ENERGY LABORATORY 2008b. NREL Research Support Facilities Request for Proposal and Conceptual Documents Amendment of Solicitation 5. Golden, CO: National Renewable Energy Laboratory.
- NATIONAL RENEWABLE ENERGY LABORATORY. 2014. *NREL Measurement and Instrumentation Data Center (MIDC) Solar Radiation Research Laboratory (SRRL) Baseline Measurement System* [Online]. Golden, CO USA: NREL. Available: http://www.nrel.gov/midc/srll_bms/ [Accessed 18 Aug 2014].
- NATURAL RESOURCES CANADA. 2014. *Interactive maps of the photovoltaic (PV) potential and solar resource of Canada* [Online]. Ottawa: Government of Canada. Available: <http://pv.nrcan.gc.ca/>; <http://pv.nrcan.gc.ca/pvmapper.php?LAYERS=2057,4240> [Accessed 27 Nov 2014].
- NATURAL RESOURCES CANADA OFFICE OF ENERGY EFFICIENCY. 2011a. *Comprehensive Energy Use Database Table - Table 20: Offices-Secondary Energy Use and GHG Emissions by End-Use* [Online]. Ottawa: Government of Canada. Available: http://oe.nrcan.gc.ca/corporate/statistics/neud/dpa/tablestrends2/com_ca_20_e_4.cfm?attr=0 [Accessed 25 Jun 2014].

- NATURAL RESOURCES CANADA OFFICE OF ENERGY EFFICIENCY. 2011b. *Energy Use Data Handbook Tables (Canada) - Canada's Secondary Energy Use by Sector, End-Use and Subsector* [Online]. Ottawa: Government of Canada. Available: <http://oee.nrcan.gc.ca/corporate/statistics/neud/dpa/showTable.cfm?type=HB§or=aaa&juris=ca&rn=2&page=6&CFID=33130633> [Accessed 16 Jun 2014].
- NIELSEN, M. V., SVENDSEN, S. & JENSEN, L. B. 2011. Quantifying the potential of automated dynamic solar shading in office buildings through integrated simulations of energy and daylight. *Solar Energy*, 85, 757-768.
- NILSSON, A. M. & JONSSON, J. C. 2010. Light-scattering properties of a Venetian blind slat used for daylighting applications. *Solar Energy*, 84, 2103-2111.
- NREL 2015. OpenStudio. 1.7.0 ed. Golden, CO: NREL.
- O'BRIEN, W., BOURDOUKAN, P., DELISLE, V. & YIP, S. 2015. Net ZEB design processes and tools. In: ATHIENITIS, A. K. & O'BRIEN, W. (eds.) *Modeling, Design, and Optimization of Net-Zero Energy Buildings*. Hoboken: Wiley.
- O'CONNOR, J., LEE, E. S., RUBINSTEIN, F. & SELKOWITZ, S. 1997. Tips for daylighting with windows: the integrated approach. *LBNL Publication*, 790.
- OLGYAY, V. & OLGAYAY, A. 1963. *Design with climate: bioclimatic approach to architectural regionalism*, Princeton, N.J., Princeton University Press.
- PAPAMICHAEL, K., KLEMS, J. & SELKOWITZ, S. Determination and application of bidirectional solar-optical properties of fenestration systems. Proceedings, 13th National Passive Solar Conference, Cambridge, MA Papamichael, K., Klems, J., Selkowitz, S, 1988.
- PENG, Q. 2009. *Modeling and daylighting design of a new window with integrated controllable louver system*. Masters, Concordia University.
- PEREZ, R., INEICHEN, P., SEALS, R., MICHALSKY, J. & STEWART, R. 1990. Modeling daylight availability and irradiance components from direct and global irradiance. *Solar Energy*, 44, 271-289.
- PEREZ, R., SEALS, R. & MICHALSKY, J. 1993. All-weather model for sky luminance distribution-Preliminary configuration and validation. *Solar Energy*, 50, 235-245.
- PETINELLI, G. & REINHART, C. 2006. Advanced Daylight Simulations Using Ecotect, Radiance, Daysim: Getting Started. Montreal, QC.
- PTC 2010. Mathcad. 15.0 ed. Needham, MA: PTC.
- REINHART, C., RAKHA, T. & WEISSMAN, D. 2014. Predicting the daylit Area - A comparison of students assessments and simulations at eleven schools of architecture. *LEUKOS - Journal of Illuminating Engineering Society of North America*, 10, 193-206.
- REINHART, C. F. A simulation-based review of the ubiquitous window-headheight to daylit zone depth rule-of-thumb. Building Simulation 2005 - 9th International IBPSA Conference, BS 2005, 15 August 2005 through 18 August 2005 2005 Montreal; Canada. 1011-1018.
- REINHART, C. F. 2006. Tutorial on the Use of DAYSIM Simulations for Sustainable Design. *Institute for Research in Construction, National Research Council Canada. Ottawa (Ont.)*.

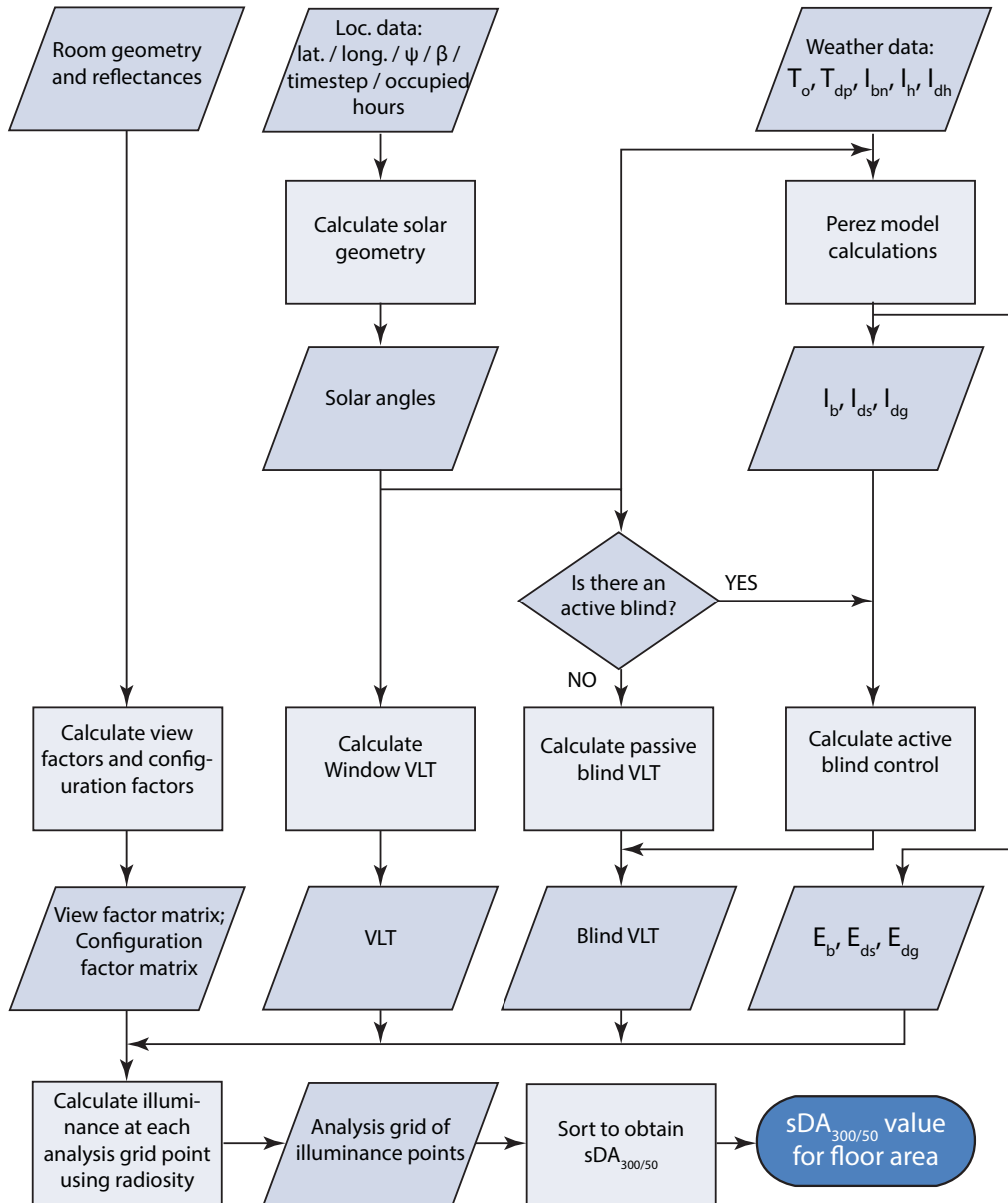
- REINHART, C. F., MARDALJEVIC, J. & ROGERS, Z. 2006. Dynamic daylight performance metrics for sustainable building design. *LEUKOS - Journal of Illuminating Engineering Society of North America*, 3, 7-31.
- REINHART, C. F. & VOSS, K. 2003. Monitoring manual control of electric lighting and blinds. *Lighting Research and Technology*, 35, 243-258.
- REINHART, C. F. & WALKENHORST, O. 2001. Validation of dynamic RADIANCE-based daylight simulations for a test office with external blinds. *Energy and Buildings*, 33, 683-697.
- ROBERTSON, K. 2005. Daylighting Guide for Buildings. Available: <http://www.cmhc-schl.gc.ca/en/inpr/bude/himu/coedar/upload/Daylighting-Guide-for-Buildings.pdf> [Accessed 20 March 2014].
- ROBINSON, D. & STONE, A. 2006. Internal illumination prediction based on a simplified radiosity algorithm. *Solar Energy*, 80, 260-267.
- ROGERS, Z. 2006. Daylighting Metric Development using Daylight Autonomy Calculations in the Sensor Placement Optimization Tool: Development Report and Case Studies. Boulder, CO: Architectural Energy Corporation.
- ROGERS, Z. 2011. SPOT Version 4.2 User's Manual. Daylighting Innovations, LLC.
- ROGERS, Z. 26 November 2013. *RE: Light Louver transmittance*. Type to CHEN, Y.
- ROYAL ARCHITECTURAL INSTITUTE OF CANADA (RAIC) 2009. *Canadian Handbook of Practice for Architects, 2nd Edition*, Ottawa.
- RUBIN, M., JONSSON, J., KOHLER, C., KLEMS, J., CURCIJA, D. & STOJANOVIC, N. 2007. Bidirectional Optical Properties of Slant Shading: Comparison Between Raytracing and Radiosity Methods. Berkeley, CA.
- SAXENA, M., HESCHONG, L., VAN DEN WYMELENBERG, K., WAYLAND, S. & ANALYTICS, I. P. 61 Flavors of daylight. ACEEE 2010 Summer Study on Energy Efficiency in Buildings, 2010 Washington, DC. American Council for an Energy-Efficient Economy Asilomar, CA.
- SEDDIGH, A., BERNTSON, E., BODIN DANIELSON, C. & WESTERLUND, H. 2014. Concentration requirements modify the effect of office type on indicators of health and performance. *Journal of Environmental Psychology*, 38, 167-174.
- SMITH-JACKSON, T. L. & KLEIN, K. W. 2009. Open-plan offices: Task performance and mental workload. *Journal of Environmental Psychology*, 29, 279-289.
- TZEMPELIKOS, A. 2005. A methodology for integrated daylighting and thermal analysis of buildings. Concordia University.
- TZEMPELIKOS, A. 2008. The impact of venetian blind geometry and tilt angle on view, direct light transmission and interior illuminance. *Solar Energy*, 82, 1172-1191.
- TZEMPELIKOS, A. & ATHIENITIS, A. K. 2007. The impact of shading design and control on building cooling and lighting demand. *Solar Energy*, 81, 369-382.
- TZEMPELIKOS, A., ATHIENITIS, A. K. & KARAVA, P. 2007. Simulation of façade and envelope design options for a new institutional building. *Solar Energy*, 81, 1088-1103.

- U.S. DEPARTMENT OF ENERGY. 2003. *2003 CBECS Survey Data - Table E3. Electricity Consumption (kWh) by End Use for Non-Mall Buildings, 2003* [Online]. Washington: U.S. Department of Energy. Available: http://www.eia.gov/consumption/commercial/data/archive/cbecs/cbecs2003/detailed_tables_2003/2003set19/2003html/e05.html ; <http://www.eia.gov/consumption/commercial/data/2003/index.cfm?view=consumption> [Accessed 25 Jun 2014].
- U.S. DEPARTMENT OF ENERGY. 2013. *EnergyPlus Energy Simulation Software - Weather Data* [Online]. USA: U.S. Department of Energy. Available: http://apps1.eere.energy.gov/buildings/energyplus/weatherdata_about.cfm [Accessed 18 Aug 2014].
- U.S. ENERGY INFORMATION ADMINISTRATION. 2013. *U.S. Energy Flow, 2013* [Online]. Washington: U.S. Department of Energy. Available: http://www.eia.gov/totalenergy/data/monthly/pdf/flow/total_energy.pdf [Accessed 01 Dec 2014].
- U.S. GENERAL SERVICES ADMINISTRATION 2007. Project Estimating Requirements for the Public Buildings Service. Washington, D.C.: U.S. General Services Administration.
- U.S. GREEN BUILDING COUNCIL 2005. *LEED for New Construction: Reference Guide, version 2.2*, U.S. Green Building Council.
- UCLA ENERGY DESIGN TOOLS GROUP 2014. Climate Consultant 5.5. Los Angeles, CA: UCLA Energy Design Tools Group.
- ULRICH, R. S. 1984. View through a window may influence recovery from surgery. *Science*, 224, 417-419.
- VAN DEN WYMELENBERG, K. 2012. Patterns of occupant interaction with window blinds: A literature review. *Energy and Buildings*, 51, 165-176.
- VINE, E., LEE, E., CLEAR, R., DIBARTOLOMEO, D. & SELKOWITZ, S. 1998. Office worker response to an automated venetian blind and electric lighting system: A pilot study. *Energy and Buildings*, 28, 205-218.
- WARD, G., MISTRICK, R., LEE, E. S., MCNEIL, A. & JONSSON, J. 2011. Simulating the daylight performance of complex fenestration systems using bidirectional scattering distribution functions within radiance. *LEUKOS - Journal of Illuminating Engineering Society of North America*, 7, 241-261.
- WIENOLD, J. & CHRISTOFFERSEN, J. 2006. Evaluation methods and development of a new glare prediction model for daylight environments with the use of CCD cameras. *Energy and Buildings*, 38, 743-757.
- WILCOX, S. & MARION, W. 2008. Users manual for TMY3 data sets. Golden, CO USA: National Renewable Energy Laboratory.
- YIP, S. & CORY, S. 2013. Use of Net Zero Energy Solution Sets for the Redesign of the Reunion Island ENERPOS Building in Christchurch. *Building Simulation 2013*. Chambéry, France: IBPSA.
- ZUO, W., MCNEIL, A., WETTER, M. & LEE, E. S. 2014. Acceleration of the matrix multiplication of Radiance three phase daylighting simulations with parallel computing on heterogeneous hardware of personal computer. *Journal of Building Performance Simulation*, 7, 152-163.

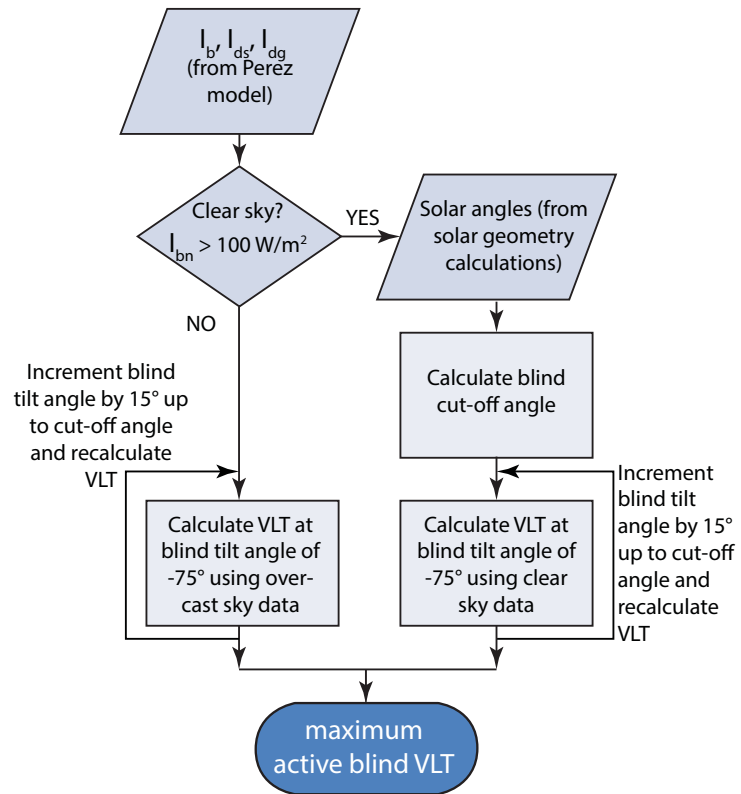
Appendices

A1. Mathematical daylighting model

A1.1. Daylighting model flowchart



A1.2. Active blind control strategy flowchart



A1.3. General building inputs

General Building Inputs

Facade orientation

$\beta_w := 90\text{deg}$	Facade tilt angle (facade is vertical)
orient_increment := 15deg	Surface azimuth: South is zero; east of south is negative
f := -3 .. 3	North wing of Phase I, South facade is 15deg east of south facade orientation index: 0 is south
$\psi_{so}(f) := f \cdot (\text{orient_increment})$	Surface azimuth: South facade
$\psi_{no}(f) := \begin{cases} (\psi_{so}(f) + 180\text{deg}) & \text{if } \psi_{so}(f) \leq 0 \\ (\psi_{so}(f) - 180\text{deg}) & \text{otherwise} \end{cases}$	Surface azimuth: North facade

Other inputs

$H_{\text{workplane}} := 0.914\text{m}$	height of workplane above finish floor
Interval_angle := 15-deg	blind tilt angle controllable interval
limit := $100 \cdot \frac{\text{W}}{\text{m}^2}$	direct normal irradiance level limit to separate overcast and clear sky conditions

Simulation time steps

```

starttime := 8
endtime := 17
t := starttime .. endtime

weeks := 1 .. 52
weekdays := 1 .. 7
n_weekdays :=
    day_counter ← 0
    row ← 0
    for week ∈ weeks
        for weekday ∈ weekdays
            day_counter ← day_counter + 1           weekday 1 is = Monday
            row ← row + 1
            nn_row ← day_counter if weekday < 6
            row ← row - 1 otherwise
        day_counter ← day_counter + 1
        row ← row + 1
        nn_row ← day_counter
    return nn

```

A1.4. Solar geometry calculations

Solar Geometry Calculations

Equation of time

$$ET(n) := \left(9.87 \cdot \sin\left(4 \cdot \pi \cdot \frac{n - 81}{364}\right) - 7.53 \cdot \cos\left(2 \cdot \pi \cdot \frac{n - 81}{364}\right) - 1.5 \cdot \sin\left(2 \cdot \pi \cdot \frac{n - 81}{364}\right) \right) \cdot \text{min}$$

Apparent solar time

$$AST(n, t) := t \cdot \text{hr} + ET(n) + \frac{(STM - LNG) \cdot \text{hr}}{15 \cdot \text{deg}}$$

Solar declination

$$\delta(n) := 23.45 \cdot \text{deg} \cdot \sin\left(360 \cdot \frac{284 + n}{365} \cdot \text{deg}\right)$$

Hour angle

$$H(n, t) := (AST(n, t) - 12 \cdot \text{hr}) \cdot \left(15 \cdot \frac{\text{deg}}{\text{hr}}\right)$$

Sunset hour angle

$$h_s(n) := \text{acos}(-\tan(L) \cdot \tan(\delta(n)))$$

Sunset time

$$t_s(n) := h_s(n) \cdot \frac{\text{hr}}{15 \cdot \text{deg}}$$

Surface sunset time

$$t_{ss}(n) := \min\left(h_s(n), \text{acos}(-\tan(L - \beta_w) \cdot \tan(\delta(n)))\right) \cdot \frac{\text{hr}}{15 \cdot \text{deg}}$$

Solar altitude

$$\alpha_s(n, t) := \begin{cases} \text{asin}\left[\frac{(\cos(L)) \cdot \cos(\delta(n)) \cdot \cos(H(n, t)) \dots}{+(\sin(L)) \cdot \sin(\delta(n))}\right] & \text{if } \text{asin}\left[\frac{(\cos(L)) \cdot \cos(\delta(n)) \cdot \cos(H(n, t)) \dots}{+(\sin(L)) \cdot \sin(\delta(n))}\right] > 0 \text{deg} \\ (0 \text{deg}) & \text{otherwise} \end{cases}$$

Solar azimuth

$$\phi(n, t) := \text{acos}\left(\frac{\sin(\alpha_s(n, t)) \cdot \sin(L) - \sin(\delta(n))}{\cos(\alpha_s(n, t)) \cdot \cos(L)}\right) \cdot \frac{H(n, t)}{|H(n, t)|}$$

Surface solar azimuth

$$\gamma_{so}(n, t, f) := \phi(n, t) - \psi_{so}(f)$$

South facing facade

$$\gamma_{no}(n, t, f) := \phi(n, t) - \psi_{no}(f)$$

North facing facade

Zenith angle

$$Z(n, t) := \text{acos}[(\cos(L)) \cdot \cos(\delta(n)) \cdot \cos(H(n, t)) + \sin(L) \cdot \sin(\delta(n))]$$

Angle of incidence

$$\theta_{so}(n, t, f) := \cos(\alpha_s(n, t)) \cdot \cos(|\gamma_{so}(n, t, f)|) \cdot \sin(\beta_w) + \sin(\alpha_s(n, t)) \cdot \cos(\beta_w)$$

$$\theta_{so}(n, t, f) := \text{acos}\left(\frac{\theta_{so}(n, t, f) + |\theta_{so}(n, t, f)|}{2}\right)$$

South facing facade

$$\theta_{no}(n, t, f) := \cos(\alpha_s(n, t)) \cdot \cos(|\gamma_{no}(n, t, f)|) \cdot \sin(\beta_w) + \sin(\alpha_s(n, t)) \cdot \cos(\beta_w)$$

$$\theta_{no}(n, t, f) := \text{acos}\left(\frac{\theta_{no}(n, t, f) + |\theta_{no}(n, t, f)|}{2}\right)$$

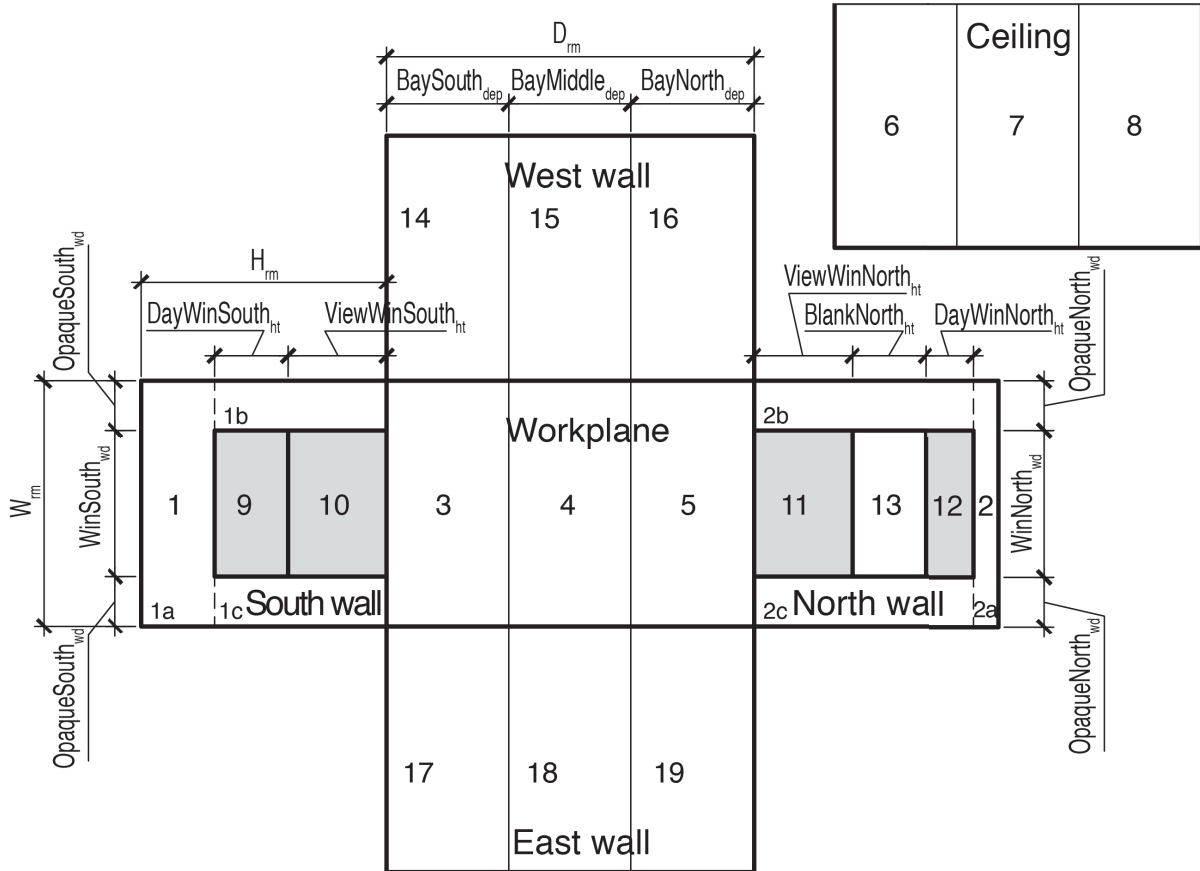
North facing facade

Profile angle

$$\lambda(n, t, f) := \begin{cases} \text{atan}\left(\frac{\tan(\alpha_s(n, t))}{\cos(\gamma_{so}(n, t, f))}\right) & \text{if } -90 \cdot \text{deg} < \gamma_{so}(n, t, f) < 90 \cdot \text{deg} \\ (90 \cdot \text{deg}) & \text{otherwise} \end{cases}$$

South facing facade

A1.5. Room geometry



$W_{rm} := 3.0m$	Width along facade
$D_{rm} = 18-m$	Depth of room
$H_{rm} := 3.048m$	Height of room above workplane
$WinSouth_{wd} := 1.8288m$	Window, South (surface 9,10): width along facade
$DayWinSouth_{ht} := 0.9144m$	Daylight window, South (surface 9): Height
$ViewWinSouth_{ht} := 1.2192m$	View window, South (surface 10): Height
$WinNorth_{wd} := 1.8288m$	Window, North (surface 11,12,13): width along facade
$DayWinNorth_{ht} := 0.762m$	Daylight window, North (surface 12): height
$ViewWinNorth_{ht} := 1.2192m$	View window, North (surface 11): height

BlankNorth_{ht} := 0.9144m Blank wall btwn daylight/view window, North (surface 13): height

$$\text{BaySouth}_{\text{ratio}} := \frac{8.6868}{18.288}$$

$$\text{BayMiddle}_{\text{ratio}} := \frac{3.1242}{18.288}$$

$$\text{BayNorth}_{\text{ratio}} := \frac{6.477}{18.288}$$

BaySouth_{dep} := BaySouth_{ratio} · D_{rm} Bay depth, South (surface 3,6): measured perp. to facade

BayMiddle_{dep} := BayMiddle_{ratio} · D_{rm} Bay depth, middle (surface 4,7): measured perp. to facade

BayNorth_{dep} := BayNorth_{ratio} · D_{rm} Bay depth, North (surface 5,8): measured perp. to facade

OpaqueSouth_{wd} := $\frac{1}{2}(W_{\text{rm}} - \text{WinSouth}_{\text{wd}})$ South wall, opaque width on each side of window

OpaqueNorth_{wd} := $\frac{1}{2}(W_{\text{rm}} - \text{WinNorth}_{\text{wd}})$ North wall, opaque width on each side of window

```
Arad := | Data1 ← Hrm · Wrm - WinSouthwd · DayWinSouthht ...
        |   + WinSouthwd · ViewWinSouthht
        | Data2 ← Hrm · Wrm - WinNorthwd · DayWinNorthht ...
        |   + WinNorthwd · ViewWinNorthht - WinNorthwd · BlankNorthht
        | Data3 ← BaySouthdep · Wrm
        | Data4 ← BayMiddledep · Wrm
        | Data5 ← BayNorthdep · Wrm
        | Data6 ← BaySouthdep · Wrm
        | Data7 ← BayMiddledep · Wrm
        | Data8 ← BayNorthdep · Wrm
        | Data9 ← WinSouthwd · DayWinSouthht
        | Data10 ← WinSouthwd · ViewWinSouthht
        | Data11 ← WinNorthwd · ViewWinNorthht
        | Data12 ← WinNorthwd · DayWinNorthht
        | Data13 ← WinNorthwd · BlankNorthht
        | Data14 ← BaySouthdep · Hrm
        | Data15 ← BayMiddledep · Hrm
        | Data16 ← BayNorthdep · Hrm
        | Data17 ← BaySouthdep · Hrm
        | Data18 ← BayMiddledep · Hrm
        | Data19 ← BayNorthdep · Hrm
        | return Data
```


A1.6. Sample view factor calculations

View factors calculated using

Athienitis, A., Building Thermal Analysis Section 6.1 (<https://www.ptcusercommunity.com/docs/DOC-4330>)
and

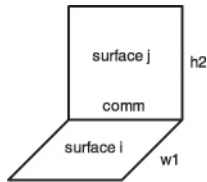
Howell, J.R., Catalog of Radiation Heat Transfer Configuration Factors, 3rd
(<http://www.thermalradiation.net/indexCat.html>)

C-14: Two finite rectangles of same length, having one common edge, and at an angle of 90deg to each other.

<http://www.thermalradiation.net/sectionc/C-14.html>

Online calculator:

<http://www.thermalradiation.net/calc/sectionc/C-14.html>



$F_{ij}(w,h)$

ORIGIN:= 1

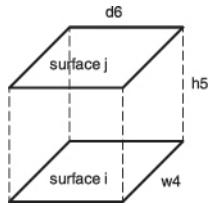
Define the following intermediate variables:

$$w = \frac{w1}{comm} \quad h = \frac{h2}{comm}$$

View factor F_{ij} from i to j:

$$F_{ij}(w,h) := \frac{w \cdot \operatorname{atan}\left(\frac{1}{w}\right) + h \cdot \operatorname{atan}\left(\frac{1}{h}\right) - \sqrt{h^2 + w^2} \cdot \operatorname{atan}\left(\frac{1}{\sqrt{h^2 + w^2}}\right) + 0.25 \ln \left[\frac{w^2 \cdot (1 + h^2 + w^2)}{(1 + w^2) \cdot (h^2 + w^2)} \right]^{w^2} \cdot \left[\frac{h^2 \cdot (1 + h^2 + w^2)}{(1 + h^2) \cdot (h^2 + w^2)} \right]^{h^2} \cdot \frac{(1 + w^2) \cdot (1 + h^2)}{(1 + h^2 + w^2)}}{\pi \cdot w}$$

C-11: Identical, parallel, directly opposed rectangles.
<http://www.thermalradiation.net/sectionc/C-11.html>
 Online calculator:
<http://www.thermalradiation.net/calc/sectionc/C-11.html>



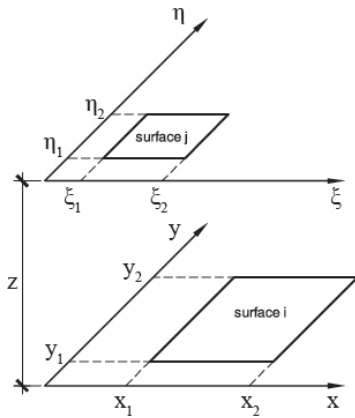
$G_{ij}(X,Y)$

ORIGIN := 1

$$X = \frac{d6}{h5} \quad Y = \frac{w4}{h5}$$

$$G_{ij}(X,Y) := \frac{2}{\pi \cdot X \cdot Y} \left[\ln \left[\frac{\sqrt{(1+X^2)(1+Y^2)}}{1+X^2+Y^2} \right] + X \cdot \sqrt{1+Y^2} \cdot \operatorname{atan} \left(\frac{X}{\sqrt{1+Y^2}} \right) \dots \right. \\ \left. + Y \cdot \sqrt{1+X^2} \cdot \operatorname{atan} \left(\frac{Y}{\sqrt{1+X^2}} \right) - X \cdot \operatorname{atan}(X) - Y \cdot \operatorname{atan}(Y) \right]$$

C-13: Rectangle to rectangle in a parallel plane.
<http://www.thermalradiation.net/sectionc/C-13.html>
 Online calculator:
<http://www.thermalradiation.net/calc/sectionc/C-13.html>



$$H_{ij}(x,y,\eta,\xi,z)$$

ORIGIN := 1

i := 1..2

j := 1..2

k := 1..2 em := 1..2

$$GG(x,y,\eta,\xi,z) := \frac{1}{2 \cdot \pi} \left[\begin{aligned} &(y - \eta) \cdot \sqrt{(x - \xi)^2 + z^2} \cdot \operatorname{atan} \left[\frac{y - \eta}{\sqrt{(x - \xi)^2 + z^2}} \right] \dots \\ &+ (x - \xi) \cdot \sqrt{(y - \eta)^2 + z^2} \cdot \operatorname{atan} \left[\frac{x - \xi}{\sqrt{(y - \eta)^2 + z^2}} \right] \dots \\ &+ \frac{-z^2}{2} \cdot \ln \left[(x - \xi)^2 + (y - \eta)^2 + z^2 \right] \end{aligned} \right]$$

$$H_{ij}(x,y,\eta,\xi,z) := \frac{1}{(x_2 - x_1) \cdot (y_2 - y_1)} \left[\sum_{em} \left[\sum_k \left[\sum_j \left[\sum_i \left[(-1)^{(i+j+k+em)} \cdot GG(x_i, y_j, \eta_k, \xi_{em}, z) \right] \right] \right] \right] \right]$$

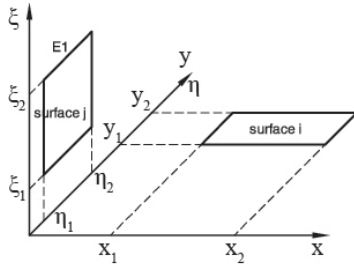
C-15: Rectangle to rectangle in a perpendicular plane; all boundaries are parallel or perpendicular to x and ξ boundaries.

<http://www.thermalradiation.net/sectionc/C-15.html>

Online calculator:

<http://www.thermalradiation.net/calc/sectionc/C-15.html>

(Note that the expression fails if the rectangles share a common edge; therefore, a "Tiny" quantity is added to avoid divide by zero error.)



$$J_{ij}(x, y, \eta, \xi)$$

ORIGIN := 1

i := 1..2 j := 1..2 k := 1..2 em := 1..2

Divide by zero error if $\eta = y$ and if $x^2 + \xi^2 = 0$

Tiny := $1.0 \cdot 10^{-10}$

avoid divide by zero error

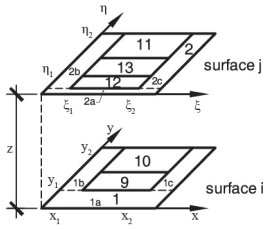
$$LL(x, \xi) := \begin{cases} \text{Tiny} & \text{if } \sqrt{x^2 + \xi^2} < \text{Tiny} \\ \sqrt{x^2 + \xi^2} & \text{otherwise} \end{cases}$$

$$KK(x, y, \eta, \xi) := \frac{(y - \eta)}{LL(x, \xi)}$$

$$GH(x, y, \eta, \xi) := \begin{cases} y \leftarrow y + \text{Tiny} & \text{if } y = \eta \\ y & \text{otherwise} \end{cases} \left[\frac{1}{2 \cdot \pi} \cdot \left[\frac{(y - \eta) \cdot \sqrt{x^2 + \xi^2} \cdot \text{atan}(KK(x, y, \eta, \xi)) \dots}{+ \frac{-1}{4} \left[(x^2 + \xi^2) \cdot \ln(1 + KK(x, y, \eta, \xi)^2) - (y - \eta)^2 \cdot \ln\left(1 + \frac{1}{KK(x, y, \eta, \xi)^2}\right)\right]} \right] \right]$$

$$J_{ij}(x, y, \eta, \xi) := \frac{1}{(x_2 - x_1)(y_2 - y_1)} \left[\sum_{em} \left[\sum_k \left[\sum_j \left[\sum_i \left[(-1)^{(i+j+k+em)} \cdot GH(x_i, y_j, \eta_k, \xi_{em}) \right] \right] \right] \right] \right]$$

South - North facade



$$A_{1a} := W_{rm} \cdot (H_{rm} - \text{DayWinSouth}_{ht} - \text{ViewWinSouth}_{ht})$$

$$A_{1b} := \text{OpaqueSouth}_{wd} \cdot (\text{DayWinSouth}_{ht} + \text{ViewWinSouth}_{ht})$$

$$A_{1c} := A_{1b}$$

$$A_{2a} := W_{rm} \cdot (H_{rm} - \text{DayWinNorth}_{ht} - \text{BlankNorth}_{ht} - \text{ViewWinNorth}_{ht})$$

$$A_{2b} := \text{OpaqueNorth}_{wd} \cdot (\text{DayWinNorth}_{ht} + \text{BlankNorth}_{ht} + \text{ViewWinNorth}_{ht})$$

$$A_{2c} := A_{2b}$$

For 1a_2a

$$x_1 := 0$$

$$x_2 := \frac{W_{rm}}{ft}$$

$$\xi_1 := 0$$

$$\xi_2 := \frac{W_{rm}}{ft}$$

$$z := \frac{D_{rm}}{ft}$$

$$F_{1a_2a} := \text{Hij}(x, y, \eta, \xi, z)$$

$$y_1 := 0$$

$$y_2 := \frac{(H_{rm} - \text{DayWinSouth}_{ht} - \text{ViewWinSouth}_{ht})}{ft}$$

$$\eta_1 := 0$$

$$\eta_2 := \frac{(H_{rm} - \text{DayWinNorth}_{ht} - \text{BlankNorth}_{ht} - \text{ViewWinNorth}_{ht})}{ft}$$

$$F_{1a_2a} = 0.0001$$

For 1a_2b

$$x_1 := 0$$

$$x_2 := \frac{W_{rm}}{ft}$$

$$\xi_1 := 0$$

$$\xi_2 := \frac{\text{OpaqueNorth}_{wd}}{ft}$$

$$z := \frac{D_{rm}}{ft}$$

$$F_{1a_2b} := \text{Hij}(x, y, \eta, \xi, z)$$

$$y_1 := 0$$

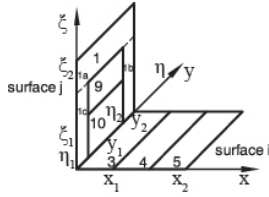
$$y_2 := \frac{(H_{rm} - \text{DayWinSouth}_{ht} - \text{ViewWinSouth}_{ht})}{ft}$$

$$\eta_1 := \frac{(H_{rm} - \text{DayWinNorth}_{ht} - \text{BlankNorth}_{ht} - \text{ViewWinNorth}_{ht})}{ft}$$

$$\eta_2 := \frac{H_{rm}}{ft}$$

$$F_{1a_2b} = 0.002$$

For South facade - Workplane



$$A_{1a} = 29.528 \text{ ft}^2 \quad \text{previously defined}$$

$$A_{1b} = 13.449 \text{ ft}^2 \quad \text{previously defined}$$

$$A_{1c} = 13.449 \text{ ft}^2 \quad \text{previously defined}$$

$$A_3 := W_{rm} \cdot \text{BaySouth}_{dep}$$

$$A_4 := W_{rm} \cdot \text{BayMiddle}_{dep}$$

$$A_5 := W_{rm} \cdot \text{BayNorth}_{dep}$$

For 3_1

For 3_1a

$$x_1 := 0$$

$$y_1 := 0$$

$$x_2 := \frac{\text{BaySouth}_{dep}}{\text{ft}}$$

$$y_2 := \frac{W_{rm}}{\text{ft}}$$

$$\xi_1 := \frac{\text{DayWinSouth}_{ht} + \text{ViewWinSouth}_{ht}}{\text{ft}}$$

$$\eta_1 := 0$$

$$\xi_2 := \frac{H_{rm}}{\text{ft}}$$

$$\eta_2 := \frac{W_{rm}}{\text{ft}}$$

$$F_{3_1a} := J_{ij}(x, y, \eta, \xi)$$

$$F_{3_1a} = 0.015$$

For 3_1b

$$x_1 := 0$$

$$y_1 := 0$$

$$x_2 := \frac{\text{BaySouth}_{dep}}{\text{ft}}$$

$$y_2 := \frac{W_{rm}}{\text{ft}}$$

$$\xi_1 := 0$$

$$\eta_1 := \frac{\text{OpaqueSouth}_{wd} + \text{WinSouth}_{wd}}{\text{ft}}$$

$$\xi_2 := \frac{\text{DayWinSouth}_{ht} + \text{ViewWinSouth}_{ht}}{\text{ft}}$$

$$\eta_2 := \frac{W_{rm}}{\text{ft}}$$

$$F_{3_1b} := J_{ij}(x, y, \eta, \xi)$$

$$F_{3_1b} = 0.012$$

For 3_1c

$$x_1 := 0$$

$$y_1 := 0$$

$$x_2 := \frac{\text{BaySouth}_{\text{dep}}}{\text{ft}}$$

$$y_2 := \frac{W_{\text{rm}}}{\text{ft}}$$

$$\xi_1 := 0$$

$$\eta_1 := 0$$

$$\xi_2 := \frac{\text{DayWinSouth}_{\text{ht}} + \text{ViewWinSouth}_{\text{ht}}}{\text{ft}}$$

$$\eta_2 := \frac{\text{OpaqueSouth}_{\text{wd}}}{\text{ft}}$$

$$F_{3_1c} := \text{Jij}(x, y, \eta, \xi)$$

$$F_{3_1c} = 0.012$$

$$F_{3,1} := F_{3_1a} + F_{3_1b} + F_{3_1c}$$

by partial summation

$$F_{3,1} = 0.039$$

$$F_{1,3} := \frac{A_{\text{rad}_3}}{A_{\text{rad}_1}} \cdot F_{3,1}$$

by reciprocity

$$F_{1,3} = 0.192$$

A1.7. Sample configuration factor calculations

ORIGIN:= 1

grid := 0.5m

$$\text{increments} := \text{floor}\left(\frac{D_{\text{rm}} - \text{grid}}{\text{grid}}\right)$$

divide room depth into 0.5 m x 0.5 m
configuration point grid with 0.5m
distance any wall to closest grid point.

range := 1..increments

j := 1..(increments + 1)

$$\text{ptj} := \begin{cases} \text{ptj}_1 \leftarrow \frac{D_{\text{rm}} - \text{increments} \cdot \text{grid}}{2} \\ \text{for } rr \in \text{range} \\ \text{ptj}_{rr+1} \leftarrow \text{ptj}_1 + rr \cdot \text{grid} \\ \text{return ptj} \end{cases}$$

coordinate system: width (i) is
measured from East facade; depth (j)
is measured from South facade.

ptj distance from South facade

i := 1..5

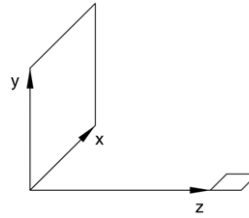
width points

set up five rows of points parallel to East facade

$$\text{pti}_1 := 0.5\text{m} \quad \text{pti}_2 := 1.0\text{m} \quad \text{pti}_3 := 1.5\text{m} \quad \text{pti}_4 := 2.0\text{m} \quad \text{pti}_5 := 2.5\text{m} \quad \text{pti}_i \text{ distance from East facade}$$

The configuration factor between a surface and a point perpendicular to the surface is:

$$\text{perp}(x, y, z) := \frac{1}{2 \cdot \pi} \cdot \left(\text{atan}\left(\frac{x}{z}\right) - \frac{z}{\sqrt{y^2 + z^2}} \cdot \text{atan}\left(\frac{x}{\sqrt{y^2 + z^2}}\right) \right)$$



Let pt.z be on the workplane (0.9m) at the centre of the rm.

Starting from the bottom, up

Surface 10, view window

$$x(i) := \text{pti}_i \quad y := \text{ViewWinSouth}_{\text{ht}} \quad z(j) := \text{ptj}_j$$

$$c_{s10}(i, j) := \begin{cases} \text{perp}[(\text{OpaqueSouth}_{\text{wd}} + \text{WinSouth}_{\text{wd}} - x(i)), y, z(j)] \dots & \text{if } (x(i) - \text{OpaqueSouth}_{\text{wd}}) \leq 0 \\ + \text{perp}[(\text{OpaqueSouth}_{\text{wd}} - x(i)), y, z(j)] & \\ \text{perp}[(x(i) - \text{OpaqueSouth}_{\text{wd}}), y, z(j)] \dots & \text{if } 0 < (x(i) - \text{OpaqueSouth}_{\text{wd}}) \leq \text{WinSouth}_{\text{wd}} \\ + \text{perp}[(\text{OpaqueSouth}_{\text{wd}} + \text{WinSouth}_{\text{wd}} - x(i)), y, z(j)] & \\ \text{perp}[(x(i) - \text{OpaqueSouth}_{\text{wd}}), y, z(j)] - \text{perp}[(x(i) - \text{OpaqueSouth}_{\text{wd}} - \text{WinSouth}_{\text{wd}}), y, z(j)] & \text{otherwise} \end{cases}$$

Surface 9, daylighting window

$$y := \text{ViewWinSouth}_{\text{ht}} + \text{DayWinSouth}_{\text{ht}}$$

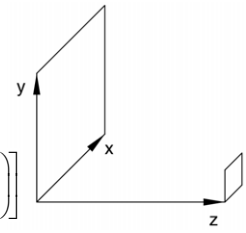
$$c_{s9}(i, j) := \begin{cases} \text{perp}[(\text{OpaqueSouth}_{\text{wd}} + \text{WinSouth}_{\text{wd}} - x(i)), y, z(j)] \dots & \text{if } (x(i) - \text{OpaqueSouth}_{\text{wd}}) \leq 0 \\ + \text{perp}[(\text{OpaqueSouth}_{\text{wd}} - x(i)), y, z(j)] - c_{s10}(i, j) & \\ \text{perp}[(x(i) - \text{OpaqueSouth}_{\text{wd}}), y, z(j)] + \dots & \text{if } 0 < (x(i) - \text{OpaqueSouth}_{\text{wd}}) \leq \text{WinSouth}_{\text{wd}} \\ + \left[\text{perp}[(\text{OpaqueSouth}_{\text{wd}} + \text{WinSouth}_{\text{wd}} - x(i)), y, z(j)] \dots \right. & \\ \left. + -c_{s10}(i, j) \right] & \\ \text{perp}[(x(i) - \text{OpaqueSouth}_{\text{wd}}), y, z(j)] \dots & \text{otherwise} \\ + \text{perp}[(x(i) - \text{OpaqueSouth}_{\text{wd}} - \text{WinSouth}_{\text{wd}}), y, z(j)] - c_{s10}(i, j) & \end{cases}$$

Surface 1, south wall

$$y := H_{\text{rm}}$$

$$c_{s1}(i, j) := \text{perp}[(W_{\text{rm}} - x(i)), y, z(j)] + \text{perp}(x(i), y, z(j)) - c_{s10}(i, j) - c_{s9}(i, j)$$

The configuration factor between a surface and a point parallel to the surface is:

$$\text{para}(x, y, z) := \frac{1}{2 \cdot \pi} \left[\left(\frac{y}{\sqrt{y^2 + z^2}} \right) \cdot \text{atan} \left(\frac{x}{\sqrt{y^2 + z^2}} \right) + \frac{x}{\sqrt{x^2 + z^2}} \cdot \text{atan} \left(\frac{y}{\sqrt{x^2 + z^2}} \right) \right]$$


Surface 6, ceiling

$$x(j) := \text{ptj}_j \quad y(i) := \text{pti}_i \quad z := H_{\text{rm}}$$

$$c_{s6}(i, j) := \begin{cases} \text{para}(x(j), y(i), z) + \text{para}[(\text{BaySouth}_{\text{dep}} - x(j)), y(i), z] \dots & \text{if } (x(j) - \text{BaySouth}_{\text{dep}}) \leq 0 \\ + \text{para}[x(j), (W_{\text{rm}} - y(i)), z] + \text{para}[(\text{BaySouth}_{\text{dep}} - x(j)), (W_{\text{rm}} - y(i)), z] & \\ \text{para}(x(j), y(i), z) - \text{para}[(x(j) - \text{BaySouth}_{\text{dep}}), y(i), z] \dots & \text{otherwise} \\ + \text{para}[x(j), (W_{\text{rm}} - y(i)), z] - \text{para}[(x(j) - \text{BaySouth}_{\text{dep}}), (W_{\text{rm}} - y(i)), z] & \end{cases}$$

Surface 7, ceiling

$$c_{s7}(i, j) := \begin{cases} \text{para}[(\text{BaySouth}_{\text{dep}} + \text{BayMiddle}_{\text{dep}} - x(j)), y(i), z] \dots & \text{if } (x(j) - \text{BaySouth}_{\text{dep}}) \leq 0 \\ + \text{para}[(\text{BaySouth}_{\text{dep}} - x(j)), y(i), z] \dots & \\ + \text{para}[(\text{BaySouth}_{\text{dep}} + \text{BayMiddle}_{\text{dep}} - x(j)), (W_{\text{rm}} - y(i)), z] \dots & \\ + \text{para}[(\text{BaySouth}_{\text{dep}} - x(j)), (W_{\text{rm}} - y(i)), z] & \\ \text{para}[(\text{BaySouth}_{\text{dep}} + \text{BayMiddle}_{\text{dep}} - x(j)), y(i), z] \dots & \text{if } 0 < (x(j) - \text{BaySouth}_{\text{dep}}) \leq \text{BayMiddle}_{\text{dep}} \\ + \text{para}[(x(j) - \text{BaySouth}_{\text{dep}}), y(i), z] \dots & \\ + \text{para}[(\text{BaySouth}_{\text{dep}} + \text{BayMiddle}_{\text{dep}} - x(j)), (W_{\text{rm}} - y(i)), z] \dots & \\ + \text{para}[(x(j) - \text{BaySouth}_{\text{dep}}), (W_{\text{rm}} - y(i)), z] & \\ \text{para}[(x(j) - \text{BaySouth}_{\text{dep}}), y(i), z] \dots & \text{otherwise} \\ + \text{para}[(x(j) - \text{BaySouth}_{\text{dep}} - \text{BayMiddle}_{\text{dep}}), y(i), z] \dots & \\ + \text{para}[(x(j) - \text{BaySouth}_{\text{dep}}), (W_{\text{rm}} - y(i)), z] \dots & \\ + \text{para}[(x(j) - \text{BaySouth}_{\text{dep}} - \text{BayMiddle}_{\text{dep}}), (W_{\text{rm}} - y(i)), z] & \end{cases}$$

Surface 8, ceiling

$$c_{s8}(i, j) := \begin{cases} \text{para}[(\text{BaySouth}_{\text{dep}} + \text{BayMiddle}_{\text{dep}} + \text{BayNorth}_{\text{dep}} - x(j)), y(i), z] \dots & \text{if } (x(j) - \text{BaySouth}_{\text{dep}}) \leq \text{BayMiddle}_{\text{dep}} \\ + \text{para}[(\text{BaySouth}_{\text{dep}} + \text{BayMiddle}_{\text{dep}} - x(j)), y(i), z] \dots & \\ + \text{para}[(\text{BaySouth}_{\text{dep}} + \text{BayMiddle}_{\text{dep}} + \text{BayNorth}_{\text{dep}} - x(j)), (W_{\text{rm}} - y(i)), z] \dots & \\ + \text{para}[(\text{BaySouth}_{\text{dep}} + \text{BayMiddle}_{\text{dep}} - x(j)), (W_{\text{rm}} - y(i)), z] & \\ \text{para}[(\text{BaySouth}_{\text{dep}} + \text{BayMiddle}_{\text{dep}} + \text{BayNorth}_{\text{dep}} - x(j)), y(i), z] \dots & \text{otherwise} \\ + \text{para}[(x(j) - \text{BaySouth}_{\text{dep}} - \text{BayMiddle}_{\text{dep}}), y(i), z] \dots & \\ + \text{para}[(\text{BaySouth}_{\text{dep}} + \text{BayMiddle}_{\text{dep}} + \text{BayNorth}_{\text{dep}} - x(j)), (W_{\text{rm}} - y(i)), z] \dots & \\ + \text{para}[(x(j) - \text{BaySouth}_{\text{dep}} - \text{BayMiddle}_{\text{dep}}), (W_{\text{rm}} - y(i)), z] & \end{cases}$$

A2. Model calibration support data

A2.1. RSF weather station irradiance data (sample)

Table A0.1: Excerpt from RSF weather station irradiance data.

Date	Time	Global [W/m ²]	Direct [W/m ²]	Diffuse [W/m ²]
1/16/2013	08:31	158.303	764.375	32.4053
1/16/2013	08:32	161.681	770.007	32.4325
1/16/2013	08:33	160.963	759.784	32.4692
1/16/2013	08:34	156.35	724.141	32.5715
1/16/2013	08:35	149.142	677.384	33.0052
1/16/2013	08:36	149.175	669.92	33.3721
1/16/2013	08:37	121.889	524.638	33.7954
1/16/2013	08:38	137.568	588.501	34.5099
1/16/2013	08:39	167.422	725.26	35.4253
1/16/2013	08:40	181.821	788.518	36.2454
1/16/2013	08:41	187.034	795.115	36.7104
1/16/2013	08:42	188.804	796.341	36.8553
1/16/2013	08:43	190.725	796.826	37.0399
1/16/2013	08:44	194.342	799.697	37.2639
1/16/2013	08:45	197.871	801.967	37.8464
1/16/2013	08:46	200.73	804.315	38.4661
1/16/2013	08:47	204.145	806.868	39.2913
1/16/2013	08:48	206.063	809.399	40.2806
1/16/2013	08:49	209.429	810.55	41.5303
1/16/2013	08:50	213.178	813.214	42.7799
1/16/2013	08:51	216.541	814.35	44.2336
1/16/2013	08:52	219.653	816.165	45.7759
1/16/2013	08:53	223.865	818.321	47.2574
1/16/2013	08:54	227.954	820.287	48.5777
1/16/2013	08:55	232.067	821.798	50.1658
1/16/2013	08:56	235.505	823.385	52.0159
1/16/2013	08:57	239.974	825.823	53.9818
1/16/2013	08:58	245.37	829.11	55.8749
1/16/2013	08:59	244.97	810.06	57.9046
1/16/2013	09:00	225.909	725.164	59.9857
1/16/2013	09:01	192.346	588.502	62.3827
1/16/2013	09:02	203.636	590.731	65.2933
1/16/2013	09:03	274.398	849.239	68.285
1/16/2013	09:04	231.634	681.07	71.1761
1/16/2013	09:05	269.375	797.433	74.3534
1/16/2013	09:06	207.785	558.276	77.3686
1/16/2013	09:07	283.471	815.614	80.6331
1/16/2013	09:08	293.88	837.313	82.9942
1/16/2013	09:09	283.152	788.798	84.7961
1/16/2013	09:10	240.16	622.29	86.6117
1/16/2013	09:11	266.86	701.179	88.8135
1/16/2013	09:12	296.653	790.988	91.0832
1/16/2013	09:13	300.715	799.568	92.5358
1/16/2013	09:14	231.87	562.905	93.1488
1/16/2013	09:15	303.226	786.979	93.8582
1/16/2013	09:16	326.532	860.765	94.1077
1/16/2013	09:17	325.685	851.487	93.8278
1/16/2013	09:18	331.046	862.758	93.2868
1/16/2013	09:19	332.417	864.068	92.6912
1/16/2013	09:20	334.428	865.696	91.8506
1/16/2013	09:21	332.625	861.082	90.5486

1/16/2013	09:22	274.209	671.872	89.1734
1/16/2013	09:23	207.159	458.416	88.3752
1/16/2013	09:24	203.237	445.131	85.3323
1/16/2013	09:25	191.22	395.046	85.9894
1/16/2013	09:26	229.599	426.419	85.4064
1/16/2013	09:27	202.518	383.438	85.5064
1/16/2013	09:28	173.706	378.468	85.7674
1/16/2013	09:29	167.865	311.467	85.8144
1/16/2013	09:30	312.996	750.279	85.967

Instrumentation : Global horizontal irradiance: TSP-700 Vent; Direct irradiance: LI-201; Diffuse irradiance: PSP (vent/cor)

A2.2. Simulation analysis grid data for LEED v2.2 verification

Table A0.2: Analysis grid illuminance for LEED v2.2 IEQ8.1; 12:00, 22 September; LightLouver; $\psi = -15^\circ$ [lx].

Analysis pts (Distance from South Wall)	Analysis pts (Distance from East Wall)				
	i1 (0.5 m)	i2 (1.0 m)	i3 (1.5 m)	i4 (2.0 m)	i5 (2.5 m)
j1 (0.5 m)	3125	4999	5534	4999	3125
j2 (1.0 m)	2665	3517	3851	3517	2665
j3 (1.5 m)	2115	2537	2706	2537	2115
j4 (2.0 m)	1669	1886	1970	1886	1669
j5 (2.5 m)	1350	1464	1507	1464	1350
j6 (3.0 m)	1130	1192	1216	1192	1130
j7 (3.5 m)	979	1014	1027	1014	979
j8 (4.0 m)	874.2	894.7	902.1	894.7	874.2
j9 (4.5 m)	799.5	811.3	815.5	811.3	799.5
j10 (5.0 m)	744.2	750.6	752.8	750.6	744.2
j11 (5.5 m)	701.2	703.8	704.6	703.8	701.2
j12 (6.0 m)	665.4	664.7	664.5	664.7	665.4
j13 (6.5 m)	632.9	628.7	627.2	628.7	632.9
j14 (7.0 m)	600.2	591.4	588.4	591.4	600.2
j15 (7.5 m)	563.1	548.5	544	548.5	563.1
j16 (8.0 m)	514	495.2	490.7	495.2	514
j17 (8.5 m)	433.5	430.4	429.9	430.4	433.5
j18 (9.0 m)	347.3	365.4	369.5	365.4	347.3
j19 (9.5 m)	298	313.9	318.6	313.9	298
j20 (10.0 m)	267	276.6	279.8	276.6	267
j21 (10.5 m)	244.9	249.4	251.1	249.4	244.9
j22 (11.0 m)	226.9	228.1	229	228.1	226.9
j23 (11.5 m)	206.5	210	211.7	210	206.5
j24 (12.0 m)	186	196.3	199.3	196.3	186
j25 (12.5 m)	179.1	190	193.5	190	179.1
j26 (13.0 m)	181.4	191.6	195.2	191.6	181.4
j27 (13.5 m)	190.5	200.9	204.6	200.9	190.5
j28 (14.0 m)	206.2	218.2	222.4	218.2	206.2
j29 (14.5 m)	229.9	245.1	250.6	245.1	229.9
j30 (15.0 m)	263.4	284.6	292.3	284.6	263.4
j31 (15.5 m)	309.5	341.6	353.5	341.6	309.5
j32 (16.0 m)	372.2	425.2	445.4	425.2	372.2
j33 (16.5 m)	458.6	555.6	593.8	555.6	458.6
j34 (17.0 m)	583.5	789	867.8	789	583.5
j35 (17.5 m)	757.9	1282	1423	1282	757.9

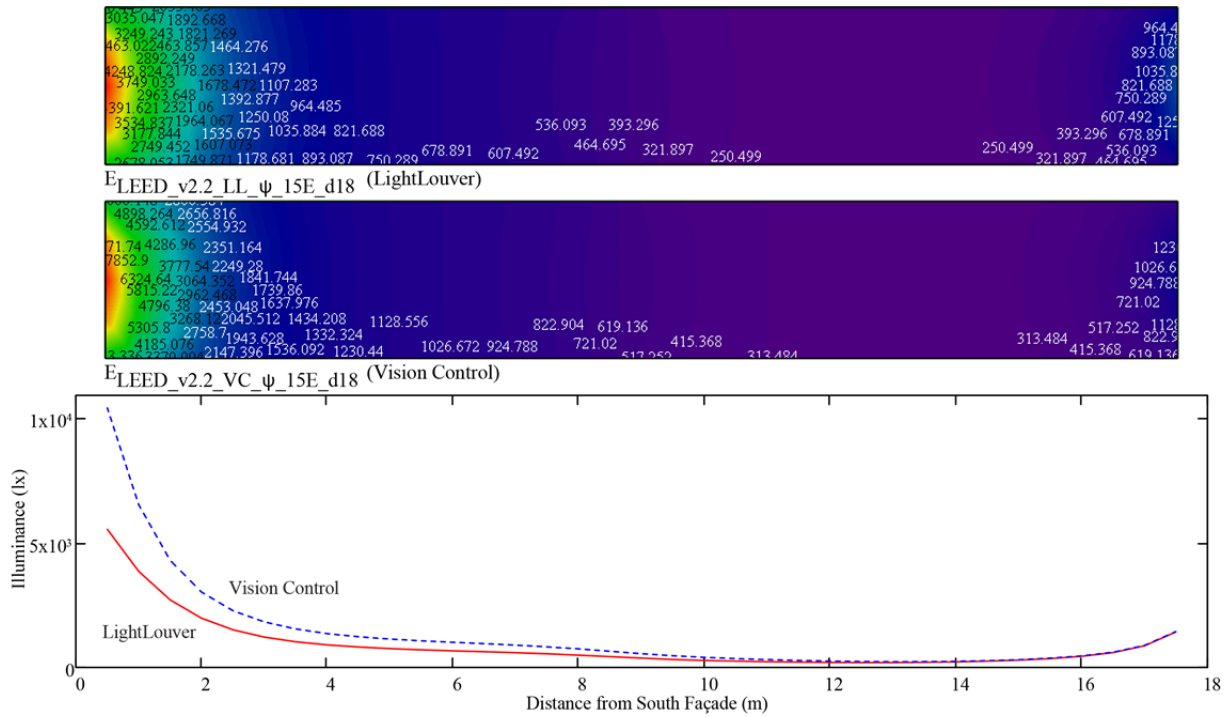
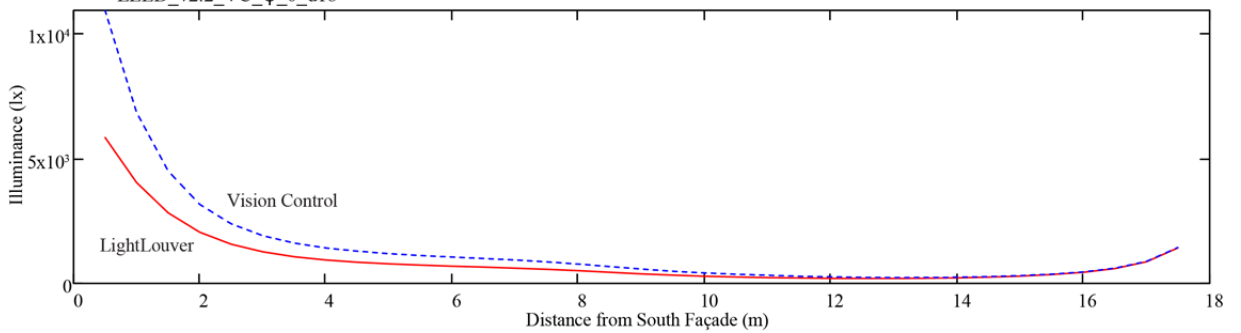
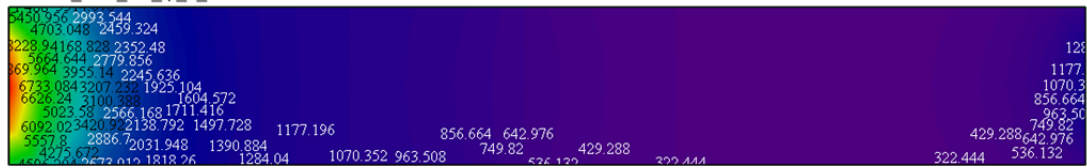
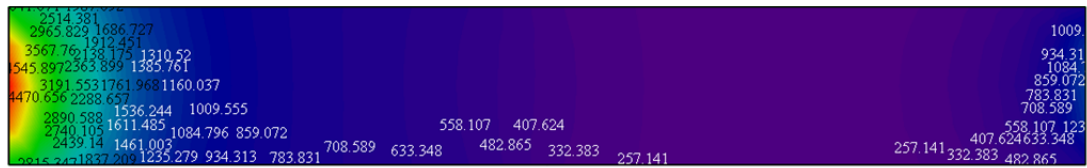


Figure A0.1: Analysis grid illuminance; 12:00, 22 September; $\psi = -15^\circ$; LightLouver (top) and Vision Control (middle); illuminance profile of LightLouver and Vision Control along centreline of cross-section (bottom) [lx].

Table A0.3: Analysis grid illuminance for LEED v2.2 IEQ8.1; 12:00, 22 September; LightLouver; $\psi = 0$ [lx].

Analysis pts (Distance from South Wall)	Analysis pts (Distance from East Wall)				
	i1 (0.5 m)	i2 (1.0 m)	i3 (1.5 m)	i4 (2.0 m)	i5 (2.5 m)
j1 (0.5 m)	3281	5260	5825	5260	3281
j2 (1.0 m)	2783	3677	4027	3677	2783
j3 (1.5 m)	2202	2643	2819	2643	2202
j4 (2.0 m)	1735	1961	2048	1961	1735
j5 (2.5 m)	1402	1521	1566	1521	1402
j6 (3.0 m)	1173	1239	1263	1239	1173
j7 (3.5 m)	1017	1054	1067	1054	1017
j8 (4.0 m)	908.1	929.4	936.9	929.4	908.1
j9 (4.5 m)	830.6	842.8	847.1	842.8	830.6
j10 (5.0 m)	773.2	779.8	782.1	779.8	773.2
j11 (5.5 m)	728.6	731.2	732.1	731.2	728.6
j12 (6.0 m)	691.4	690.7	690.3	690.7	691.4
j13 (6.5 m)	657.6	653.2	651.6	653.2	657.6
j14 (7.0 m)	623.6	614.4	611.3	614.4	623.6
j15 (7.5 m)	585	569.6	564.9	569.6	585
j16 (8.0 m)	533.7	514.1	509.3	514.1	533.7
j17 (8.5 m)	449.7	446.5	445.9	446.5	449.7
j18 (9.0 m)	359.7	378.6	382.8	378.6	359.7
j19 (9.5 m)	308.2	324.7	329.5	324.7	308.2
j20 (10.0 m)	275.7	285.6	288.9	285.6	275.7

j21 (10.5 m)	252.3	256.9	258.7	256.9	252.3
j22 (11.0 m)	233.2	234.4	235.3	234.4	233.2
j23 (11.5 m)	211.5	215.1	216.7	215.1	211.5
j24 (12.0 m)	189.6	200.2	203.3	200.2	189.6
j25 (12.5 m)	181.9	193	196.6	193	181.9
j26 (13.0 m)	183.7	194.1	197.7	194.1	183.7
j27 (13.5 m)	192.3	202.9	206.6	202.9	192.3
j28 (14.0 m)	207.8	219.9	224.1	219.9	207.8
j29 (14.5 m)	231.3	246.6	252	246.6	231.3
j30 (15.0 m)	264.6	285.9	293.6	285.9	264.6
j31 (15.5 m)	310.6	342.8	354.7	342.8	310.6
j32 (16.0 m)	373.3	426.2	446.5	426.2	373.3
j33 (16.5 m)	459.6	556.7	594.8	556.7	459.6
j34 (17.0 m)	584.5	790	868.9	790	584.5
j35 (17.5 m)	758.9	1283	1424	1283	758.9



A2.3. Analysis grid resolution

Table A0.4: Comparison of illuminance analysis grids: Golden, LightLouver and Vision Control blind, 1.0 m x 1.0 m and 0.5 m x 0.5 m grid, $sDA_{300/50}$ [%].

$sDA_{300/50}$	ψ Orientation													
	-45°		-30°		-15°		0		15°		30°		45°	
	low VLT	high VLT	low VLT	high VLT	low VLT	high VLT	low VLT	high VLT	low VLT	high VLT	low VLT	high VLT	low VLT	high VLT
1.0 m x 1.0 m														
LightLouver	28	35	33	41	39	44	39	44	33	44	33	41	28	35
Vision Control	33	35	39	41	44	44	39	44	39	46	33	41	30	35
0.5 m x 0.5 m														
LightLouver	29	36	34	43	35	46	35	46	35	43	32	39	29	35
Vision Control	31	36	37	43	41	49	41	47	38	43	32	38	31	35
RER *														
LightLouver	-5.7	-2.6	-1.6	-6.0	11.1	-3.6	11.1	-3.6	-4.8	2.6	3.4	3.3	-5.7	0.5
Vision Control	9.1	-2.6	6.1	-6.0	9.6	-9.1	-4.1	-5.9	2.9	6.8	3.4	7.8	-3.0	0.5

* Relative error: the 0.5 m x 0.5 m grid is the reference

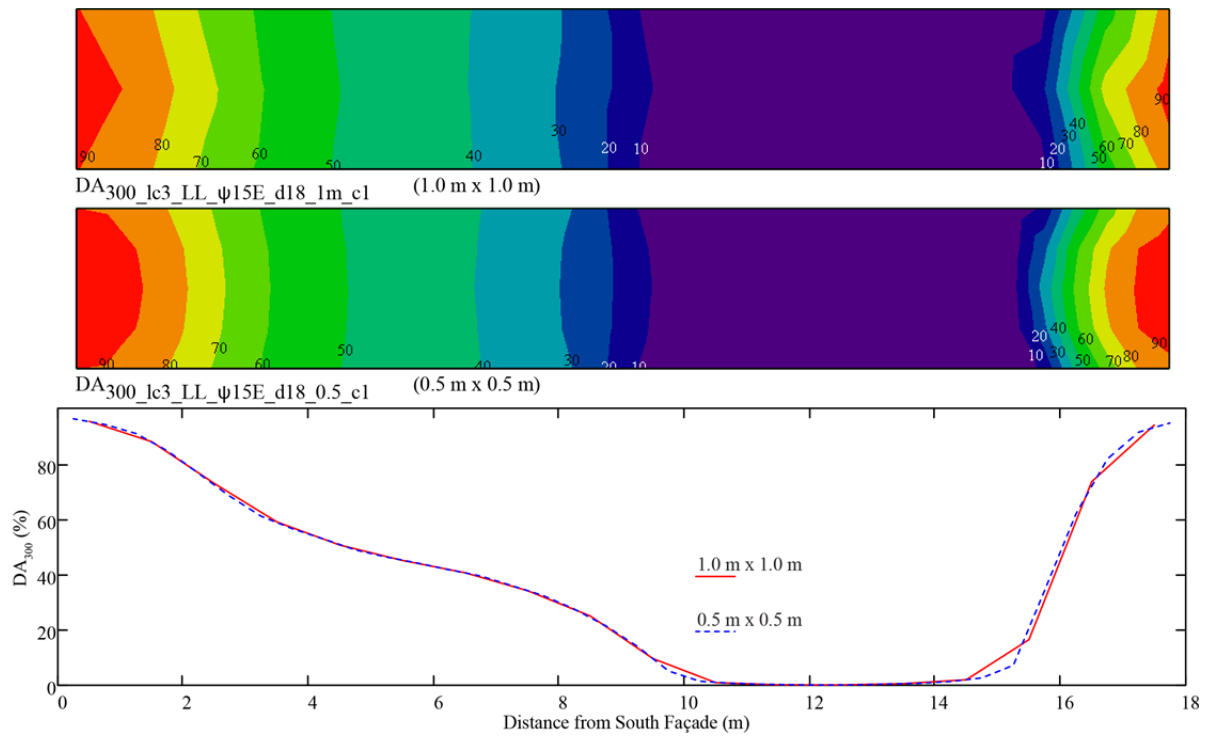


Figure A0.3: Comparison of illuminance analysis grids: Golden, LightLouver blind, $\psi = -15^\circ$; DA_{300} contour plot (1.0 m x 1.0 m grid at top, 0.5 m x 0.5 m grid in middle) and DA_{300} X-Y plot (bottom) [%].

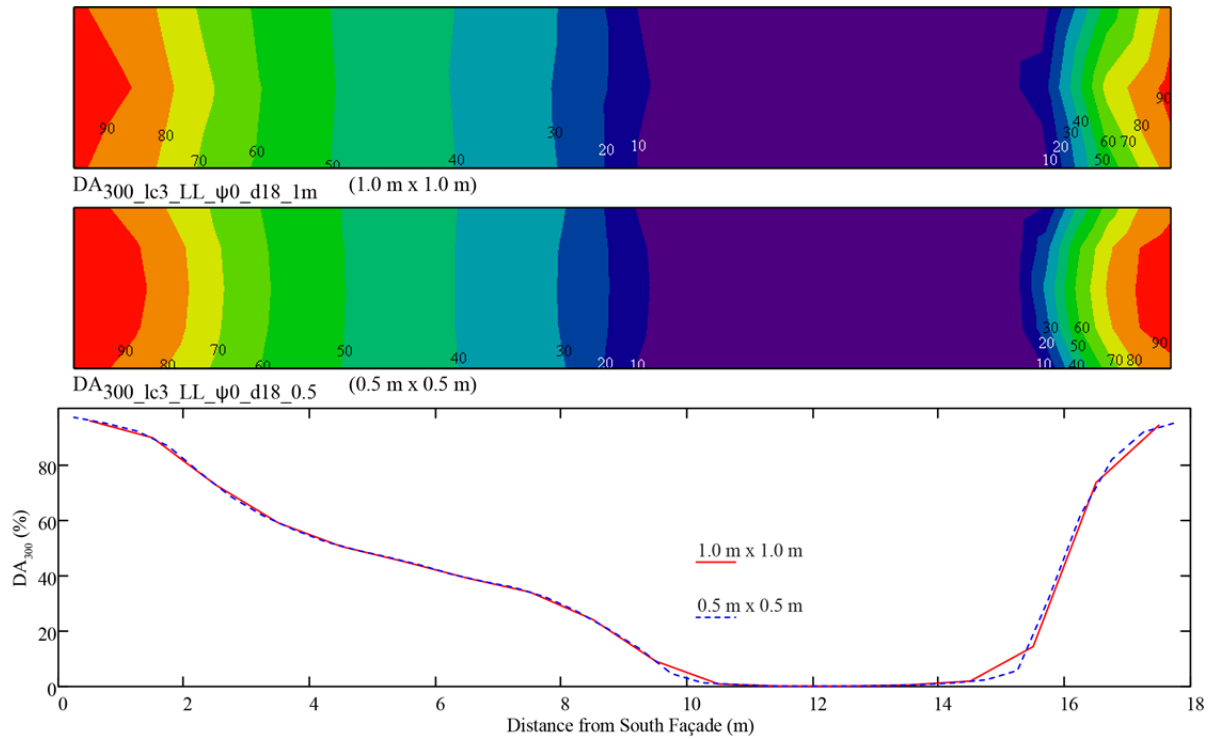


Figure A0.4: Comparison of illuminance analysis grids: Golden, LightLouver blind, $\psi = 0$; DA_{300} contour plot (1.0 m x 1.0 m grid at top, 0.5 m x 0.5 m grid in middle) and DA_{300} X-Y plot (bottom) [%].

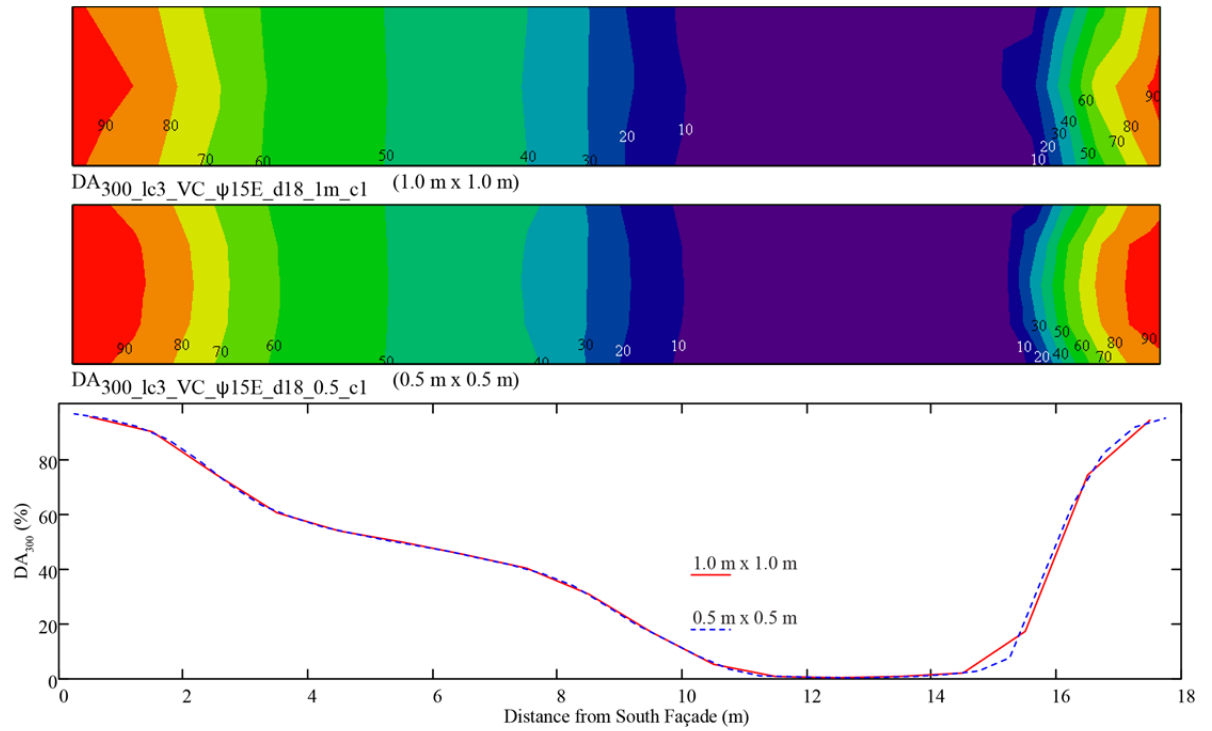


Figure A0.5: Comparison of illuminance analysis grids: Golden, Vision Control blind, $\psi = -15^\circ$; DA_{300} contour plot (1.0 m x 1.0 m grid at top, 0.5 m x 0.5 m grid in middle) and DA_{300} X-Y plot (bottom) [%].

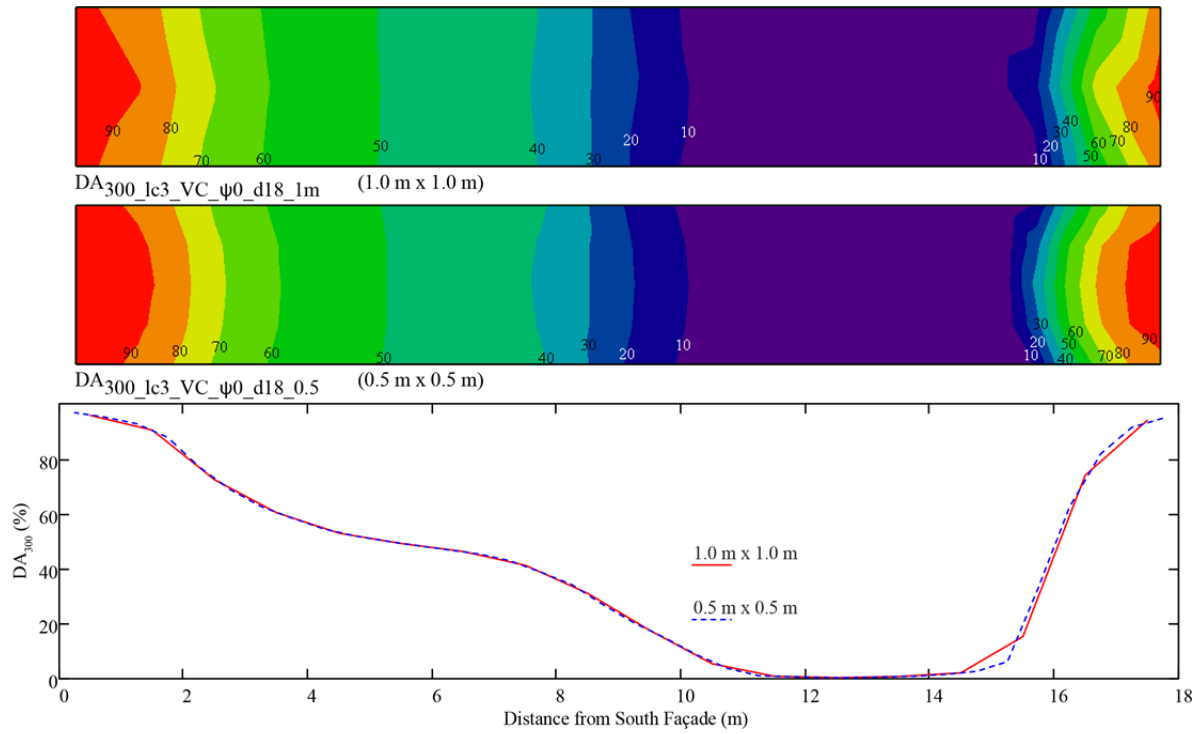


Figure A0.6: Comparison of illuminance analysis grids: Golden, Vision Control blind, $\psi = 0$; DA_{300} contour plot (1.0 m x 1.0 m grid at top, 0.5 m x 0.5 m grid in middle) and DA_{300} X-Y plot (bottom) [%].

A3. Supporting data for methodology part 2

A3.1. Comparative analysis of the LightLouver and Vision Control blinds (existing location)

Table A0.5: LightLouver and Vision Control blind spatial daylight autonomy, $sDA_{300/50}$ [%].

	$\psi = -15^\circ$ (15E) North wing	$\psi = 0$ South wing
0.5 m x 0.5 m		
LightLouver	35	35
Vision Control	41	41

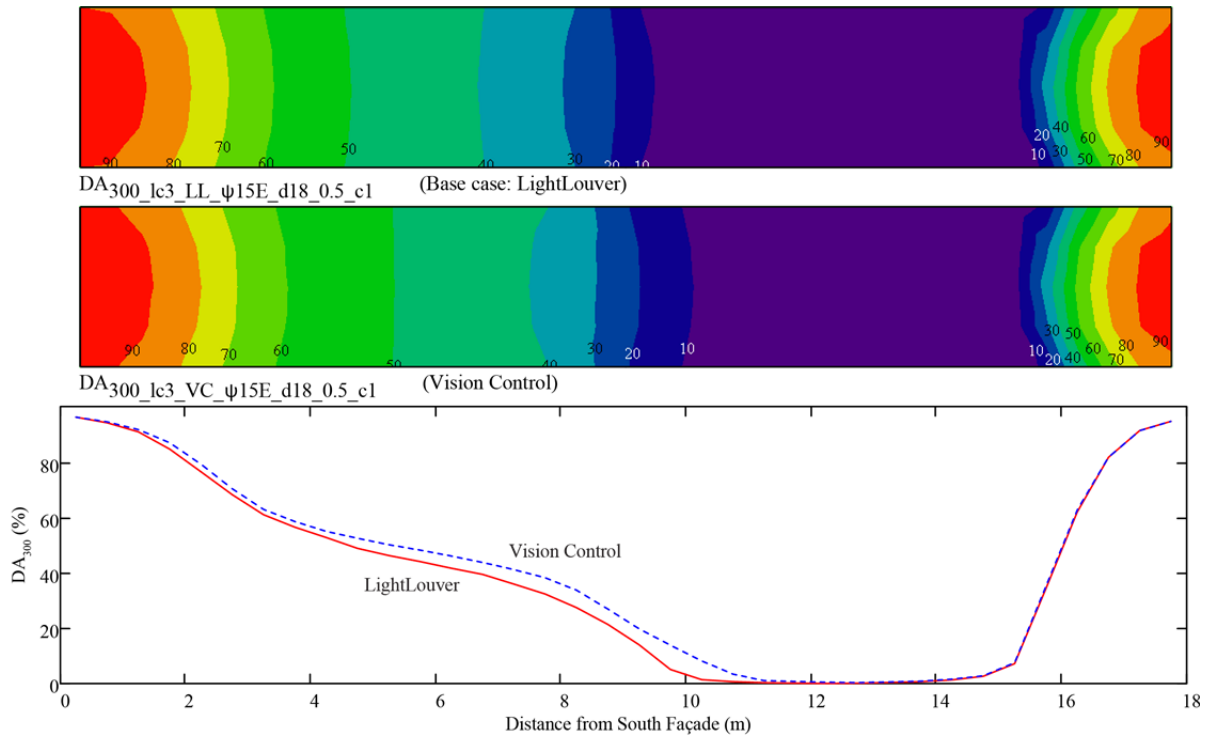


Figure A0.7: Base case: Golden, LightLouver and Vision Control blinds, $\psi = -15^\circ$; DA_{300} contour (top, middle) and X-Y (bottom) plots [%].

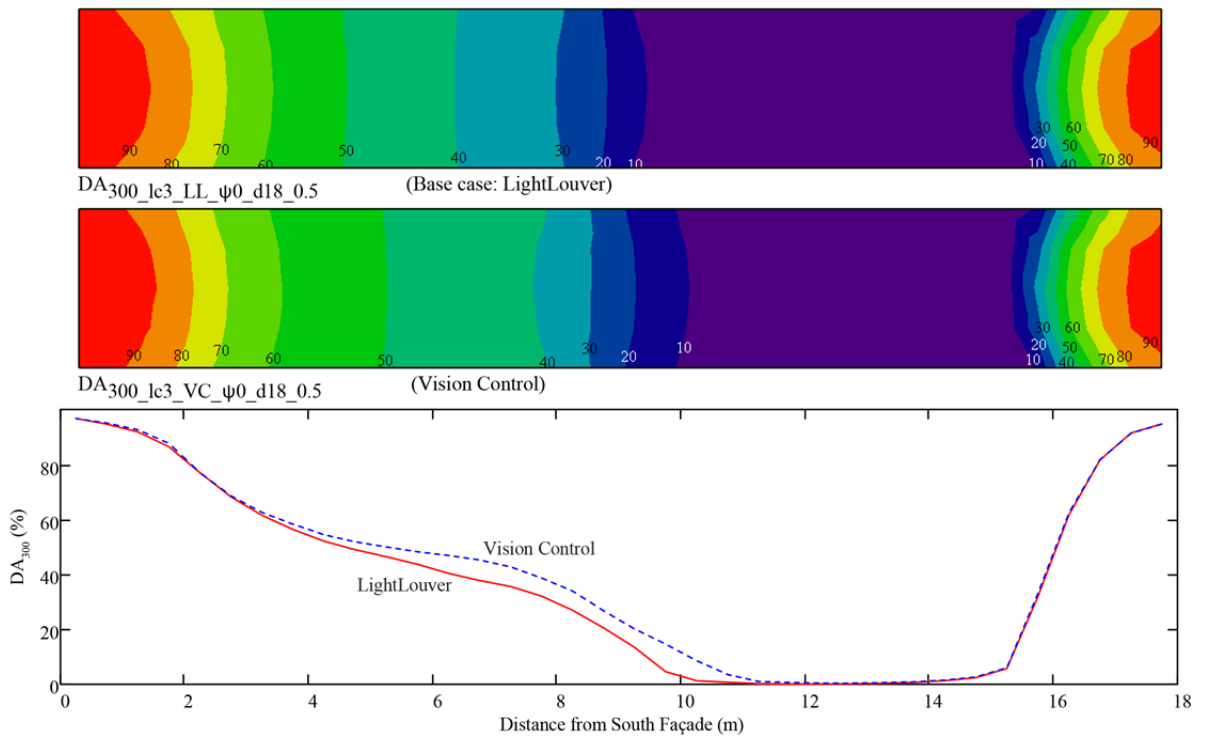


Figure A0.8: Base case: Golden, LightLouver and Vision Control blinds, $\psi = 0^\circ$; DA_{300} contour (top, middle) and X-Y (bottom) plots [%].

A3.2. Base building: location, window properties, daylight redirecting

blind, orientation

Table A0.6 shows the simulation results for the base building (i.e. the building with existing dimensions) at different locations, orientations, and window properties with both daylight redirecting blinds.

Table A0.6: Base bldg. results by location, window properties, daylight redirecting blind, orientation; sDA_{300/50} [%].

sDA _{300/50} [%]	Orientation ψ ; c1 = low VLT windows; c2= high VLT windows													
	-45°		-30°		-15°		0		15°		30°		45°	
Bldg. depth = 18 m	c1	c2	c1	c2	c1	c2	c1	c2	c1	c2	c1	c2	c1	c2
Golden (lc3)														
LightLouver (cfs1)	28	35	33	41	39	44	39	44	33	44	33	41	28	35
Vision Control (cfs2)	33	35	39	41	44	44	39	44	39	46	33	41	30	35
Montreal (lc2)														
LightLouver (cfs1)	28	35	33	35	33	39	30	39	33	39	33	39	28	33
Vision Control (cfs2)	30	35	35	39	39	44	39	44	39	44	39	39	33	35
Vancouver (lc4)														
LightLouver (cfs1)	19	28	20	28	24	28	24	28	24	28	20	28	19	28
Vision Control (cfs2)	20	28	24	28	24	28	24	28	24	28	24	28	20	28
St. John's (lc5)														
LightLouver (cfs1)	24	28	20	28	24	28	24	28	24	28	24	28	20	28
Vision Control (cfs2)	28	28	24	28	24	28	24	30	24	28	24	28	28	28
Phoenix (lc6)														
LightLouver (cfs1)	44	56	44	56	39	52	39	52	39	52	44	56	33	41
Vision Control (cfs2)	44	52	44	52	44	52	41	50	44	52	44	52	33	37

A3.3. Base building: from Golden to Montreal

Changing the EPW weather file from Golden to Montreal while keeping all other parameters the same has the effect of decreasing sDA_{300/50} performance by 15 % for the North wing ($\psi = -15^\circ$) and by 23 % for the South wing ($\psi = 0$) (Table A0.7). One possible explanation for why the sDA_{300/50} performance decreases only for $\psi = 0$ in Montreal is that there are more occurrences of large incidence angles when the solar-surface azimuth is

small, resulting in lower visible transmittance through the glass. Figure A0.9 and Figure A0.10 compare in graphic format the performance of the LightLouver in the two cities for $\psi = -15^\circ$ and $\psi = 0$.

Table A0.7: Base bldg.: Golden and Montreal, low VLT, LightLouver performance, $sDA_{300/50}$ [%].

$sDA_{300/50}$, low VLT	ψ orientation						
	-45°	-30°	-15°	0	15°	30°	45°
Golden (lc3)	28	33	39	39	33	33	28
Montreal (lc2)	28	33	33	30	33	33	28

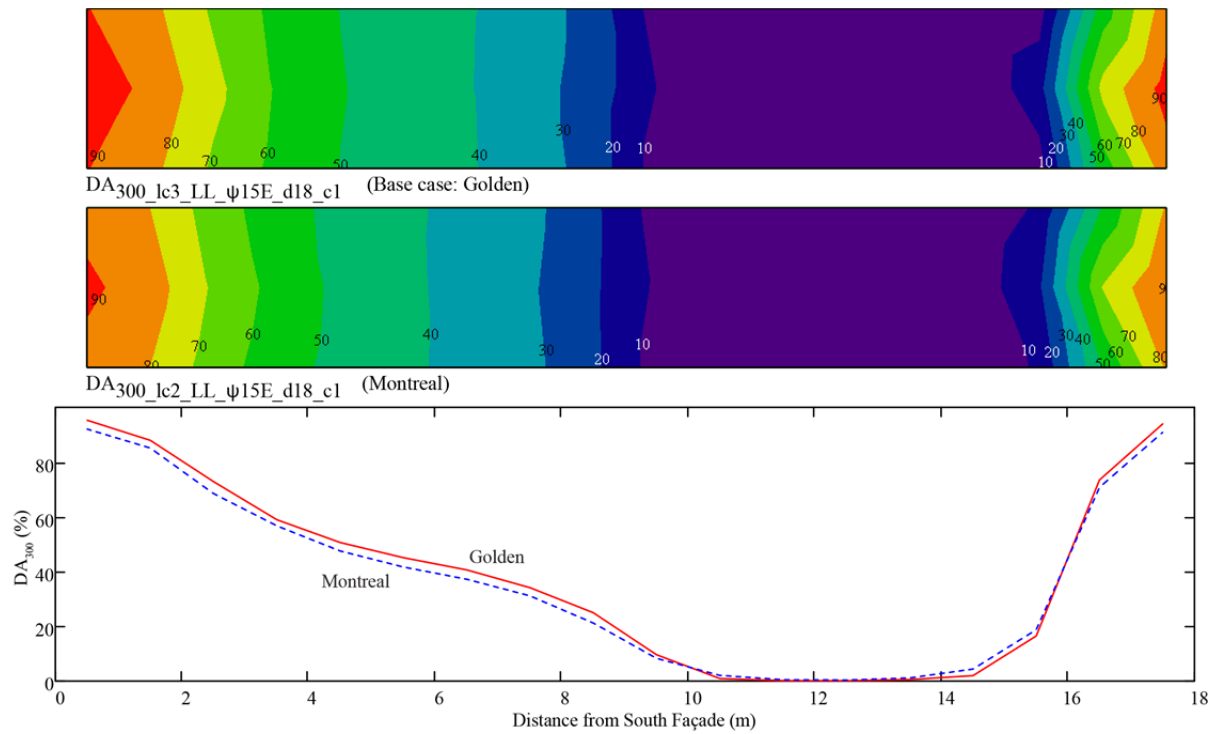


Figure A0.9: Base bldg.: Golden and Montreal, LightLouver blind, $\psi = -15^\circ$; DA_{300} contour (top, middle) and X-Y (bottom) plots [%].

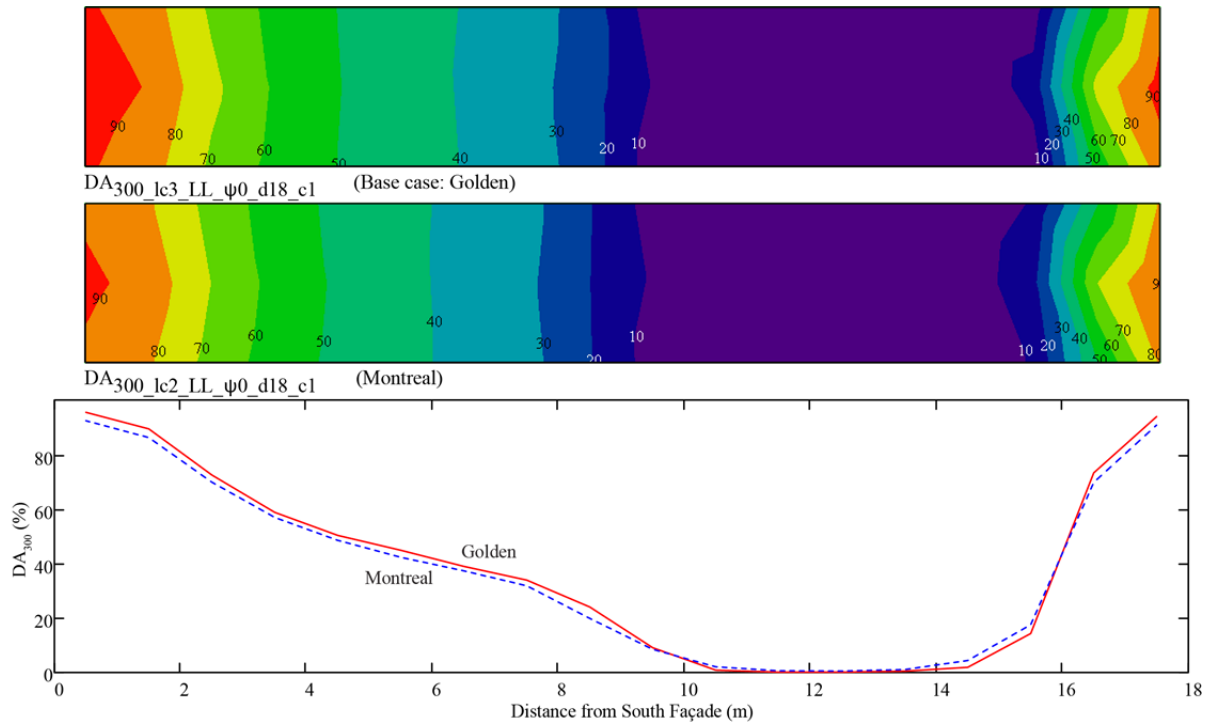


Figure A0.10: Base bldg.: Golden and Montreal, LightLouver blind, $\psi = 0$; DA_{300} contour (top, middle) and X-Y (bottom) plots [%].

A3.4. Base building: from Golden to Phoenix

Going southward, the base building is simulated in Phoenix and compared to the results in Golden using the same low VLT windows (c1) as in the existing RSF building (Table A0.8, Figure A0.11, and Figure A0.12). Although the daylighting performance in Phoenix is better than in Golden, it is not at façade orientations one normally expects. At $\psi = -15^\circ$ and $\psi = 0$, the daylighting performance in Phoenix is no better than that of Golden. It is only when moving the facade orientation away from due South that the daylighting performance gains in Phoenix are realized – as much as 57 % in the case of $\psi = -45^\circ$.

Table A0.8: Base bldg.: Golden and Phoenix, low VLT, LightLouver performance, $sDA_{300/50}$ [%].

LightLouver	ψ orientation						
	-45°	-30°	-15°	0	15°	30°	45°
Low VLT, 1.0 m x 1.0 m							
Golden (lc3)	28	33	39	39	33	33	28
Phoenix (lc6)	44	44	39	39	39	44	33

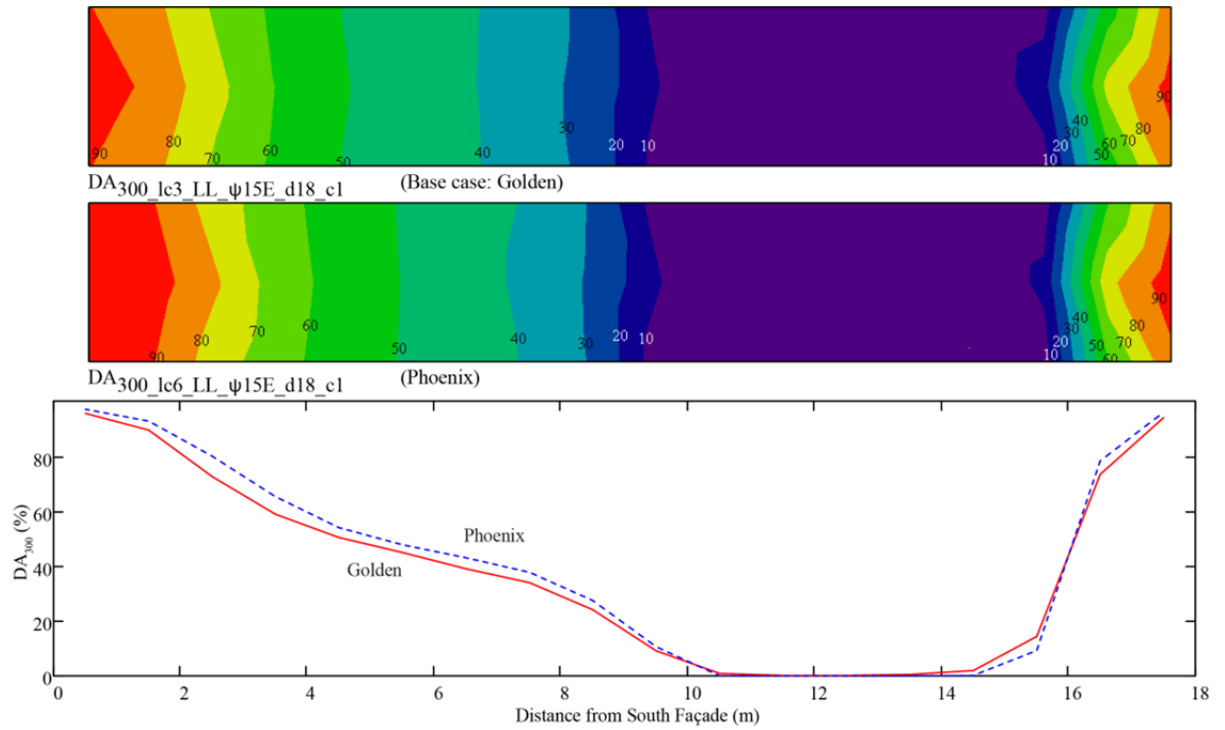


Figure A0.11: Base bldg.: Golden and Phoenix, LightLouver blind, $\psi = -15^\circ$; DA_{300} contour (top, middle) and X-Y (bottom) plots [%].

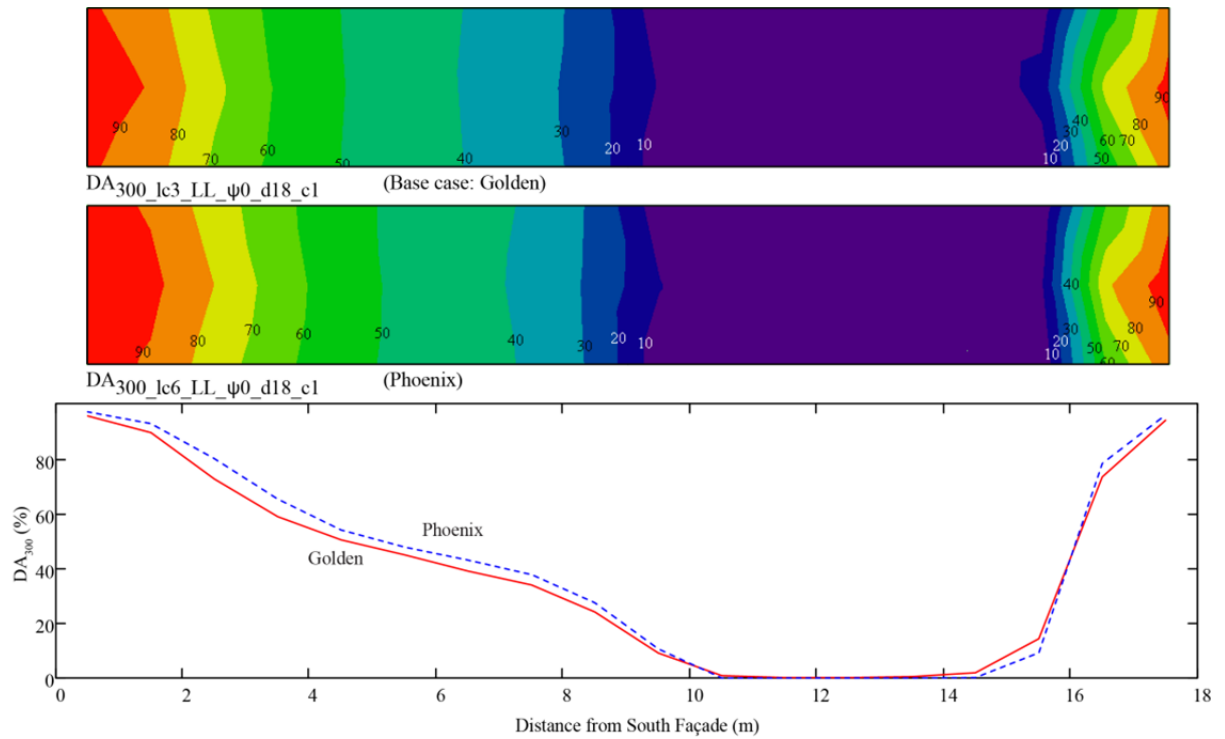


Figure A0.12: Base bldg.: Golden and Phoenix, LightLouver blind, $\psi = 0^\circ$; DA_{300} contour (top, middle) and X-Y (bottom) plots [%].

A3.5. Base building: all locations, low VLT, daylight redirecting blind, $\psi = -45^\circ$ to 45°

Table A0.9, shows the variation in DA₃₀₀ performance of the base building in orientations from $\psi = -45^\circ$ to $\psi = 45^\circ$ with the LightLouver and Vision Control blinds. Figure A0.13 and Figure A0.14 show the DA₃₀₀ performance of the LightLouver.

For Golden, the results show that the best daylighting performance (sDA_{300/50}) of 39 % occurs when facades are oriented between -15° and 15° . LightLouver daylighting performance decreases by 28 % at facade orientations of -45° and 45° . Running the same simulations with the Vision Control blind yields different results. The VC performed best with sDA_{300/50} = 44 % at a facade orientation of -15° . From there the sDA_{300/50} drops to 30 % at 45° for a relative decrease in performance of 32 %.

When comparing the two blinds, we see that at each façade orientation tested, the VC daylighting performance is better except for $\psi = 0$ and $\psi = 30^\circ$ where it is the same as for the LL. The VC daylighting performance increase is as much as 18 % depending on façade orientation. It can be concluded that in Golden, for most orientations, the VC will improve daylighting performance of the RSF as compared to the LL. A similar result is found for the other locations.

Table A0.9: Base bldg. results by location, low VLT, daylight redirecting blind, orientation; sDA_{300/50} [%].

sDA _{300/50} , low VLT, 1.0mx1.0m Location / blind	Orientation ψ						
	-45°	-30°	-15°	0	15°	30°	45°
Golden (lc3)							
LightLouver	28	33	39	39	33	33	28
Vision Control	33	39	44	39	39	33	30
Montreal (lc2)							
LightLouver	28	33	33	30	33	33	28
Vision Control	30	35	39	39	39	39	33
Vancouver (lc4)							
LightLouver	19	20	24	24	24	20	19
Vision Control	20	24	24	24	24	24	20
St. John's (lc5)							
LightLouver	24	20	24	24	24	24	20
Vision Control	28	24	24	24	24	24	28
Phoenix (lc6)							
LightLouver	44	44	39	39	39	44	33
Vision Control	44	44	44	41	44	44	33

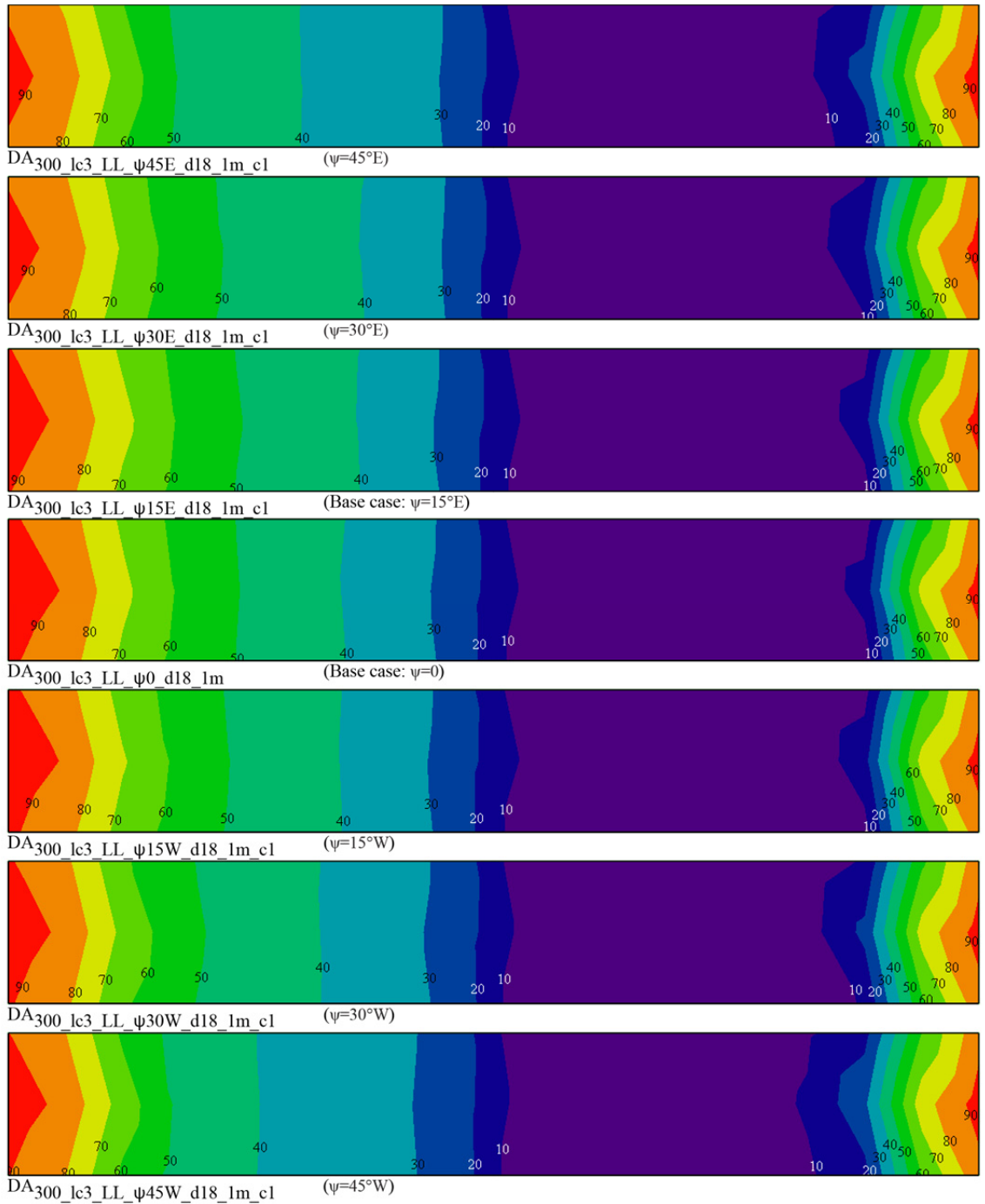


Figure A0.13: Base bldg.: Golden, low VLT, LightLouver blind, $\psi = -45^\circ$ to 45° ; DA₃₀₀ contour (top, middle) and X-Y (bottom) plots [%].

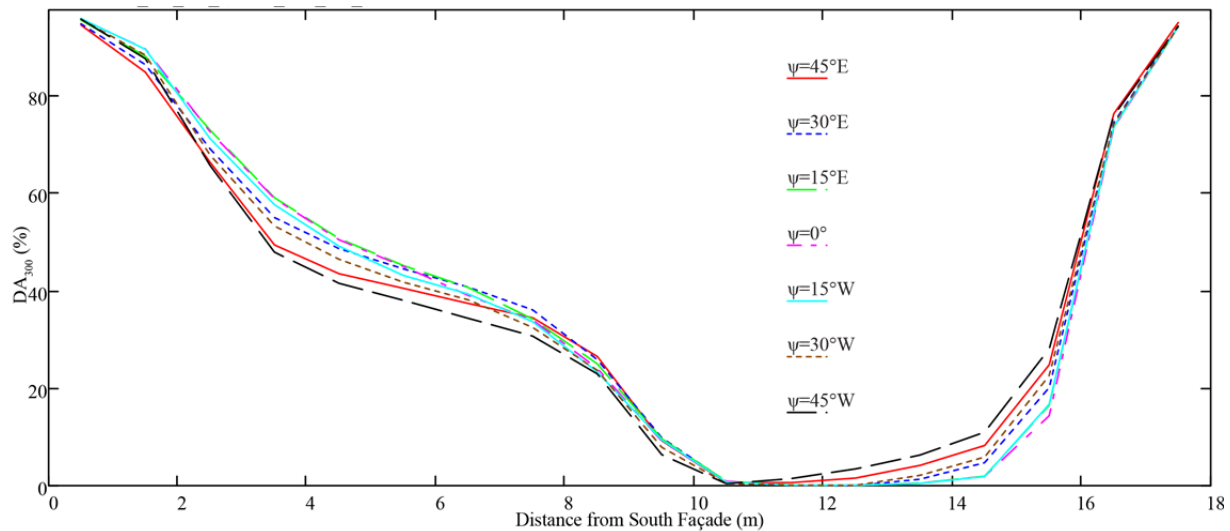


Figure A0.14: Base bldg.: Golden, low VLT, LightLouver blind, $\psi = -45^\circ$ to 45° ; DA_{300} contour (top, middle) and X-Y (bottom) plots [%].

A3.6. Changing window visible light transmittance (VLT) properties

In Table A0.10, Figure A0.15, and Figure A0.16 we see the expected effect of increasing the visible transmittance at normal incidence from 70 % in the low VLT daylighting window to 76 % in the high VLT daylighting window and from 59 % in the low VLT view window to 68 % in the high VLT view window, while keeping all other parameters the same in the base case. Although this is not necessarily a practical design option for the Golden climate, it will be useful in the later comparisons with the Canadian climates.

Table A0.10: Golden, LightLouver and Vision Control, window VLT comparison; $sDA_{300/50}$ [%].

Golden, 1.0x1.0	ψ Orientation						
	-45°	-30°	-15°	0	15°	30°	45°
LightLouver							
Low VLT	28	33	39	39	33	33	28
High VLT	35	41	44	44	44	41	35
Vision Control							
Low VLT	33	39	44	39	39	33	30
High VLT	35	41	44	44	46	41	35

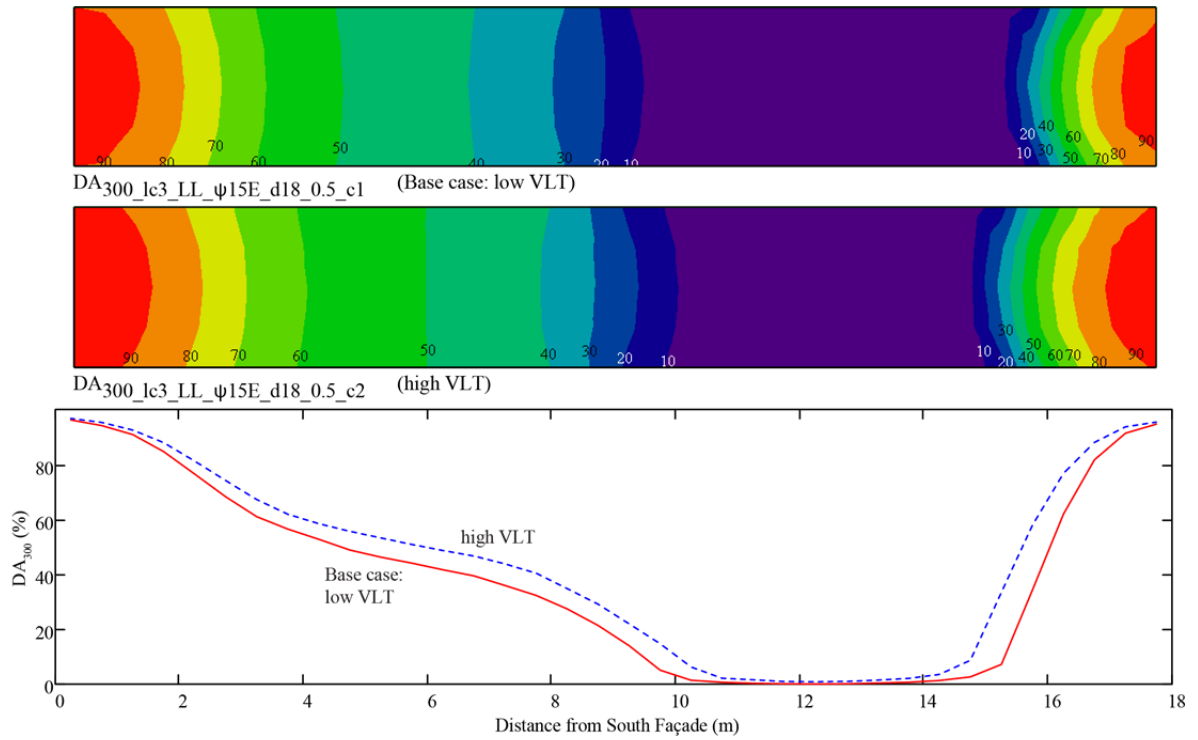


Figure A0.15: Base bldg.: Golden, low and high VLT, LightLouver blind, $\psi = -15^\circ$; DA_{300} contour (top, middle) and X-Y (bottom) plots [%].

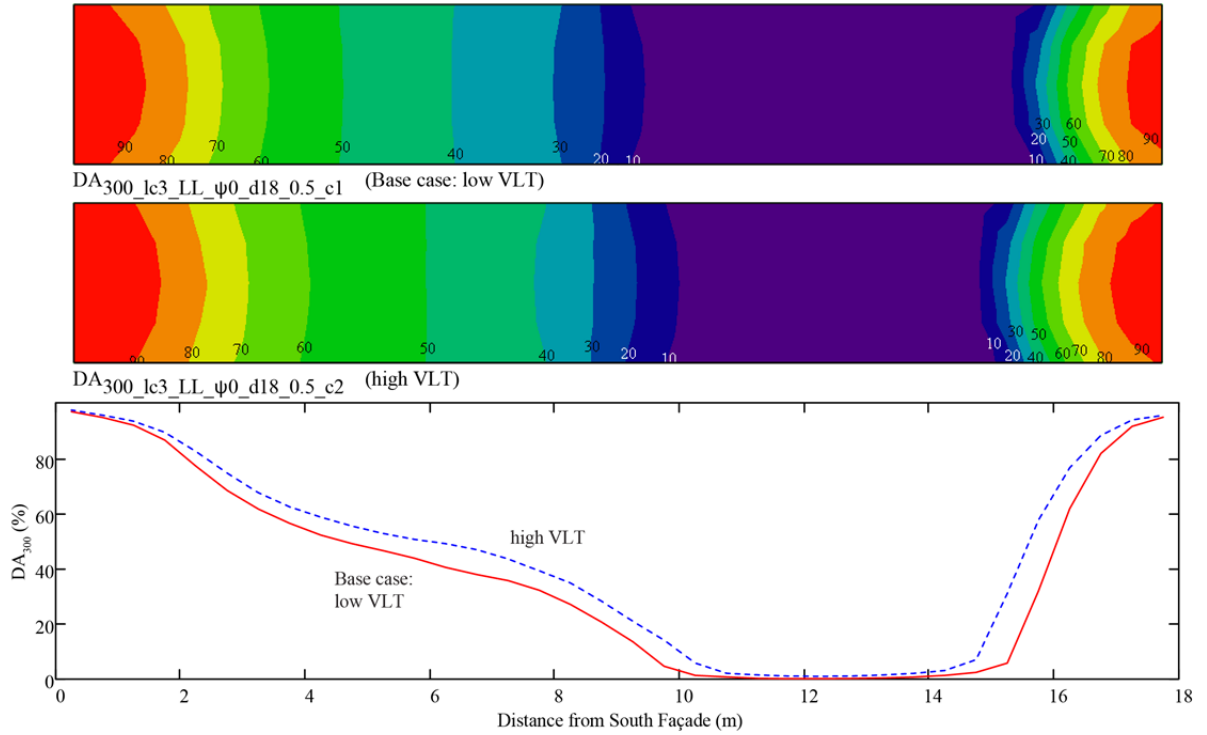


Figure A0.16: Base bldg.: Golden, low and high VLT, LightLouver blind, $\psi = 0^\circ$; DA_{300} contour (top, middle) and X-Y (bottom) plots [%].

A3.7. Configuration A: a taller daylighting window

The first fenestration change is to increase the South daylighting window height by 0.736 m from 0.914 m to 1.650 m, by raising its head height. The sill height, window width, and side-to-side position in the wall have not been altered. A secondary effect is an increase to its surface area and hence, window to wall ratio. The new WHH_s is 3.783 m. The overall window to wall ratio of the South façade (WWR_s) increases from 33 % to 44 %.

As expected, the increased WHH_s leads to an increase in $sDA_{300/50}$ (Table A0.11, Figure A0.17, and Figure A0.18). For $\psi = -15^\circ$ and $\psi = 0$, the taller daylighting window leads to a 44 % increase in $sDA_{300/50}$ performance compared to that of the base building. However, the biggest gains are at $\psi = 15^\circ$, -30° , and -45° , of 70 %, 64 %, and 57 % respectively. This gain can be explained by the fact that the reference daylighting performance of $\psi = 15^\circ$, -30° , and -45° is fairly poor to begin with and the increased window area helps to greatly improve the daylighting performance.

Table A0.11: Base bldg. and configuration A, Golden, low VLT, LightLouver, orientation; $sDA_{300/50}$ [%].

Golden, 1.0 mx1.0 m, low VLT	ψ orientation						
	-45°	-30°	-15°	0	15°	30°	45°
LightLouver							
Base bldg.	28	33	39	39	33	33	28
Config. A	44	54	56	56	56	50	41

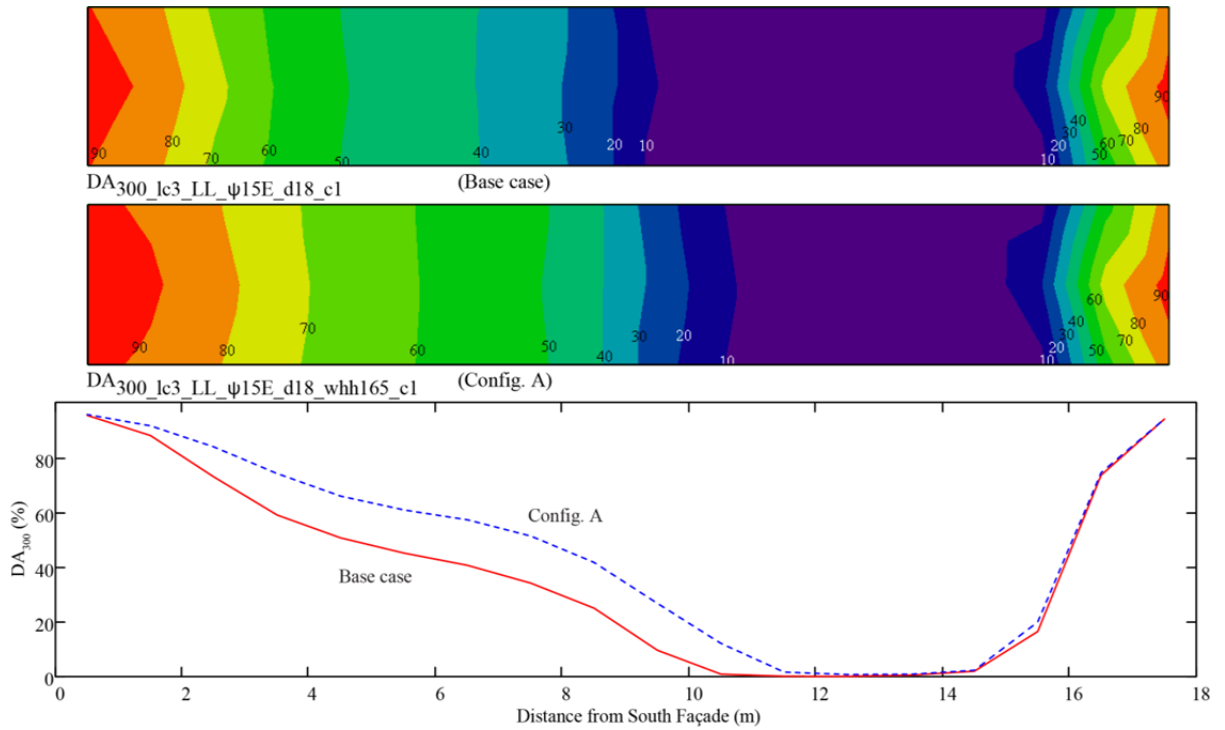


Figure A0.17: Base bldg. and configuration A, Golden, low VLT, LightLouver blind, $\psi = -15^\circ$; DA₃₀₀ contour (top, middle) and X-Y (bottom) plots [%].

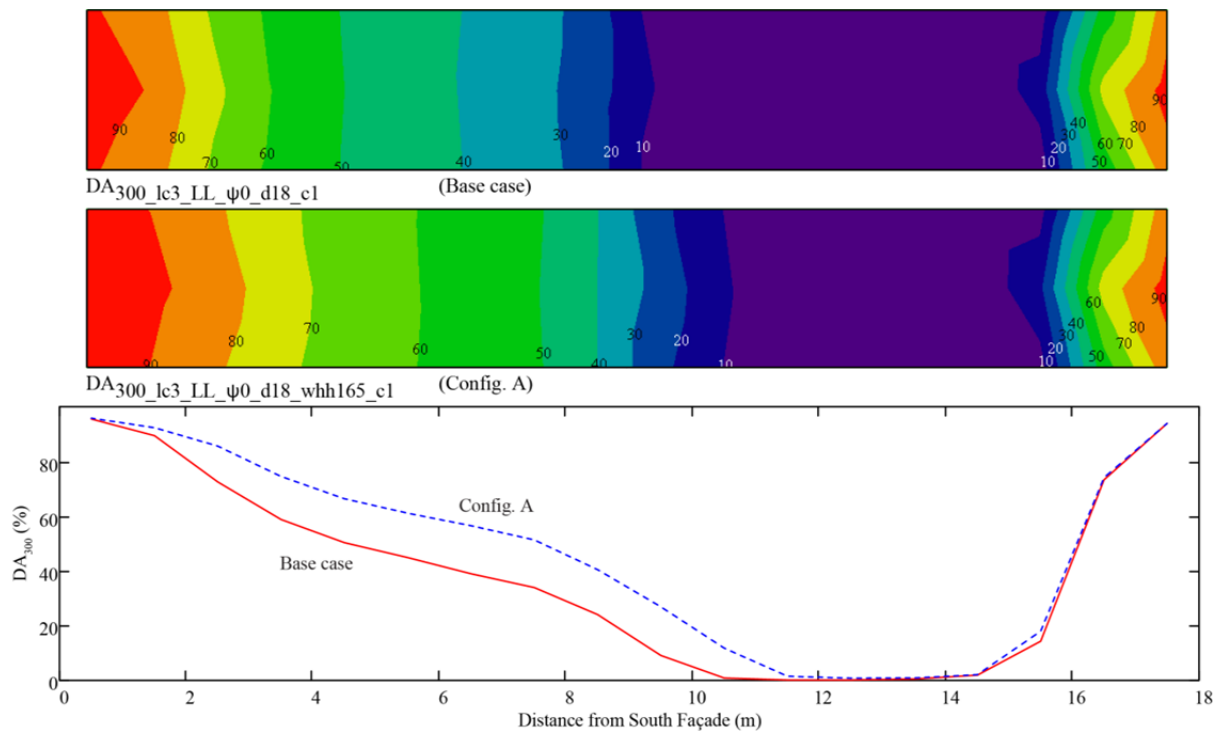


Figure A0.18: Base bldg. and configuration A, Golden, low VLT, LightLouver blind, $\psi = 0^\circ$; DA₃₀₀ contour (top, middle) and X-Y (bottom) plots [%].

A3.8. Configuration B: increase daylighting window head height to ceiling height

The South daylighting window is made taller still, from the reference 0.736 m to 1.800 m. This makes the WHH_s 3.933 m, which is just 30 mm below the room height of 3.963 m. The objective here is to measure the daylighting effect from having the tallest window possible while respecting the overall floor to ceiling clear height. Like in configuration A, the sill height, window width, and side-to-side position in the South wall have not been altered.

For $\psi = -15^\circ$ and $\psi = 0$, this configuration results in a 44 % increase in sDA_{300/50} performance over that of the base building (Table A0.12, Figure A0.19, and Figure A0.20) which is identical to that of configuration A. On the other hand, the biggest relative sDA_{300/50} performance gains are for $\psi = -45^\circ, -30^\circ, 15^\circ$, at 79 %, 70 %, and 70 % respectively. These are the same orientations that benefited in configuration A.

Table A0.12: Base bldg. and configuration B, Golden, low VLT, LightLouver, orientation; sDA_{300/50} [%].

Golden, LL, c1 1.0x1.0, D18	ψ Orientation						
	-45°	-30°	-15°	0	15°	30°	45°
Reference (base bldg.)	28	33	39	39	33	33	28
Configuration B	50	56	56	56	56	50	44

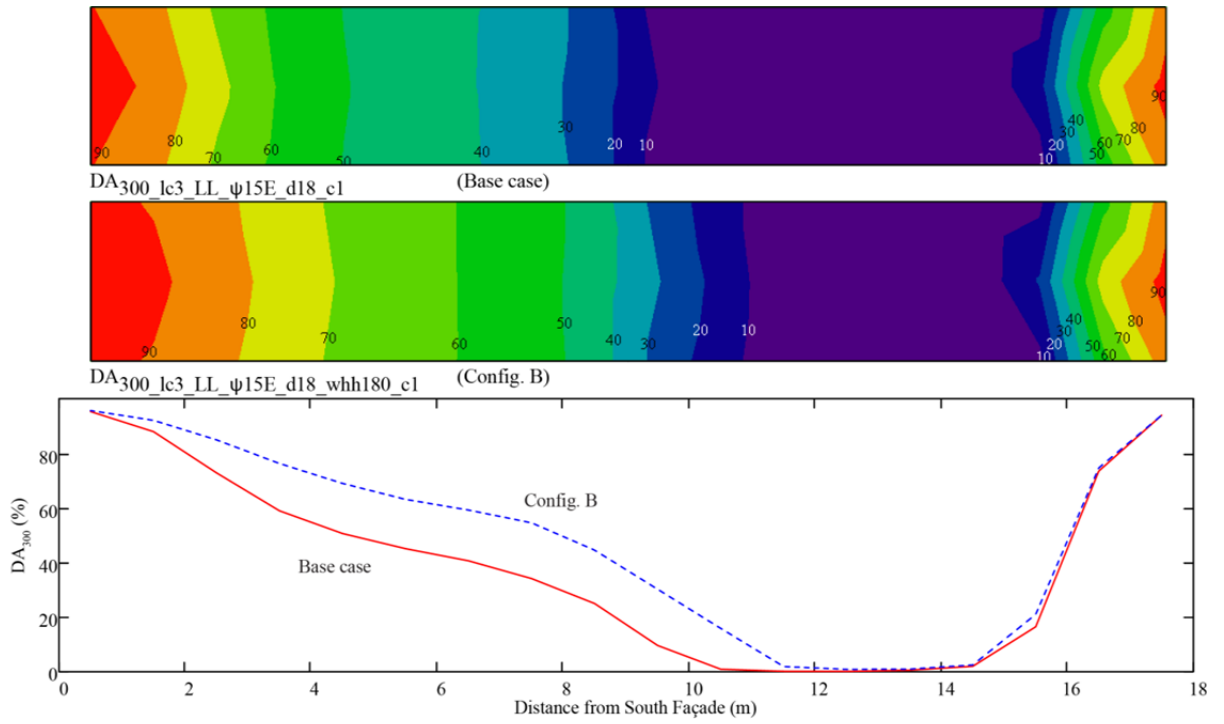


Figure A0.19: Base bldg. and configuration B, Golden, low VLT, LightLouver blind, $\psi = -15^\circ$; DA₃₀₀ contour (top, middle) and X-Y (bottom) plots [%].

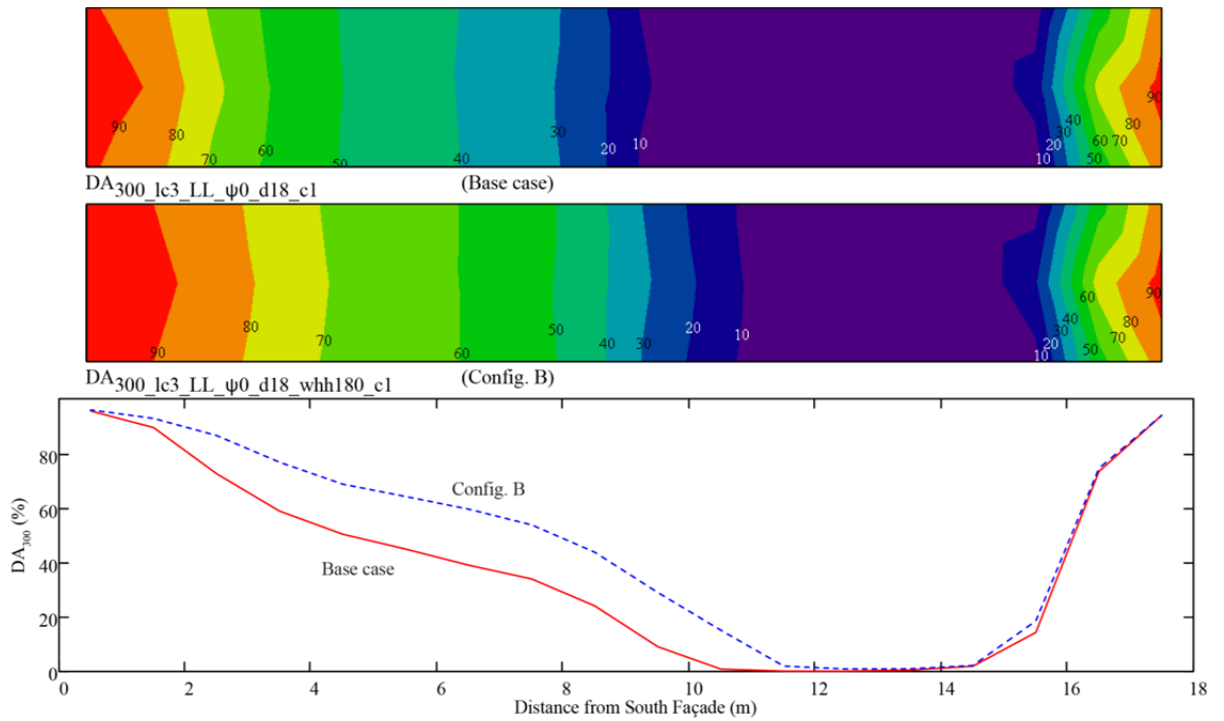


Figure A0.20: Base bldg. and configuration B, Golden, low VLT, LightLouver blind, $\psi = 0^\circ$; DA₃₀₀ contour (top, middle) and X-Y (bottom) plots [%].

A3.9. Configuration C: increase daylighting window height and window width

The previous configuration, B, showed that increasing the height of the South daylighting window, $DayWinSouth_{ht}$, from 1.650 m to 1.800 m, produced no improvement in $sDA_{300/50}$ for the central ψ angles of 0 and $\pm 15^\circ$.

For the configuration C, we revert back to a WHH_s of 1.650 m as in configuration A. The South facade’s windows’ width was increased from 1.829 m to 2.100 m. Note that for the purpose of modelling simplification, there is only one variable assigned to the South facade’s windows’ width. The limitation of this simplification is that the width of the South facade’s view window and the South facade’s daylighting window is always the same. This limitation is encountered in the next configuration, D, as well.

The results are very similar to those for configuration A. The notable differences are at $\psi = \pm 30^\circ, \pm 45^\circ$ where the $sDA_{300/50}$ is improved. The “better” solar orientations of $\psi = 0, \pm 15^\circ$ performed identically as in configuration A. See Table A0.13, Figure A0.21, and Figure A0.22.

Table A0.13: Base bldg. and configuration C, Golden, low VLT, LightLouver, orientation; $sDA_{300/50}$ [%].

Golden, LL, c1, 1.0x1.0, D18	ψ Orientation						
	-45°	-30°	-15°	0	15°	30°	45°
Reference (base bldg.)	28	33	39	39	33	33	28
Configuration C	50	56	56	56	56	56	50

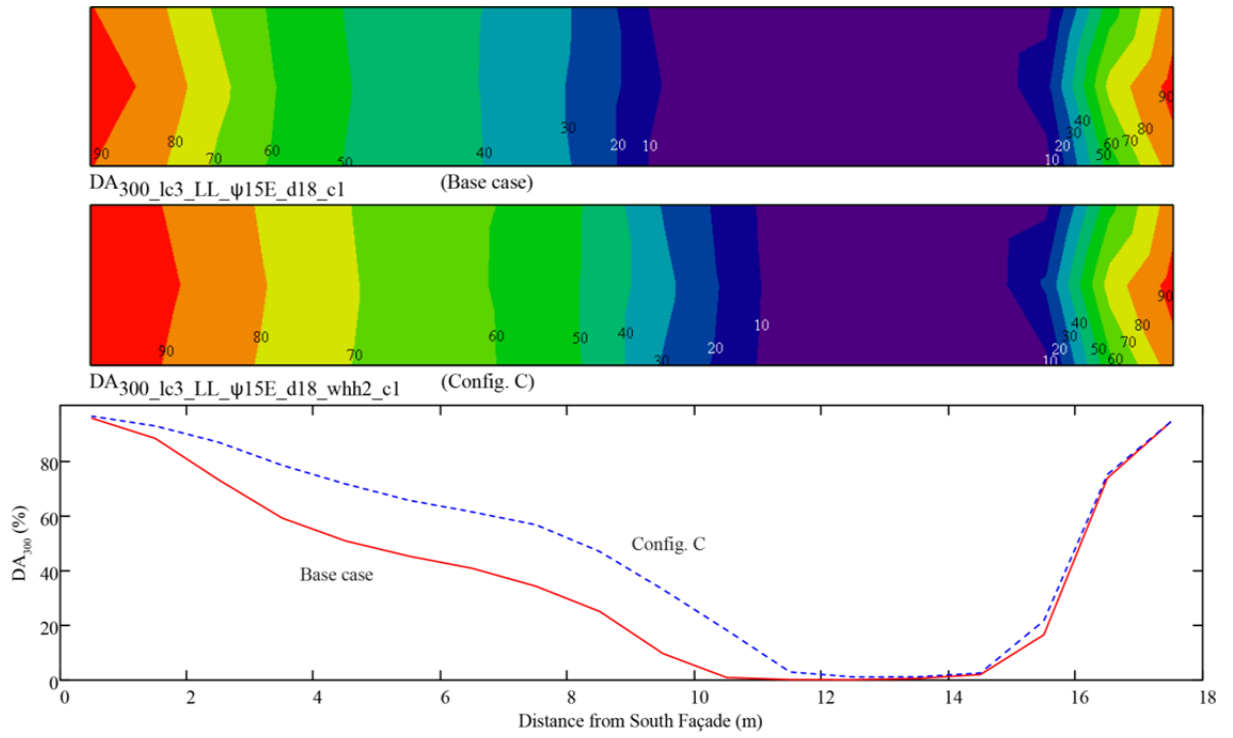


Figure A0.21: Base bldg. and configuration C, Golden, low VLT, LightLouver blind, $\psi = -15^\circ$; DA₃₀₀ contour (top, middle) and X-Y (bottom) plots [%].

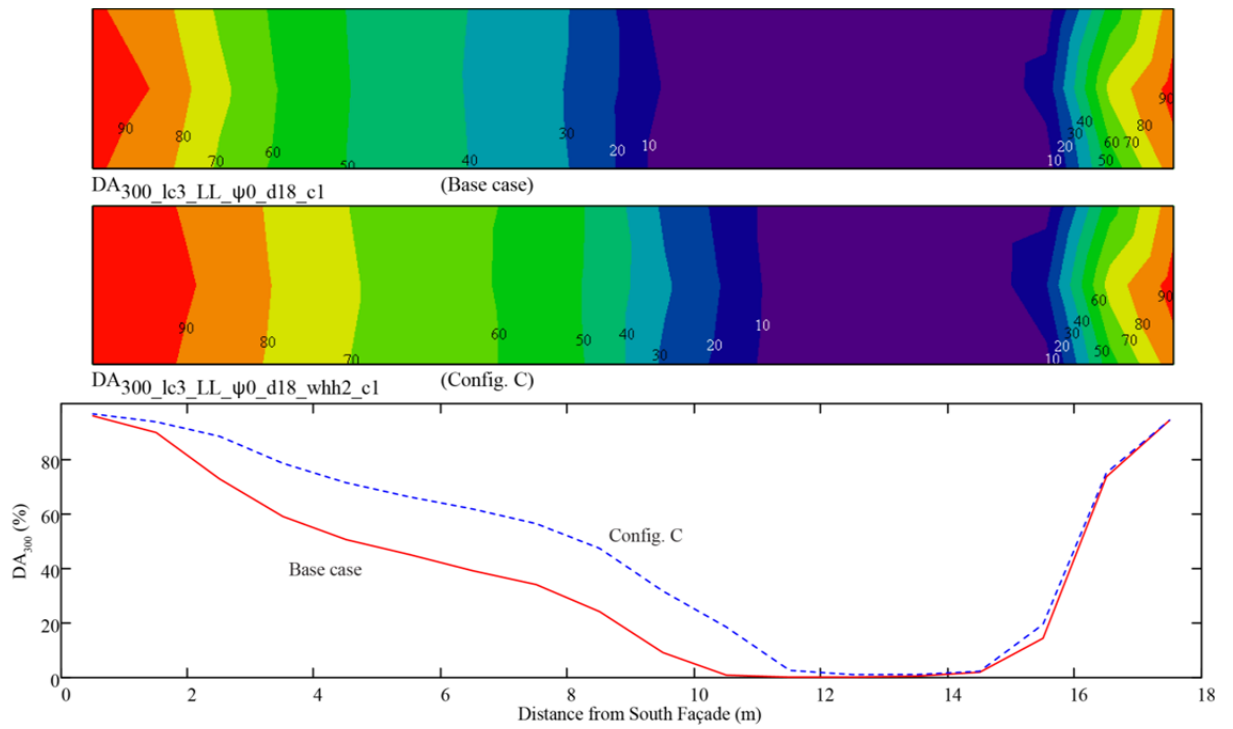


Figure A0.22: Base bldg. and configuration C, Golden, low VLT, LightLouver blind, $\psi = 0^\circ$; DA₃₀₀ contour (top, middle) and X-Y (bottom) plots [%].

A3.10. Configuration D: increase daylighting window WWR and WHH

In this configuration a large WWR_{ds} of 40 % is considered while keeping the WWR_{vs} the same as in the base building. Again, due to the way the simplified model was made, the window dimensions had to be adjusted to arrive at the same WWR_{vs} of 18.8 % while increasing the WWR_{ds} to 40 %, to make a total WWR_s of 59 %. The $WinSouth_{wd}$, $DayWinSouth_{ht}$, and $ViewWinSouth_{ht}$ were modified.

The results show that the $sDA_{300/50}$ at all façade orientation angles reaches a minimum of 56 % – thereby attaining the “nominally acceptable” level for a daylit space for $sDA_{300/50}$. In fact, for $\psi = -30, -15^\circ, 0,$ and 15° , the $sDA_{300/50}$ reaches 61 % which is greater than what is achieved with the previous configurations. See Table A0.14, Figure A0.23, and Figure A0.24.

Table A0.14: Base building and configuration D, Golden, low and high VLT, LightLouver and Vision Control blind, orientation; $sDA_{300/50}$ [%].

lc3, 1.0x1.0, D18	ψ Orientation; c1 = low VLT windows; c2= high VLT windows													
	-45°		-30°		-15°		0		15°		30°		45°	
	c1	c2	c1	c2	c1	c2	c1	c2	c1	c2	c1	c2	c1	c2
Reference (base bldg.)														
LightLouver	28	35	33	41	39	44	39	44	33	44	33	41	28	35
Vision Control	33	35	39	41	44	44	39	44	39	46	33	41	30	35
Configuration D														
LightLouver (cfs1)	56	63	61	63	61	63	61	63	61	63	56	63	56	57
Vision Control (cfs2)	56	63	61	63	61	63	61	63	61	63	61	63	56	57

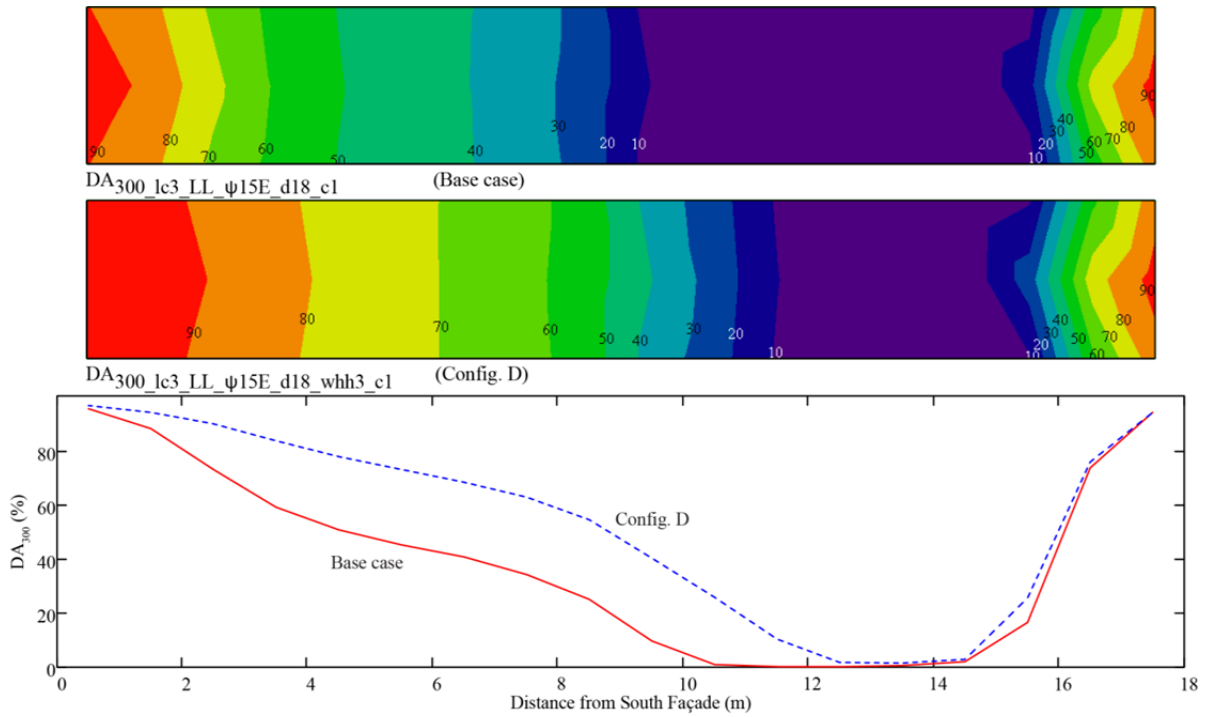


Figure A0.23: Base bldg. and configuration D, Golden, low VLT, LightLouver blind, $\psi = -15^\circ$; DA₃₀₀ contour (top, middle) and X-Y (bottom) plots [%].

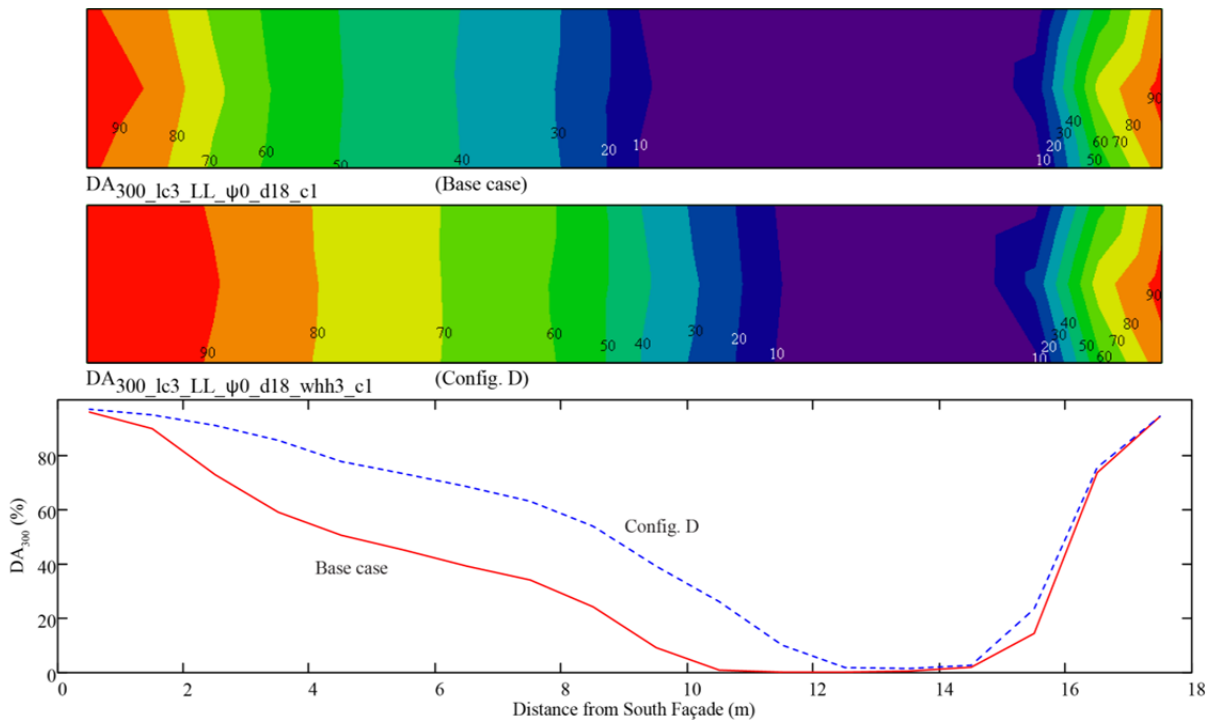


Figure A0.24: Base bldg. and configuration D, Golden, low VLT, LightLouver blind, $\psi = 0^\circ$; DA₃₀₀ contour (top, middle) and X-Y (bottom) plots [%].

A3.11. Configuration E: increasing WHH without changing WWR

For this configuration, the South façade window head height is increased without increasing the window to wall ratio. This is done by making the South façade windows slightly narrower (from 1.829 m to 1.400 m) and taller (from WHHs 3.048 m to 3.701 m) than in the base building. The results in Table A0.15 show that for certain conditions this can lead to improved sDA_{300/50} performance. For example, for $\psi = 15^\circ$, and -30° , the sDA_{300/50} performance increase is 18 % and in the case of $\psi = -45^\circ$, it is 7 %. See Figure A0.25 and Figure A0.26.

Table A0.15: Base bldg. and configuration E, Golden, low VLT, LightLouver, orientation; sDA_{300/50} [%].

Golden, LL, c1, 1.0x1.0 D18	ψ Orientation						
	-45°	-30°	-15°	0	15°	30°	45°
Reference (base bldg.)	28	33	39	39	33	33	28
Configuration E	30	39	39	39	39	33	28

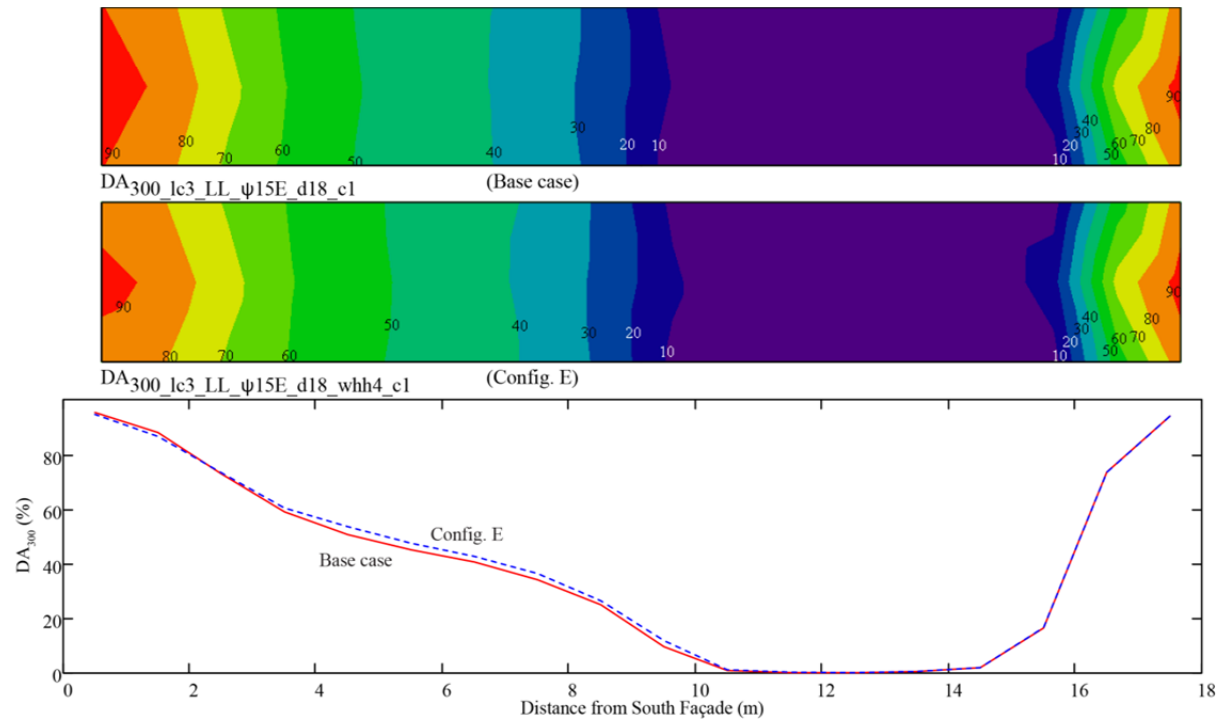


Figure A0.25: Base bldg. and configuration E, Golden, low VLT, LightLouver blind, $\psi = -15^\circ$; DA₃₀₀ contour (top, middle) and X-Y (bottom) plots [%].

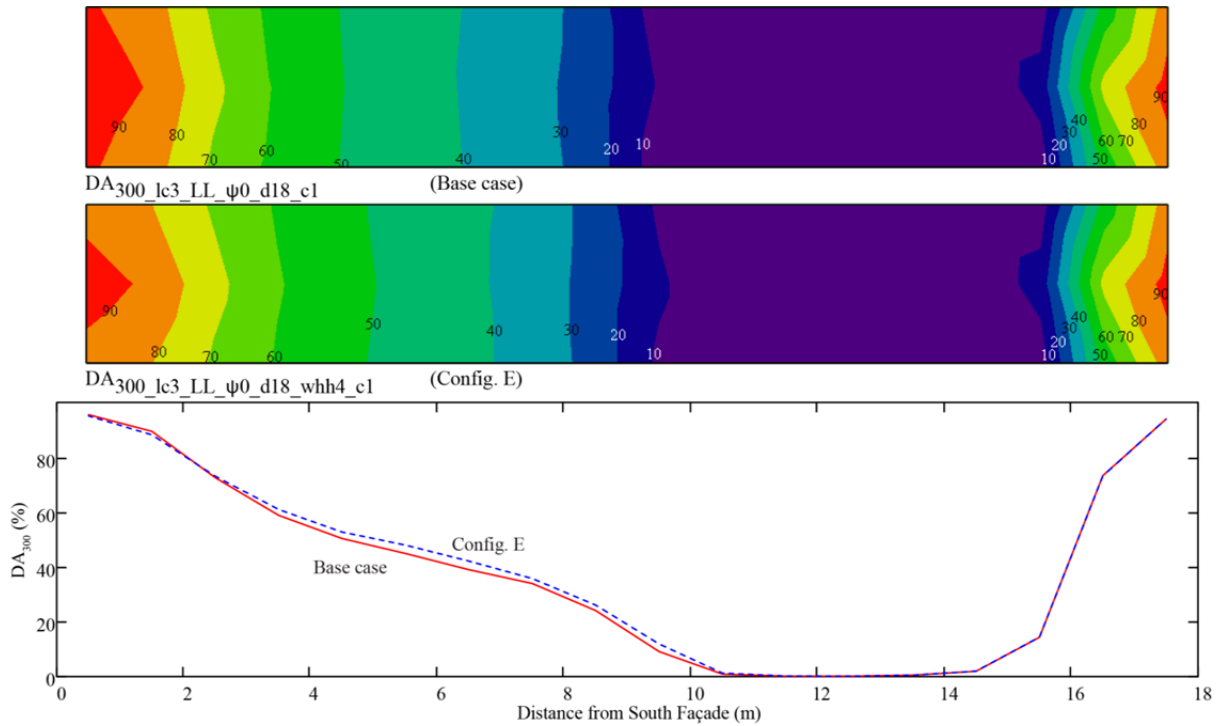


Figure A0.26: Base bldg. and configuration E, Golden, low VLT, LightLouver blind, $\psi = 0$; DA₃₀₀ contour (top, middle) and X-Y (bottom) plots [%].

A3.12. Configuration F: lower WHH on North façade

One last parameter tested in this series of window geometry configurations is the window head height on the North façade, WHH_n. The base building at the North façade positions the North daylighting window higher up than the corresponding daylighting window on the South façade (see Figure 4.8 or Table 4.11). The North daylighting window is lowered to the same height as the South daylighting window for this configuration. Results in Table A0.16 show no difference in sDA_{300/50} between the higher North daylighting window height and the lower North daylighting window height. It is only in looking at the X-Y plots in Figure A0.27 and Figure A0.28 that we can see a change in DA₃₀₀ near the North façade. This leads us to conclude that height positioning of the North daylighting window has no significant impact on the overall sDA_{300/50} values of the building cross-section being studied. This permits us to eliminate the North facade daylighting window height from the list of parameters that may contribute to near-optimal design values for daylight illuminance.

Table A0.16: Base bldg. and configuration F, Golden, low VLT, LightLouver, orientation; sDA_{300/50} [%].

Golden, LL, c1, 1.0x1.0 D18	ψ Orientation						
	-45°	-30°	-15°	0	15°	30°	45°
Reference (base bldg.)	28	33	39	39	33	33	28
Configuration F	28	33	39	39	33	33	28

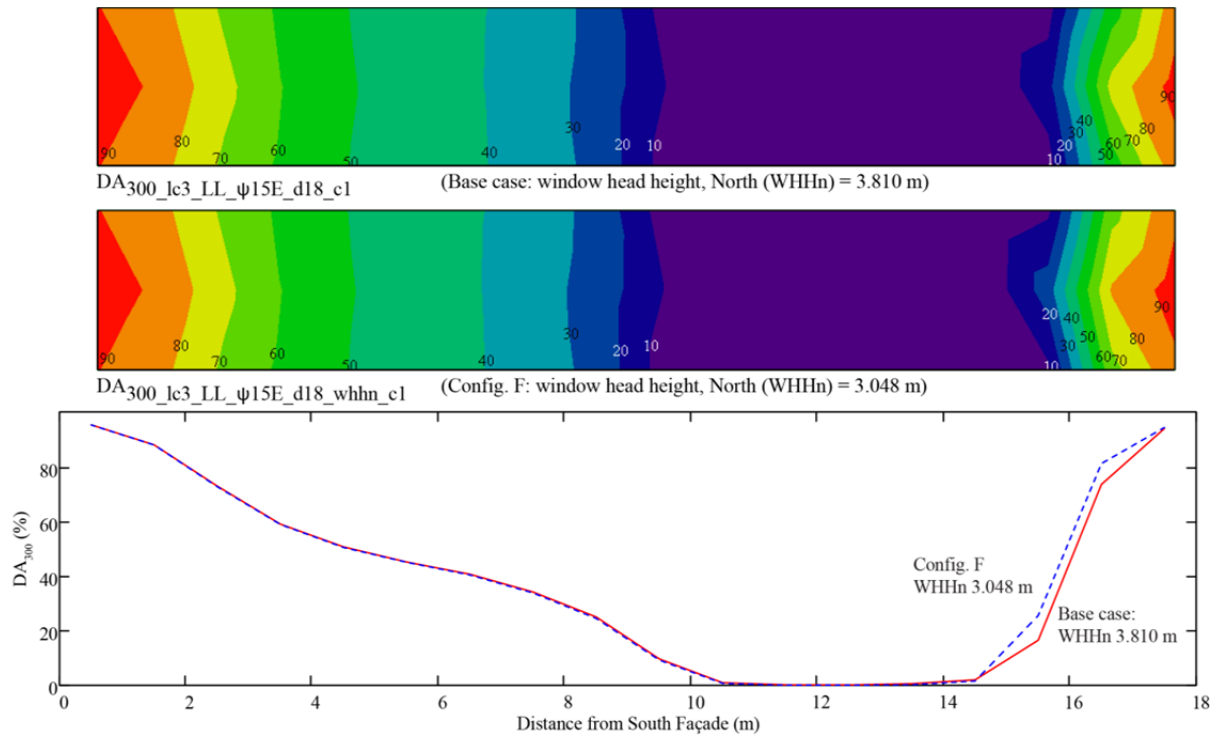


Figure A0.27: Base bldg. and configuration F, Golden, low VLT, LightLouver blind, ψ = -15°; DA₃₀₀ contour (top, middle) and X-Y (bottom) plots [%].

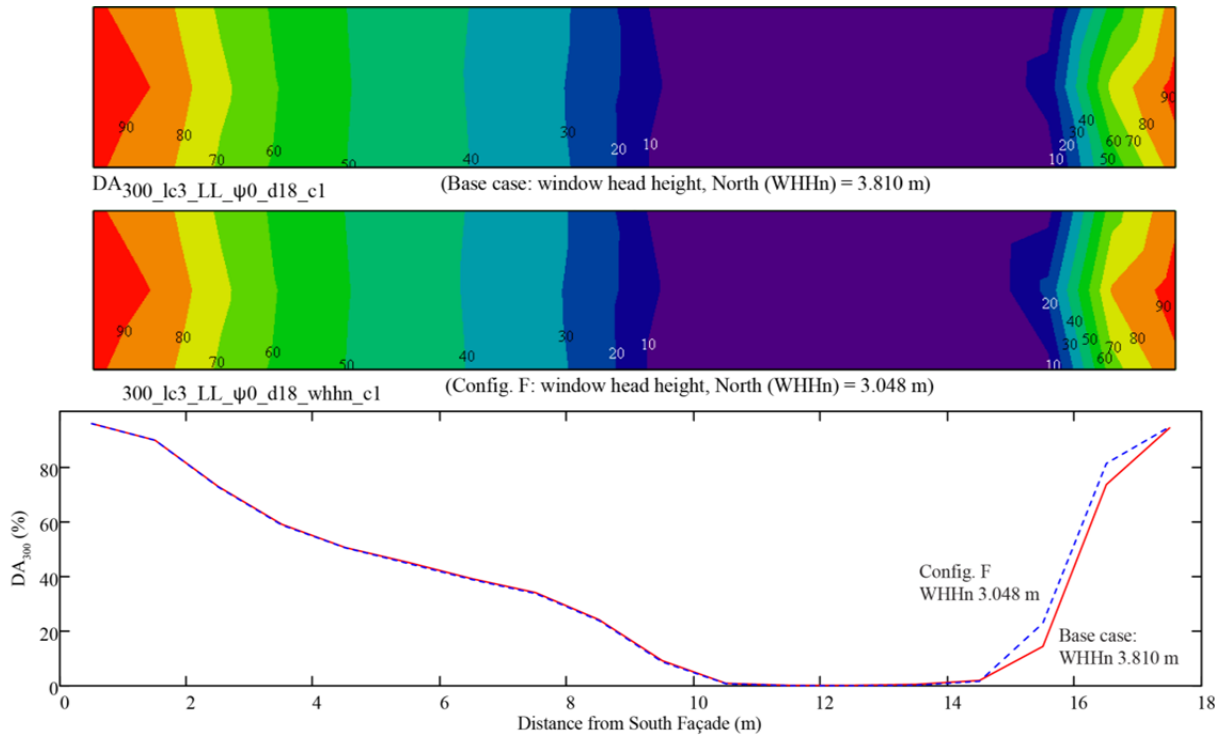


Figure A0.28: Base bldg. and configuration F, Golden, low VLT, LightLouver blind, $\psi = 0$; DA_{300} contour (top, middle) and X-Y (bottom) plots [%].

A3.13. All window to wall ratio and window head height configurations

Table A0.17, Figure A0.29, and Figure A0.30 group together all the previous configurations tested. It shows that configuration B and C have the same $sDA_{300/50}$ performance for most orientations. Therefore, for most orientations, choosing a *taller* daylighting window (configuration B) will lead to the same predicted $sDA_{300/50}$ as choosing a *wider* daylighting window (configuration C).

Table A0.17: Comparison of fenestration configurations for Golden; sDA_{300/50} [%].

D18		Orientation ψ													
Golden, 1.0 m x 1.0 m		-45°		-30°		-15°		0		15°		30°		45°	
Configuration blind		low VLT	high VLT	low VLT	high VLT	low VLT	high VLT	low VLT	high VLT	low VLT	high VLT	low VLT	high VLT	low VLT	high VLT
base bldg	LightLouver (cfs1)	28	35	33	41	39	44	39	44	33	44	33	41	28	35
	Vision Control (cfs2)	33	35	39	41	44	44	39	44	39	46	33	41	30	35
A	LightLouver (cfs1)	44	52	54	57	56	57	56	56	56	57	50	57	41	52
	Vision Control (cfs2)	50	52	56	57	56	63	56	56	56	57	54	57	44	52
B	LightLouver (cfs1)	50	57	56	57	56	63	56	61	56	57	50	57	44	52
	Vision Control (cfs2)	50	57	56	57	56	63	56	63	56	63	56	57	50	52
C	LightLouver (cfs1)	50	57	56	63	56	63	56	61	56	63	56	57	50	57
	Vision Control (cfs2)	56	57	56	63	61	63	61	63	56	63	56	57	50	57
D	LightLouver (cfs1)	56	63	61	63	61	63	61	63	61	63	56	63	56	57
	Vision Control (cfs2)	56	63	61	63	61	63	61	63	61	63	61	63	56	57
E	LightLouver (cfs1)	30	37	39	46	39	50	39	50	39	44	33	41	28	35
	Vision Control (cfs2)	33	35	39	46	44	50	44	50	39	46	35	41	33	35

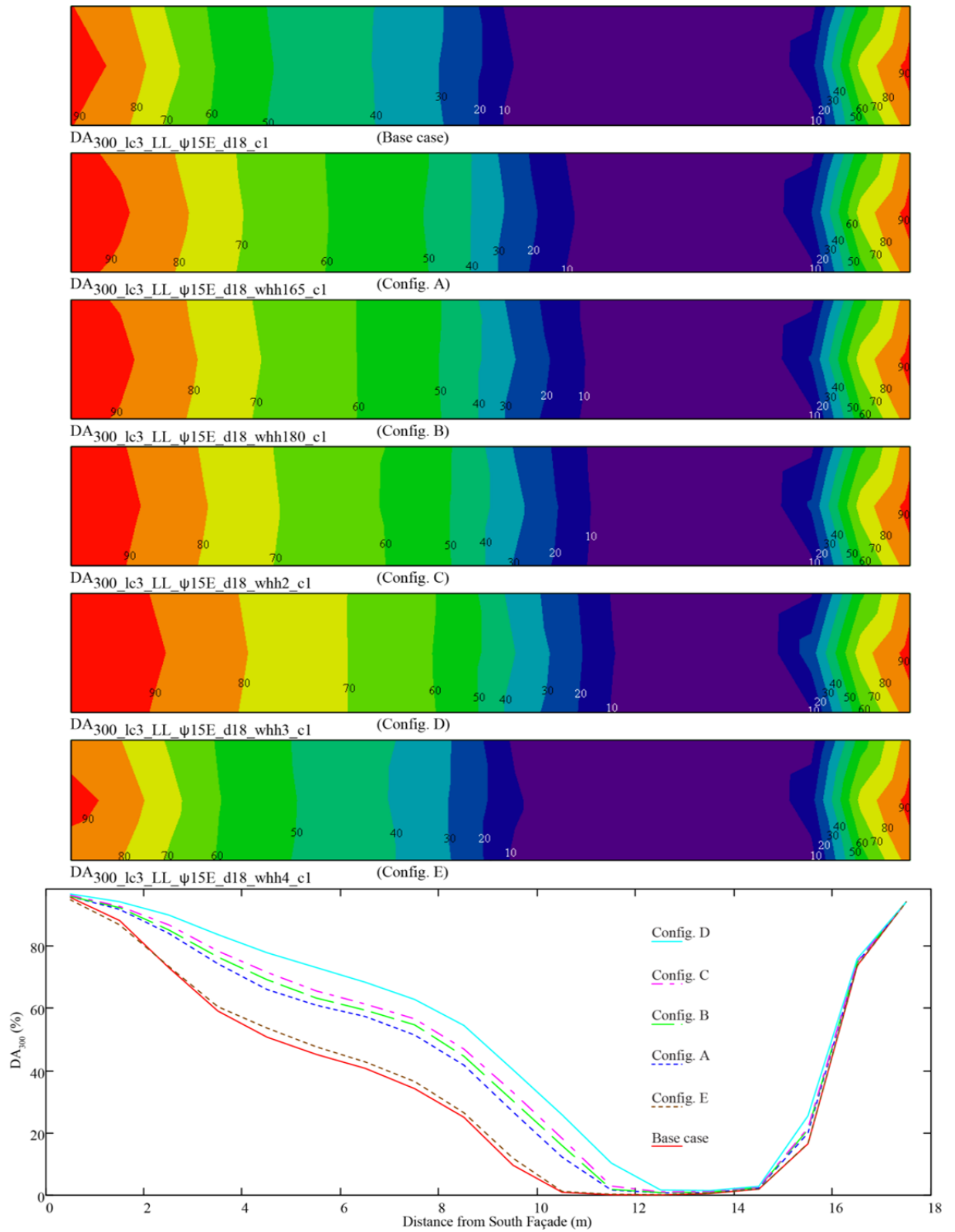


Figure A0.29: Fenestration configuration comparison: Golden, low VLT, LightLouver blind, $\psi = -15^\circ$; DA₃₀₀ contour (top, middle) and X-Y (bottom) plots [%].

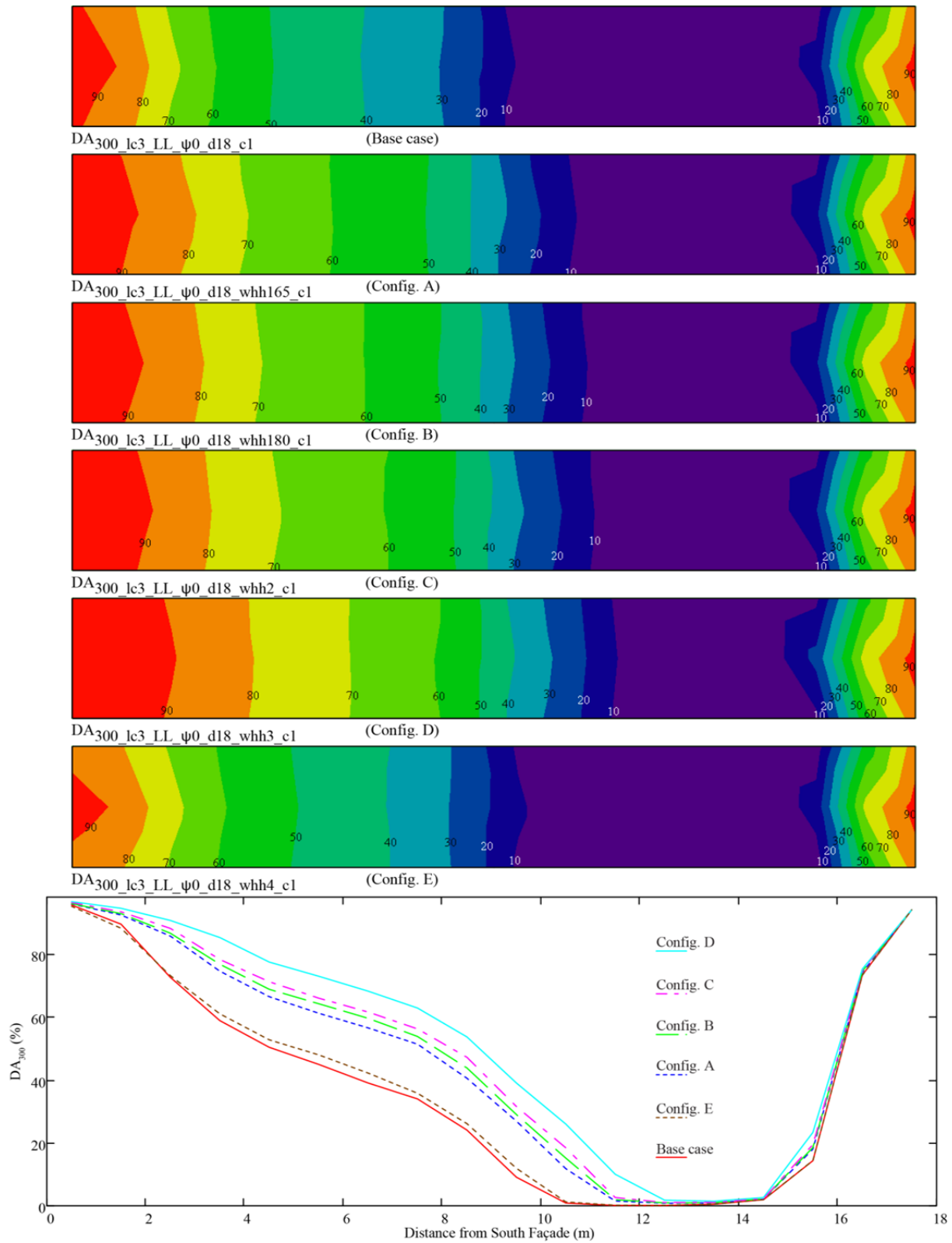


Figure A0.30: Fenestration configuration comparison: Golden, low VLT, LightLouver blind, $\psi = 0$; DA_{300} contour (top, middle) and X-Y (bottom) plots [%].

A3.14. Design inquiry: maximum building depth for daylit open-plan area

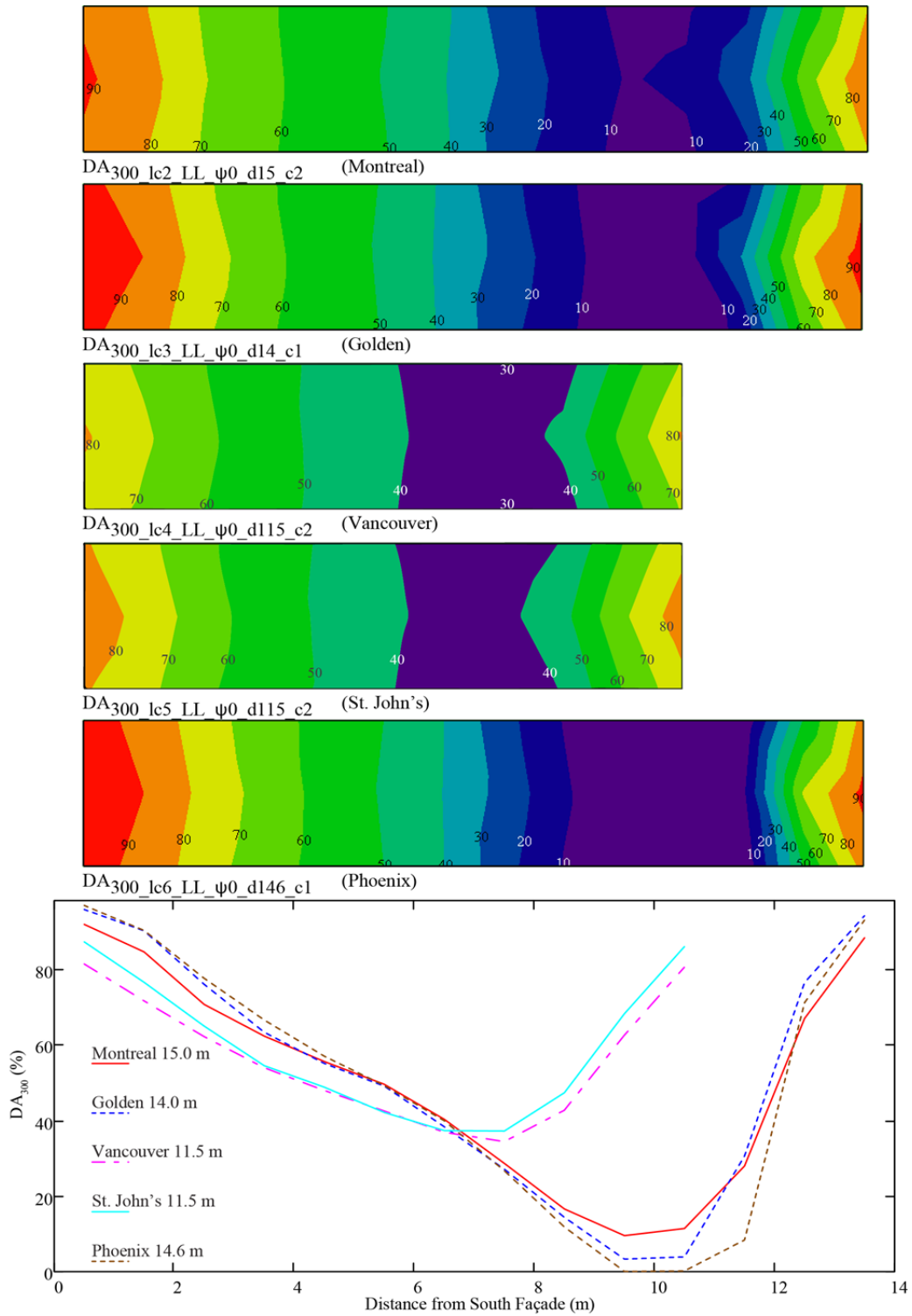


Figure A0.31: Base bldg. maximum building depth for nominally acceptable daylighting illuminance: all locations, LightLouver blind, $\psi = 0$; DA₃₀₀ contour (top, middle) and X-Y (bottom) plots [%].

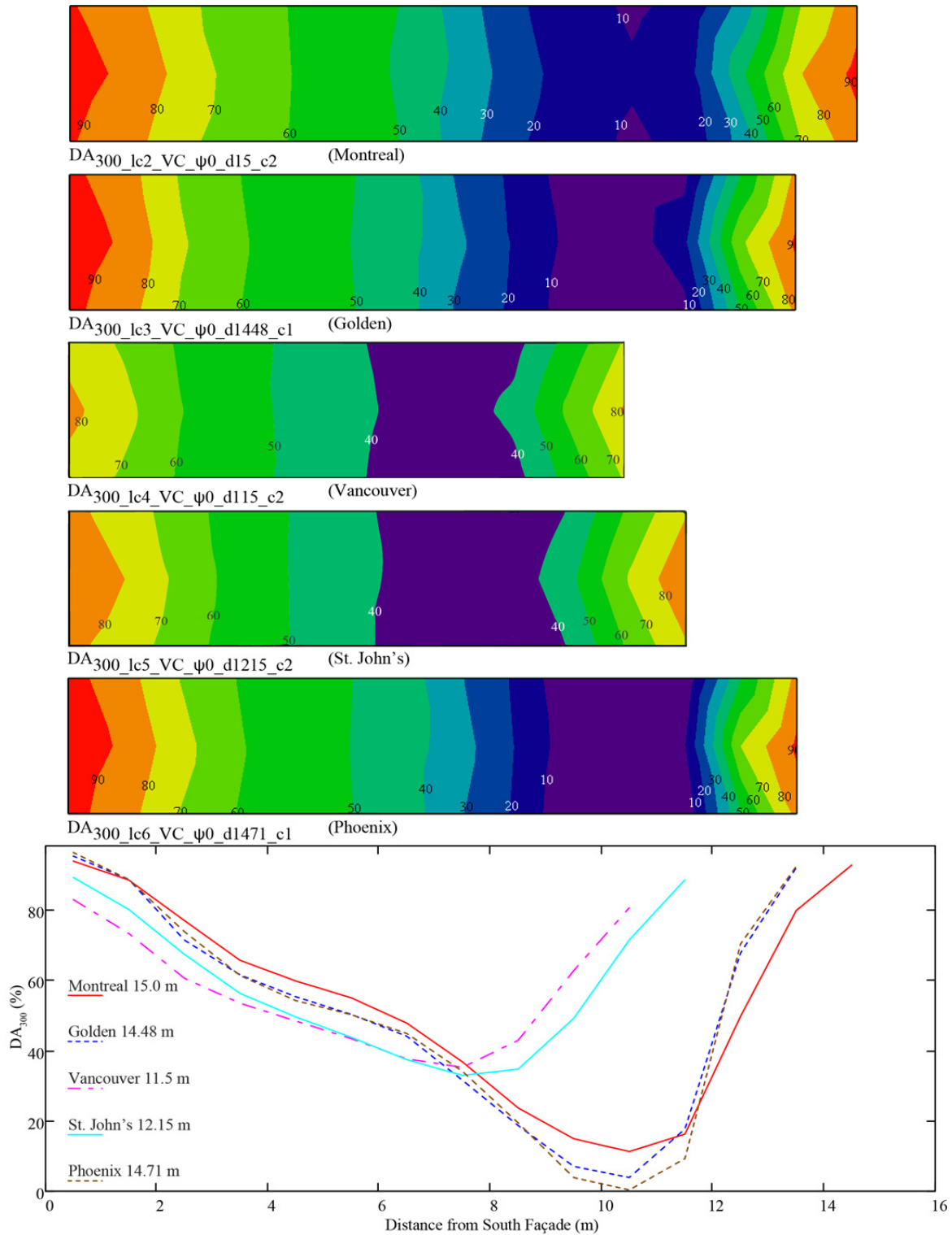
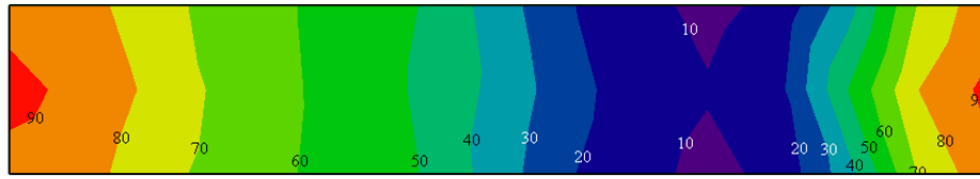
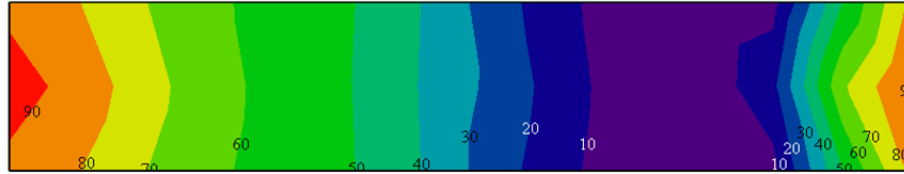


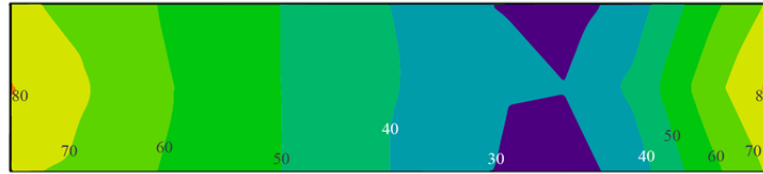
Figure A0.32: Base bldg. maximum building depth for nominally acceptable daylighting illuminance: all locations, Vision Control blind, $\psi = 0$; DA_{300} contour (top, middle) and X-Y (bottom) plots [%].



DA₃₀₀_lc2_LL_ψ0_d15_whh4_c2 (Montreal)



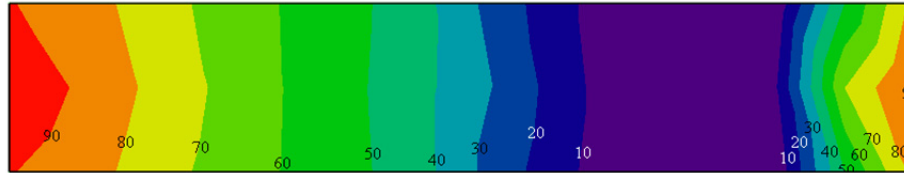
DA₃₀₀_lc3_LL_ψ0_d1441_whh4_c1 (Golden)



DA₃₀₀_lc4_LL_ψ0_d1228_whh4_c2 (Vancouver)



DA₃₀₀_lc5_LL_ψ0_d124_whh4_c2 (St. John's)



DA₃₀₀_lc6_LL_ψ0_d1467_whh4_c1 (Phoenix)

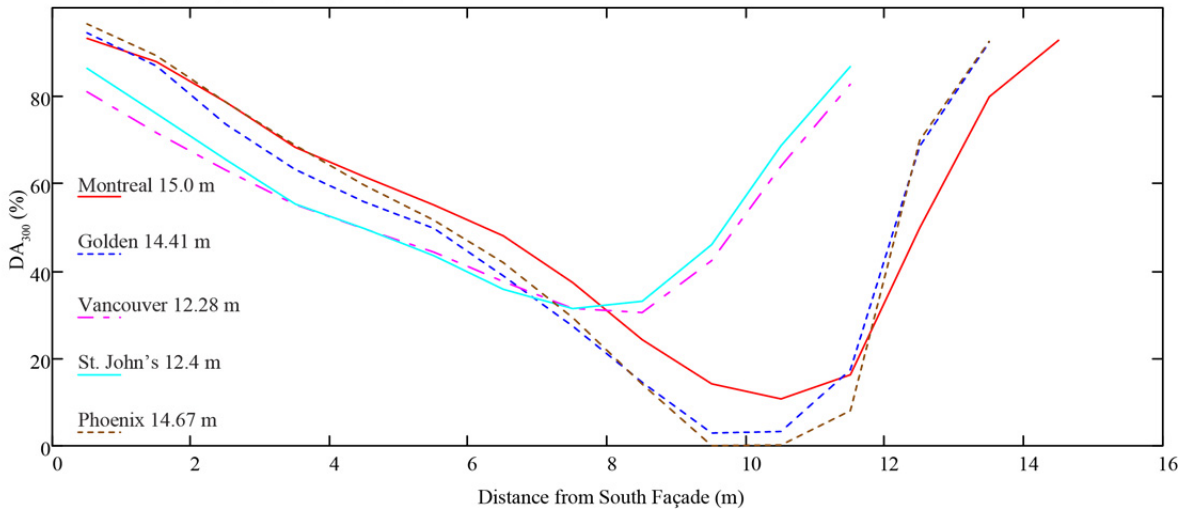


Figure A0.33: Configuration E: maximum building depth for nominally acceptable daylighting illuminance: all locations, LightLouver blind, $\psi = 0$; DA₃₀₀ contour (top, middle) and X-Y (bottom) plots [%].

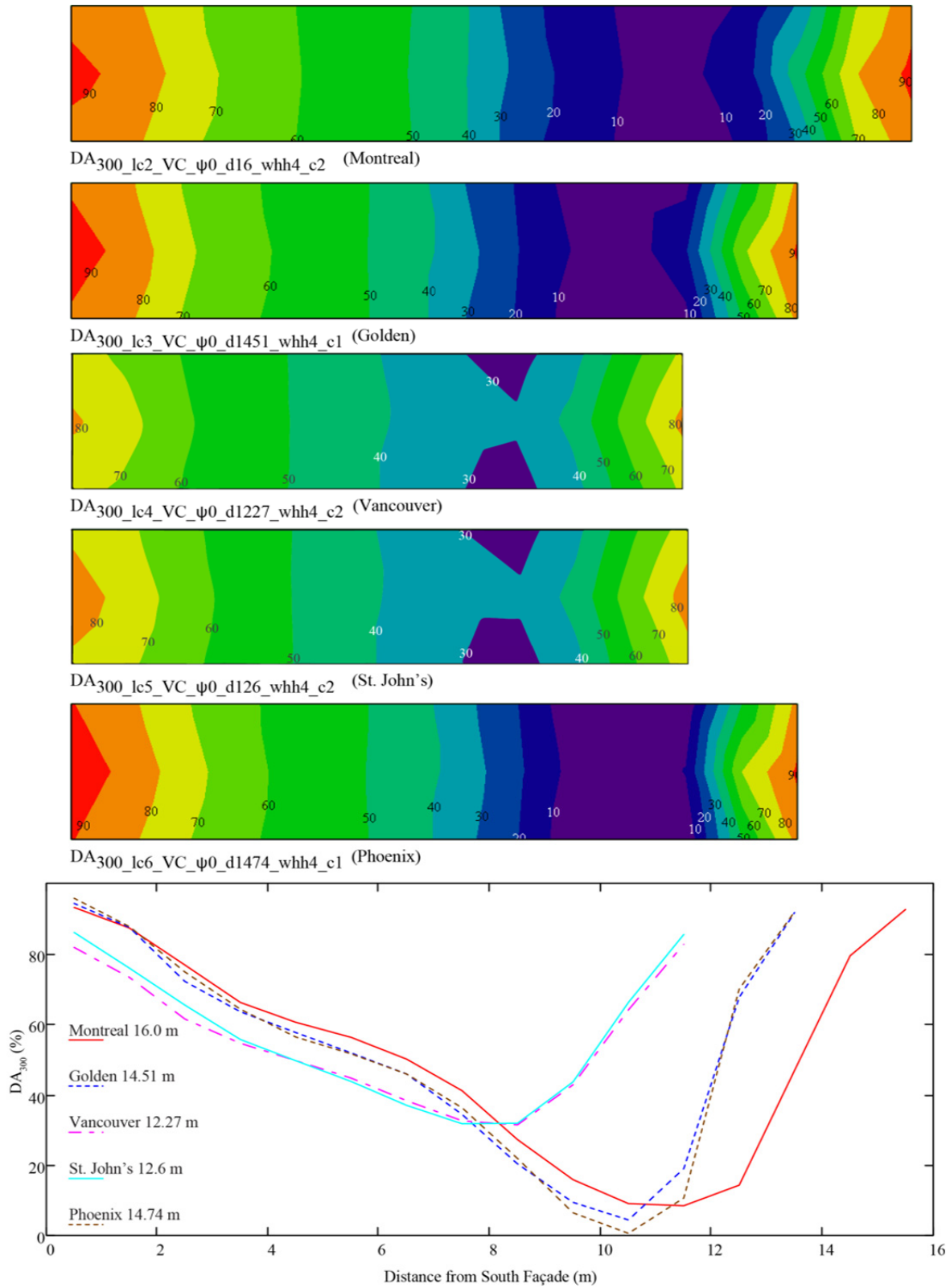


Figure A0.34: Configuration E: maximum building depth for nominally acceptable daylighting illuminance: all locations, Vision Control blind, $\psi = 0$; DA_{300} contour (top, middle) and X-Y (bottom) plots [%].

A4. Tables of simulation results

A4.1. Base building, building depth 11 m

base building D11	Orientation													
1.0 x 1.0	-45°		-30°		-15°		0		15°		30°		45°	
Location / blind	low VLT	high VLT	low VLT	high VLT	low VLT	high VLT	low VLT	high VLT	low VLT	high VLT	low VLT	high VLT	low VLT	high VLT
Montreal														
LightLouver (cfs1)	67	100	67	94	64	88	64	88	64	88	67	94	67	100
Vision Control (cfs2)	70	100	76	94	76	88	73	94	76	88	76	94	70	100
Golden														
LightLouver (cfs1)	67	100	70	100	70	94	70	94	67	94	67	100	67	100
Vision Control (cfs2)	82	100	76	100	76	94	76	94	76	94	70	100	82	100
Vancouver														
LightLouver (cfs1)	45	67	45	58	48	67	48	64	55	67	45	58	45	67
Vision Control (cfs2)	48	58	55	58	55	58	48	64	55	58	55	58	55	58
St. John's														
LightLouver (cfs1)	45	67	45	64	55	67	55	67	55	67	55	67	48	73
Vision Control (cfs2)	55	70	55	73	55	67	55	67	55	67	55	73	55	73
Phoenix														
LightLouver (cfs1)	94	100	85	100	76	100	76	100	76	100	94	100	100	100
Vision Control (cfs2)	100	100	94	100	76	100	76	94	82	100	94	100	100	100

A4.2. Base building, building depth 12 m

base building D12	Orientation													
1.0 x 1.0	-45°		-30°		-15°		0		15°		30°		45°	
Location / blind	low VLT	high VLT	low VLT	high VLT	low VLT	high VLT	low VLT	high VLT	low VLT	high VLT	low VLT	high VLT	low VLT	high VLT
Montreal														
LightLouver (cfs1)	50	75	58	75	58	75	58	69	58	75	58	75	58	75
Vision Control (cfs2)	61	78	64	75	67	75	67	69	67	75	67	75	61	75
Golden														
LightLouver (cfs1)	61	81	61	78	64	75	67	75	58	75	61	78	61	81
Vision Control (cfs2)	61	78	69	81	69	78	67	78	69	75	61	78	61	81
Vancouver														
LightLouver (cfs1)	42	53	36	50	36	50	39	50	36	50	42	53	42	53
Vision Control (cfs2)	42	53	42	50	44	50	44	50	44	50	42	53	42	53
St. John's														
LightLouver (cfs1)	42	53	42	53	44	53	50	53	44	53	42	53	42	53
Vision Control (cfs2)	42	53	50	53	50	53	50	61	50	61	50	61	50	53
Phoenix														
LightLouver (cfs1)	72	100	69	94	69	86	69	78	69	89	69	100	78	100
Vision Control (cfs2)	83	100	69	94	69	81	69	78	69	86	78	100	94	100

A4.3. Base building, building depth 13 m

base building D13	Orientation													
1.0 x 1.0	-45°		-30°		-15°		0		15°		30°		45°	
Location / blind	low VLT	high VLT	low VLT	high VLT	low VLT	high VLT	low VLT	high VLT	low VLT	high VLT	low VLT	high VLT	low VLT	high VLT
Montreal														
LightLouver (cfs1)	46	62	54	64	54	64	54	64	54	64	54	64	46	69
Vision Control (cfs2)	46	67	59	69	62	64	62	64	62	64	62	69	54	69
Golden														
LightLouver (cfs1)	46	69	54	69	59	69	59	64	54	69	54	69	46	69
Vision Control (cfs2)	54	69	62	69	62	69	62	69	62	69	54	69	49	69
Vancouver														
LightLouver (cfs1)	33	41	33	46	33	46	33	46	33	46	33	41	33	41
Vision Control (cfs2)	33	41	33	41	36	46	41	46	36	46	33	46	38	44
St. John's														
LightLouver (cfs1)	38	44	38	49	38	46	38	46	38	49	38	49	38	49
Vision Control (cfs2)	38	49	38	49	46	49	46	46	46	49	46	49	41	49
Phoenix														
LightLouver (cfs1)	64	79	62	77	62	77	62	72	62	77	64	82	64	90
Vision Control (cfs2)	67	90	64	77	62	72	62	69	64	72	64	82	67	90

A4.4. Base building, building depth 14 m

base building D14	Orientation													
1.0 x 1.0	-45°		-30°		-15°		0		15°		30°		45°	
Location / blind	low VLT	high VLT	low VLT	high VLT	low VLT	high VLT	low VLT	high VLT	low VLT	high VLT	low VLT	high VLT	low VLT	high VLT
Montreal														
LightLouver (cfs1)	43	52	43	52	50	60	50	60	50	60	50	60	43	52
Vision Control (cfs2)	43	52	50	60	57	60	57	60	57	60	55	60	43	52
Golden														
LightLouver (cfs1)	43	57	50	60	50	60	55	60	50	60	50	64	43	57
Vision Control (cfs2)	43	57	55	64	57	64	57	60	57	60	50	64	43	57
Vancouver														
LightLouver (cfs1)	31	36	31	36	31	43	31	43	31	43	31	36	31	36
Vision Control (cfs2)	31	36	31	36	31	43	33	43	31	43	31	36	31	36
St. John's														
LightLouver (cfs1)	36	38	36	38	36	43	36	43	36	43	36	43	36	40
Vision Control (cfs2)	36	38	36	45	38	43	43	43	38	43	36	43	36	45
Phoenix														
LightLouver (cfs1)	57	71	57	71	57	71	57	67	57	71	57	71	52	74
Vision Control (cfs2)	57	74	57	71	57	71	57	69	57	71	57	71	52	74

A4.5. Base building, building depth 14.5 m

base building D14.5	Orientation													
1.0 x 1.0	-45°		-30°		-15°		0		15°		30°		45°	
Location / blind	low VLT	high VLT	low VLT	high VLT	low VLT	high VLT	low VLT	high VLT	low VLT	high VLT	low VLT	high VLT	low VLT	high VLT
Montreal														
LightLouver (cfs1)	36	43	38	50	45	57	45	57	45	57	38	55	38	52
Vision Control (cfs2)	43	45	50	57	45	57	50	57	50	57	50	57	43	52
Golden														
LightLouver (cfs1)	38	x	50	x	45	x	45	x	50	x	43	x	36	x
Vision Control (cfs2)	43	x	50	x	57	x	52	x	50	x	43	x	43	x
Vancouver														
LightLouver (cfs1)	24	36	26	36	29	31	29	33	31	38	26	36	24	36
Vision Control (cfs2)	26	36	31	36	29	36	29	38	31	36	31	36	26	36
St. John's														
LightLouver (cfs1)	26	36	26	36	31	38	31	43	31	38	31	36	26	36
Vision Control (cfs2)	31	36	31	36	31	43	31	43	31	38	31	38	31	36
Phoenix														
LightLouver (cfs1)	57	67	57	67	57	67	57	60	57	67	57	67	50	71
Vision Control (cfs2)	57	67	57	67	57	67	57	60	57	67	57	64	45	71

x = not calculated

A4.6. Base building, building depth 15 m

base building D15	Orientation													
1.0 x 1.0	-45°		-30°		-15°		0		15°		30°		45°	
Location / blind	low VLT	high VLT	low VLT	high VLT	low VLT	high VLT	low VLT	high VLT	low VLT	high VLT	low VLT	high VLT	low VLT	high VLT
Montreal														
LightLouver (cfs1)	36	42	40	49	47	56	47	53	47	56	40	56	40	49
Vision Control (cfs2)	40	42	47	56	53	56	53	56	53	56	47	56	40	49
Golden														
LightLouver (cfs1)	40	49	47	56	47	60	47	60	47	56	40	53	36	42
Vision Control (cfs2)	40	49	47	56	53	62	53	60	53	56	47	49	40	42
Vancouver														
LightLouver (cfs1)	24	33	29	33	29	36	29	40	29	40	29	33	24	33
Vision Control (cfs2)	29	33	29	33	29	36	29	40	29	36	29	33	29	33
St. John's														
LightLouver (cfs1)	33	33	33	33	33	40	29	40	33	40	33	36	33	33
Vision Control (cfs2)	33	36	33	36	36	40	31	40	33	40	33	40	33	36
Phoenix														
LightLouver (cfs1)	53	67	53	62	53	62	53	62	53	62	53	67	47	60
Vision Control (cfs2)	53	67	58	67	58	62	53	62	53	67	53	67	47	60

A4.7. Base building, building depth 16 m

base building D16	Orientation													
1.0 x 1.0	-45°		-30°		-15°		0		15°		30°		45°	
Location / blind	low VLT	high VLT	low VLT	high VLT	low VLT	high VLT	low VLT	high VLT	low VLT	high VLT	low VLT	high VLT	low VLT	high VLT
Montreal														
LightLouver (cfs1)	33	40	38	46	40	50	44	50	44	50	38	46	33	40
Vision Control (cfs2)	38	40	44	52	44	50	50	50	44	50	44	52	38	42
Golden														
LightLouver (cfs1)	38	42	44	52	44	52	44	54	44	52	38	46	31	40
Vision Control (cfs2)	38	40	44	52	50	58	50	56	44	52	40	46	38	40
Vancouver														
LightLouver (cfs1)	23	31	27	31	27	33	27	38	27	33	23	31	23	31
Vision Control (cfs2)	27	31	27	31	27	33	27	38	27	33	27	31	27	31
St. John's														
LightLouver (cfs1)	27	31	31	31	27	33	27	38	27	33	31	31	31	31
Vision Control (cfs2)	31	31	31	31	27	38	29	38	27	33	31	33	31	31
Phoenix														
LightLouver (cfs1)	50	58	50	58	50	58	50	58	50	58	50	58	38	56
Vision Control (cfs2)	50	58	54	58	54	58	50	58	50	58	50	63	38	50

A4.8. Base building, building depth 17 m

base building D17	Orientation													
1.0 x 1.0	-45°		-30°		-15°		0		15°		30°		45°	
Location / blind	low VLT	high VLT	low VLT	high VLT	low VLT	high VLT	low VLT	high VLT	low VLT	high VLT	low VLT	high VLT	low VLT	high VLT
Montreal														
LightLouver (cfs1)	29	37	35	41	35	47	37	47	35	47	35	41	31	37
Vision Control (cfs2)	31	37	41	43	41	47	41	47	41	47	41	47	35	37
Golden														
LightLouver (cfs1)	31	37	35	49	41	49	41	47	37	49	35	43	29	37
Vision Control (cfs2)	35	37	41	49	47	53	47	51	41	49	35	43	31	37
Vancouver														
LightLouver (cfs1)	22	29	22	29	25	29	25	31	25	29	22	29	22	29
Vision Control (cfs2)	22	29	25	29	25	29	25	31	25	29	25	29	22	29
St. John's														
LightLouver (cfs1)	25	29	29	29	25	29	25	31	25	29	25	29	29	29
Vision Control (cfs2)	29	29	29	29	25	31	25	35	25	31	25	29	29	29
Phoenix														
LightLouver (cfs1)	47	55	47	59	47	55	41	55	47	55	47	59	35	53
Vision Control (cfs2)	47	55	51	55	47	55	47	55	47	55	47	55	35	47

A4.9. Base building, building depth 18 m

base building D18	Orientation													
1.0 x 1.0	-45°		-30°		-15°		0		15°		30°		45°	
Location / blind	low VLT	high VLT	low VLT	high VLT	low VLT	high VLT	low VLT	high VLT	low VLT	high VLT	low VLT	high VLT	low VLT	high VLT
Montreal														
LightLouver (cfs1)	28	35	33	35	33	39	30	39	33	39	33	39	28	33
Vision Control (cfs2)	30	35	35	39	39	44	39	44	39	44	39	39	33	35
Golden														
LightLouver (cfs1)	28	35	33	41	39	44	39	44	33	44	33	41	28	35
Vision Control (cfs2)	33	35	39	41	44	44	39	44	39	46	33	41	30	35
Vancouver														
LightLouver (cfs1)	19	28	20	28	24	28	24	28	24	28	20	28	19	28
Vision Control (cfs2)	20	28	24	28	24	28	24	28	24	28	24	28	20	28
St. John's														
LightLouver (cfs1)	24	28	20	28	24	28	24	28	24	28	24	28	20	28
Vision Control (cfs2)	28	28	24	28	24	28	24	30	24	28	24	28	28	28
Phoenix														
LightLouver (cfs1)	44	56	44	56	39	52	39	52	39	52	44	56	33	41
Vision Control (cfs2)	44	52	44	52	44	52	41	50	44	52	44	52	33	37

A4.10. Configuration A, building depth 18 m

configuration A D18	Orientation													
1.0 x 1.0 whh165	-45°		-30°		-15°		0		15°		30°		45°	
Location / blind	low VLT	high VLT	low VLT	high VLT	low VLT	high VLT	low VLT	high VLT	low VLT	high VLT	low VLT	high VLT	low VLT	high VLT
Montreal														
LightLouver (cfs1)	44	52	50	57	54	56	54	56	54	56	50	56	44	52
Vision Control (cfs2)	44	52	56	57	56	56	56	56	56	56	56	57	50	52
Golden														
LightLouver (cfs1)	44	52	54	57	56	57	56	56	56	57	50	57	41	52
Vision Control (cfs2)	50	52	56	57	56	63	56	56	56	57	54	57	44	52
Vancouver														
LightLouver (cfs1)	30	33	30	39	31	39	31	44	31	44	30	39	26	33
Vision Control (cfs2)	30	33	30	39	35	39	35	44	35	41	30	39	30	33
St. John's														
LightLouver (cfs1)	33	35	33	39	31	44	35	44	31	41	30	39	33	39
Vision Control (cfs2)	33	39	39	39	35	44	41	44	35	44	39	44	39	39
Phoenix														
LightLouver (cfs1)	56	63	56	63	56	63	56	63	56	63	56	63	50	61
Vision Control (cfs2)	56	57	61	63	61	63	56	63	56	63	56	63	50	61

A4.11. Configuration B, building depth 18 m

configuration B D18	Orientation													
1.0 x 1.0 whh180	-45°		-30°		-15°		0		15°		30°		45°	
Location / blind	low VLT	high VLT	low VLT	high VLT	low VLT	high VLT	low VLT	high VLT	low VLT	high VLT	low VLT	high VLT	low VLT	high VLT
Montreal														
LightLouver (cfs1)	44	56	50	57	56	56	56	56	56	56	54	57	50	57
Vision Control (cfs2)	50	52	56	57	56	61	56	61	56	61	56	57	50	57
Golden														
LightLouver (cfs1)	50	57	56	57	56	63	56	61	56	57	50	57	44	52
Vision Control (cfs2)	50	57	56	57	56	63	56	63	56	63	56	57	50	52
Vancouver														
LightLouver (cfs1)	30	39	30	39	35	44	35	44	35	44	30	39	30	39
Vision Control (cfs2)	30	39	35	39	35	44	41	44	41	44	35	39	30	39
St. John's														
LightLouver (cfs1)	33	39	35	39	35	44	35	44	35	44	35	44	33	39
Vision Control (cfs2)	39	39	39	44	41	50	41	50	41	50	44	44	39	44
Phoenix														
LightLouver (cfs1)	61	63	61	63	56	63	56	63	56	63	61	63	56	61
Vision Control (cfs2)	56	63	61	63	61	63	61	63	61	63	61	63	56	61

A4.12. Configuration C, building depth 18 m

configuration C D18	Orientation													
1.0 x 1.0 whh2	-45°		-30°		-15°		0		15°		30°		45°	
Location / blind	low VLT	high VLT	low VLT	high VLT	low VLT	high VLT	low VLT	high VLT	low VLT	high VLT	low VLT	high VLT	low VLT	high VLT
Montreal														
LightLouver (cfs1)	50	57	54	57	56	61	56	61	56	61	56	57	50	57
Vision Control (cfs2)	50	57	56	63	56	61	61	61	61	61	56	63	56	57
Golden														
LightLouver (cfs1)	50	57	56	63	56	63	56	61	56	63	56	57	50	57
Vision Control (cfs2)	56	57	56	63	61	63	61	63	56	63	56	57	50	57
Vancouver														
LightLouver (cfs1)	30	39	35	44	35	50	41	50	37	50	31	44	30	39
Vision Control (cfs2)	35	39	35	44	41	44	44	50	41	50	35	44	35	39
St. John's														
LightLouver (cfs1)	33	39	39	44	37	50	41	50	37	50	39	44	39	44
Vision Control (cfs2)	39	44	44	44	46	50	46	50	44	50	44	50	44	44
Phoenix														
LightLouver (cfs1)	61	63	61	63	61	63	61	63	61	63	61	63	56	67
Vision Control (cfs2)	61	63	61	63	61	63	61	63	61	63	61	67	56	61

A4.13. Configuration D, building depth 18 m

configuration D D18	Orientation													
1.0 x 1.0 whh3	-45°		-30°		-15°		0		15°		30°		45°	
Location / blind	low VLT	high VLT	low VLT	high VLT	low VLT	high VLT	low VLT	high VLT	low VLT	high VLT	low VLT	high VLT	low VLT	high VLT
Montreal														
LightLouver (cfs1)	56	57	56	63	61	61	61	61	61	61	56	63	56	63
Vision Control (cfs2)	56	57	61	63	61	63	61	61	61	63	61	63	56	63
Golden														
LightLouver (cfs1)	56	63	61	63	61	63	61	63	61	63	56	63	56	57
Vision Control (cfs2)	56	63	61	63	61	63	61	63	61	63	61	63	56	57
Vancouver														
LightLouver (cfs1)	41	50	41	50	46	56	46	56	46	56	41	50	37	50
Vision Control (cfs2)	41	50	46	50	46	56	52	56	52	56	46	50	41	50
St. John's														
LightLouver (cfs1)	44	50	44	54	46	56	46	56	46	56	50	56	44	54
Vision Control (cfs2)	50	50	50	56	56	56	52	56	56	56	56	56	54	56
Phoenix														
LightLouver (cfs1)	61	72	61	69	61	65	61	65	61	65	61	72	61	67
Vision Control (cfs2)	61	69	61	65	61	65	61	63	61	65	61	69	61	67

A4.14. Configuration D, building depth 18.5 m

configuration D D18.5	Orientation													
1.0 x 1.0 whh3	-45°		-30°		-15°		0		15°		30°		45°	
Location / blind	low VLT	high VLT	low VLT	high VLT	low VLT	high VLT	low VLT	high VLT	low VLT	high VLT	low VLT	high VLT	low VLT	high VLT
Montreal														
LightLouver (cfs1)	x	x	x	x	x	x	x	x	x	x	x	x	x	x
Vision Control (cfs2)	x	x	x	x	x	x	x	x	x	x	x	x	x	x
Golden														
LightLouver (cfs1)	56	x	61	x	57	x	57	x	57	x	56	x	56	x
Vision Control (cfs2)	56	x	61	x	57	x	57	x	61	x	61	x	56	x
Vancouver														
LightLouver (cfs1)	x	50	x	46	x	52	x	52	x	52	x	50	x	44
Vision Control (cfs2)	x	44	x	50	x	50	x	52	x	52	x	50	x	44
St. John's														
LightLouver (cfs1)	x	50	x	50	x	56	x	56	x	56	x	54	x	50
Vision Control (cfs2)	x	50	x	54	x	56	x	56	x	56	x	56	x	56
Phoenix														
LightLouver (cfs1)	61	x	61	x	61	x	61	x	61	x	61	x	61	x
Vision Control (cfs2)	61	x	61	x	61	x	61	x	61	x	61	x	56	x

x = not calculated

A4.15. Configuration E, building depth 10 m

configuration E D10	Orientation													
1.0 x 1.0 whh4	-45°		-30°		-15°		0		15°		30°		45°	
Location / blind	low VLT	high VLT	low VLT	high VLT	low VLT	high VLT	low VLT	high VLT	low VLT	high VLT	low VLT	high VLT	low VLT	high VLT
Montreal														
LightLouver (cfs1)	93	100	93	100	83	100	83	100	83	100	93	100	93	100
Vision Control (cfs2)	100	100	100	100	87	100	87	100	93	100	100	100	100	100
Golden														
LightLouver (cfs1)	100	100	100	100	93	100	93	100	93	100	100	100	100	100
Vision Control (cfs2)	100	100	100	100	100	100	93	100	100	100	100	100	100	100
Vancouver														
LightLouver (cfs1)	60	93	60	87	60	73	60	73	60	87	60	87	63	93
Vision Control (cfs2)	60	87	60	87	60	73	63	73	60	83	63	87	63	87
St. John's														
LightLouver (cfs1)	63	93	63	87	60	87	60	83	60	93	63	93	63	93
Vision Control (cfs2)	63	87	73	93	70	87	70	87	70	93	73	93	73	100
Phoenix														
LightLouver (cfs1)	100	100	100	100	100	100	100	100	100	100	100	100	100	100
Vision Control (cfs2)	100	100	100	100	100	100	100	100	100	100	100	100	100	100

A4.16. Configuration E, building depth 11 m

configuration E D11	Orientation													
1.0 x 1.0 whh4	-45°		-30°		-15°		0		15°		30°		45°	
Location / blind	low VLT	high VLT	low VLT	high VLT	low VLT	high VLT	low VLT	high VLT	low VLT	high VLT	low VLT	high VLT	low VLT	high VLT
Montreal														
LightLouver (cfs1)	67	100	67	94	70	94	67	94	70	94	70	94	70	100
Vision Control (cfs2)	82	100	76	100	76	94	76	94	76	94	76	100	76	100
Golden														
LightLouver (cfs1)	76	100	76	100	76	100	76	94	76	100	76	100	76	100
Vision Control (cfs2)	82	100	76	100	76	100	76	94	76	100	82	100	85	100
Vancouver														
LightLouver (cfs1)	48	67	48	67	48	67	48	67	55	67	48	67	48	67
Vision Control (cfs2)	55	67	55	67	55	67	48	67	55	67	55	67	55	67
St. John's														
LightLouver (cfs1)	48	73	55	73	55	67	55	67	55	67	55	73	55	73
Vision Control (cfs2)	55	73	55	73	55	67	64	67	55	67	64	73	55	73
Phoenix														
LightLouver (cfs1)	94	100	94	100	76	100	76	100	82	100	94	100	100	100
Vision Control (cfs2)	100	100	94	100	82	100	76	100	88	100	100	100	100	100

A4.17. Configuration E, building depth 12 m

configuration E D12	Orientation													
1.0 x 1.0 whh4	-45°		-30°		-15°		0		15°		30°		45°	
Location / blind	low VLT	high VLT	low VLT	high VLT	low VLT	high VLT	low VLT	high VLT	low VLT	high VLT	low VLT	high VLT	low VLT	high VLT
Montreal														
LightLouver (cfs1)	61	78	58	75	64	75	67	75	58	75	58	75	61	81
Vision Control (cfs2)	61	81	69	78	67	75	67	78	67	78	69	78	69	81
Golden														
LightLouver (cfs1)	61	86	69	86	67	78	67	78	67	78	61	81	61	86
Vision Control (cfs2)	69	81	69	86	69	83	67	78	69	78	69	81	69	89
Vancouver														
LightLouver (cfs1)	42	53	36	50	44	58	44	58	44	58	42	53	42	53
Vision Control (cfs2)	44	53	44	53	44	50	44	58	44	53	44	53	44	53
St. John's														
LightLouver (cfs1)	42	53	42	53	50	61	50	61	50	61	50	61	44	56
Vision Control (cfs2)	50	53	50	61	50	61	50	61	50	61	50	61	50	61
Phoenix														
LightLouver (cfs1)	78	100	69	100	69	89	69	86	69	89	72	100	83	100
Vision Control (cfs2)	89	100	72	100	69	86	69	78	69	89	83	100	94	100

A4.18. Configuration E, building depth 13 m

configuration E D13	Orientation													
1.0 x 1.0 whh4	-45°		-30°		-15°		0		15°		30°		45°	
Location / blind	low VLT	high VLT	low VLT	high VLT	low VLT	high VLT	low VLT	high VLT	low VLT	high VLT	low VLT	high VLT	low VLT	high VLT
Montreal														
LightLouver (cfs1)	43	52	50	60	50	60	50	60	50	60	50	60	43	60
Vision Control (cfs2)	43	57	57	60	57	60	57	64	57	64	57	60	50	64
Golden														
LightLouver (cfs1)	43	64	50	64	57	67	57	67	55	60	50	64	43	64
Vision Control (cfs2)	50	64	57	64	57	67	57	67	57	60	50	64	45	64
Vancouver														
LightLouver (cfs1)	31	38	31	43	31	43	31	43	31	43	31	38	31	36
Vision Control (cfs2)	31	38	31	38	33	43	38	43	33	43	31	43	36	36
St. John's														
LightLouver (cfs1)	36	40	36	45	36	43	38	43	36	43	36	43	36	45
Vision Control (cfs2)	36	40	38	45	43	43	43	45	43	43	43	43	38	45
Phoenix														
LightLouver (cfs1)	57	74	57	71	57	71	57	71	57	71	57	71	52	79
Vision Control (cfs2)	64	79	62	71	62	71	57	71	62	71	60	71	52	81

A4.19. Configuration E, building depth 14 m

configuration E D14	Orientation													
1.0 x 1.0 whh4	-45°		-30°		-15°		0		15°		30°		45°	
Location / blind	low VLT	high VLT	low VLT	high VLT	low VLT	high VLT	low VLT	high VLT	low VLT	high VLT	low VLT	high VLT	low VLT	high VLT
Montreal														
LightLouver (cfs1)	43	52	50	60	50	60	50	60	50	60	50	60	43	60
Vision Control (cfs2)	43	57	57	60	57	60	57	64	57	64	57	60	50	64
Golden														
LightLouver (cfs1)	43	64	50	64	57	67	57	67	55	60	50	64	43	64
Vision Control (cfs2)	50	64	57	64	57	67	57	67	57	60	50	64	45	64
Vancouver														
LightLouver (cfs1)	31	38	31	43	31	43	31	43	31	43	31	38	31	36
Vision Control (cfs2)	31	38	31	38	33	43	38	43	33	43	31	43	36	36
St. John's														
LightLouver (cfs1)	36	40	36	45	36	43	38	43	36	43	36	43	36	45
Vision Control (cfs2)	36	40	38	45	43	43	43	45	43	43	43	43	38	45
Phoenix														
LightLouver (cfs1)	57	74	57	71	57	71	57	71	57	71	57	71	52	79
Vision Control (cfs2)	64	79	62	71	62	71	57	71	62	71	60	71	52	81

A4.20. Configuration E, building depth 15 m

configuration E D15	Orientation													
1.0 x 1.0 whh4	-45°		-30°		-15°		0		15°		30°		45°	
Location / blind	low VLT	high VLT	low VLT	high VLT	low VLT	high VLT	low VLT	high VLT	low VLT	high VLT	low VLT	high VLT	low VLT	high VLT
Montreal														
LightLouver (cfs1)	40	49	42	56	47	56	47	56	47	56	47	56	40	49
Vision Control (cfs2)	40	49	53	56	53	60	53	62	53	62	53	56	42	49
Golden														
LightLouver (cfs1)	40	49	47	56	53	62	53	62	47	60	47	56	40	49
Vision Control (cfs2)	42	53	53	56	53	62	53	62	53	60	47	56	40	53
Vancouver														
LightLouver (cfs1)	24	33	29	36	29	40	29	40	29	40	29	33	24	33
Vision Control (cfs2)	29	33	29	33	29	40	36	40	31	40	29	36	29	33
St. John's														
LightLouver (cfs1)	33	33	33	36	33	40	29	40	33	40	33	40	33	36
Vision Control (cfs2)	33	36	33	40	40	40	36	40	36	40	36	40	33	40
Phoenix														
LightLouver (cfs1)	58	67	60	67	53	62	53	62	53	67	60	67	47	67
Vision Control (cfs2)	58	67	60	67	60	62	53	62	60	67	60	67	47	60

A4.21. Configuration E, building depth 16 m

configuration E D16	Orientation													
1.0 x 1.0 whh4	-45°		-30°		-15°		0		15°		30°		45°	
Location / blind	low VLT	high VLT	low VLT	high VLT	low VLT	high VLT	low VLT	high VLT	low VLT	high VLT	low VLT	high VLT	low VLT	high VLT
Montreal														
LightLouver (cfs1)	38	46	38	46	44	50	44	50	44	50	44	52	38	46
Vision Control (cfs2)	38	42	44	52	50	54	50	56	50	56	50	52	38	46
Golden														
LightLouver (cfs1)	38	46	44	52	46	58	50	58	44	56	40	52	38	42
Vision Control (cfs2)	38	46	50	52	50	58	50	58	50	56	44	52	38	42
Vancouver														
LightLouver (cfs1)	23	31	27	31	27	38	27	38	27	38	27	31	23	31
Vision Control (cfs2)	27	31	27	31	27	38	29	38	27	38	27	31	27	31
St. John's														
LightLouver (cfs1)	27	31	31	31	27	38	27	38	27	38	31	33	31	31
Vision Control (cfs2)	31	31	31	33	33	38	33	38	29	38	31	38	31	33
Phoenix														
LightLouver (cfs1)	56	58	56	58	50	58	50	58	50	58	56	63	44	56
Vision Control (cfs2)	56	63	56	58	56	58	50	58	56	58	56	63	44	56

A4.22. Configuration E, building depth 17 m

configuration E D17	Orientation													
1.0 x 1.0 whh4	-45°		-30°		-15°		0		15°		30°		45°	
Location / blind	low VLT	high VLT	low VLT	high VLT	low VLT	high VLT	low VLT	high VLT	low VLT	high VLT	low VLT	high VLT	low VLT	high VLT
Montreal														
LightLouver (cfs1)	31	37	35	41	41	47	41	47	41	47	35	47	35	43
Vision Control (cfs2)	35	37	41	49	47	47	47	53	47	53	41	47	35	43
Golden														
LightLouver (cfs1)	35	43	41	49	41	55	41	53	41	49	35	45	31	37
Vision Control (cfs2)	35	43	43	49	47	55	47	53	47	49	41	43	35	37
Vancouver														
LightLouver (cfs1)	22	29	25	29	25	31	25	35	25	35	22	29	22	29
Vision Control (cfs2)	22	29	25	29	25	31	25	35	25	31	25	29	22	29
St. John's														
LightLouver (cfs1)	25	29	29	29	25	31	25	35	25	31	25	29	29	29
Vision Control (cfs2)	29	29	29	29	25	35	27	35	25	35	25	31	29	29
Phoenix														
LightLouver (cfs1)	53	61	53	61	47	59	47	55	47	59	53	61	41	53
Vision Control (cfs2)	53	55	53	59	53	55	47	55	53	55	53	55	37	47

A4.23. Configuration E, building depth 18 m

configuration E D18	Orientation													
1.0 x 1.0 whh4	-45°		-30°		-15°		0		15°		30°		45°	
Location / blind	low VLT	high VLT	low VLT	high VLT	low VLT	high VLT	low VLT	high VLT	low VLT	high VLT	low VLT	high VLT	low VLT	high VLT
Montreal														
LightLouver (cfs1)	30	35	33	39	35	44	39	44	39	44	33	39	30	35
Vision Control (cfs2)	33	35	39	44	39	44	44	44	41	44	39	44	33	37
Golden														
LightLouver (cfs1)	30	37	39	46	39	50	39	50	39	44	33	41	28	35
Vision Control (cfs2)	33	35	39	46	44	50	44	50	39	46	35	41	33	35
Vancouver														
LightLouver (cfs1)	20	28	20	28	24	30	24	30	24	30	20	28	20	28
Vision Control (cfs2)	20	28	24	28	24	30	24	33	24	30	24	28	20	28
St. John's														
LightLouver (cfs1)	24	28	24	28	24	30	24	30	24	30	24	28	20	28
Vision Control (cfs2)	28	28	24	28	24	33	26	33	24	30	24	30	28	28
Phoenix														
LightLouver (cfs1)	44	57	50	57	44	56	44	52	44	56	50	57	33	46
Vision Control (cfs2)	44	52	50	56	50	56	44	52	50	56	50	52	33	41

A4.24. Configuration F, building depth 18 m

configuration F D18	Orientation													
1.0 x 1.0 whhn3048	-45°		-30°		-15°		0		15°		30°		45°	
Location / blind	low VLT	high VLT	low VLT	high VLT	low VLT	high VLT	low VLT	high VLT	low VLT	high VLT	low VLT	high VLT	low VLT	high VLT
Montreal														
LightLouver (cfs1)	28	35	33	35	33	41	33	39	33	39	33	41	28	35
Vision Control (cfs2)	30	35	35	41	39	46	39	44	39	46	39	41	33	35
Golden														
LightLouver (cfs1)	28	35	33	41	39	46	39	46	33	46	33	41	28	35
Vision Control (cfs2)	33	35	39	41	39	46	39	46	39	46	33	41	30	35
Vancouver														
LightLouver (cfs1)	22	28	24	28	24	28	24	28	28	28	24	28	22	28
Vision Control (cfs2)	24	28	28	28	24	28	24	28	28	28	28	28	24	28
St. John's														
LightLouver (cfs1)	24	30	24	28	28	28	28	28	28	28	28	28	24	28
Vision Control (cfs2)	28	30	28	28	28	28	28	30	28	28	28	28	28	28
Phoenix														
LightLouver (cfs1)	44	52	44	56	39	52	39	52	39	52	44	56	33	44
Vision Control (cfs2)	44	52	44	52	44	52	41	46	44	52	44	52	33	41